CRANFIELD UNIVERSITY

ALESSANDRO E. CONTINI

CALORIMETRIC INVESTIGATIONS OF A SERIES OF ENERGETIC POLYPHOSPHAZENES

DEFENCE ACADEMY OF THE UNITED KINGDOM

PhD THESIS

CRANFIELD UNIVERSITY

DEFENCE ACADEMY OF THE UNITED KINGDOM

DEPARTMENT OF ENVIRONMENTAL AND ORDNANCE SYSTEMS

PhD THESIS

Academic Year 2004-2005

Alessandro E. Contini

Calorimetric Investigations of a Series of Energetic Polyphosphazenes

Supervisor: Dr A.J. Bellamy

September 2005

© Cranfield University 2005. All rights reserved. No part of this publication may be reproduced without the written permission of the copyright owner.

ABSTRACT

Energetic, fluorinated, linear polyphosphazenes are currently under investigation as potential, high-density binders for new, polymer bonded explosive compositions. A series of such polymers was synthesised and the enthalpy of combustion of each member of the series was measured by static bomb calorimetry. This was performed after combusting appropriate secondary thermochemical standards to model the combustion stoichiometry of the hetero-atoms nitrogen, fluorine and phosphorus. The water-soluble combustion products were identified and quantified using ^{19}F NMR spectroscopy and Ion Chromatography. Since some of the combustion products are hydrolytically unstable, it was found necessary to stabilise the initial combustion product mixtures by using a buffer solution instead of pure water in the bomb, and then to determine the composition of the stabilised product mixtures in order to obtain meaningful values for the enthalpies of combustion and thence enthalpies of formation. The thermochemical measurements themselves were made with pure water in the bomb. The composition and structures of the various polyphosphazenes were correlated with their energies of combustion and enthalpies of formation. The latter were calculated using the latest CODATA values of enthalpy of formation of the combustion products. The 'combustion' of the polyphosphazenes under a nitrogen atmosphere was also investigated with the view to calculating the enthalpies of detonation of each member of the series. Three conference papers which include the results of this work have been published and are included in Appendices C-E.

KEY WORDS

Energetic polyphosphazenes, heat of combustion, heat of formation, heat of detonation.

ACKNOWLEDGEMENTS

I would like to thank first of all my supervisor, Dr Tony Bellamy, for his help, encouragement, guidance and great patience. He has done well to 'put up' with my general stubbornness and eccentric 'Italianness' for three whole years! Financial sponsoring of this project by AWE Aldermaston is also greatfully acknowledged. My gratitude is also extended to Dr Peter Golding, Dr Steve Trussell and other members of the AWE Polymer Synthesis Group, for their general advice, and to Dr Hugh Davies, Thermochemical Modelling Team, NPL Teddington, for his valuable criticism and suggestions.

Special thanks go to Dr Alistair MacCuish and Dr Matt Andrews for all of their contributions and for literally bringing me, from feather-quill and ink-bottle, into the world of 21st century word-processing. Other people in the department to whom I am indebted include Roger Cox, for the PC interfacing of the digital thermometer unit, Jenny Lovell, Marjorie Saunders and Maggie Harris for their great help with consumables, and for always providing me with just the right 'bit' at the right time, Dr Phil Gill and Anjum Agha for the recording of mass spectra; Richard Hall, for mending my broken glassware and Dr Mike Williams for his sense of humour. I am also indebted to my landlady, Anne Ward, for her friendship, to her Terrier dog, Poppy, for constantly reminding me of the most fundamental principles in life i.e. eating and sleeping, and, last but not least, to my uncle and aunt in Derby, John and Maureen Hadway, for the many Sunday roasts and Chinese dinners consumed together.

Finally, a special *thank you* goes to my parents for everything they have done to get me to this point.

To Mum and Dad

FAVOURITE QUOTE

Play It by Ear…

GLOSSARY

A	Ampere
AWE	Atomic Weapons Establishment
COSY	Correlation Spectroscopy
C_p	Heat capacity at constant pressure
Da	Dalton
DEPT	Distortionless Enhancement by Polarisation Transfer
DFPA	Difluorophosphoric acid
DSC	Differential Scanning Calorimetry
DC	Direct current
EGDN	Ethyleneglycol dinitrate
ES%	Energetic Substituent Percentage
eV	Electronvolt
GAP	Glycidyl Azide Polymer
GC-MS	Gas Chromatography- Mass Spectrometry
GPC	Gel Permeation Chromatography
H	Enthalpy
HCTP	Hexachlorocyclotriphosphazene
HE	High Explosive
HFPA	Hexafluorophosphoric acid
HMX	1,3,5,7-Tetranitro-1,3,5,7-tetraazacyclooctane
HNS	2,2',4,4',6,6'-Hexanitrostilbene
HPLC	High Pressure Liquid Chromatography
HTPB	Hydroxy-terminated polybutadiene
IC	Ion Chromatography
ICTAC	International Confederation for Thermal Analysis and Calorimetry
IM	Insensitive Munitions
IUPAC	International Union of Pure and Applied Chemistry
IR	Infra Red
J (1)	Coupling constant

J (2)	Joule
K	Kelvin
K-W	Kistiakowsky-Wilson
MFPA	Monofluorophosphoric acid
Mod K-W	Modified Kistiakowsky-Wilson
M_n	Number average molecular weight
M_w	Weight average molecular weight
NENA	Nitratoethylnitramines
NIST	National Institute for Standards Testing
NG	Nitroglycerine
NMR	Nuclear Magnetic Resonance
NPL	National Physical Laboratory
NTO	3-Nitro-1,2,4-triazol-5-one
OB	Oxygen balance
PETN	Pentaerytritol tetranitrate
PolyAMMO	Poly(3-azidomethyl-3-methyloxetane)
PolyBAMO	Poly(3,3-bisazidomethyloxetane)
PBX	Polymer Bonded Explosive
PDI	Polydispersity Index
Perspex	Trademark for poly(methyl methacrylate) in sheet form
PolyGLYN	Poly(glycidylnitrate)
PolyNIMMO	Poly(3-nitratomethyl-3-methyloxetane)
polyNEO	Poly(2-nitratoethyloxirane)
PTFE	Polytetrafluoroethylene
Polymer 1	Random linear poly[P-2-nitratoethoxy/P-2,2,2-trifluoro-ethoxyphosphazene]
Polymer 2	Random linear poly[P-2,3-dinitratoprop-1-oxy/P-2,2,2-trifluoroethoxyphosphazene
Polymer 3	Random linear poly[P-3,4-dinitratobut-1-oxy/P-2,2,2-trifluoroethoxyphosphazene]
Polymer 4	Random linear poly[P-4,5-dinitratopent-1-oxy/P-2,2,2-trifluoroethoxyphosphazene]

Polymer 5	Random linear poly[P-5,6-dinitratohex-1-oxy/P-2,2,2-trifluoroethoxyphosphazene]
RDX	1,3,5-Trinitro-1,3,5-triazacyclohexane
RM	Reference materials
RT	Room temperature
SI	International System of Units
S-R	Springhall-Roberts
STP	Standard Temperature and Pressure
TATB	1,3,5-Triamino-2,4,6-trinitrobenzene
THF	Tetrahydrofuran
T_g	Glass transition temperature
TNT	1,3,5-Trinitrotoluene
TMS	Tetramethylsilane
TrMS	Trimethylsilyl

SYMBOLS

Δ	Difference
ΔU_c	Internal energy of combustion
ΔH_c	Enthalpy of combustion
ΔH_d	Enthalpy of detonation
ΔH_f	Enthalpy of formation
δ	Chemical shift
ε	Heat equivalent of the calorimeter
Ω	Oxygen balance or OB

LIST OF CONTENTS

LIST OF FIGURES

LIST OF TABLES

1 INTRODUCTION

1.1 POLYMER BONDED EXPLOSIVES

During the manufacture of munitions, the crystalline high explosive (HE) filler is usually embedded in a polymeric matrix in order to reduce the sensitivity of the former towards accidental initiation. This stratagem, coupled with the use of new, less heat- and impact-sensitive explosives,[1,2,3] aims to develop and augment a whole new class of safer weapons, which are generally described as insensitive munitions (IM).[4,5,6,7]

The first polymer bonded explosive (PBX) was developed in 1952 at Los Alamos Scientific Laboratories in the US and it consisted of a composition of RDX crystals embedded in plasticized polystyrene.[8] A variety of PBX formulations, based on an inert polymeric matrix, such as urethane cross-linked hydroxyl-terminated polybutadiene (HTPB)[9,10] were subsequently developed.[8] The loss of explosive performance caused by the presence of a relatively low-density, 'inert' polymeric binder however, soon led to the development of novel polymers which were themselves energetic and thus, could actively contribute to the explosive performance of the PBXs.

Common, in-service energetic binders include polyNIMMO, *poly(3-nitratomethyl -3-methyloxetane),*[11](II, Figure 1.1), polyGLYN, *poly(glycidylnitrate)*[12,13] (I, Figure 1.1), GAP *(glycidyl azide polymer)*[14](III), polyAMMO, *poly(3-azidomethyl-3-methyloxetane)*[15] (IV) and polyBAMO, *poly(3,3-bisazidomethyloxetane)*,[15] (V). Another energetic polymer, polyNEO, *poly(2-nitratoethyloxirane)* has been recently reported.[16] These polymers owe their energetic properties to the presence of one nitrato group (polyNIMMO, polyGLYN and polyNEO) or one or two azido groups per monomer unit (GAP, polyAMMO and polyBAMO).

In addition to the energetic binder, additional non-polymeric energetic compounds can also be added to PBXs in order to decrease even further the sensitivity of the explosive filler or to impart specific physical and/or mechanical properties to the composition, and these take the name of *energetic plasticizers*. Common plasticizers include K10,[8] (a mixture of di- and tri-nitroethylbenzene), NENAs (nitroethylnitramines),[17,18] GLYN oligomer and EGDN (ethyleneglycol dinitrate), a close relative of nitroglycerine.

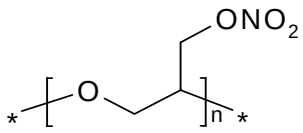

(I) polyGLYN

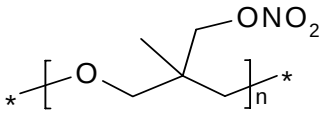

(II) polyNIMMO

Figure 1.1 Structures of (I) polyGLYN and (II) polyNIMMO.

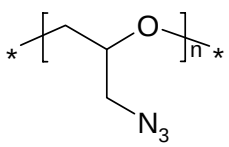

(III) GAP

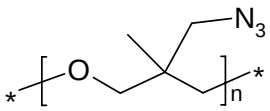

(IV) polyAMMO

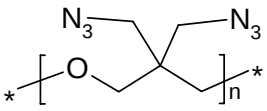

(V) polyBAMO

Figure 1.2 Structures of (III) GAP, (IV) polyAMMO and (V) polyBAMO.

1.2 POLYPHOSPHAZENES

Current, in-service, energetic binders are typically linear carbon-based polymers (Section 1.1) which display low energy densities and relatively high glass transition temperatures (T_g).[19] The high T_g of the binder usually requires the addition of a suitable plasticizer to the final PBX compositions[8,4] in order to lower the T_g to an acceptable level. Although plasticisation is a viable solution to ameliorate the binder's high T_g, it also leads, in time, to the migration of plasticizer[20] to the surface of the explosive filler, with the effect of seriously

compromising[19] the low-temperature performance of the PBX. One of the main problems with energetic binders is therefore the difficulty in developing materials which display high energy-densities and low T_gs, a combination of properties which would ultimately allow the formulation of PBXs of higher solids loading and yet good physical and IM properties.

In search of a viable alternative to carbon-based binders, novel systems based on a *linear polyphosphazene* backbone[21] are currently under investigation[19] as potential high-density, high-energy density (HED) and low T_g binders for new, polymer bonded explosive compositions.

Polyphosphazenes are polymeric materials based on a formally 'unsaturated' phosphorus-nitrogen backbone which can contain up to a maximum of 15000 $-R_2P=N-$ units;[22] the final MW of the polymer and its polydispersity[23] depending on the synthetic route adopted for its preparation.[24,25,26,27,28] Like silicones and polysilanes, polyphosphazenes are *semi-organic* polymers, having the repeat unit ($N=PR_2$) as shown in Figure 1.3, where R can be a halogen, an organic group or an organometallic unit.[21]

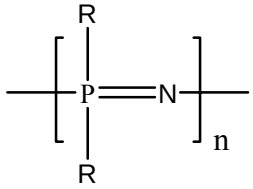

Figure 1.3 Unit monomer structure of a generic, linear polyphosphazene.

Other oligomeric or non-polymeric compounds that are closely related to polyphosphazenes, are usually classified into *phosphoranimines* or *mono*phosphazenes (e.g. $X_3P=NR$), *di*phosphazenes (e.g. $X_3P=N-P(O)X_2$) and *cyclo*phosphazenes, $(-X_2P=N-)_n$ with n = 3, 4, 5 up to 17.[29]

Although the chemistry of polyphosphazenes dates back to the first half of the 19th century,[30,31,32,33] the real breakthrough in the field was achieved in the mid 1960s, with the discovery and optimisation by Allcock *et al.*[21] of the thermal and Lewis acid catalysed ring opening/substitution routes for preparing various substituted

linear polyphosphazenes. Although most of this chemistry is relatively recent, more than 700 examples of linear polyphosphazenes have been synthesised to date and extensive reviews of these materials and their syntheses have been published.[34,35]

The physical properties of polyphosphazenes vary widely with the nature of the substituents. Solubility in appropriate solvents,[21,22] hydrophilicity,[36] crystallinity,[37] electrical conductivity,[38,39] mechanical strength,[40] glass transition temperature[21,22] and flame retardancy[41,42]can all be tailored to suit many specific applications by careful selection of the side groups.[21] At the time of writing, the main fields of application of polyphosphazenes include fuel-cell technology,[43] advanced biomedical materials[44,45] and filtration technology.[46]

1.2.1 Phosphazene-based energetic binders

The synthesis of novel, high-energy phosphazene-based binders for PBX formulation has been attempted by various workers over the last two decades. The first reported[47] case focused on the synthesis of energetic cyclic compounds such as *cyclotriphosphazene polynitramines*, which may be prepared by reaction of hexachlorocyclotriphosphazene (HCTP, VI in Figure 1.4) with 1,2-diaminoethane and selective nitration of the amino groups of the product (VII). Although generally obtained in good yields, these compounds were found to be highly heat- and impact-sensitive, to the extent that even small samples had to be handled behind a protective shield.

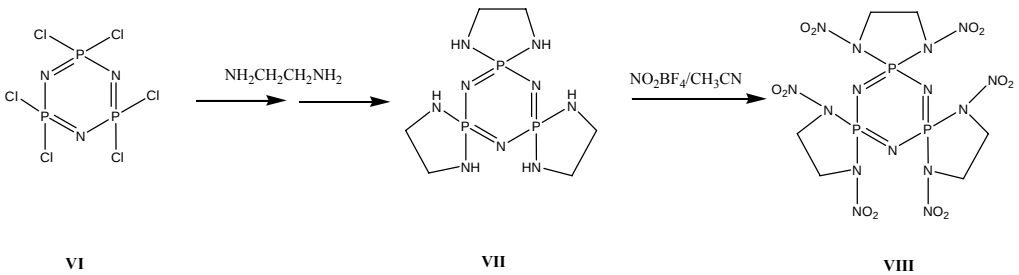

Figure 1.4 General scheme for the synthesis of 1,1,3,3,5,5-tris-spiro(N,N'-dinitroethylenediamino)cyclotriphosphazene (VIII).

A later, similar approach[48] aimed for the partial and complete substitution of the chlorine atoms of HCTP with a range of short-chain, oxirane-bearing alkoxides, which may be energised by ring-opening nitration using N_2O_5 in dichloromethane or concentrated HNO_3. The purity and yields of the isolated products however were very low.

In the very first reported[49] attempt to synthesise a low T_g, high molecular weight, *linear poly[dinitratoalkoxyphosphazene],* other workers successfully prepared the energetic monophosphazene *tris(2,2-dinitroprop-1-oxy)-N-(trimethylsilyl) phosphoranimine* (X in Figure 1.5), which was then polymerised anionically to yield energetic, *linear poly[bis(2,2-dinitroprop-1-oxy)phosphazene]* (XI), directly. Although obtained in good yields, the energetic intermediate to the phosphoranimine, *tris(2,2-dinitropropyl)phosphite* (IX), was unfortunately found to either self-ignite or decompose explosively over time, and this, coupled to the very low molecular weight of the final polymer (i.e. up to 4 monomer units only), precluded further work in this direction.

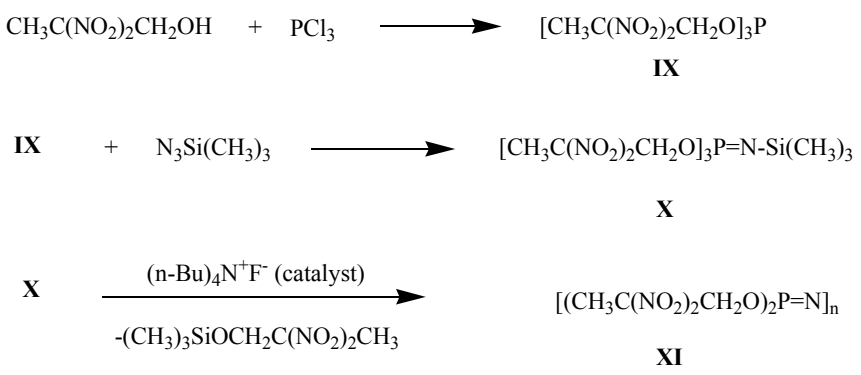

Figure 1.5 Synthetic sequence for linear poly[bis(2,2-dinitroprop-1-oxy) phosphazene] via direct anionic polymerisation of an energetic phosphoranimine.

Despite the initial discouraging efforts, an alternative and promisingly scalable route to the synthesis of high molecular weight, low T_g, linear polynitratoalkoxyphosphazenes, was recently developed[19] by the Polymer Synthesis Group of AWE Aldermaston, UK. The new approach exploits the good leaving-group ability[50,51] of the 2,2,2-trifluoroethoxide groups of *linear*

poly[bis(2,2,2-trifluoroethoxy)phosphazene] upon macromolecular nucleophilic substitution with suitable alkoxides. After nitrolysis of protected sites in the alkoxy groups, a series of energetic, fluorinated, random mixed substituted linear polyphosphazenes (Figure 1.6) are produced.

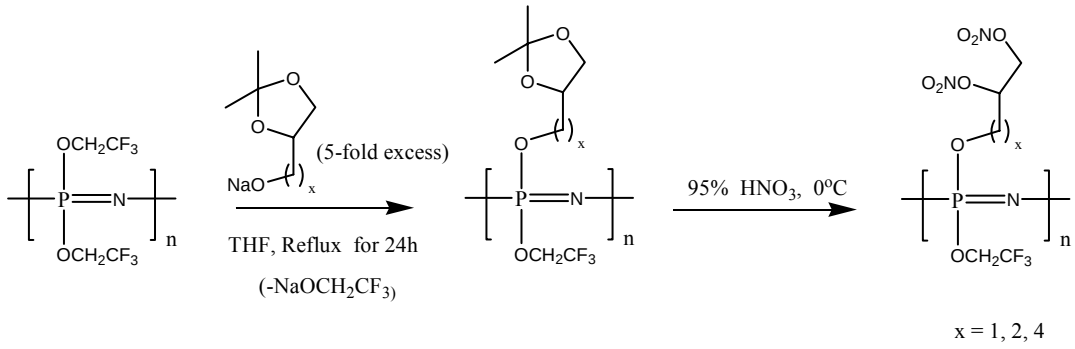

Figure 1.6 General scheme of the AWE synthesis of three homologous random mixed substituent, energetic polyphosphazenes.

The major advantages of this method include the relatively low cost of the starting material, the mild nitration conditions required, the low polydispersities and the high molecular weights of the final polymers (5000-10000 *Da*, corresponding to 20-40 repeat units[19]).

An additional positive aspect of this method is the possibility of variation, within certain limits, of the degree of side-chain substitution (the *energetic substituent percent*, ES%) by adjustment of the substitution reaction conditions.[50] This would enable a range of potential PBX binders to be synthesised, with different energy densities, glass transition temperatures and other important physical properties, such as density and viscosity. A possible disadvantage however, is the impossibility of achieving complete substitution (i.e. ES%=100) of the 2,2,2-trifluoroethoxide groups of linear poly[*bis*(2,2,2-trifluoroethoxy)phosphazene] upon nucleophilic substitution.[19,50] Stoichiometric substitution on phosphorus may be obtained only by replacing the starting high-polymer template with the highly moisture-sensitive[52] linear poly[dichlorophosphazene]. [50,53]

In this work, the standard enthalpies of formation of four *random linear poly(2,2,2-trifluoroethoxy/dinitratoalkoxy)phosphazenes* and of a *random linear*

poly(2,2,2-trifluoroethoxy/mononitratoalkoxy)phosphazene prepared by the AWE method, (the simplified structures of which are given in Figure 1.7), were calorimetrically measured. Whilst Figure 1.7 depicts the five polymers in a simplistic manner, Figure 1.8 illustrates how, in reality, all the materials have a random mixed substituent structure.

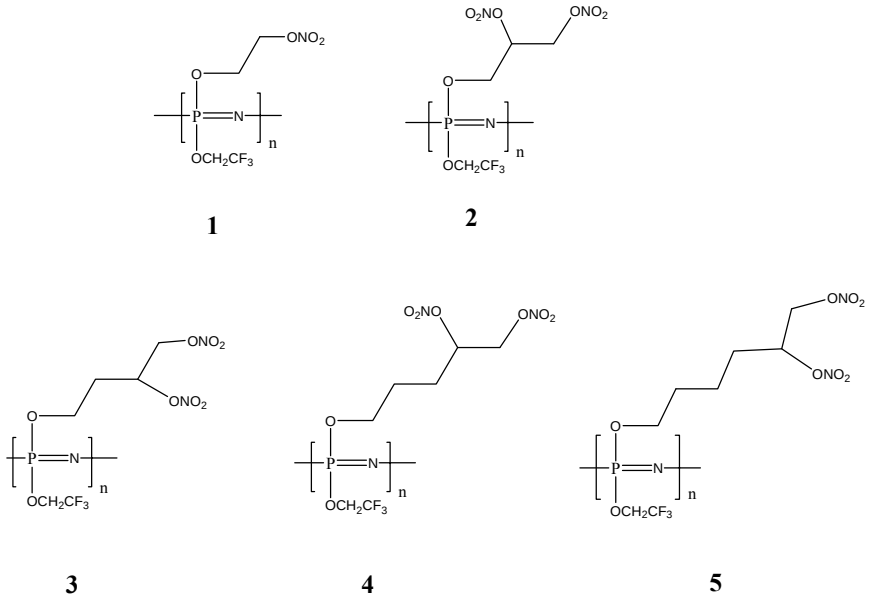

Figure 1.7 Nitrate ester functionalised polyphosphazenes calorimetrically investigated in this work

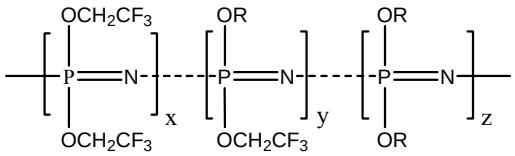

R =	$CH_2CH_2ONO_2$	**1**
	$CH_2CH(ONO_2)CH_2ONO_2$	**2**
	$CH_2CH_2CH(ONO_2)CH_2ONO_2$	**3**
	$CH_2CH_2CH_2CH(ONO_2)CH_2ONO_2$	**4**
	$CH_2CH_2CH_2CH_2CH(ONO_2)CH_2ONO_2$	**5**

Figure 1.8 Random structures of the five energetic, linear polyphosphazenes.

Although none of the polymers studied in this work would be capable of sustaining detonation independently, the materials are energetic by virtue of the nitrate ester functionalities present on the side-chains. Preliminary small-scale

hazard tests (mallet-impact, mallet friction, flame and electric spark) are however consistent with the materials exhibiting a low explosive hazard.[19]

1.2.2 Synthesis of linear poly[bis(2,2,2-trifluoroethoxy)-phosphazene]

1.2.2.1 Synthesis of tris-P-(2,2,2-trifluoroethoxy)-N-(trimethylsilyl)-phosphoranimine

As mentioned in Section 1.2.1, the non-energetic precursor to all of the polyphosphazenes synthesised in this work is high molecular weight, linear *poly[bis(2,2,2-trifluoroethoxy)phosphazene]*. The latter may be prepared by polymerisation (Section 1.2.2.2) of *tris-P-(2,2,2-trifluoroethoxy)-N-(trimethylsilyl)phoshoranimine* (XIV in Figure 1.9), which, in turn, is obtained by reacting *trimethylsilylazide* (XII) with an *equimolar* amount of *tris(2,2,2-trifluoroethyl)phosphite* (XIII). This reaction, which was first successfully attempted in 1977 by Flindt and Rose,[54] is a variation of the much earlier discovered (1919) reaction of an azide with a phosphine, now known as *Staudinger coupling*.[55] Although linear poly[bis(2,2,2-trifluoroethoxy) phosphazene] may also be prepared by thermal ring-opening[56] of hexachlorocyclotriphosphazene (HCTP), followed by macromolecular halogen substitution of the resulting linear polymer, the Flindt and Rose method is now almost universally preferred when better control on the molecular weight and polydispersity of the final product is required.[21] Whilst the progress of the 'condensation' reaction can be monitored by IR spectroscopy and also by ^{1}H, ^{19}F, ^{29}Si, and ^{31}P NMR spectroscopy,[54] making the Flindt and Rose approach convenient to the modern polymer chemist, its main disadvantages remain in the long reaction time (70 h) and the relatively high temperature (110˚C) required for the reaction to go to completion. These can lead to degradation of the phosphoranimine product and hence low reaction yields.

The method currently employed[53] by AWE Aldermaston to prepare tris-P-(2,2,2-trifluoroethoxy)-N-(trimethylsilyl)phosphoranimine, and which was also adopted in this work, utilised essentially the original Flindt and Rose reaction conditions,

albeit with a two-fold excess (3 equivalents) of trimethylsilylazide. The excess trimethylsilylazide is believed[57] to increase the reaction yields, whilst acting as a solvent for the product.

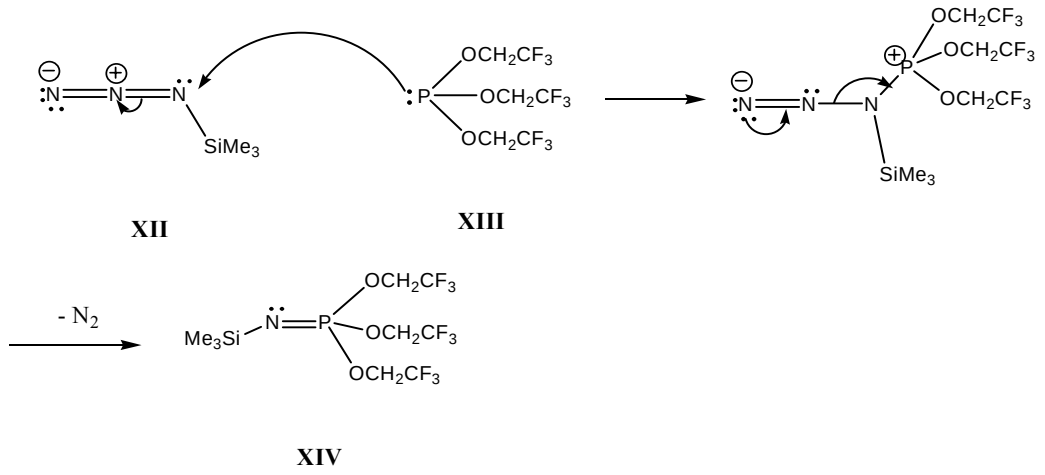

Figure 1.9 Proposed mechanism for the reaction of trimethylsilylazide (XII) with tris(2,2,2-trifluoroethyl)phosphite (XIII) to give tris-P-(2,2,2-trifluoroethoxy)-N-(trimethylsilyl)phosphoranimine (XIV).

1.2.2.2 Polymerisation of tris-P-(2,2,2-trifluoroethoxy)-N-(trimethylsilyl)-phosphoranimine

Due to the fast-growing interest in semi-organic polyphosphazenes, and in particular, in high MW, *linear* poly[bis(2,2,2-trifluoroethoxy)phosphazene] in both established and emerging high-tech fields (in particular, biomedicine,[58,59] flame retardants[60] and semi-organic membrane technology[61]), a number of investigations have been recently carried out in order to develop novel, high-yield routes to this polymer with low values of the polydispersity index, starting from the N-silylated monomer P-*tris*(2,2,2-trifluoroethoxy)-*N*-(trimethylsilyl) phosphoranimine, $Me_3SiN{=}P(OCH_2CF_3)_3$ (Section 1.2.2.1). The three 'options' currently available to induce polymerisation of this and other N-silylated phosphoranimines are the *uncatalysed thermal,*[62] the *'living cationic'*[63,64] and the *anionic* polymerisation reactions. The latter technique was employed for the

synthesis of linear poly[bis(2,2,2-trifluoroethoxy)phosphazene] in this work, (Section 4.2.1.2).

1.2.2.2.1 Anionic polymerisation of $Me_3SiN=P(OCH_2CF_3)_3$

The polymerisation of $Me_3SiN=P(OCH_2CF_3)_3$ can be induced by various 'anionic' initiators e.g. nucleophilic organic salts and compounds such as tetrabutylammonium fluoride ($Bu_4N^+F^-$), N-methylimidazole and a variety of basic compounds including amines, amides and aryloxides,[63,64,65] to give high MW polymer of low polydispersity in good yields. The advantage of using a specific initiator is the possibility of varying (within limits) the final MW and polydispersity of the product, when the reaction is carried out in solution (i.e. in diglyme), as opposed to neat. The possibility to vary the MW depends[64] on each initiator's own ability to slightly influence the kinetics of the reaction. The presence of the anionic initiator also lowers the polymerisation temperatures to around 100ºC, depending on the monomer being polymerised. The relatively low reaction temperature enables phosphoranimine monomers bearing thermally sensitive side groups on phosphorus to be polymerised. These would not 'survive' prolonged exposure to high temperatures.

The overall mechanism of anionic polymerisation of $Me_3SiN=P(OCH_2CF_3)_3$, which is presented in Figures 1.10, 1.11 and 1.12, is quite complex and involves[21] initiation (Figure 1.10), chain growth (Figure 1.11, A), chain 'transfer to monomer' (Figure 1.11, B) and finally, a 'macrocondensation of oligomeric chains' (Figure 1.12), which effectively terminates the process. The initiation step is thought[64] to involve the displacement of the silyl group from the monomer by the lone pair of the 'silylphilic' initiator, generating a 'free' phosphazene anion which then attacks the phosphorus atom of another molecule of monomer. In this process, which rapidly repeats itself several times, trifluoroalkoxide is eliminated and this can then attack the end silyl group of an oligomeric chain to yield what is currently believed[21] to be the 'true' propagation initiator (Figure 1.10). The propagator, as the name implies, can then either react with momomer to *propagate* the chain to medium or high molecular weights via a *chain-growth* mechanism (A in Figure 1.11), it can induce a '*chain transfer*' to monomer (B in

Figure 1.11), or it can attack the pentavalent end-phosphorus of another oligomeric chain, (*macrocondensation*), thus terminating the process (Figure 1.12). The reported[64] highest molecular weights for the anionic polymerisation of $Me_3SiN{=}P(OCH_2CF_3)_3$ are in excess of 20000 (corresponding to ~80 monomer units). Judging from Figure 1.12, it would appear that the high MW chains formed by macrocondensation would bear a trimethylsilyl (TrMS) moiety at one end. Previous experiments[64] have indeed confirmed that there are TrMS end-groups present on the polymer chains, although these usually remain undetected by ^1H NMR spectroscopy because of their low abundance, relative to the protons of the substituent groups on phosphorus.

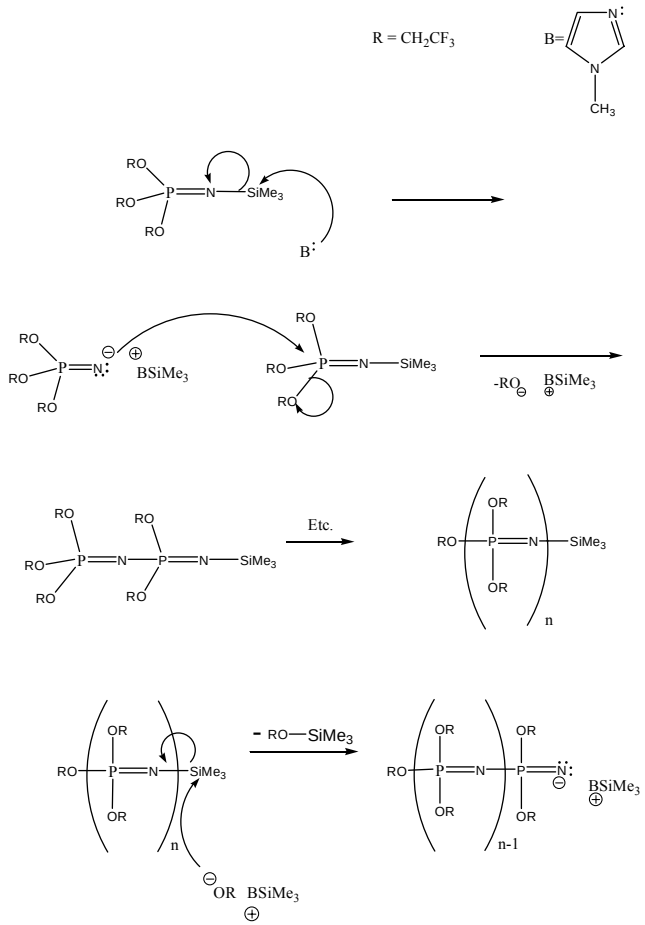

Figure 1.10 Rationalisation[21] for the formation of the oligomeric 'propagation initiator'. Anionic initiator employed: N-methylimidazole (B).

A: Chain propagation

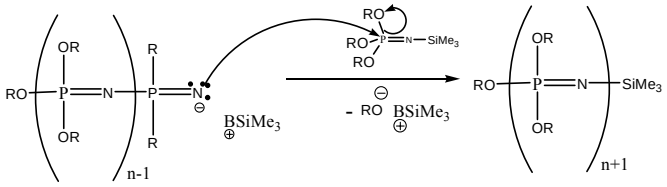

B: Chain transfer to monomer

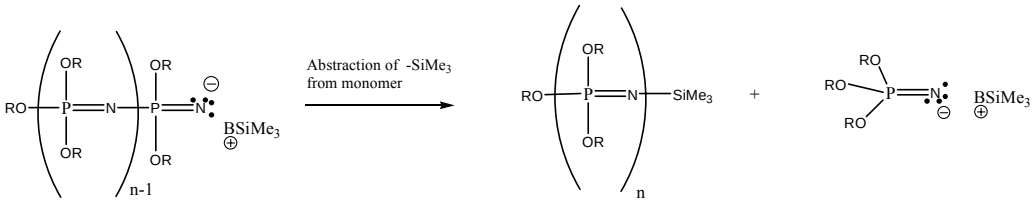

Figure 1.11 Simplified mechanism[21] re-adapted to the initiator N-methylimidazole (B) for: (A) chain propagation and (B) chain 'transfer' to monomer.

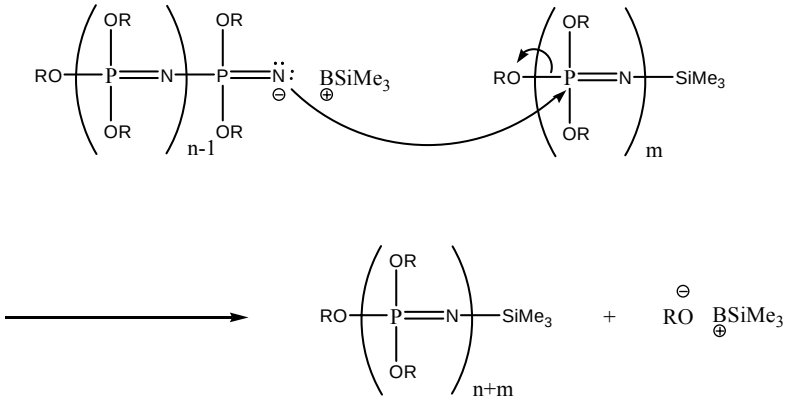

Figure 1.12 Macrocondensation[21,64] of the nucleophilic 'chain propagator' with another chain, with expulsion of trifluoroethoxide, to yield high MW polymer (B= N-methylimidazole).

1.3 STANDARD ENTHALPY OF FORMATION

The standard enthalpy of formation of a compound (sometimes abbreviated as enthalpy of formation or standard heat of formation, ΔH°_f)[66] is best defined as the *standard enthalpy change when the compound is formed from its elements in their standard states*, that is, their most stable form, under chosen standard conditions of temperature and pressure (STP), which are defined by IUPAC as $P = 10^5$ Pa (= 1 bar = 0.9869atm) and T = 25ºC (298.15K). [67,68,69] The standard enthalpy of formation of a compound can be either positive or negative, depending on whether the formation reaction of the former is *endo*- or *exo*-thermic, respectively. By convention, the standard enthalpy of formation of all elements, under STP conditions, is set equal to zero.[70, 71]

The beauty of the latter assumption lies in the possibility, granted by Hess's law[67] (see Section 1.6), of calculating the standard enthalpy change for a multitude of chemical reactions for which direct calorimetric measurement would be difficult or impossible to perform, by knowing the standard enthalpies of formation of *all* the reactants and products of reaction. If aqueous solutions are also involved, the standard state refers to *infinite dilution* at 25ºC, which is usually denoted as '*aq.*'[67,71] When hydrated acids, bases or salts are concerned, the standard enthalpies of formation of the hydrated hydrogen ion is arbitrarily taken to be *zero,* as for elemental hydrogen.[67]

The standard enthalpy of formation of organic compounds (including energetic materials) is routinely measured by oxygen combustion calorimetry.[77,72] When the combustion data is not available however, the group additivity method[73,74,75] can sometimes be used, pending availability of bond energy data. Highly accurate values of the standard formation enthalpy of a multitude of organic, organo-metallic and inorganic compounds, and also free atoms and hydrated ions, are regularly compiled in extensive tables which are available in the open literature.[76,77]

In explosive science, the standard enthalpy of formation is a particularly important parameter, since it allows semi-empirical calculation,[8] via the application of

Hess's law to the detonation products, of the *standard enthalpy of detonation* (ΔH°_{d}) of energetic compounds (both crystalline explosives[78] and energetic polymers[79]). As a consequence of Hess's law, the *more positive* (larger quantity in modulus) the enthalpy of formation of an explosive is, the higher will be its enthalpy of detonation.[8] In the specialised literature, it is not unusual, for example, to read statements such as "…*the highly endothermic energetic material*...", with reference to novel, highly brisant explosives.

The standard enthalpy of detonation (also commonly referred to as '*Q*', the unit mass enthalpy of explosion) is arguably the thermodynamic quantity which best describes explosive performance,[80] as it indicates the total energy available to perform mechanical work and hence damage to the surroundings.[81] Although ΔH°_{d} may also be directly measured by means of specially designed 'detonation' or 'explosion' calorimeters,[82,83,84] it is preferable, in the case of energetic polymers of low-oxygen balance,[79] to derive it semi-empirically. In order to do this, the nature and stoichiometry of formation of the detonation products are either derived experimentally[85]or theoretically predicted. This prediction has traditionally been carried out by means of the long-established Kistiakowsky-Wilson (*K-W*) and related rules,[8] and, only recently, by the use of thermodynamic computer codes.[86] However, while computer code 'detonation modelling' for energetic CHNO compounds is often far from accurate,[87,88] systems which contain elements other than CHNO pose even more complications,[89,90] since, as some authors[86] have recently stated: *"...the accurate determination of product decomposition species for energetic materials with complex elemental composition remains a major unresolved problem."*

1.4 RELATION BETWEEN INTERNAL ENERGY OF COMBUSTION AND ENTHALPY OF COMBUSTION

The derivation of the standard enthalpy of formation of an organic compound requires the experimental measurement of its *standard enthalpy of combustion,* ΔH^{o}_{c}. If the combustion reaction under calorimetric investigation is carried out under constant-volume conditions, as in a pressurised steel vessel (bomb), no

work of expansion can be performed and the heat of the reaction will be equal to the *internal energy* change ΔU_c. Only if a constant pressure apparatus is used, the measured heat of reaction would, by definition, be equal to the *enthalpy* change of reaction. From combining the First Law of Thermodynamics with the ideal Gas Law, an equation (Equation 1) can be derived[70,66,91] which effectively describes the difference between ΔU_c and ΔH_c for a given reaction.

$$\Delta H_c = \Delta U_c + \Delta(PV) \quad (1)$$

Assuming the ideal gas law to apply[67] at the typical oxygen bomb pressure (30 atm), then $\Delta(PV)$ will be equal to ΔnRT and Equation 1 can thus be written as

$$\Delta H_c = \Delta U_c + \Delta nRT \quad (2)$$

where Δn is the difference between the gaseous moles of products and reactants, R is the universal gas constant and T is the absolute temperature. If all reactants and products are solids or liquids, the change in volume which accompanies a reaction at constant pressure is very small, usually less than 0.1%,[66] and the magnitude of the thermal contribution due to expansion work of condensed matter is usually less than 5 J.[66] This error can be included in the overall experimental uncertainty interval, which, for most experimental determinations, is usually far greater. For reactions at very high pressures however (e.g. at the bottom of the ocean or deep in the Earth's fluid mantle), $\Delta(PV)$ can be significant even for condensed phases.

When gases are involved in the reaction however, an appreciable value of $\Delta(PV)$ can occur and the difference between internal energy and enthalpy of reaction can be significant. To give a practical example, the case of the complete combustion of ethanol in pressurised oxygen may be considered. The stoichiometry of exhaustive combustion for ethanol can be written as:

$$C_2H_5OH_{(l)} + 3O_{2(g)} \rightarrow 2CO_{2(g)} + 3H_2O_{(l)}$$

The standard internal energy change of this reaction, measured[66] by constant-volume bomb calorimetry is $\Delta U^o_c = -1364.47\ kJ\ mol^{-1}$. The complete oxidation

reaction involves 2 moles of product gas and 3 moles of reactant gas. The change *Δn* will therefore be –1 mol. Assuming the ideal gas law to apply at the bomb internal pressure, then Δ(PV) will be equal to ΔnRT and therefore (Equation 3) to:

$$(-1)RT = -8.314\ Jmol^{-1}K^{-1} \times 298.15\ Jmol^{-1} = -2.48\ kJmol^{-1} \quad (3)$$

As a consequence, the standard enthalpy change will be given by Equation 4:

$$\Delta H_c = -1364.47 + (-2.48) = -1366.95\ kJmol^{-1} \quad (4)$$

and the difference between internal energy and enthalpy of reaction is now large enough[66] (2.48 kJ mol^{-1}, 0.2%) to be significant.

1.5 STANDARD ENTHALPY OF COMBUSTION: MEASUREMENT VERSUS CALCULATION

If experimental combustion data were not available, enthalpies of combustion could be calculated by application of two semi-empirical criteria, namely *oxygen consumption calorimetry*[92,93] and the *molar group additivity of the heats of formation.*

Oxygen consumption calorimetry relies on the experimental observation that a wide range of organic compounds display approximately the same heat of complete combustion *per gram of diatomic oxygen* consumed. Although this method may at first seem convenient to use, it has the main disadvantage of requiring an accurate knowledge of the molar amount of oxygen consumed in the balanced combustion equation. This is easily predictable for CHNO compounds, but when a sample of complex atomic composition is burnt, the molar amount of oxygen needed for complete combustion becomes harder to accurately predict, especially if the nature of the combustion products is unknown.

The principle of *additivity of the heats of formation* is a consequence of Hess's law and the fact that enthalpies of reaction are state functions.[70] In practice, the enthalpy of combustion may also be calculated by subtracting the sum of the heats

of formation of all the reaction products from the sum of the heats of formation of all the reactants,[67] following prior calculation of all heats of formation via the group additivity method (Section 1.3). The main problem with this approach lies in the lack of energy data regarding less common, hetero-atomic groups such as P=N and P-O which this method would require for the thermochemical study of polyphosphazenes.

1.6 HESS'S LAW

Hess's law takes its name from the Russian chemist *German M. Hess* (1806-50) who first established it experimentally in 1840. The law, which has been described[77] as constituting the basis of thermochemistry, states that *the amount of thermal energy exchanged in a reaction carried out at constant volume or constant pressure, is independent of any intermediate reactions but only depends on the initial and final chemical states, e.g. on the internal energy or enthalpy of the reactants and of the final products of reaction*.[66] From Hess's law, which is also known[66,67] as Law of Constant Heat Summation, it follows that both the enthalpy, ΔH and the internal energy, ΔU, are *state functions*, and only depend upon the *initial* and *final* states of the reaction.

Hess's law is extremely useful for the determination of those enthalpies of reaction that cannot be experimentally measured. A simple example would be the heat liberated when carbon (graphite) and oxygen gas react to form carbon monoxide (CO). Oxidation of carbon does not normally stop at CO but gives CO_2 instead,[94] making the *carbon* → *CO* reaction impossible to measure experimentally. According to Hess's Law the problem can be solved by measuring, at a given temperature, the heat of formation of carbon dioxide from its elements and, at the same temperature, the heat liberated by the formation of CO_2 from burning carbon monoxide in oxygen gas. The formation of CO_2 from its elements can in fact occur either through a single, direct reaction, as described by Equation 5,

$$C_{(graphite)} + O_{2\,(g)} \rightarrow CO_{2\,(g)} \qquad \Delta H_1 = -393.5 \text{ kJ mol}^{-1} \qquad (5)$$

or through the intermediate formation of carbon monoxide (Equations 6 and 7):

$C_{(graphite)} + 0.5O_{2\,(g)} \rightarrow CO_{(g)}$ $\quad \Delta H_x = ?$ $\quad kJ\ mol^{-1}$ (6)

$CO_{(g)} + 0.5O_{2\,(g)} \rightarrow CO_{2\,(g)}$ $\quad \Delta H_2 = -283.0$ $\quad kJ\ mol^{-1}$ (7)

The pathway of the complete reaction can be summarised with a 'Hess's law energy diagram', as shown in Figure 1.13.

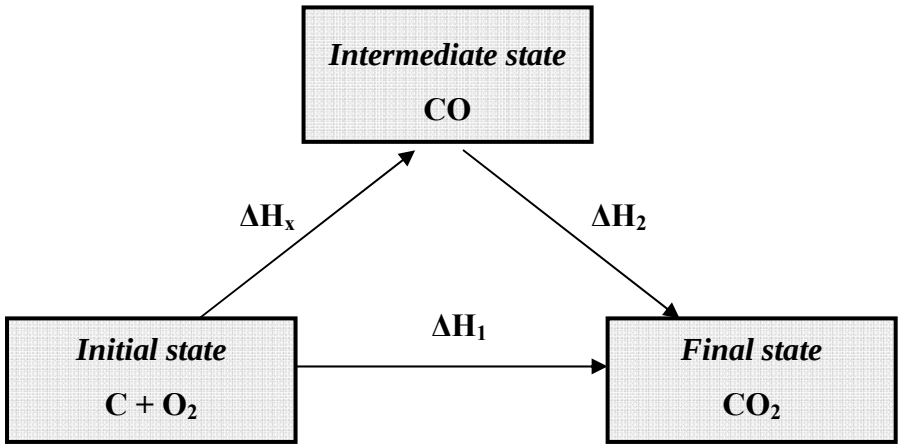

Figure 1.13 Hess's law energy diagram for the reaction of graphite with oxygen to give carbon dioxide.

Because both *ΔH* and *ΔU* are state functions, their final values are not influenced by the intermediate steps of the reaction and ΔH_x, in this case the heat of formation of CO can be calculated (Equation 8) by direct subtraction of ΔH_2 from ΔH_1, which gives

$\Delta H_x = -393.5 - (-283) = -110.5\ kJ\ mol^{-1}$ (8)

which is the value[94] of the heat of formation of carbon monoxide from its elements.

Extending the given example to the combustion reaction of other compounds, it can be stated that *the heat of formation of any compound can be conveniently calculated from the sum of the enthalpies of combustion at temperature T of the constituent elements minus the enthalpy of combustion of the compound itself, at the same temperature T* (in the previous example; $\Delta H_x = \Delta H_1 - \Delta H_2$).

In other words, the heat of formation (expressed either as ΔH or ΔU) of any compound can be calculated from the difference between *the sum of the heats of formation of all of the combustion products*, at a given temperature *T,* (expressed either as ΔH or ΔU), and *the heat of combustion of the compound itself* (expressed either as ΔH or ΔU), at the same temperature, *T*, as diagrammatically shown for a hypothetical energetic polyphosphazene, by the Hess's law energy diagram presented in Figure 1.14.

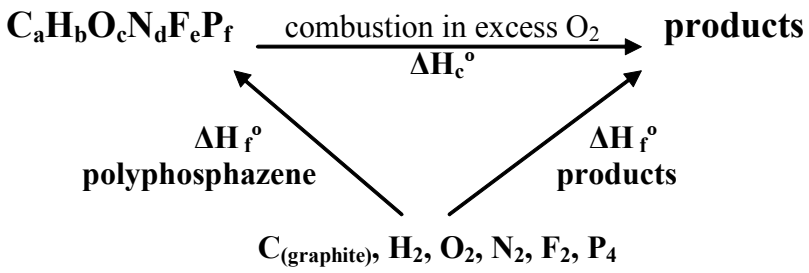

Figure 1.14 Hess's law combustion enthalpy diagram for a hypothetical energetic polyphosphazene.

The validity of Hess's law has enabled thermochemists to compile extensive tables of heats of formation of innumerable combustible substances, amongst which is a wide variety of organic fuels and explosives.

1.7 CALORIMETRY

Thermochemical investigations are routinely conducted in a *calorimeter* (from Latin, *Calor* = *heat* and from Greek, *Metron* = *measure*)[95] and the branch of thermochemistry devoted to the measurements of enthalpies of reaction takes the name of *calorimetry.* Although many types of calorimeters exist, all of them are essentially variations of the same basic principle: the reaction or physical process to be studied occurs inside the boundaries of a closed space, the reaction chamber, at a defined initial temperature T_i, in *controlled thermal contact*[77] with the 'jacket'

at its temperature T_j. The temperature control of the jacket may be 'active' as in the case of an adiabatic calorimeter, or 'passive' in the case of a heat sink, if present. The reaction chamber and its jacket, with devices for stirring, heating, cooling (if any) and temperature measurement constitute the *calorimetric system*. Calorimeters can be sophisticated and expensive or simple and cheap, thus catering for a wide variety of purposes which require different degrees of accuracy. Static combustion bomb calorimeters, a relatively simple design, are for example, often employed for routine calorific measurements of coal, coke and liquid fuels,[96] combustible wastes, food and supplements for human nutrition, combustible building materials,[93] explosives and propellants,[78] and even for energy balance studies in ecology.

A calorimeter can be operated under constant pressure, with a vent to allow the pressure to be maintained at the atmospheric value, or at constant volume, which is usually the condition chosen in the study of combustion reactions.

Because of the large number of existing designs, there is still no formal method of classification for calorimeters. Recently published work[97] however, suggests a broad classification based on three main criteria:

1. The measuring principle
2. The mode of operation
3. The principle of construction

1. *The measuring principle* subdivides calorimeters into three categories, namely *heat conduction, heat accumulation* and *heat exchange* calorimeters.
2. *The mode of operation* subdivides calorimeters into another three categories, namely *isothermal* instruments, in which reaction chamber and its jacket are held at a constant temperature ($\Delta T = 0$, T_j and T_i constant), *isoperibol* instruments, in which the jacket is held at constant temperature whilst the reaction chamber temperature may alter ($\Delta T \neq 0$, T_j constant), and finally *adiabatic* instruments, where, ideally, no heat exchange takes

place between the reaction chamber and the jacket because they are both maintained at the same temperature, which, of course, may increase or decrease during the reaction. (ideally $\Delta T = 0$, $T_j = T_i$ not constant).

3. *The principle of construction* differentiates calorimeters between single measuring systems or twin (differential) systems.

Another classification approach, which is often used in calorimetry text-books, consists in dividing the various calorimeters into 'special purpose classes'. We may therefore distinguish between solution calorimeters, flame calorimeters, combustion (bomb) calorimeters, reaction hazard calorimeters, heat flow (isothermal) calorimeters and differential scanning calorimeters.[97] Each one of these types can, in some cases, be further subdivided into more variants, which essentially cater for very specific applications.

In conclusion, it can be said that calorimeter design and construction is a very demanding science, especially for processes involving very small heat changes.

1.8 OXYGEN BOMB CALORIMETRY

The enthalpy change that occurs when a liquid or solid material is burnt quantitatively in a strongly oxidative atmosphere, usually pure oxygen or fluorine under pressure (in the latter case we speak of fluorine bomb calorimetry[98]), is a very powerful tool for determining thermochemical data regarding the material burnt. For this purpose a stainless steel pressure vessel (*a bomb*) is always employed. The bomb sits in a *calorimetric bucket*, sometimes also called *calorimetric pail*, filled with an accurately known volume of water, which is constantly stirred by a rotating paddle. The bomb can be a twin-valve or, as in the early days of calorimetry, a much less convenient single-valve model. Having an inlet as well as an outlet valve allows the operator to 'flush' the air trapped in the bomb with oxygen gas prior to pressurising it for the experiment. Operational pressures are usually in the range of 25 to 30 atm. The charged bomb together with the bucket and the water it contains constitute the *calorimetric system*. The water bucket can be surrounded by either a simple insulating shield of polystyrene

in the cheapest designs ('plain jacket' calorimeters), or, at the other extreme, a micro-processor-controlled thermostatic water jacket. The function of the jacket is very important, as it distinguishes between the three previously mentioned modes of operation, namely *adiabatic, isoperibol and isothermal*.[97] The isoperibol configurations are today preferred to adiabatic and isothermal designs, as they are simpler designs capable of delivering better precision as opposed to the rapidly changing jacket temperature required in an adiabatic calorimeter. Isoperibol *micro-bomb* combustion calorimeters which are capable of very high accuracy have also been recently developed.[99,100,101] These burn samples of less than 25 mg, (instead of the typical 1g sample mass burnt in ordinary, *macro-bomb* systems).

The calorimetric bomb, which can be machined from ordinary stainless steel or from halogen-resistant alloys, contains two electrodes connected by a length of metallic wire (usually Pt, NiCr alloy or Fe) which serves as the fuse. On application of an intense electrical current (generally a few amps) the wire glows and ignites a cotton thread which leads from the wire to the sample, and this in turns ignites the sample to be burnt. The sample, which is usually placed inside a high-melting, inert, metal crucible, is pressed into pellets in order to reduce the reacting surface area. This is done to avoid small deflagrations which would scatter unburnt material outside the crucible, and thus invalidating the combustion experiment.

It is common practice to add[98] a small volume of distilled water to the bomb at the outset in order to generate a more homogeneous, final thermodynamic state after the combustion has taken place. When burning, organic materials generate water which condenses on the internal walls of the bomb. This thin film of water is very effective at bringing into solution any gaseous combustion products, but the final concentrations usually vary in different parts of the bomb. Adding a small volume of water to the bottom of the bomb aids in achieving a more uniform distribution of the product solutions and also provides a saturated water-vapour atmosphere for the reaction, in some cases influencing the stoichiometry of combustion in a desirable way.

As a general rule,[98] a volume of water (in ml) equal to the number of cubic decimetres (l) of the bomb volume should be added, although in practice it is found that using a larger volume (up to 20 ml for a 350 ml bomb) yields the most desirable final states.[102] This consideration brings us to the main classification of combustion bomb calorimeters, which divides them into *rotating* and *static* instruments.

1.8.1 Rotating bomb calorimeters

When samples containing sulphur, nitrogen, phosphorus and halogens are burnt in oxygen, the corresponding oxy-acids and halogeno-acids are formed. The formation of the oxy-acids is usually regarded to be the result of 'side-reactions' which needs to be thermochemically corrected for, because of the relatively large heat of formation of these species. The formation of the halogeno-acids, on the other hand, is regarded as part of the preferred calorimetric reaction and needs to be accounted for only in terms of enthalpy of dilution. It is clear however, that it is important, whatever the nature of the acids generated in the bomb, to end up with a homogeneous state, immediately after the sample has extinguished.

In order to fulfil this requirement, Sunner and other workers,[103] in the early 1950s developed the first *rotating* bomb calorimeter, as an advancement on a *moving* bomb design (the bomb was simply agitated) developed in 1933 by Popov.[98] In the rotating bomb design, a motor-driven mechanism allows the bomb to rotate about its horizontal axis for a period of time (of the order of minutes), allowing the water film to thoroughly mix with the water added by the operator, and also to achieve the necessary final degree of homogeneity of the resulting acidic bomb solution.

Usually, a constant temperature jacket surrounds the body of water in which the bomb rotates, making these instruments isoperibolic systems. The mechanical drive and gear system are both immersed in the same body of water as the bomb and are an integral part of the calorimetric system. A small centrifugal pump ensures that good circulation is achieved throughout the volume of water. Rotating bomb calorimeters are suitable for work of the highest accuracy and

precision[77] and are consequently used only in standardising institutions or in specialised chemistry departments.

1.8.2 Static bomb calorimeters

Static bomb calorimeters are simpler instruments, and as the name implies, they are *not* designed to tumble the bomb after a combustion experiment. They are therefore more limited in scope and are most likely encountered in undergraduate, physical chemistry laboratories and in the fuel and food-testing industries. Calorimetric work on samples containing the hetero-atomic species S, N, P, Si and the halogens *can* however be accomplished with these instruments, although the accuracy and precision of the measured enthalpies of combustion is lower than what can be achieved using the rotating bomb design. In modern instruments the mercury-in-glass thermometer is often replaced by a very sensitive thermocouple (± 0.0001 K), and the water temperature, which can be sampled over very small time intervals, is typically logged by a PC interfaced to the digital thermometer unit. Cost partly justifies the use of an adiabatic, static bomb design for the work described in this thesis, provided that the losses of accuracy and precision are taken into account when directly comparing the measured enthalpy values with those given in the literature, as these are nearly always derived using a rotating bomb design. Figure 1.15[104] shows the schematic of a classic adiabatic static bomb calorimeter.

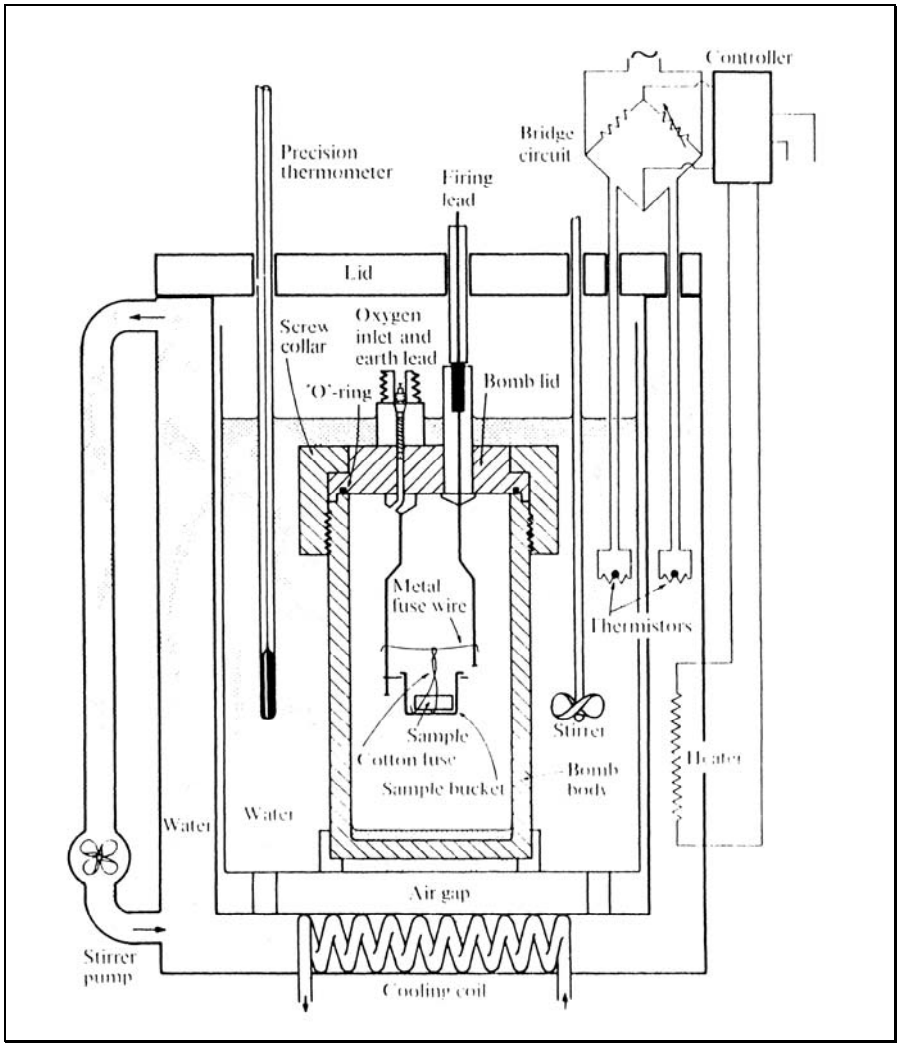

Figure 1.15 Schematic of an adiabatic bomb calorimeter (© G.P. Matthews. Extracted from *Experimental Physical Chemistry*, G.P. Matthews, Clarendon Press, Oxford, 1985).

1.8.3 The thermochemistry of bomb calorimetry

Although the thermochemistry of combustion calorimeters is extensively treated elsewhere,[66,95,98] the basic principles will be briefly set out in this chapter for the sake of completeness.

Before the 'calorific content' of any compound can be measured with a bomb calorimeter, the heat capacity of the system (also called *heat equivalent* or *water equivalent* and often denoted with the Greek letter ε) must first be determined. For calibration purposes, a thermochemical standard substance, with a known

(standard) internal energy of combustion, is normally used (this is usually referred to as the *primary calorimetric standard*). The heat transferred to the calorimeter from the combustion of the thermochemical standard can be written as (Equation 9):

$$Q_{st}=n_{st}\Delta U_c \tag{9}$$

where n_{st} is the number of moles and ΔU_c is the molar internal energy of combustion of the substance burnt. As mentioned in Section 1.8.2, the combustion is usually initiated by passing a current through a fuse wire and is then transferred to the standard substance by a strand of cotton thread. Cotton (cellulose) is chosen as it burns quantitatively to carbon dioxide and water in pressurised oxygen. The two heat contributions (to the total heat gain of the calorimeter) can be accounted for by knowing the values of the heat of combustion of cellulose ($Q_{cellulose}$) and, for the work of highest accuracy, also that of the fuse wire (Q_{fuse}) which can also burn in pressurised oxygen. If the final change in temperature of the calorimeter is ΔT, then the heat capacity of the system, C_{sys}, (Equation 10) will be:

$$C_{sys}=\frac{Q_{st}+Q_{cellulose}+(Q_{fuse})}{\Delta T} \tag{10}$$

where the *system* consists of the bomb, thermometer or thermistor probes, stirring paddle, calorimetric pail and water, in addition to the combustion products and any unreacted starting materials which can be found in the event of incomplete combustion. It is normally assumed[77,98] that the heat capacity of the system remains constant over the small temperature change observed during the typical experiment (usually $\leq$ 2K).

Once the heat capacity of the system is known, it is possible to measure the heat of combustion of the compound of interest. If the change in temperature for the combustion of n_{comp} moles of the compound burnt is ΔT_{comp} then the heat evolved is given by Equation 11:

$$Q_{sys} = C_{sys}\,\Delta T_{comp} \tag{11}$$

At this point the energy of combustion of the cotton thread and, if necessary, that of the fuse wire, are usually subtracted (Equation 12) from the total amount of

heat absorbed by the system to obtain the heat of combustion of the compound (Q_{comp}):

$$Q_{comp} = Q_{sys} - (m_{NiCr}\, Q_{NiCr})-(m_{cellulose}\, Q_{cellulose}) \quad (12)$$

and since the combustion reaction occurs at constant volume we can write Equation 13:

$$\Delta U_{comp} = \frac{Q_{comp}}{n_{comp}} \quad (13)$$

where n_{comp} is the amount of material burnt in moles or grams and ΔU_c can therefore be expressed in molar energy units ($Jmol^{-1}$) or in the more common 'massic' energy units (Jg^{-1}). The combustion enthalpy of the compound, ΔH_c, is then normally derived as explained in Section 1.4. The value of ΔH_c thus derived, however, relates to the actual temperature and pressure inside the bomb and some minor corrections should be made to convert the experimentally measured result to standard temperature and pressure. The temperature dependence of enthalpy may be assessed using Equation 14:

$$\Delta H_{T2} - \Delta H_{T1} = \Delta Cp\, \Delta T \quad (14)$$

where ΔCp is given by the heat capacities of the products minus the heat capacities of the reactants. Equation 14 assumes that the heat capacities are constant over the small temperature range of the experiment, whereas in reality they vary slightly.[66,70] This small correction may be neglected as the error is reported[98] to be less than 0.1% of the final measured enthalpy change. In calorimetric work of the highest accuracy, the often negligible effect of bomb pressure deviation from 1 bar on the final enthalpy values, is usually also accounted for by using the *Washburn corrections*[105] (Section 2.2.2.3), after the name of the first American calorimetrist who, in the 1930s, first pioneered this side of calorimetry.

1.9 OVERALL AIM OF WORK AND SPECIFIC OBJECTIVES

The ultimate, long term aim of the work described in this thesis, is to develop a method for calculating the energy released upon detonation (self-oxidation) by a series of novel, energetic polyphosphazenes and to *graphically* correlate the enthalpies of detonation with the chemical properties of each polymer. This should enable energetic polyphosphazenes with specific thermochemical properties to be identified.

However the work described here, focussed primarily on the first necessary step to achieving the long-range goal. That is the measurement of the standard enthalpy of combustion, and the derivation of the standard enthalpy of formation, of each member of the series. This was achieved by the joint application of oxygen bomb combustion calorimetry and instrumental analysis [Nuclear Magnetic Resonance (NMR) spectroscopy and Ion exchange Chromatography, (IC)] of the final, water-soluble combustion products of each polymer. The work subdivides into three main areas:

1. To successfully synthesise and characterise, following established procedures,[19] a series of energetic polyphosphazenes, in the quantities sufficient for the accurate calorimetric investigations.
2. To elucidate, as far as possible, the nature and the stoichiometry of formation of the products of complete combustion in excess oxygen of the polymers, which is necessary for the derivation of the enthalpies of formation. Whilst the detonation and combustion products arising from propellants and explosives based upon C, H, N and O is well established, in fact very little is currently known[86,106] about the nature of the products arising from energetic systems that contain other elements, such as fluorine and phosphorus.
3. To experimentally measure the enthalpies of combustion and hence derive the enthalpies of formation of each member of the polymer series.

2 RESULTS AND DISCUSSION

2.1 SYNTHESIS AND CHARACTERISATION OF THE ENERGETIC POLYMERS 1-5

2.1.1 Synthesis of Polymers 2, 3 and 5

The energetic polyphosphazenes 2, 3 and 5 were the first polymers originally synthesised by *AWE Aldermaston* as potential, novel energetic binders.[19] At the outset of the work herein described, calorimetric characterisation was sought exclusively for those materials. Later into the project however, following their successful synthesis by the author, Polymers 1 and 4 were also added to the existing series, in order to extend the calorimetric investigation to a 'more complete' range of homologous polyphosphazenes. As a result, Polymers 2, 3 and 5 were also the first polyphosphazenes to be synthesised and characterised in this work.

The precursors to Polymers 2, 3 and 5 were synthesised following the AWE general procedure[19] (Sections 4.2.2.1 and 4.2.2.2), i.e. by reacting linear poly[bis(2,2,2-trifluoroethoxy)phosphazene], (synthesised as described in Sections 4.2.1.1 and 4.2.1.2), with a 5-fold excess of the sodium salts of the required protected triols, according to the general scheme shown in Figure 1.6 (Section 1.2.1). The excess nucleophile ensured that a high degree of 2,2,2-trifluoroethoxy group replacement would be achieved within the 24 h reaction period. The isolation and purification of the non-energetic alkoxylated precursors from the reaction mixture is described in the next section (Section 2.1.1.1).

After purification, the non-energetic precursors were nitrated with a large excess (~200-fold molar) of cold 95% nitric acid (as described in Section 4.2.2.3). This treatment served to nitrolyse the protecting ketal groups of the alkoxy substituents of the precursor, generating the corresponding di-nitrate ester moieties (Figure 2.1). The excess of acid also acts as a solvent for the nitrated products and as a heat sink to absorb the heat of reaction.

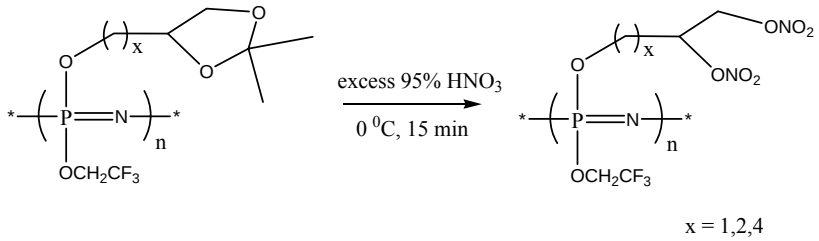

Figure 2.1 Nitrolysis of the ketal protecting groups of Polymers 2, 3 and 5 in HNO_3.

In the original procedure the reaction mixtures were quenched in cold distilled water after 15 min. The resulting suspension was then left standing overnight to allow the polymers to settle at the bottom of the beaker. An alternative to this lengthy procedure was later devised, whereby the suspensions were mechanically stirred for approximately 1 hour. During this time the particles of polymer quickly coalesced onto the walls of the beaker and onto the stirrer, leaving a clear supernatant liquid which could be decanted with minimal loss of product. The wet, water-swollen polymers were then rinsed and dried as described in Section 4.2.2.3. The three dry polymers were isolated as yellow-brown, highly viscous, sticky liquids. The purity, molecular weight and polydispersity of the materials matched those of the corresponding polymers synthesised by AWE (as assessed by ^{1}H and ^{19}F NMR spectroscopy and Gel Permeation Chromatography).

A total of *three* batches of Polymer 2 and *two* batches of both Polymers 3 and 5 were prepared. Table 2.1 shows the estimated *energetic substituent percentage* (ES%) of each batch, as judged by ^{1}H NMR spectroscopy.

Polymer	Batch No.	Yield (g)	Yield %	ES%
2	1	0.81	70	65
	2	5.30	67	70
	3	3.63	68	78
3	1	0.53	62	59
	2	3.09	76	61
5	1	0.40	51	50
	2	3.28	72	51

Table 2.1 Yield and estimated ES% for the different batches of Polymers 2, 3 and 5 synthesised in this work.

2.1.1.1 Isolation and purification of the non-energetic precursors

During the initial synthetic work on Polymers 2, 3 and 5, a new, simplified, high recovery technique for the isolation and purification of the non-energetic alkoxylated precursors from the excess sodium alkoxide was found. The need to develop an alternative purification method stemmed from the low recoveries (30-50%) that were typically achieved with the multi-step purification method routinely used by AWE prior to this work. In the original procedure, the impure precursors, normally obtained as a dark wax after evaporation of the THF from the substitution reaction mixture, were repeatedly dissolved in acetone (in which the excess alkoxide is insoluble) which was then filtered. The polymers were then re-precipitated into cold *n*-hexane until an acceptable purity (as assessed by ^{1}H NMR spectroscopy) was achieved. Typically five or six washings were required.

In the new approach, the viscous, dark-brown product was dissolved directly in a large volume of water (Section 4.2.2.2). In theory, the high molecular weight alkoxylated precursors should not be soluble in water but in practice, at this stage, it was found that the impure products dissolved completely after approximately 2 h with vigorous stirring. Later tests revealed that the time to achieve complete dissolution could be halved by warming the initial suspensions (up to 40ºC). The

resultant aqueous solutions were, as expected, strongly alkaline (pH=13-14), due to the presence, in the waxy residue, of unreacted sodium alkoxide.

To re-precipitate the polymers, the aqueous solutions were acidified to pH 2, by addition of aqueous HCl and the polymer extracted into chloroform. After being washed repeatedly with water in order to eliminate the last traces of acid and free alcohol, the organic phase was evaporated to yield the pure product as a brown viscous liquid. The purity of the materials, as assessed by ^{1}H and ^{19}F NMR spectroscopy, was found to be comparable or even superior to that of samples purified using the original acetone/n-hexane procedure. In addition, Gel Permeation Chromatographic (GPC) analysis carried out at AWE on samples purified by the 'acid-treatment' showed no evidence of chain degradation.

No references were found in the literature that would explain the observed solubility of the precursor polyphosphazenes in aqueous alkali and their subsequent acidic re-precipitation. Since prolonged treatment of the impure waxy products with aqueous NaOH (at the same concentration that would ensue when the excess alkoxide reacts with the water) did not dissolve them, it is proposed that the excess sodium alkoxide may reversibly attack the phosphorus sites of the polymer generating the water-soluble ionic species XV, according to the scheme shown in Figure 2.2 (simplified structures shown). Upon acidification of the solution, the formal double P=N bond would then be regenerated, via expulsion of 2,2,2-trifluoroethoxide, to yield the water-insoluble, non-energetic, precursor XVI. Since previous studies[34,107] on the basicity of the skeletal nitrogen of a range of substituted polyphosphazenes have shown that protonation of the backbone nitrogen upon addition of aqueous mineral acids occurs only when the substituents on phoshorus are alkyl groups, the possible formation of a water-insoluble polymeric hydrochloride[34] was ruled out. No further work was done to further investigate this matter.

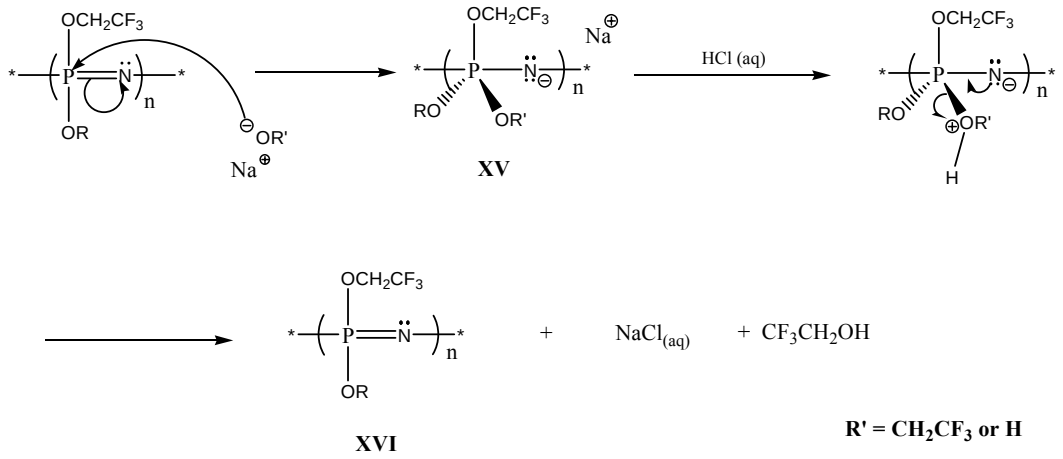

Figure 2.2 Proposed scheme for the formation of the water-soluble ionic polymer XV and its subsequent aqueous hydrolysis to yield the water-insoluble polyphosphazene XVI.

2.1.1.2 Synthesis of Polymer 3: formation of isomeric impurities during the protection of butane-1,2,4-triol

The protection of butane-1,2,4-triol with acetone, as a preliminary step in the synthesis of the first batch of the non-energetic precursor to Polymer 3 {random linear poly[P-2-(2',2'-dimethyl-1',3'-dioxolan-4'-yl)ethoxy/P-2,2,2-trifluoroethoxyphospazene]}, gave a product which appeared to be contaminated from its ^{13}C NMR spectrum. The contaminant was not the starting triol (Section 4.2.6.1). It was thought that an isomeric condensation product could have formed. When butane-1,2,4-triol is reacted with excess acetone, the isomeric acetonide XVIII (Figure 2.3) is known[108,109] to form in appreciable amounts (highest reported[108] quantity: 23 mol % with respect to XVII, the main, desired, product of reaction). The formation of a further possible cyclic isomer, XIX, which could form by ketalization of the hydroxyl groups at positions 1 and 4 of butane-1,2,4-triol, has not however been reported in the literature, possibly because the formation of the seven-membered ring structure is thermodynamically unfavourable.

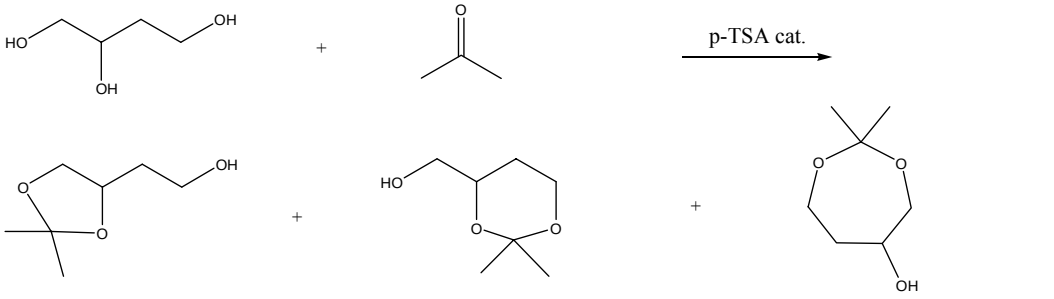

XVII 4-(2'-hydroxyethyl)2,2-dimethyl-1,3-dioxolan

XVIII 2,2-dimethyl-4-hydroxymethyl-1,3-dioxan

XIX 2,2-dimethyl-5-hydroxy-1,3-dioxepan

Figure 2.3 Acetonation of butane-1,2,4-triol: the three possible isomeric products of reaction.

The ^{13}C NMR shifts of the detected impurity could only be grossly compared to those given in the literature[110] for ketal XVIII, as the authors recorded their ^{13}C NMR spectra in the neat liquid (acetone-d_6 was used in this work). The experimental figures, however, were found to be in excellent agreement with those published, as shown in Figure 2.4.

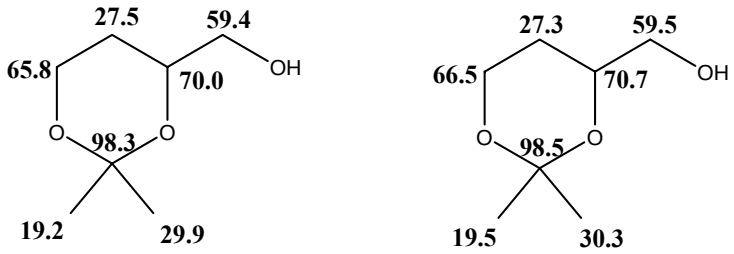

Figure 2.4 ^{13}C chemical shifts (ppm) referenced to TMS of 2,2-dimethyl-4-hydroxymethyl-1,3-dioxan as reported[110](left), and as found in this work (right).

The alkoxide salt of the isomeric acetonide XVIII (Figure 2.3) would ultimately have the same formula weight as the main alkoxylating precursor *sodium 2-(2',2'-dimethyl-1',3'-dioxolan-4'-yl)ethoxide* and hence would not cause any difference in formula weight to the unit monomer of Polymer 3. However there is no guarantee that the former alcohol displays identical nucleophilicity upon the macromolecular substitution of linear poly[bis(2,2,2-trifluoroethoxy)

phosphazene]. The purity of the protected alcohol (XVII) was not measured and the product was used as such to prepare Polymer 3.

2.1.2 Synthesis of Polymer 1

Polymer 1, (random linear poly[P-2-nitratoethoxy/P-2,2,2-trifluoroethoxy phosphazene]) XXI in Figure 2.5, was synthesised by reacting sodium 2-t-butoxyethanol (XX) with linear poly[bis(2,2,2-trifluoroethoxy)phosphazene] and by subsequently nitrating the polymeric product with excess, cold nitric acid (Section 2.1.1.1), according to the general scheme shown in Figure 2.5. The t-butoxy moiety acts as a protecting group for the β-hydroxyl group in the alkoxide and is cleaved off upon nitration[111,112] in excess HNO_3 to yield the corresponding nitrate ester; the nitrolysis is presumably facilitated by the inherent stability of the tertiary carbocation which is formed as an intermediate.

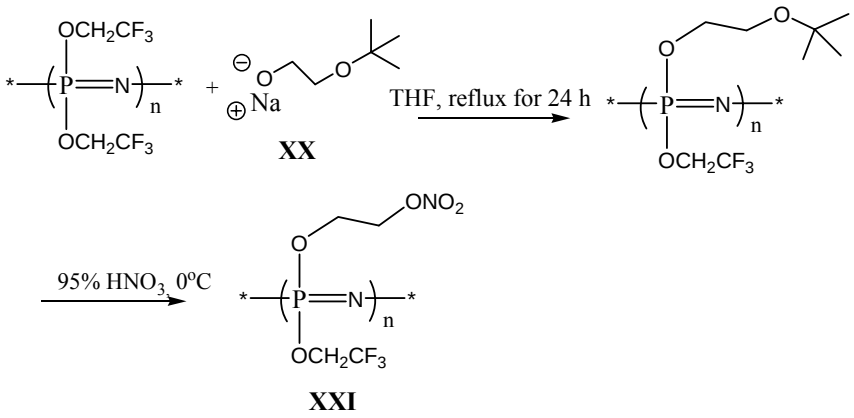

Figure 2.5 General scheme for the alkoxilation of linear poly[bis(2,2,2-trifluoroethoxy)phosphazene] with sodium 2-t-butoxyethoxide (XX) to yield Polymer 2 (XXI, simplified structure).

Diethyl ether was found to be an effective solvent for the extraction of the non-polymeric by-products which were detected by ^{1}H NMR spectroscopy in the nitrated polymer (Section 4.2.3.2). From the chemical shifts of these contaminants, they appeared to contain t-butyl moieties in slightly different chemical environments. In an attempt to identify at least one contaminant, the proton chemical shifts observed were compared with the literature[113] values for

2-methyl-2-nitratopropane recorded in the same deuterated solvent. The figure reported was close but not exactly coincident with any of the shifts observed in the spectrum of the extract. The mixture was thought to be composed mainly of the nitrated derivatives of t-butyl alcohol and possibly of 2-t-butoxyethanol, but no further work was undertaken to positively identify these species. Only one batch (yield 4.64g, 79%) of Polymer 1 was synthesised. The material had an estimated ES% of 76.

2.1.2.1 Synthesis of fully substituted Polymer 1

Samples of fully substituted (ES% =100) Polymer 2 were subsequently prepared[53] by AWE, by reacting poly(dichlorophosphazene) with an excess of sodium 2-(tetrahydro-2-pyran-2-yloxy)ethoxide and by subsequent nitrolysis (excess 95% nitric acid) of the tetrahydropyranyl protecting groups, according to the scheme shown in Figure 2.6.

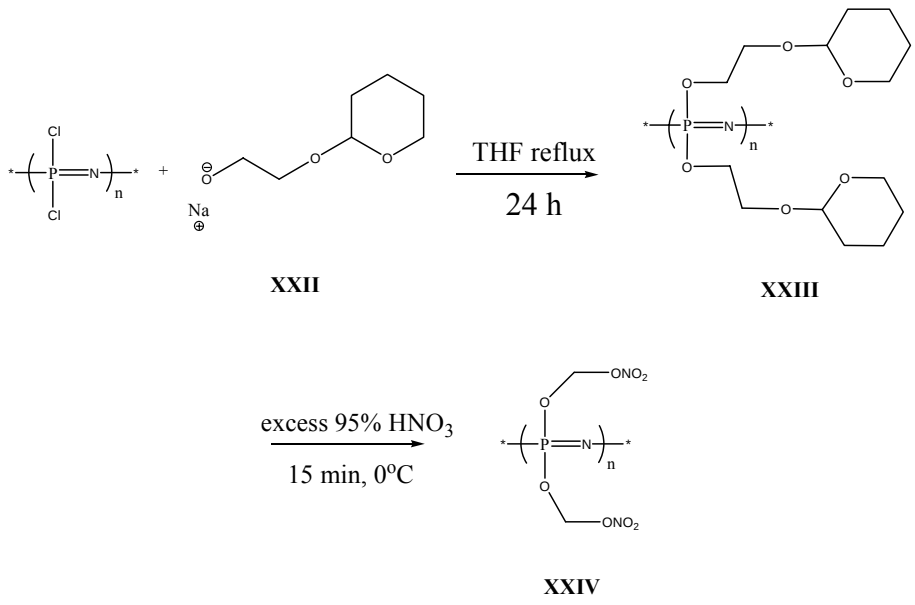

Figure 2.6 Reaction of poly(dichlorophosphazene) with sodium 2-(tetrahydro-2-pyran-2-yloxy)ethoxide (XXII) to yield poly[bis(P-tetrahydro pyranyl-2-oxyethoxy)phosphazene] and its subsequent nitration to give fully substituted Polymer 2, poly[bis(2-nitratoethoxy)phosphazene] (XXIV).

2.1.3 Synthesis of Polymer 4

Since Polymer 1 had been synthesised, it became desirable to attempt the synthesis of Polymer 4 (random linear poly[P-4,5-dinitratopent-1-oxy/P-2,2,2-trifluoroethoxyphosphazene]) in order to 'complete' the series of energetic polyphosphazenes, from Polymer 1 to Polymer 5.

Pentane-1,2,5-triol, which is required for the preparation of Polymer 4, was not commercially available from the common laboratory chemicals suppliers and alternative vendors only sold this product in bulk quantities. It was therefore decided to synthesise the triol in our laboratory using a literature procedure. From the three different routes for the preparation of pentane-1,2,5-triol that were found in the literature, the one chosen[114] is based on the zinc-catalysed *ring-opening acetylation* of tetrahydrofurfuryl alcohol in excess acetic anhydride. This yields 1,2,5-triacetoxypentane (Section 4.2.7.1). The latter is then hydrolysed (O-deacylation) to pentane-1,2,5-triol in aqueous acidic medium according to the mechanism shown in Figure 2.9, (Section 4.2.7.4). The reported[114] overall yields for this reaction are good, i.e. 63-71%. Alternative methods for the laboratory preparation of pentane-1,2,5-triol use more expensive starting materials and typically yield the product in lower yields. One alternative procedure[115] for example, that can be employed for the preparation of enantiomerically pure pentane-1,2,5-triol, involves diazotization and subsequent reduction of glutamic acid, according to Figure 2.7.

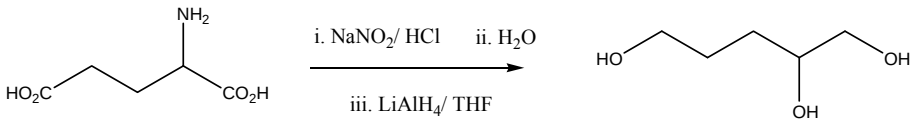

Figure 2.7 General scheme for the laboratory preparation of enantiomerically-pure pentane-1,2,5-triol starting from glutamic acid.

Another stereoselective approach[116] adopts the reductive ring-opening of butyrolactone-4-carboxylic acid (5-oxotetrahydrofuranyl-2-carboxylic acid), as shown in Figure 2.8.

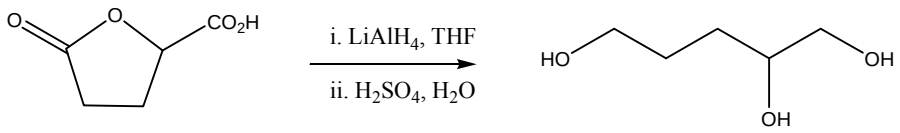

Figure 2.8 General scheme for the laboratory preparation of enantiomerically-pure pentane-1,2,5-triol starting from butyrolactone-4-carboxylic acid.

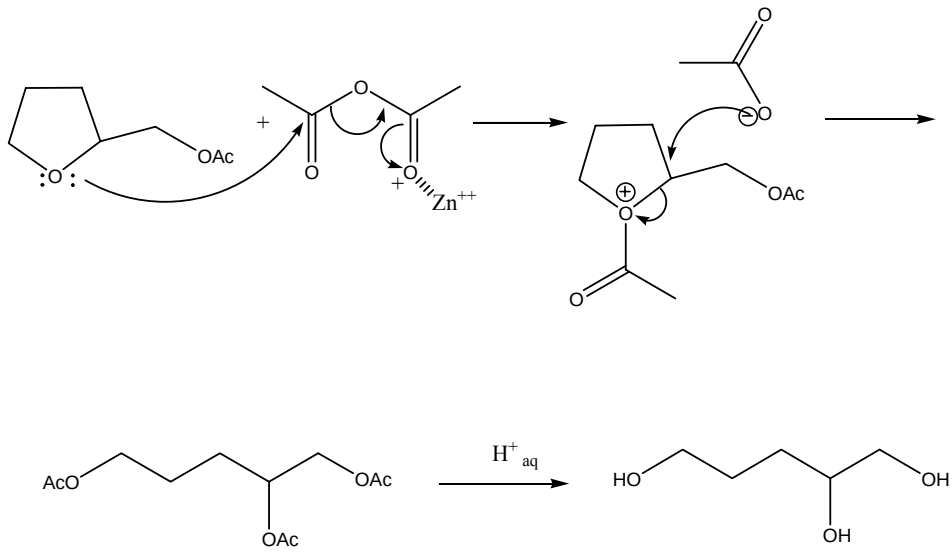

Figure 2.9 Proposed mechanism for the reaction of tetrahydrofurfuryl alcohol with acetic anhydride to give 1,2,5-triacetoxypentane, which is subsequently hydrolysed in aqueous acid medium to give pentane-1,2,5-triol.

During the preparation of 1,2,5-triacetoxypentane, the product distilled very slowly and the distillation had to be interrupted after 9 h at the end of the working day, well before all of the product had distilled. The tediously slow rate of distillation suggested that the product was forming 'during' the distillation, the process being possibly driven forward by the removal of product from the reaction mixture. The dark, syrupy residue was retained for later distillation of the remaining product. An impurity observed in both the ^{1}H and ^{13}C NMR spectra of the product was at first believed to be tetrahydrofurfuryl acetate, and in order to verify this, a small amount of authentic material (as judged by ^{1}H and ^{13}C NMR

spectroscopy) was prepared (Section 4.2.7.3), but the chemical shifts did not match those of the impurity. A sample of pentane-1,2,5-triol prepared from acid-hydrolysis of this material was also found to contain traces of an unidentified impurity. These were at first believed to be the mono- and/or di-acetoxy by-products. GC-MS (EI, 70eV) of both the triacetoxypentane and the trihydroxypentane however failed to unambiguously identify the impurity(ies). According to the instrumental library of mass spectra, the trace compounds corresponded to structures which could not have been responsible for the observed $^{1}H/^{13}C$ NMR peaks. One trace impurity that was detected in the triacetoxypentane sample, but with a low matching score, was tetrahydrofurfuryl acetate. However, no signals for this compound were visible in the ^{1}H and ^{13}C NMR spectra of the sample.

Interestingly, when the low pressure distillation of the residual triacetoxypentane from the syrupy liquor was resumed six months later (Section 4.2.7.2), the rate of product distillation was found to be dramatically improved and the resulting distillate was free from impurities, as judged from both the ^{1}H and ^{13}C NMR spectra. Acid hydrolysis of this product also yielded a sample of pentane-1,2,5-triol of much higher purity than before (Section 4.2.7.5). The improved purity was thought to arise as a consequence of the long time that had elapsed. Presumably, the remainder of the ring-opened by-products which may have distilled azeotropically with the desired product during the first attempted distillation, would have had time to react, in the presence of residual acid, to yield 1,2,5-triacetoxypentane. In view of this observation, a revision of the ring-opening reaction conditions (i.e. temperature and reaction time) may be necessary for future scale-up. The pure sample of pentane-1,2,5-triol was used to synthesise Polymer 4. Only one batch (yield 2.30 g, 56%) of this polymer was synthesised. The material had an estimated ES% of 67.

The ‘doubled appearance’ of one of the ^{1}H NMR signals (assigned to C-5 C*H*H) of the non-energetic precursor to Polymer 4 (Section 4.2.7.7) suggested the presence of some degree of isomerism of the C5 alkoxy chains of the polymer. In order to establish whether the conjugate base of 4-(3’-hydroxypropyl)-2,2-dimethyl-1,3-dioxolan would undergo isomerisation upon alkoxide generation

using sodium hydride in THF, a sample of protected alcohol was reacted with NaH (1 equivalent) in THF for 3 h, after which time the starting material was recovered by work-up with glacial acetic acid and rotary-evaporation of the solvent. The ^{1}H and ^{13}C NMR spectra of the recovered material however revealed no structural changes, suggesting that no rearrangement would occur in the presence of strong base. Since no ^{13}C nor ^{1}H-^{1}H correlation NMR spectra of the precursor polymer were recorded, the cause for the 'double' ^{1}H NMR peak remained unclear. No double peaks were observed in the ^{1}H NMR spectrum of the nitrated product (Polymer 4).

2.1.4 Synthesis of less-substituted and fully substituted Polymers 2, 3 and 5

It was mentioned in Section 1.2.1 that the reaction of linear poly[bis(2,2,2-trifluoroethoxy)phosphazene] with alkoxides leads to *partial* substitution of the 2,2,2-trifluoroethoxy groups (typically in the 50-70 molar % range, depending on nucleophile size) even when a large excess of nucleophile is employed in the reaction.[19,50] In this work, only one sample of a 'less-substituted' Polymer 2 was prepared by nitrating a further product of reaction of (2',2'-dimethyl-1',3'-dioxolan-4'-yl)methoxide and linear poly[bis(2,2,2-trifluoroethoxy) phosphazene]. These were reacted in a 1:1 molar ratio instead of the usual 5:1 molar ratio, and for a reaction time of 6 h instead of 24 h (Section 4.2.5.1). Even under these conditions, the degree of 2,2,2-trifluoroethoxy group displacement was still relatively high, i.e. 31%. Lower degrees of 2,2,2-trifluoroethoxy group replacement were later obtained for Polymers 2, 3 and 5 by workers at AWE however, using the corresponding *lithium* alkoxides instead of the sodium analogues, according to the reaction conditions listed in Table 2.2.

Polymer	% Energetic precursor side-groups (ES%)	Alkoxide:Polymer Molar ratio	Li / Na salt	Reaction time (in refluxing THF) h
2	**16**	2:1	Li	18
	36	1:1	Na	1.25
	46	1:1	Na	3.75
	62	2.2:1	Na	18
	72	2.2:1	Na	23
3	**6**	0.5:1	Li	18
	17	1:1	Li	18
	22	3:1	Li	18
	28	5:1	Li	18
	52	2.2:1	Na	18
	68	5:1	Na	18
5	**9**	0.5:1	Li	18
	24	1:1	Li	18
	41	5:1	Li	18
	51	3:1	Na	06
	77	5:1	Na	18

Table 2.2 Replacement of 2,2,2-trifluoroethoxy group in Polymers 2, 3 and 5 achieved by AWE using different reaction conditions; (courtesy of the Polymer Synthesis Group, AWE Aldermaston).

Samples of *fully*-substituted Polymers 2, 3 and 5 (i.e. ES% =100) were also prepared by AWE, by reaction of linear poly(dichloro)phosphazene [obtained by the living cationic polymerisation of tris(chloro)-N-(trimethylsilyl)-phosphoranimine[117]] with an excess of the required sodium alkoxides.[53]

2.1.5 Investigation of alternative nitration methods

Although the use of 95% HNO_3 yields nitrated polyphosphazenes of high purity (as judged by ^1H NMR spectroscopy), the development of an alternative method for the nitration of the non-energetic precursors to Polymers 1-5 will eventually become indispensable for the future scaled-up manufacture of these binders. Whilst on a small laboratory scale (i.e. ≤5 g) it is relatively safe to nitrate the precursors by direct addition of cold, 95% nitric acid, it would be unpractical to scale-up this procedure as it may lead to an uncontrollable exotherm. Ideally, the nitrating agent should be added slowly to a solution of the precursor dissolved in an inert solvent. In order to investigate alternatives to 95% nitric acid, the nitration of the precursor to Polymer 2 was attempted using a series of 'solvent-based' nitration conditions viz. HNO_3/chloroform (Section 4.2.9.1) and N_2O_5/dichloromethane (Section 3.2.9.2).

2.1.5.1 Two-phase nitration using $HNO_3/CHCl_3$

Although the ^1H NMR spectrum of the product showed no major differences in signal patterns and integral ratios from that of a sample of material that had been nitrated using cold 95% HNO_3 alone, a weak, broad envelope was observed at about 4 ppm. As this displayed the typical broadness of polymeric protons, it was suggested that it may arise from products of cross-linking between single polyphosphazene chains, the structures of which are suggested in Figure 2.10.

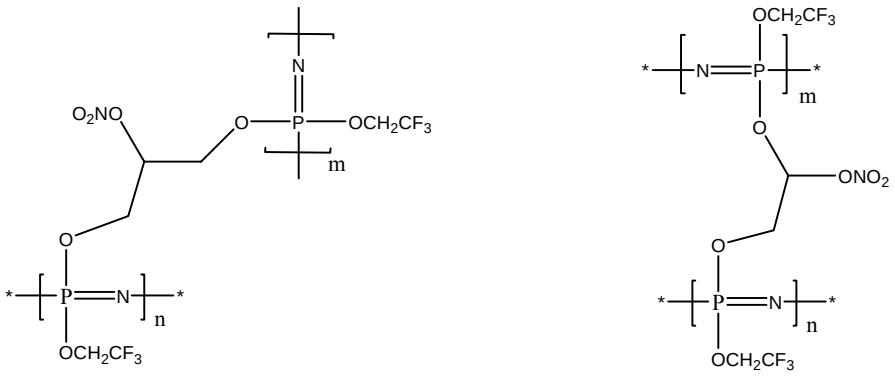

Figure 2.10 Proposed structures of possible cross-linked polymers.

2.1.5.2 Nitration using N_2O_5 /CH_2Cl_2

The nitration of the precursor to Polymer 2 was also attempted using N_2O_5 in dichloromethane. A total of four modification of the same general method, by which different amounts of N_2O_5 were added to the polymer dissolved in CH_2Cl_2, were investigated. The results suggested that a combination of a large excess of N_2O_5 (~10 equivalents) coupled with the minimum amount of solvent could yield the desired energetic product with an acceptable purity but more research would be needed to optimise the reaction conditions. Nevertheless neither of the alternative nitrating methods investigated yielded products of comparable quality to those obtained using 95% nitric acid alone.

2.1.6 Evaluation of side group ratios and estimation of monomer unit empirical formula

In order to establish the ratio of trifluoroethoxy to alkoxy substituent groups, which varies for Polymers 1-5 and which is required for calculating the correct average molecular weight of the unit monomers, five modelling equations were derived for the non-energetic polymeric precursors of Polymers 1-5, in which the unit fraction of alkoxy groups was expressed as a function of the relative integral of low to high field signals in the respective ^{1}H NMR spectra, low field signals arising from H on carbon adjacent to O and high field signals arising from H on carbon not adjacent to O. Since the broadened low field signals arising from the methylene protons of the alkoxy groups was not sufficiently resolved from the signal of the methylene unit of the 2,2,2-trifluoroethoxy group (apart from the case of the precursor to Polymer 1), the entire low field envelope was, out of necessity, considered as a whole unit, when calculating the ratio to the integral of the high field signals. The equations were developed by assigning the unit fraction $\boldsymbol{x}$ ($0<\boldsymbol{x}<1$) to the alkoxy substituents and the difference ($1-\boldsymbol{x}$) to the 2,2,2-trifluoroethoxy groups. The value of ES% is given by $100\boldsymbol{x}$. The ratio of the low- to high-field signal integrals is given by $\boldsymbol{y}$. Since the number of protons present in the two different groups is known, Equations 15-18 can be easily derived. In order to improve the resolution of the methylene and methine protons low field signals, the deuteriated solvents CD_3COOD, C_6D_6, CD_3CN, $(CD_3)_2SO$

and $CDCl_3$ were explored as potential NMR solvents for the precursors. None of these, however, yielded better resolution than acetone-d_6, which was used as the solvent of choice.

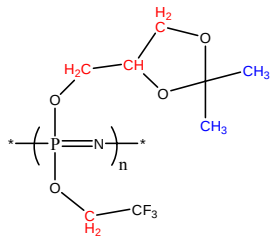

Precursor to Polymer 2

$$y = \frac{[5x + 2(1-x)]}{6x}$$

Solving for x: $$x = \frac{2}{6y - 3}$$ (15) †

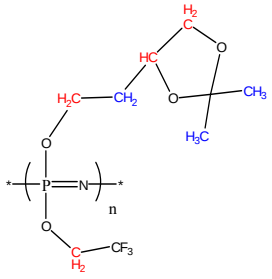

Precursor to Polymer 3

$$y = \frac{[5x + 2(1-x)]}{8x}$$

Solving for x: $$x = \frac{2}{8y - 3}$$ (16) †

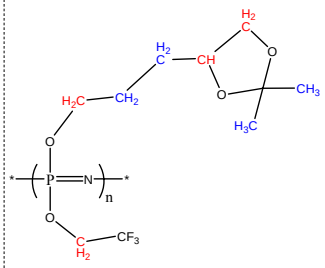

Precursor to Polymer 4

$$y = \frac{[5x + 2(1-x)]}{10x}$$

Solving for x: $$x = \frac{2}{10y - 3}$$ (17) †

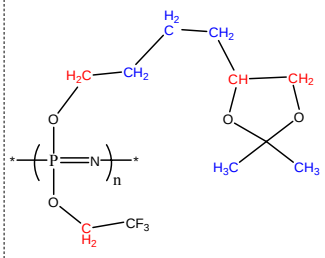

Precursor to Polymer 5

$$y = \frac{[5x + 2(1-x)]}{12x}$$

Solving for x: $$x = \frac{2}{12y - 3}$$ (18) †

† Where x is the unit fraction of non-fluorinated alkoxy substituent and y is the ratio of the integrals of low-field to high-field NMR proton signals (as colour-coded in the formulas above).

In the simplified monomer structures shown above, the red protons (attached to C adjacent to O) gave low-field signals, whereas the blue protons (attached to C *not* adjacent to O), gave high-field signals.

By contrast, the equation developed for the precursor to Polymer 1 (Equation 19) was derived using a different set of protons (as indicated by the colours of the protons in the simplified structure below) since the ^{1}H NMR signals of this material, albeit broadened, were all sufficiently resolved to avoid using the t-butyl proton signal, which appeared to be partially overlapped by a signal due to an impurity, possibly 2-t-butoxyethanol (Figure 2.11). The use of the t-butyl signal gave a low figure (69%) for the ES% value instead of the more accurate value (76%).

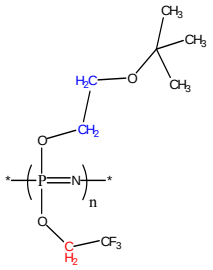

Precursor to Polymer 1

$$y = \frac{2(1-x)}{4x}$$

Solving for x:

$$x = \frac{2}{4y+2} \qquad (19)$$

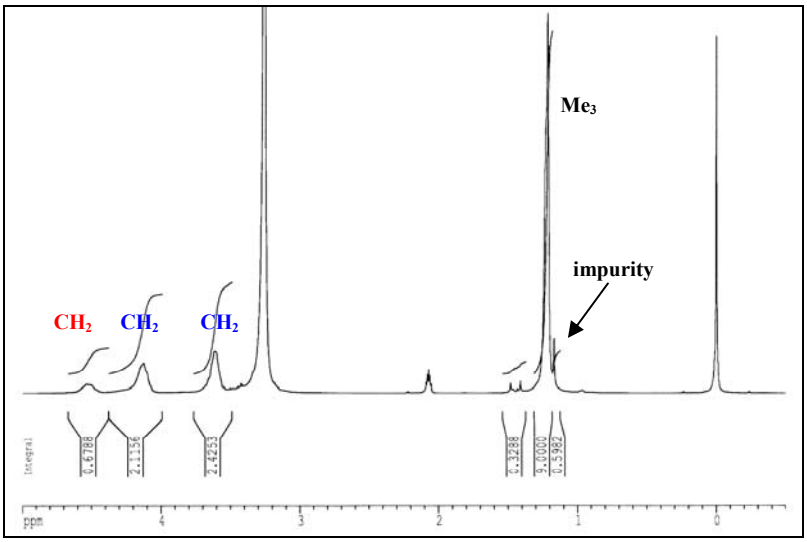

Figure 2.11 ^{1}H NMR spectrum (acetone-d_6 + H_2O) of the non-energetic precursor to Polymer 1, linear poly[P-2-t-butoxyethoxy-P-2,2,2-trifluoro-ethoxyphosphazene].

A set of analogous equations were also developed for the nitrated products (Polymers 1-5) and these were used to 'double-check' the values of percentage of alkoxy substituent obtained from the ^{1}H NMR spectra of the respective purified

precursors. The two values correlated well (within 1%) for all polymers with the exception of Polymer 5. The high-field signals of the precursor to Polymer 5 appeared to be overlapped by the signal due to residual 4-(3'-hydroxypropyl)-2,2-dimethyl-1,3-dioxolan. Application of Equation 17 to this spectrum yielded a suspiciously high degree of side-chain substitution (80%). As a consequence, the ES% was estimated from the ^{1}H NMR spectra (acetone-d_6 and DMSO-d_6) of the much cleaner nitrated material (67%).

From the ES% figures (which were rounded to the nearest integer to account for accuracy of the NMR integration, recently measured to be around 1%[118]), the molecular weights of the average monomer units of all batches of Polymers 1-5 were thus derived, using the IUPAC 1995 recommended atomic weights.[119]

Table 2.3 shows a comparison of the values of elemental wt% of Polymers 1-5 as calculated from the ^{1}H NMR spectroscopy data against those directly measured by elemental analysis. The experimental C and H wt% values agreed reasonably well with those calculated from the ^{1}H NMR data, although for the N wt% values, the agreement was less satisfactory. Fluorine elemental analysis was carried out only on Polymer 3. The latter also yielded a value which was in very poor agreement with the expected value. Since fears of a possible interference by phosphorus upon combustion of the PF-containing samples in the fluorine mass analyser were assuaged by Butterworth Laboratories, the cause for the observed disparities remained unknown.

Energetic Polymer (ES% by ^{1}H NMR)	C wt% (EA)	C wt% (^{1}H NMR)	H wt% (EA)	H wt% (^{1}H NMR)	N wt% (EA)	N wt% (^{1}H NMR)	F wt% (EA)	F wt% (^{1}H NMR)
1 (76)	18.86	18.93	2.60	2.80	13.24	13.91	-	13.91
2 (70)	18.41	18.12	2.37	2.30	13.62	14.80	-	9.55
3 (61)	21.97	21.46	2.90	2.83	13.56	13.34	7.45	12.47
4 (67)	25.3	24.7	3.55	3.50	12.60	13.20	-	9.63
5 (51)	27.71	26.23	3.85	3.59	12.25	11.50	-	15.18

Table 2.3 Comparison of CHN wt% values of selected batches of Polymers 1-5 as directly measured by elemental analysis (EA) and as calculated using ^{1}H NMR spectroscopic data.

Energetic Polymer	Energetic substituent (% by ^{1}H NMR)	Energetic substituent (average % by CHN elemental analysis)	Unit empirical formula (calculated from ^{1}H NMR estimated ES%)
1	**76**	**74**	$C_{4.00}H_{7.04}N_{2.52}O_{6.56}F_{1.44}P_{1.00}$
2	**31**	**-**	$C_{4.62}H_{5.86}N_{2.24}O_{5.72}F_{4.14}P_{1.00}$
	65	**-**	$C_{5.30}H_{7.90}N_{3.60}O_{9.80}F_{2.10}P_{1.00}$
	70	**69**	$C_{5.40}H_{8.20}N_{3.80}O_{10.40}F_{1.80}P_{1.00}$
	78	**-**	$C_{5.56}H_{8.68}N_{4.12}O_{11.37}F_{1.32}P_{1.00}$
3	**59**	**-**	$C_{6.36}H_{9.90}N_{3.36}O_{9.08}F_{2.46}P_{1.00}$
	61	**62**	$C_{6.44}H_{10.10}N_{3.44}O_{9.32}F_{2.34}P_{1.00}$
4	**67**	**67**	$C_{8.02}H_{13.38}N_{3.68}O_{10.04}F_{1.98}P_{1.00}$
5	**50**	**-**	$C_{8.00}H_{13.00}N_{3.00}O_{8.00}F_{3.00}P_{1.00}$
	51	**54**	$C_{8.08}H_{13.18}N_{3.04}O_{8.12}F_{2.94}P_{1.00}$
	68[a]	-	$C_{9.44}H_{16.24}N_{3.72}O_{10.16}F_{1.92}P_{1.00}$

[a] Synthesised by the Polymer Synthesis Group, AWE Aldermaston.

Table 2.4 Percent energetic substituent of Polymers 1-5 as estimated by ^{1}H NMR spectroscopy and CHN elemental analysis (selected batches only).

2.1.7 Polymer oxygen balance

The *oxygen balance* (often referred to as Ω or *OB*) is defined[8,95] as the weight percentage of oxygen required to achieve the stoichiometric, exhaustive oxidation of all of the atomic species present in a compound or mixture of compounds (energetic or non-energetic alike). By convention, any carbon is oxidised to CO_2 and any hydrogen to water. If the molecule also contains nitrogen, gaseous N_2 is formed. If the halogens are present, these react to form the corresponding hydracids consuming hydrogen. The remaining hydrogen then converts to water. If other hetero-atoms are present in the molecule, these are oxidised to the highest valence oxide attainable for that element upon stoichiometric combustion[95] (i.e. $P \rightarrow P_2O_5$,[95] $S \rightarrow SO_3$,[95] $Eu \rightarrow Eu_2O_3$[120]). Thus, if the molecular oxygen content is sufficient to stoichiometrically oxidise the other atomic species present in the molecule to the highest attainable oxidation state, the oxygen balance of the compound is *zero* and the material is said to be (fully) *oxygen balanced* (i.e. ethylene glycol dinitrate, $\Omega = 0$). Consequently, a negative oxygen balance will be typical of oxygen-deficient compounds (i.e. most secondary explosives) and a positive oxygen-balance of oxygen-rich compounds or mixtures (i.e. nitroglycerine and all pyrotechnic compositions).

For high polymers ('ordinary' polymers and energetic systems alike), the same rules are valid if applied to the monomer unit empirical formula.[121,122] In the author's view however, this is a simplification, as the chain terminating groups of most organic and inorganic polymers have a different formula to that of the inner monomers. As a consequence, this should not be neglected for oligomers for which a large error in the calculation of Ω would arise.

The ideal, exhaustive combustion reaction of Polymers 1-5 may be conveniently described by a general stoichiometric equation (Equation 20):

$$C_aH_bN_cO_dP_eF_{g\ (l)} + \left[a + \frac{(b-g)}{4} + \frac{5e}{4}\right]O_{2\ (g)} \rightarrow aCO_{2(g)} + \frac{(b-g)}{2}H_2O_{(l)} + \frac{c}{2}N_{2(g)} + \frac{e}{2}P_2O_{5(s)} + gHF_{(g)} \qquad (20)$$

If the empirical formulas of the unit monomers are known, then the oxygen balance of the polymers may be conveniently calculated by application of Equation 21.

$$\Omega = \frac{\frac{d}{2} - \left[a + \frac{b-g+5e}{4}\right]}{MW\left(C_aH_bN_cO_dP_eF_g\right)} \times 3200 \qquad (21)$$

The calculated values of Ω for Polymers 1-5 are presented in Table 2.5, alongside those of the carbon-based energetic polymers polyNIMMO, polyGLYN and GAP. Although all of the five polyphosphazenes are oxygen-deficient, with Polymer 2 exhibiting the least negative oxygen balance, all the polymers are less oxygen-deficient than the latter carbon-based systems.

Energetic Polymer	Energetic substituent (% by ^{1}H NMR)	Unit empirical formula (calculated from ^{1}H NMR estimated ES%)	Ω (to CO_2, H_2O, P_2O_5 and HF)
1	76	$C_{4.00}H_{7.04}N_{2.52}O_{6.56}F_{1.44}P_{1.00}$	-42.5
2	31	$C_{4.62}H_{5.86}N_{2.24}O_{5.72}F_{4.14}P_{1.00}$	-37.5
	65	$C_{5.30}H_{7.90}N_{3.60}O_{9.80}F_{2.10}P_{1.00}$	-28.4
	70	$C_{5.40}H_{8.20}N_{3.80}O_{10.40}F_{1.80}P_{1.00}$	-27.3
	78	$C_{5.56}H_{8.68}N_{4.12}O_{11.37}F_{1.32}P_{1.00}$	-25.6
3	59	$C_{6.36}H_{9.90}N_{3.36}O_{9.08}F_{2.46}P_{1.00}$	-44.3
	61	$C_{6.44}H_{10.10}N_{3.44}O_{9.32}F_{2.34}P_{1.00}$	-44.1
4	67	$C_{8.02}H_{13.38}N_{3.68}O_{10.04}F_{1.98}P_{1.00}$	-58.1
5	50	$C_{8.00}H_{13.00}N_{3.00}O_{8.00}F_{3.00}P_{1.00}$	-67.5
	51	$C_{8.08}H_{13.18}N_{3.04}O_{8.12}F_{2.94}P_{1.00}$	-67.8
	68	$C_{9.44}H_{16.24}N_{3.72}O_{10.16}F_{1.92}P_{1.00}$	-71.4
PolyGLYN	-	$C_{3.00}H_{5.00}O_{4.00}N_{1.00}$	-60.5
PolyNIMMO	-	$C_{5.00}H_{9.00}O_{4.00}N_{1.00}$	-114.3
GAP	-	$C_{3.00}H_{5.00}O_{1.00}N_{3.00}$	-121.2

Table 2.5 Values of the oxygen balance (%) of Polymers 1-5 and of three carbon-based energetic polymers.

2.1.8 Glass-transition temperature measurements

The glass transition temperature (T_g) of selected batches of Polymers 1-5 was measured by differential scanning calorimetry (DSC). The samples were subjected to two identical cooling/heating cycles according to the temperature profile shown in Figure 2.12.

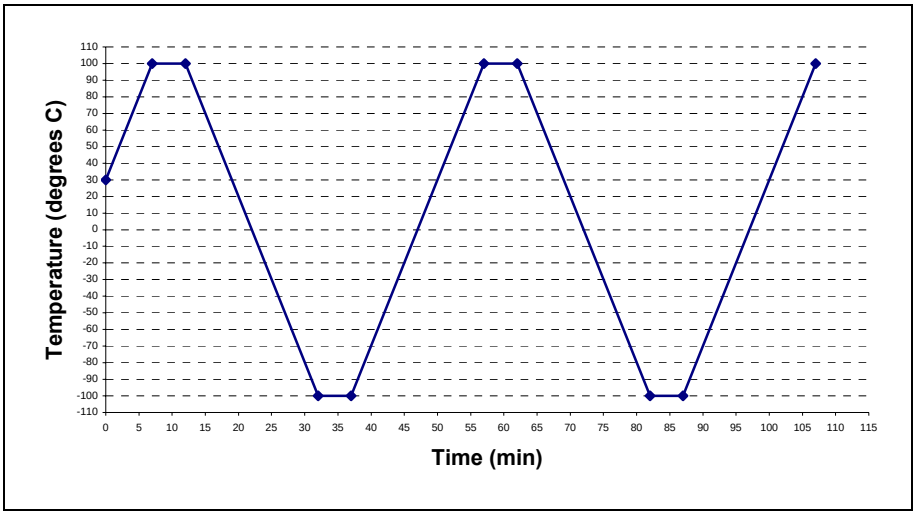

Figure 2.12 DSC temperature profile. All heating and cooling ramps have a rate of 10ºCmin^{-1}. The isotherms are of 5 min in duration.

As shown in Table 2.5, the T_g values of the polymers were generally found to decrease with the increasing size of alkoxy substituent. Polymer ESTC2 was an exception however and exhibited a lower than expected T_g despite the small size of the alkoxy substituent and the relatively high ES% value. This is in apparent contrast with the observed 'waxy' nature of this polymer at ambient temperature, when compared to the other polymers, which appeared more mobile at room temperature (Figure 2.13). The low T_g values exhibited by the higher homologous members of the polymer series (Polymers 4 and 5) may be rationalised in terms of their larger alkoxy substituents, which may hinder the formation of specific interactions between the nitrato groups of adjacent polymer chains. No other physical characterisation measurements (i.e. density or viscosity) were carried out on the polymers.

Energetic Polyphosphazene	ES% (by ^{1}H NMR)	T_g (°C)	
		Peak	Onset
1	76	-41.1	-47.2
2	70	-19.0	-27.9
3	61	-19.0	-29.1
4	67	-30.1	-38.6
5	51	-40.1	-48.2

Table 2.6 DSC measured T_g values of Polymers 1-5 (selected batches only).

Figure 2.13 A picture of Polymers (from left to right): 1 (ES%=76), 2 (ES% =70), 3 (ES%=61%) and 5 (ES%=51), showing apparent trend of decreasing viscosity.

2.2 CALORIMETRY

2.2.1 Calorimeter calibration and thermochemical standard substances

Calibration, or the determination of the heat equivalent of the calorimeter, as it is more commonly known, is performed prior to measuring the energy of combustion of any 'unknowns' in order to determine the heat capacity of the *complete* calorimetric system. Bomb calorimeters can be calibrated using electrical energy. In this method, which is reported to be extremely accurate,[98] an electric current of known intensity (A) is passed through a resistive conductor inside the bomb, for a known period of time and the temperature rise of the system is carefully monitored before, during and after re-equilibration. By knowing the resistance of the conductor and the time of current application, the electrical energy 'fed' to the calorimeter can be calculated with great accuracy. Electrical calibration has the disadvantage of requiring more complex instrumentation and therefore it is generally only used by standardising laboratories.

The second and almost universally adopted method used to calibrate a bomb calorimeter relies on the combustion of a known quantity of a suitable, primary, thermochemical standard substance, which has a known internal energy of combustion (usually referred to as the *primary calorimetric standard*). For generic work involving the combustion of CHO compounds, benzoic or succinic acids are generally used as primary standards. The standard (internal) energy of combustion of very pure benzoic acid is accurately known and is readily available from thermochemical tables. Most standardising institutions usually despatch their samples of standard benzoic acid with a certificate of analysis which also certifies the energy of combustion of the compound with any associated uncertainties. The *minimum* requirements for a substance to be used as a primary standard are:[95,98]

1. It should be obtainable in a pure state,
2. it should be stable,
3. it should *not* be hygroscopic and should be *dry* before use,
4. it should not be volatile,
5. it should be easily formed into pellets,
6. it should ignite readily in pressurised oxygen, and
7. it should burn completely without leaving sooty residues in the crucible.

It is clear that the accuracy of all of the data obtained with a combustion calorimeter relies entirely on the quality of the measured heat capacity of the system, and in turn on the reliability of the certified standard sample of benzoic acid. This is the reason why a primary standard must satisfy the above-mentioned minimum requirements and benzoic acid has been repeatedly shown[95] to fully satisfy all of them.

If the sample to be investigated calorimetrically contains one or more of the elements N, S, P, Cl, Br or I, then a *calorimetric secondary standard* should also be employed. The function of the secondary standard is different from that of the primary standard. When a compound containing any of the above-mentioned elements undergoes combustion in oxygen, the chemistry of the reaction is more complex than that of an ordinary CHO compound. As a consequence, the final calorimetric result for these substances will also depend on the 'side-reaction' combustion products which need to be accurately quantified in order to correct for their enthalpies of formation and/or dilution. An appropriate secondary standard, or *calorimetric test substance,* is therefore used to check the accuracy of the analytical and calorimetric techniques for that particular atomic species, by allowing a direct comparison with the data published by other investigators; test substances essentially 'standardise' the *chemical part* of the calorimetric investigation.

The chemical part of the experiment will often require different bomb conditions to the standard conditions required for the calorimetric part; for instance, as in this work, the distilled water may be replaced by a buffer solution to prevent the decomposition of analytes. As these non-standard conditions are not appropriate for obtaining 'standard' calorimetric data, the experiment must be divided into two sets of burns; a calorimetric set, carried out under, or as close as possible to standard conditions, and a separate, parallel chemical set for analysis purposes, from which no calorimetric data is retained. The set of c*hemical burns* allows correction to be made for any 'side-reaction' deviating from the *idealised combustion process* that may be occuring during the calorimetric part of the experiment.

The stoichiometry of the idealised combustion reaction (in excess oxygen) of a large variety of secondary standards is revised periodically by national and international standardising organisations. The first official list of recommended test substances (reference materials, RM) for combustion calorimetry was published[98] in 1959 and then revised[95] in 1979 by the IUPAC Commission on Experimental Thermochemistry. An up-to-date and more complete list, was published in 1999 by ICTAC. [123]

Unfortunately, no references were found in the literature describing the bomb calorimetric combustion of compounds containing more than a *single* hetero-atomic species. Three secondary standards were therefore chosen to model the combustion stoichiometry of each hetero-atomic species present in the energetic polyphosphazenes and in their non-energetic precursor poly[bis(2,2,2-trifluoroethoxy)phosphazene], namely *phosphorus, fluorine* and *nitrogen*. For reference purposes, the primary and secondary standards that were used in this work are described in Section 2.2.1.1.

2.2.1.1 Thermochemical standards used in this work

- Benzoic acid

By international agreement in 1959, benzoic acid was chosen as the principal reference substance for measuring the energy equivalent of oxygen-bomb calorimeters. The compound also serves to 'kindle' materials which are difficult to burn and, in some cases, also to direct the overall stoichiometry of reaction towards a more desirable final state. Suitable grades of benzoic acid with a certified value of the energy of combustion are available from NIST in the US, from NPL in the UK and other standardising laboratories in China and the Russian Federation. The stated purity, achieved by repeated re-crystallization followed by sublimation or by zone-refining, is usually greater than 99.995%. The standard specific energy of combustion of benzoic acid is defined as the (constant volume) energy evolved when 1g of the substance burns under standard conditions.[123]

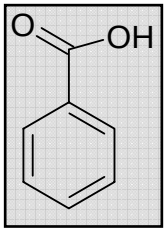

Benzoic acid, $C_7H_6O_2$, physical state at RT: non hygroscopic solid, MW: 122.1234 $gmol^{-1}$, *recommended*[123] *value of energy of combustion* (298.15 K): $\mathbf{\Delta U_c^\circ = -(26434 \pm 1)\ Jg^{-1}}$ Intended use: primary standard used to calibrate the calorimeter.

Combustion reaction in excess oxygen:

$$\mathbf{C_7H_6O_{2\,(s)} + 7.5O_{2\,(g)} \rightarrow 7CO_{2(g)} + 3H_2O_{(l)}}$$

- Triphenylphosphine oxide

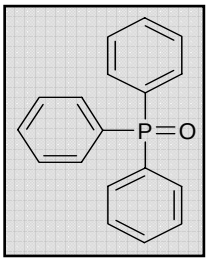

Triphenylphosphine oxide, $C_{18}H_{15}OP$ physical state at RT: non-hygroscopic solid, MW: 278.2903 $gmol^{-1}$, *recommended*[123] *value of energy of combustion* (298.15 K): $\mathbf{\Delta U_c^\circ = -(35789.3 \pm 4.5)\ Jg^{-1}}$ Intended use: secondary standard for the combustion of phosphorus-containing compounds.

Idealised combustion reaction in excess oxygen:

$\mathbf{C_{18}H_{15}OP_{(s)} + 22.5\ O_{2(g)} \rightarrow 18CO_{2(g)} + H_3PO_4(6H_2O)_{(l)}}$

- *para*-Fluorobenzoic acid

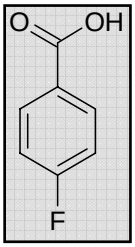

4-Fluorobenzoic acid, $C_7H_5O_2F$, physical state at RT: non-hygroscopic solid, MW: 140.1139 $gmol^{-1}$, *recommended*[123] *value of energy of combustion* (298.15 K): $\mathbf{\Delta U_c^\circ = -(21860 \pm 4)\ Jg^{-1}}$ Intended use: secondary standard for the combustion of fluorine-containing compounds of low fluorine content.

Idealised combustion reaction in excess oxygen:

$\mathbf{C_7H_5O_2F_{(s)} + 7O_{2(g)} + 18H_2O_{(l)} \rightarrow 7CO_{2(g)} + HF(20H_2O)_{(l)}}$

- 1,2,4-(1H)-Triazole

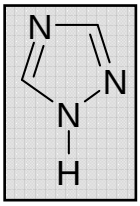

1,2,4-(1H)-Triazole, $C_2H_3N_3$, physical state at RT: non-hygroscopic solid, MW: 69.0660 $gmol^{-1}$, *recommended*[123] *value of energy of combustion* (298.15 K): $\mathbf{\Delta U_c^\circ = -(19204.2 \pm 4.1)\ Jg^{-1}}$ Intended use: secondary standard for the combustion of nitrogen-containing compounds.

Idealised combustion reaction in excess oxygen:

$\mathbf{C_2H_3N_{3(s)} + 2.75O_{2(g)} \rightarrow 2CO_{2(g)} + 1.5H_2O_{(l)} + 1.5N_{2(g)}}$

2.2.1.2 Experimental derivation of ε (the heat equivalent of the calorimeter)

A Gallenkamp 'Autobomb 305' static adiabatic bomb calorimeter (Figures 2.14 and 2.15), fitted with a Parr 1108-Cl halogen-resistant bomb (Figures 2.16, 2.17 and 2.18), was used for all of the calorimetric investigations carried out in this work. Two sets of calibration were performed: manual and automated. The manual calibration was carried out prior to automation (i.e. interfacing to a PC) of the calorimeter. The procedures followed to perform both manual and automated calibrations are described in Section 4.1.1.1. Surprisingly, the standard deviation of the 'automated' calibration mean value of system heat capacity was found to be half of that of the 'manually' derived one, even though the number of replicate experiments was half of those of the 'manual' calibration. Since the values of energy of combustion of the secondary standards that were burnt to ensure the accuracy of the technique, were calculated using the 'manually' derived heat equivalent value, and since these were found to be already in excellent agreement with the literature values, both 'manual' (Table 2.7) and 'automated' (Table 2.8) heat equivalent values are presented.

To ensure that a reproducibly constant volume of water would be poured into the pail of the calorimeter prior to performing any experiment, a specially designed glass funnel was made (Figure 2.19 and Section 4.1.1). The pail, filled with water, was then placed in a thermostatic bath set to 27ºC (Figure 2.20) along with the bomb to ensure that the same value of starting temperature (27.0 ± 0.5 ˚C) would be rapidly reached by the system before firing the bomb, therefore minimising the effect of the temperature dependence of the system's heat capacity. The temperature of the water in the pail was constantly monitored by a high precision mercury-in-glass thermometer. A fast transfer of the pail and charged bomb from the thermostatic bath in the adiabatic jacket of the calorimeter minimised the effect of temperature re-equilibration.

Calibration run	Weight of firing cotton (g)	Weight of benzoic acid (g)	ΔT corr (K)	ε (J K^{-1}) rounded to 4 signif. figures
1	0.0482	1.2088	3.005	10920
2	0.0694	1.0608	2.692	10880
3	0.0659	1.2091	3.042	10890
4	0.0678	1.2205	3.069	10910
5	0.0434	1.2088	3.010	10880
6	0.0493	1.1248	2.805	10920
7	0.0736	1.0990	2.795	10860
8	0.0398	1.0650	2.691	10730
9	0.0414	1.0719	2.697	10780
10	0.0411	1.1661	2.905	10870
11	0.0488	1.1481	2.886	10820
12	0.0434	1.2156	3.038	10830
13	0.0403	1.1560	2.874	10890
14	0.0492	1.1929	2.978	10590
15	0.0477	1.2180	3.029	10910
16	0.0603	0.9548	2.416	10890
17	0.0525	1.1602	2.904	10880
18	0.0408	1.2431	3.105	10820
19	0.0724	1.2186	3.092	10840
20	0.0493	1.2025	3.023	10810
Mean and standard deviation				**10850 ± 80 (±0.7%)**

Table 2.7 Experimental results for the 'manual' calibration of the Gallenkamp calorimeter (ΔT_{corr}= corrected temperature rise).

Calibration run	Weight of firing cotton (g)	Weight of benzoic acid (g)	ΔT corr (K)	ε (J K^{-1}) rounded to 4 signif. figures
1	0.0807	1.2186	2.619	10930
2	0.0797	0.9667	2.598	10890
3	0.0973	1.0594	2.543	10870
4	0.0569	1.0579	2.587	10900
5	0.0641	1.0879	2.613	10880
6	0.0799	1.9940	2.596	10940
7	0.0875	1.0238	2.530	10880
8	0.0869	1.0120	2.594	10810
9	0.0868	0.9874	2.620	10880
Mean and standard deviation				**10890 ± 40 (±0.3%)**

Table 2.8 Experimental results for the 'automated' calibration of the Gallenkamp calorimeter (ΔT_{corr} = corrected temperature rise).

Figure 2.14 The Gallenkamp 305 'Autobomb' static adiabatic calorimeter

Figure 2.15 The Gallenkamp 305 'Autobomb' static adiabatic calorimeter with jacket lid raised.

Figure 2.16 The Parr 1108-Cl twin-valve, halogen-resistant 'Hastelloy' bomb

Figure 2.17 Parr 1108-Cl bomb's three main components

Figure 2.18 Parr 1108-Cl bomb twin-valve lid with crucible in place

Figure 2.19 The water dispensing glass funnel

Figure 2.20 The thermostatic bath with the bomb and water-filled pail

2.2.2 Measurement of the internal energy of combustion (ΔU_c)

The 'calorimetric part' of the measurement of ΔU_c consists in performing a number of replicate combustion experiments on samples of the substance under investigation. Seven replicate combustion experiments are reported[77] to be enough to achieve a satisfactory final uncertainty interval which, for precision bomb calorimetry, may be as low as ±0.01%.[77] As the precision of a calorimetric measurement (i.e. the magnitude of the uncertainty interval) is inversely proportional to the square of the number of replicate observations,[129] it is usually not worth increasing the number of these over ten.

In the typical combustion experiment, the sample, if solid, is pressed into a pellet, weighed and placed in the crucible along with the fuse and the cotton thread for ignition. If it is liquid, it is usually admixed with a known amount of 'kindling hydrocarbon oil' to aid combustion. The heat released by the hydrocarbon must be subtracted from the total energy change observed during the experiment. A small volume of water is also added[95] to the bomb prior to sealing it. The volume of water added to the 'measuring' experiments must however be identical to that added to the calibration experiments, to avoid a systematic error due to the different heat capacity of the system between calibration and measurement.

The bomb is flushed with oxygen in order to expel the residual air trapped inside it. This is done because nitrogen, which is the main constituent of air (78% v/v), would react in the hot oxygen-rich flame envelope, giving rise to small quantities of nitric acid which require thermochemical correction. The same process is known[124] to occur during thunder-storms when nitrogen is 'fixated' into nitric acid in the extremely hot ionised paths of lightening strikes.

Although, in this work, high purity oxygen gas was used for all of the experiments (Section 4.1.1), the degree of air nitrogen 'fixation' occurring in the bomb was investigated, by burning the same quantity (1g) of benzoic acid after (a) flushing the bomb three times, (b) flushing the bomb only once, and (c) after pressurising the bomb without flushing. The quantity of nitric acid formed was

detected in the bomb washings by alkali titration and also as nitrate ion by ion exchange chromatography (IC). Figure 2.21 shows the relative peak areas for experiments (a), (b) and (c). For experiment (c) 24 mmol of HNO_3 in total were detected, suggesting that almost 3% of the nitrogen in the air 'trapped' inside the bomb was fixated to NO_2. When the bomb was flushed three times however (experiment a), negligible amounts of nitric acid were formed (close to the limit of detection of the instrument for $NO_3^- \approx 0.1$ ppm wt/vol).

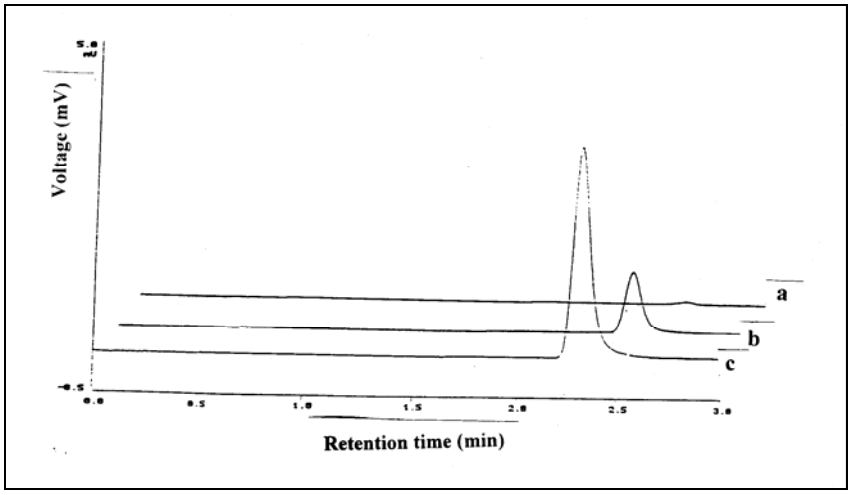

Figure 2.21 Ion chromatograms for experiments (a) bomb flushed three times, (b) bomb flushed only once, and (c) bomb not flushed.

The value of 'starting temperature', which ideally should be identical for calibration and measuring experiments (in practice this varied within ± 0.5 K), was chosen to be close but slightly above the recommended standard bomb temperature of 298.15 K (25°C). As 27ºC was above the annual average ambient temperature of the laboratory in which all experiments were conducted (no air conditioning was available in the room), negative 'drift' fore- and after-period lines on the calorimetric thermographs could be achieved (Section 2.2.2.1), simplifying the determination of the *'end of chemical heat evolution'* (also referred to as the 'end-point', Section 2.2.2.2). This operation is extremely important for the reproducible estimation of the corrected temperature rise of the experiments. The maximum error arising from conducting the calorimetric

experiments 2K above the standard bomb temperature was estimated to fall well within the 'automated' experimental uncertainty.

2.2.2.1 Observation of temperature over time

A bomb calorimetric experiment is usually divided into three main periods, as shown in Figure 2.22. There is a *fore-period,* in which the temperature change of the calorimeter is due completely to physical processes, namely heat transfer between the calorimeter and the surroundings (thermal leakage) and heat of stirring (Joule heating). Thermal leakage can be positive or negative and obeys Newton's law of cooling. A truly adiabatic system should, of course, rectify physical heat gain and loss, although in practice perfect adiabaticity is almost impossible to achieve: in the system used in this work, the 'compensating' thermistor probes of the 'Wheatstone bridge' circuit, the rotating stirrer and the thermocouple of the digital thermometer are all metallic and hence good heat conductors to and from the external environment. Minor temperature drifts (approximately 0.002 K min^{-1}) were therefore observed regardless of 'jacket balance control' fine tuning.

When the bomb is fired, the fore-period is followed by the *main period*, which usually lasts 15 min, in which the principal part of the temperature rise due to evolution of chemical energy takes place. The duration of the main period depends mainly on the *lag* of the bomb, which is governed by the heat capacity and thermal conductivity of the bomb material. The main period is then followed by a *final period* or *after-period* in which the temperature change of the system is again due entirely to thermal leakage and heat of stirring.

The length of the fore- and after-periods is usually 20 min for each, although in this work they have been extended to 40 min each so that a better estimation of the temperature drift rates could be achieved. During these 'physical' periods, temperature readings are either recorded manually (usually at intervals of 30 s) or, in modern systems, automatically by a computer interfaced to the digital thermometer unit. Sampling intervals can therefore be as low as one wants them to be; in this work an interval of 3 s was adopted. The frequency of the temperature readings ultimately governs the accuracy of the determination of the

end point at the end of the main period. The advantages of automatically logging temperatures include the obvious fact that the operator does not have to manually record data for an hour or more, which may cause losses in accuracy and precision of the raw calorimetric data.

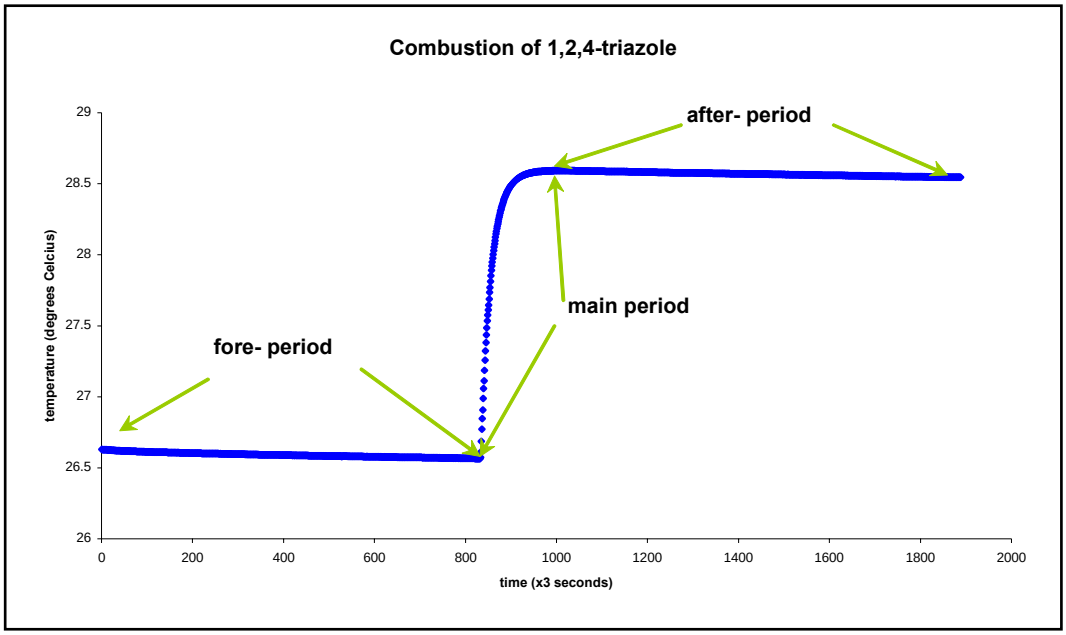

Figure 2.22 Thermograph showing temperature profile over time for the combustion of 1 g of 1,2,4-triazole for which the fore-, main and after-periods are identified. Temperature was logged automatically every 3 s.

The *corrected* temperature rise (ΔT_{corr}) of the system after a combustion experiment is calculated in order to subtract the thermal effect of temperature drift from the main period of the experiment, thereby giving the value of chemical heat only from the burning sample. The correction is based on the assumption that the rate of temperature change due to thermal leakage and heat of stirring is constant (within the temperature range of the typical experiment). Different methods have been developed to calculate the corrected temperature rise. In the *Regnault-Pfaundler* method[98] ΔT_{corr} is calculated by Equation 22 where K is the *cooling constant* of the calorimeter which can be found empirically, u is the rate of temperature rise due to stirring, Tj and Tc are the temperatures of the jacket and of the calorimetric proper respectively. T_1 and T_2 are the integration limits and are

the start and end temperature values of the main period, ($T_2 - T_1$ = *uncorrected* temperature rise observed)

$$\Delta(Tc) = u(T_2 - T_1) + k(Tj - Tc)(T_2 - T_1) \quad (22)$$

Other methods to determine ΔT_{corr} are essentially graphical in nature and are extremely laborious. In the *Dickinson* method[98] for example, areas below and above the main period of the thermogram are 'made equal' and the 'end-point' temperature is detected on the thermographic curve where the two areas meet. This procedure can be accomplished by counting the squares on graph paper or by using specialised software.

There exists however a simplified version of the *Regnault-Pfaundler* method which corrects the observed temperature rise empirically and without introducing the calorimeter's cooling constant and the temperature rise due to stirring into the equation. This method is suggested by Parr[125] for isothermal calorimetry and is routinely used by other investigators.[126]The corrected temperature rise for all experiments carried out in this work were computed using this method.

The net corrected temperature rise ΔT_{corr} for each combustion test was computed by using Equation 23:

$$\Delta T_{corr} = t_c - t_a - r_1(b-a) - r_2(c-b) \quad (23)$$

which effectively subtracts the observed temperature drift before and after a firing, where:

a = time corresponding to the end of the fore-period (i.e. immediately before the temperature rise due to release of chemical heat, typically 3-5 s after firing the bomb).

b = time (to the nearest 3 s) when the temperature reaches 60% of the total *uncorrected* rise. At this point the temperature drift can be shown[127,128] to 'switch' from the fore-period rate to the after-period rate.

c = end-point (end of the main period and *start* of the after-period)

For clarity, the points *a*, *b* and *c* have been identified on the thermograph shown in Figure 2.23.

t_a = temperature at time *a*

t_c = temperature at time *c*

r_1 = rate (temperature units over time units) at which temperature was rising (or falling) during the 40 min period before firing. In this work it was found that better R^2 values for the linear regression line through the data-points of the fore-period, could be obtained by interpolating only the last 20 min of the fore-period, during which the temperature drift was found to be more linear.

r_2 = rate at which temperature was rising (or falling) during the 40 min period after time *c*. If the temperature was falling instead of rising after time *c*, r_2 is negative and the quantity $-r_2(c-b)$ becomes positive and must be added when computing the corrected temperature rise. The same applies to the fore-period correction term $-r_1(b-a)$. For the combustion of benzoic acid (typical temperature rise for 1 g sample ≈ 2.5K), the magnitude of the error which would be incurred had the corrections for the effect of temperature drift not be applied, fluctuated between 0.5 and 1%. For less calorific samples however (i.e. 200 mg of a high explosive) the error would be much greater (up to 4% for a typical temperature rise of approximately 0.5K).

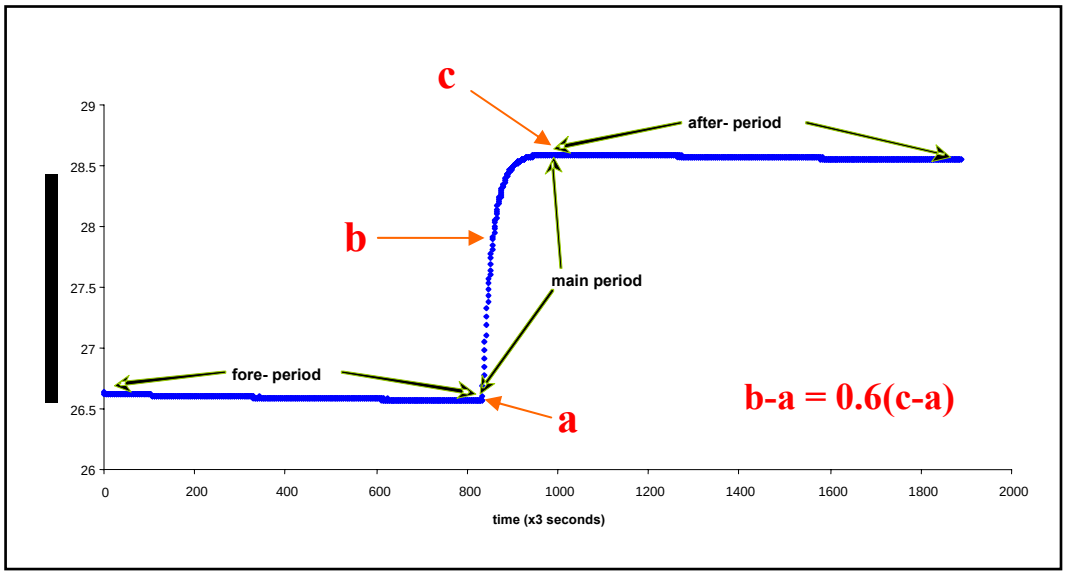

Figure 2.23 Identification of the points *a*, *b* and *c* of the calorimetric thermogram shown in Figure 2.22.

2.2.2.2 Estimation of end-point

Without access to specialised software, the most critical part of the analysis of the raw calorimetric data is the determination of the 'end-point', which can effectively be described as the last temperature value recorded for the *main period* of the calorimetric 'sigmoid', corresponding to the precise instant when all chemical evolution of heat from the burning sample has finally ceased and has given way to physical heat evolution processes only, which are then responsible for the observed after-period temperature drift. If the after-period temperature drift is positive, the sigmoid presents no maximum and the end-point can only be estimated by judging where the after-period data-points start to 'deviate' significantly from the regression line. This method is obviously imprecise because an arbitrary choice must be made to decide what is the unacceptable magnitude of the deviation from the line. To solve the problem it is sufficient to start the calorimetric experiment at an initial temperature value slightly above ambient (300 K in this work) which furnishes, after combustion of the sample, negatively sloped after-period drift lines (Figure 2.24). In this way, the function will always present a maximum, which unambiguously indicates the end-point. Although first or second order derivation of the function would be the best tools to estimate the position of the maximum, it is possible to identify its position also by simply re-scaling the ordinate axis of the thermogram, with the aid of an electronic spreadsheet as shown in Figure 2.25.

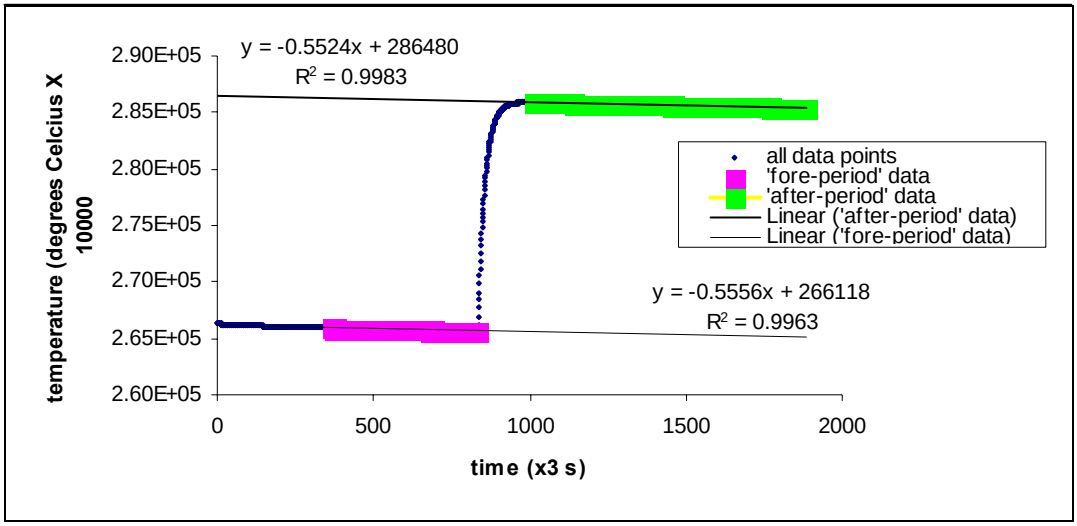

Figure 2.24 Assessment of linearity of the temperature drift lines for the fore- and after-periods.

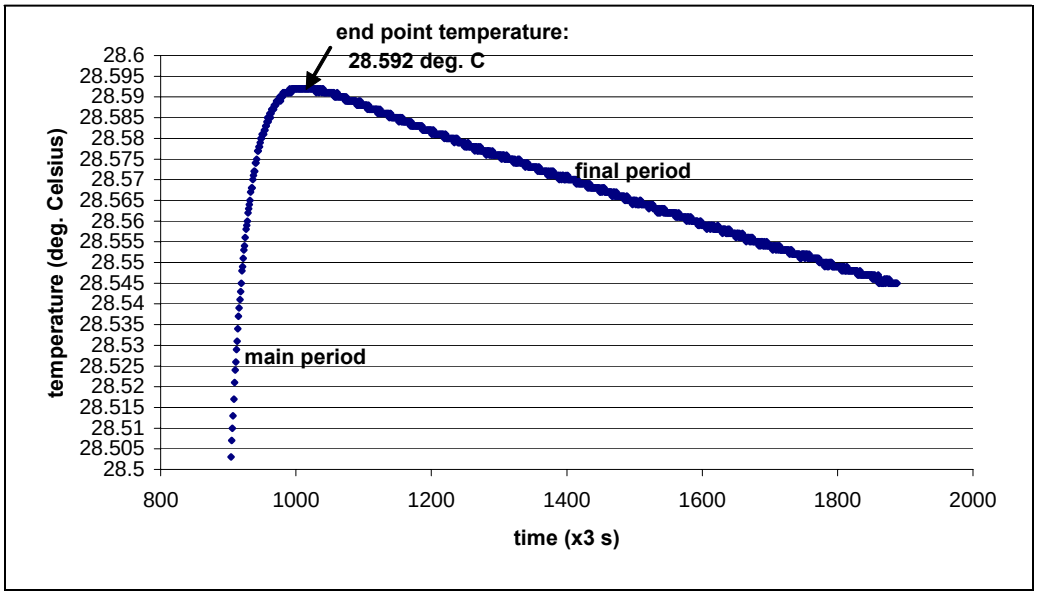

Figure 2.25 Determination of end-point by re-scaling of the ordinate axis

2.2.2.3 Washburn Corrections

It is common practice, for work of the highest accuracy, to make small corrections for the effect of pressure and other physical variables that can interfere with the measured energy values. These minor corrections take their name after E.W. Washburn who first published[105] them in 1933 for general CHO compounds.

Before then the Washburn corrections were generally ignored.[98] However, as the magnitude of these corrections is usually smaller than 0.1%,[105] they were neglected in this work. In brief, the Washburn corrections account for:

Compression of condensed phases. Since the solid (or liquid) compound to be burnt and the water initially present in the bomb are compressed to a greater pressure than 1 atm, a small thermal correction for the compression energy 'stored' in the system is required. The effect of compression is usually calculated by solving a differential equation which includes the 'coefficient of cubical expansion' and in which the independent variable is the pressure in the bomb.

Compression of the gaseous phase. Since neither the initial nor the final gas phase in the bomb are at very low pressure, a thermal correction for non-ideality of the gases is required. Because of the complexity of the calculations involved, several assumptions and simplifications are usually made.

Solution of the gases in the aqueous phase. In the initial state, some oxygen will be dissolved in the water added to the bomb, and in the final state, some of the product gases will be dissolved in the aqueous phase. Thermal corrections for the enthalpy of solution of these gases in water are required.

Vaporization of water. When water is placed in the bomb, the gas phase becomes saturated with water vapour and remains so throughout the experiment. The concentration of water vapour in the gas phase may change from the initial to the final state. This may happen because the partial pressure of water vapour over the final liquid phase may differ from that over pure water. A small correction for this vaporisation 'imbalance' is accounted for.

Dilution of the aqueous phase. The energy of dilution of the gaseous products in the liquid phase depends on the final concentration. In a series of replicate experiments it is impossible to end up with the same final concentration every time. To solve the problem, a correction is made for dilution of the formed species to an *arbitrarily chosen* reference concentration, e.g. $HF \cdot 20H_2O$ for the combustion of organo-fluorine compounds.

Non-isothermal reaction. As previously mentioned (Section 1.8.3), it is a standard practice to correct the measured enthalpy of combustion to standard temperature

(298.15 K). This can be done by application of Equation 14 (Section 1.8.3). To derive the quantity ΔC_p , (i.e. the difference in the system's heat capacity *before* and *after* the combustion reaction), *Cp* must be accurately known for the compound to be burnt, the complex gas mixture produced upon combustion and the final aqueous bomb solution. The *Cp* values of complex gaseous mixtures and novel compounds are difficult to find in the open literature and without the required specialised instrumentation to carry out the measurements, it may be difficult to fully correct for non-isothermal conditions.

2.2.2.4 Estimation of uncertainties

In most thermochemical investigations, *systematic* errors arise from a number of sources, including the calibration of the calorimeter and the 'train of operations' associated with the chemical (i.e. analytical) part of the calorimetric experiment. These errors would affect the accuracy of the technique but *not* the precision of the final results. This situation leads to poor agreement of the data found by different laboratories for the same compound.

In thermochemistry the uncertainty intervals are generally expressed as twice the standard deviation of the mean[98] which is given by Equation 24:

$$\bar{s} = \sqrt{\frac{\sum_{X1}^{Xn} (x_i - \bar{x})^2}{n-1}} \qquad (24)$$

In order to reduce the magnitude of the above-mentioned discrepancies, however, Rossini[98] recommended that the uncertainty of the mean value of a small set of *n* calorimetric observations should be expressed as $2/\sqrt{n}$ times its standard deviation (calculated with Equation 24). It would appear that most investigators have adopted Rossini's recommendation, ending up with surprisingly small uncertainty intervals for their energy values. In the author's opinion the use of Rossini's recommendation would be justified only if a 'note of warning' was added alongside each uncertainty value that is estimated in this way. In this work, Rossini's recommendation was *not* followed.

The propagation of calorimetric error was estimated by application of Equation 25,[129] in which $s\Delta Uc$ is the final 'propagated' uncertainty, ΔU_c is the mean observed energy of combustion of the substance burnt with uncertainty $s\Delta U_c$, and ΔU_{ba} is the mean value of the calorimeter's heat equivalent with associated uncertainty $s\Delta U_{ba.}$

$$\frac{\bar{s}\,\Delta U_{\mathrm{c}}}{\Delta U_{\mathrm{c}}} = \sqrt{\left[\left(\frac{\bar{s}\Delta U_{\mathrm{c}}}{\Delta U_{\mathrm{c}}}\right)^2 + \left(\frac{\bar{s}\Delta U_{\mathrm{ba}}}{\Delta U_{\mathrm{ba}}}\right)^2\right]} \qquad (25)$$

In turn, the mean value of the heat equivalent of the calorimeter (ΔU_{ba}) will be affected by the overall uncertainty given by Equation 26, where ΔU_{cal} is the mean value of the heat equivalent ΔU_{cal}, with associated uncertainty $s\Delta U_{cal}$, ΔU_{cotton} is the energy of combustion of the cotton thread with associated uncertainty $s\Delta U_{cotton}$, and $\Delta U_{primary}$ is the certified energy of combustion of benzoic acid with its uncertainty $s\Delta U_{primary}$.

$$\frac{\bar{s}\,\Delta U_{\mathrm{ba}}}{\Delta U_{\mathrm{ba}}} = \sqrt{\left[\left(\frac{\bar{s}\Delta U_{\mathrm{cal}}}{\Delta U_{\mathrm{cal}}}\right)^2 + \left(\frac{\bar{s}\Delta U_{\mathrm{cotton}}}{\Delta U_{\mathrm{cotton}}}\right)^2 + \left(\frac{\bar{s}\Delta U_{\mathrm{primary}}}{\Delta U_{\mathrm{primary}}}\right)^2\right]} \qquad (26)$$

In this work the completeness of combustion in all experiments was checked by visually inspecting the interior of the bomb for residues of uncombusted material and/or excessive soot in the crucible. In order to determine whether a suspicious result of a replicate experiment was 'in statistical control', the *Q test* was employed. This test is reported to be[129] the most statistically correct for a small number of observations. A ratio Q (rejection quotient) is calculated by arranging the data in decreasing order of numbers. The difference between the suspect number and its nearest neighbour, is divided by the *range,* i.e. the difference between the highest and the lowest number. Referring to Figure 2.24, $Q = a/w$. This ratio is then compared with tabulated values of Q. If it is equal or greater than the tabulated value, the suspected observation should be rejected. Tabulated

values of Q at 90%, 95% and 99% confidence levels are found in standard Q tables.

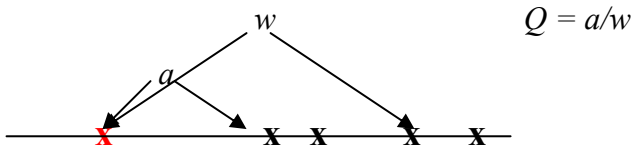

Figure 2.26 Illustration of the calculation of Q. The suspect value is coloured red.

2.2.3 Measurement of the internal energy of combustion of conventional explosives and energetic polymers

The (internal) energy of combustion of the conventional explosives TNT (2,4,6-trinitrotoluene), RDX (1,3,5-trinitro-1,3,5-triazacyclohexane), HMX (1,3,5,7-tetranitro-1,3,5,7-tetraazacyclooctane), and NTO (3-nitro-1,2,4-triazol-5-one), and of the energetic binders polyGLYN and polyNIMMO were measured and compared with the values given in the literature. All of the materials, apart from the NTO which was synthesised and re-crystallised in our laboratory, were of UK commercial origin. No purity assessments were made and all materials were used as provided. As these measurements constituted an early attempt to verify the accuracy and precision capabilities of the bomb calorimeter prior to its automation, no corrections for the formation of nitric acid (Section 2.2.6) were made. Temperatures were logged manually in all experiments and the 'manually' derived value for the heat equivalent of the calorimeter (Table 2.7) was used to determine all values of the energy of combustion. Despite the 'crudeness' of these early investigations, the experimental energy values agreed well with those given in the literature, suggesting that the magnitude of the required corrections was within the final uncertainty intervals (Tables 2.9 to 2.12). The measured value for the energy of combustion of RDX was found to be higher than any of the figures given in the literature. HPLC analysis was employed to check the quality of the RDX sample, which was found to be free of by-products such as HMX or hexamine. The cause for the deviation is unknown. Due to the energetic nature of

the materials, only small quantities were burnt in each experiment (~0.2g). All samples were weighed and combusted inside special *gelatine capsules* (Parr No. 3601), the energy of combustion of which was previously measured to be 21850 ± 200 Jg^{-1}. In some cases the combined weight of the cotton thread fuse and capsule was, out of necessity, only slightly less than that of the explosive and this was thought to be the major cause of the low precision observed for these early measurements.

A word of caution may be added about the poor quality of the thermodynamic data for high explosives found in the literature, which are sometimes inconsistent and are often expressed in kcal kg^{-1} without any estimated uncertainty range. As a consequence, only an indicative comparison could be made with such data, after converting them into Jg^{-1}, the energy unit adopted by the *International System of Units* (SI).[95] In these preliminary calorimetric experiments only three significant figures were retained for the evaluation of the mean combustion energy values.

Combustion experiment	Sample weight (g)	Weight of firing cotton (g)	ΔT corr (K)	$-\Delta U_c$ ($J\ g^{-1}$)
1	0.2371	0.0843	0.721	15100
2	0.2152	0.0651	0.673	14900
3	0.2774	0.0658	0.777	15300
4	0.3057	0.0739	0.791	14800
Mean and S.D. %SD Literature value				**15000 ± 200 (±1.5%) 15137[130] (ΔU^o_c)**

Table 2.9 Experimental measurement of the internal energy of combustion of TNT

Combustion experiment	Sample weight (g)	Weight of firing cotton (g)	ΔT corr (K)	$-\Delta U_c$ ($J\ g^{-1}$)
1	0.1671	0.0511	0.489	10000
2	0.1656	0.0503	0.483	9800
3	0.1857	0.0617	0.522	9900
4	0.2020	0.0680	0.535	9300
5	0.1816	0.0504	0.510	10600
6	0.1904	0.0533	0.510	9800
7	0.1045	0.0576	0.443	10200
Mean and S.D.				**9900 ± 100 (±1%)**
Literature values				**8510[131] (ΔU^o_c)** **9443[132] (ΔH^o_c)**

Table 2.10 Experimental measurement of the internal energy of combustion of RDX

Combustion experiment	Sample weight (g)	Weight of firing cotton (g)	ΔT corr (K)	$-\Delta U_c$ ($J\ g^{-1}$)
1	0.1753	0.0517	0.482	9100
2	0.2130	0.0736	0.563	9700
3	0.2380	0.0626	0.547	8800
4	0.2064	0.0575	0.516	9000
5	0.1919	0.0447	0.504	10100
6	0.2078	0.0921	0.598	10200
7	0.2012	0.0724	0.550	9700
Mean and S.D.				**9500 ± 200 (±2%)**
Literature values				**9419[132] (ΔU^o_c)** **9330[133] (ΔH^o_c)**

Table 2.11 Experimental measurement of the internal energy of combustion of HMX

Combustion experiment	Sample weight (g)	Weight of firing cotton (g)	ΔT corr (K)	$-\Delta U_c$ (J g^{-1})
1	0.1009	0.1323	0.538	7700
2	0.2135	0.1207	0.599	7700
3	0.1744	0.1102	0.557	7900
4	0.1743	0.1465	0.612	7600
5	0.1630	0.1215	0.563	7600
6	0.1050	0.0871	0.463	7300
7	0.1731	0.1390	0.589	7600
Mean and S.D.				**7600 ± 200 (±2.5%)**
Literature values				**7592[134] (ΔU^o_c)** **7310.9±8.0[135](ΔU^o_c)**

Table 2.12 Experimental measurement of the internal energy of combustion of NTO

Three different specimens of polyNIMMO and one of polyGLYN were combusted. All of the polymers were viscous and sticky liquids at room temperature and considerable care had to be taken to load the appropriate amount of material in the gelatine capsules prior to weighing. This was accomplished using a thin glass rod. The loaded capsules were also punctured with a fine hypodermic needle to prevent disruptive burning upon ignition of the capsule, thus reducing material loss from the crucible. A total of seven calorimetric experiments were performed for each sample and the results are shown in Tables 2.13 to 2.16. Excellent agreement was found with the standard combustion energy values given in the literature[121] for the two polymers: ΔU_c^o polyNIMMO = -19500 Jg^{-1}, ΔU_c^o polyGLYN = -14700 Jg^{-1}.

Combustion experiment	Sample weight (g)	Weight of firing cotton (g)	ΔT corr (K)	$-\Delta U_c$ ($J\ g^{-1}$)
1	0.2657	0.0496	0.832	20220
2	0.3743	0.0831	1.087	20070
3	0.3658	0.0635	1.043	20190
4	0.2389	0.0822	0.828	19920
5	0.2938	0.0707	0.907	19760
6	0.4813	0.0599	1.239	19830
7	0.4513	0.0851	1.141	19850
Mean and S.D.				**20000 ± 180 (± 1%)**

Table 2.13 Experimental measurement of the internal energy of combustion of polyNIMMO, specimen 'BX PP370'

Combustion experiment	Sample weight (g)	Weight of firing cotton (g)	ΔT corr (K)	$-\Delta U_c$ ($J\ g^{-1}$)
1	0.2834	0.0886	0.895	18920
2	0.2915	0.1045	0.937	18980
3	0.2524	0.0981	0.866	19360
4	0.2862	0.0963	0.939	19910
5	0.3323	0.1221	1.057	19590
6	0.2898	0.1062	0.949	19430
7	0.3905	0.1114	1.146	19580
Mean and S.D.				**19390 ± 350 (±1.8%)**

Table 2.14 Experimental measurement of the internal energy of combustion of polyNIMMO, specimen 'ICI blend PP57'

Combustion experiment	Sample weight (g)	Weight of firing cotton (g)	ΔT corr (K)	$-\Delta U_c$ ($J\ g^{-1}$)
1	0.5134	0.1075	1.398	20280
2	0.4415	0.0900	1.217	19890
3	0.3636	0.1220	1.117	19670
4	0.4065	0.0959	1.161	19880
5	0.4598	0.1092	1.277	19760
6	0.5131	0.1039	1.345	19310
7	0.4208	0.0983	1.200	19820
Mean and S.D.				**19800 ± 290 (±1.4%)**

Table 2.15 Experimental measurement of the internal energy of combustion of polyNIMMO, specimen 'PP278'

Combustion experiment	Sample weight (g)	Weight of firing cotton (g)	ΔT corr (K)	$-\Delta U_c$ ($J\ g^{-1}$)
1	0.5109	0.0792	0.990	13330
2	0.4394	0.1202	0.983	13090
3	0.4005	0.0861	0.894	13470
4	0.4853	0.1000	1.039	13810
5	0.4053	0.0757	0.876	13290
6	0.4867	0.1338	1.074	13320
7	0.4244	0.0814	0.930	13810
Mean and S.D.				**13450 ± 270 (±2%)**

Table 2.16 Experimental measurement of the internal energy of combustion of polyGLYN, specimen 'blend 3.23'

2.2.4 Oxygen combustion calorimetry of phosphorus-containing compounds

There is a limited amount of information available in the literature regarding the combustion calorimetry of organo-phosphorus compounds. This might be due in part to the difficulties that arise when combusting phosphorus-containing organic compounds in an oxygen bomb:

1. Different phosphorus oxy-acids are formed in varying amounts in different parts of the bomb, especially when using a static bomb. This is due to the polyvalent nature of phosphorus and also to the varying degree of hydration of the oxides of phosphorus that are generated during the combustion. These oxy-acids need to be quantified in order to calculate the necessary corrections to the final energy of combustion caused by their energies of dilution.
2. It is often difficult to obtain complete, clean combustion reactions because the burning phosphorus-containing compound tends to become covered by phosphorus acids and oxides, which effectively passivate the surface and sooty residues are often found in the crucible after firing.
3. Most of the common crucible materials are attacked by the phosphorus acids. Only pure gold would appear to be totally inert to the acids generated upon combustion of phosphorus containing compounds.[95]

Early workers have attempted[95] to solve the first problem by allowing time for the water added to the bomb to evaporate and then condense on the walls of the bomb prior to firing, whilst others have increased the amount of water added to the bomb and also substituted the water with a 60% aqueous solution of perchloric acid,[136] which would function as a hydrolytic agent to convert any polycondensed acids into phosphoric acid. The latter expedient was successful but introduced complications to the analysis of the final system and a complex sequence of comparison experiments were needed. It would seem that the only practical solution to the problem of obtaining a well defined, homogeneous final state lies in the use of a rotating bomb calorimeter (Section 1.8.1), but as the corrections due to the formation of condensed phosphorus acids are reported[136] to amount to

only a fraction of a percent, the purchase of an expensive rotating bomb calorimeter would only be justified if very high accuracy, thermochemical data is sought.

The data found in the literature regarding the formation of different phosphorus acids was also grossly inconsistent. Bedford and Mortimer[137] found quantitative conversion to phosphoric acid using a static bomb whereas other workers[138] found variable amounts of *diphosphoric* (commonly known as pyrophosphoric) and *tripolyphosphoric* acids even when using a rotating bomb. This might be a reflection of the variable accuracies of the different analytical techniques available to the authors at the time. Two such papers for example[136,137] date back to the early 1960s and late 1970s respectively, whereas another relevant paper[138] was published in the late 1980s.

To address the second problem mentioned earlier, some workers[137] made use of paraffin oil as an auxiliary or 'kindling' substance to enhance the efficiency of the combustion process, but despite this, some carbon residues were still found in the crucible. It appears that the mass of the metallic crucible in which the combustion occurs and hence its heat capacity plays an important role in determining the efficiency of the reaction. A fused silica crucible would certainly 'quench' the high temperatures considerably less than any metallic crucible, but in practice the choice of such refractory materials is precluded by the low resistance to attack by acids, especially strong hydro-halogen acids which are generated during the combustion of halogen-containing compounds.

Regarding the third problem, gold and platinum crucibles should be used for very high accuracy, calorimetric investigations, but in this work an ordinary high temperature resistant nickel-chromium alloy crucible was used instead. The inner surface of the crucible which is directly exposed to the flame was found to become coated with a thin and uniform white layer (possibly a mixture of Ni and Cr oxides) after the first few firings, but as no further deterioration was observed, it was assumed that the surface had effectively become passivated to further attack and no further precautions were taken.

2.2.4.1 Standards for organo-phosphorus compounds

In the past, early workers[137] have adopted *triethyl phosphate* and even *white phosphorus* admixed with *Perspex*[139] as phoshorus reference standards, but several problems arose in both cases; triethyl phosphate is a liquid at room temperature and it had to be sealed into small glass ampoules prior to firing, whereas white phosphorus was prone to early oxidation in the pressurised bomb prior to ignition.

As previously mentioned (Section 2.2.1.1) the phosphorus reference standards of choice in this work were triphenylphosphine oxide and triphenylphosphine (Section 4.1.1.2). Although triphenylphosphine is no longer recognised as an official secondary standard for organo-phosphorus compounds,[123] it was nevertheless decided to calorimetrically assess this compound as well as triphenylphosphine oxide in order to gain more insight into the combustion stoichiometry of this class of substances.

2.2.4.2 Measurement of the standard internal energy of combustion of triphenylphoshine and triphenylphosphine oxide

A total of ten replicate combustion experiments were performed on triphenylphosphine oxide and as many as thirteen on triphenylphosphine (Section 4.1.1.2). The experimental results are given in Tables 2.17 and 2.19, respectively. The combustions were found to be almost complete with very little carbon residue being left in the crucible. No auxiliary substances were added to the sample pellet in the crucible apart from the cotton thread ignition promoter.

After each replicate combustion experiment, the filtered bomb washings were analysed for phosphoric acid by IC (Section 4.1.3) and titrimetry (0.1 M standard NaOH to a methyl-orange end point,[140] [Section 2.2.4.3]). Using this data, the corrections due to the energy of solution of crystalline phosphoric acid (ΔU^{o}_{s} $H_3PO_{4(s)}$ = 12.12 kJ mol^{-1}, taken from Bedford and Mortimer[137]) were estimated, as an average for the unit mass of sample burnt, to be 25 J (g of sample)$^{-1}$ for triphenylphosphine oxide and 30 J (g of sample)$^{-1}$ for triphenylphosphine. The energy of combustion of soot (amorphous carbon) to carbon dioxide was not

accounted for, as the black residue found in the crucible after each firing was not chemically identified. The energy of ignition and the Washburn corrections to standard states were neglected. The overall uncertainties affecting the mean energy of combustion of the two compounds were estimated by propagating the uncertainties associated with the precision of the calorimetric techniques to (a) the heat equivalent of the calorimeter and (b) the value for the energy of combustion of benzoic acid used in the calibration experiments (Section 2.2.2.4). Both estimated uncertainty intervals were larger than those affecting the calibration of the calorimeter (i.e. combustion of benzoic acid). This disparity was attributed to (a) the use of a static bomb technique and (2) the less clean combustion reactions of the phosphorus compounds as opposed to the very clean combustion of benzoic acid.

Only one replicate result for triphenylphosphine was rejected, by application of the Q-test at the 90% confidence level[129] (Section 2.2.2.4). A comparison of the measured values of the energy of combustion of the two compounds with those given in the literature indicated an excellent agreement. The experimental values were slightly higher than the figures quoted by earlier workers who used a rotating bomb technique, and were in closer agreement with those obtained using a static adiabatic calorimeter similar to the one used in this work (Tables 2.18 and 2.20). The uncertainties quoted for both compounds[137] are considerably smaller than those estimated in this work. This was attributed to the use, by these authors, of Rossini's recommendation (Section 2.2.2.4) and to the high precision thermometers used. In this work, the nominal accuracy of the digital thermometer was only ±0.001 K. Nevertheless, the uncertainties affecting the experimental data amounted to less than ±1%.

Combustion experiment	Mass of firing cotton (g)	Mass of sample (g)	ΔT corr (K)	**$-\Delta U_c$ (J g^{-1}) rounded to 4 signif. figures**
1	0.0750	0.5438	1.928	**36030**
2	0.0749	0.5509	1.948	**35960**
3	0.0582	0.5526	1.942	**36260**
4	0.0725	0.6145	2.171	**36260**
5	0.0690	0.5484	1.945	**36250**
6	0.0785	0.5646	1.999	**35970**
7	0.0774	0.6370	2.253	**36230**
8	0.0711	0.6083	2.136	**36040**
9	0.0749	0.6451	2.270	**36120**
10	0.0530	0.5092	1.780	**36100**
Mean and SD %SD				**36120 ± 120 ±0.3%**
$-(-\Delta U_{sol}^{\circ} H_3PO_{4(s)})$ and after propagation of uncertainty				**$-\Delta U_c^{\circ}$= 36090 ± 180 ± 0.5%**

Table 2.17 Experimental results for the standard internal energy of combustion of triphenylphosphine oxide.

This work	**-36090 ± 180**
Bedford and Mortimer (static bomb)[137]	**-35945 ± 45**
Harrop and Head (rotating bomb with water added to bomb)[136]	**-35786 ± 3**
Harrop and Head (rotating bomb with $HClO_4$ added to bomb)[136]	**-36002 ± 4**
Kirklin and Domalsky (rotating bomb)[138]	**-35789 ± 2**

Table 2.18 Values (J g^{-1}) of the standard internal energy of combustion (ΔU_c°) of triphenylphosphine oxide given in the literature.

Combustion experiment	Mass of firing cotton (g)	Mass of sample (g)	ΔT corr (K)	**$-\Delta U_c$ (J g^{-1}) rounded to 4 signif. figures**
1	0.0723	0.5174	1.990	**39260**
2	0.0659	0.5630	2.162	**39600**
3	0.0812	0.5583	2.159	**39400**
4	0.0789	0.5732	1.931	**34120**
5	0.0601	0.5638	2.151	**39510**
6	0.0707	0.6162	2.357	**39480**
7	0.0590	0.5687	2.159	**39350**
8	0.0574	0.7001	2.633	**39360**
9	0.0738	0.6460	2.459	**39280**
10	0.0777	0.5896	2.258	**39200**
11	0.0747	0.6670	2.550	**39500**
12	0.0594	0.6671	2.513	**39330**
13	0.0624	0.6546	2.479	**39420**
Mean and SD %SD				**39400±120 ±0.3%**
$-(-\Delta U_{sol}{}^{\circ}H_3PO_{4(s)})$ and after propagation of uncertainty				**$-\Delta U_c{}^{o}$ = 39370 ± 190 ± 0.5%**

Table 2.19 Experimental results for the standard internal energy of combustion of triphenylphosphine. Experiment 4 was rejected by virtue of the Q-test (highlighted in grey).

This work	**-39370 ± 190**
Bedford and Mortimer (static bomb)[137]	**-39248 ± 37**
Harrop and Head (rotating bomb with water added to bomb)[136]	**-39200 ± 3**
Harrop and head (rotating bomb with $HClO_4$ added to bomb)[136]	**-39204 ± 57**

Table 2.20 Values (J g^{-1}) for the standard internal energy of combustion ($\Delta U_c{}^{o}$) of triphenylphosphine given in the literature.

2.2.4.3 Stoichiometry of combustion reaction and product analysis

The combustion in excess oxygen of triphenylphoshine and triphenylphosphine oxide refer[138] to the following idealized reactions:

$$(C_6H_5)_3P_{(s)} + 23O_{2\,(g)} \rightarrow 18CO_{2\,(g)} + (H_3PO_4 + 6H_2O)_{(aq)} \quad (27)$$

$$(C_6H_5)_3PO_{(s)} + 22.5O_{2\,(g)} \rightarrow 18CO_{2\,(g)} + (H_3PO_4 + 6H_2O)_{(aq)} \quad (28)$$

In Equations 27 and 28 the only phosphorus-containing product of reaction is phosphoric acid, H_3PO_4, but in reality, as already mentioned, diphosphoric acid ($H_4P_2O_7$) and traces of tripolyphosphoric acid ($H_5P_3O_{10}$), and possibly even higher polycondensed species, are also formed.[136,138] In this work, phosphoric acid was analysed as phosphate anion PO_4^{3-} by Ion exchange Chromatography which was chosen as the analytical technique of choice following the work of Kirklin and Domalski[138] who stated that ion chromatography should prove "*a promising alternative method* [to titrimetry] *for determining the extent of side reactions that occur during the bomb process"*. The IC column employed (Section 3.1.3) could also be used to analyse fluoride and nitrate at the same time as the phosphate anion. The ion chromatograph was calibrated for orthophosphate, nitrate and fluoride with standard solutions of analytical reagent grade KH_2PO_4, KNO_3 and NaF.

Each data point on the plot was taken as the mean of four replicate runs for the same standard. This procedure enabled the concentration range of 'maximum instrumental precision' for each anion[141] to be identified, so that the sample solution could be diluted to closely match an 'optimum' concentration value. For the orthophosphate anion this range was found to lie between 7 and 10 ppm (wt/vol) with an average instrumental response precision of ±0.4%. The calibration plot for orthophosphate is shown in Figure 2.25. The calibration line was not made to intercept the origin of the axes as a much better correlation coefficient (R^2>0.999) could be obtained in this way.

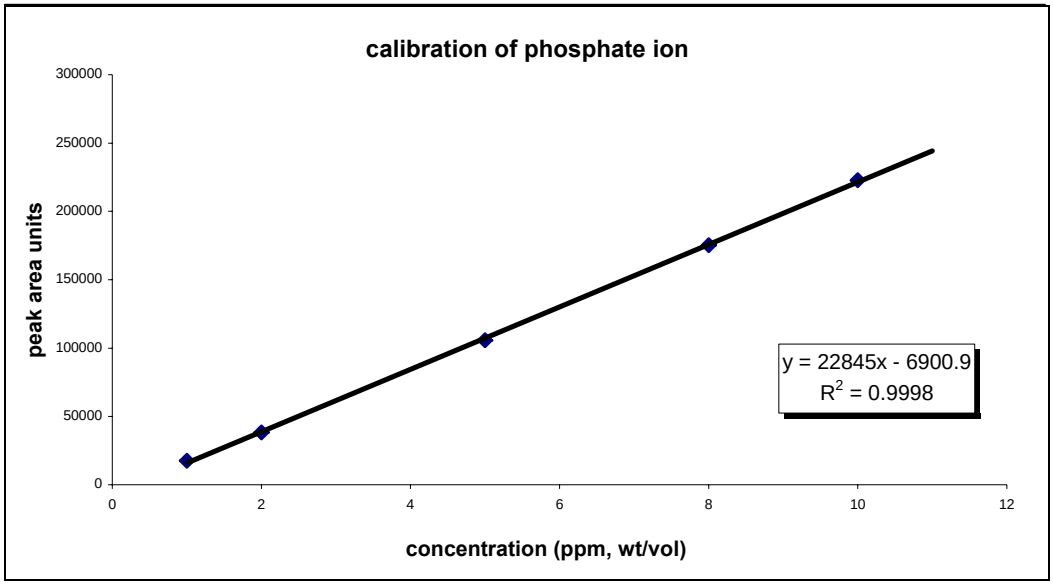

Figure 2.27 IC calibration line for phosphate, in the concentration range 1 to 10 ppm (wt/vol).

During the 'chemical part' of the calorimetric investigations, the initial amount of water added to the bomb prior to sealing it was only 1± 0.05 ml, following the experimental work of Kirklin and Domalski.[138] Although only phosphate was detected in the resulting bomb solutions of both phosphorus standards, Kirklin and Domalsky reported[138] small quantities of diphosphate $P_2O_7^{4-}$ and tripolyphosphate $P_3O_{10}^{5-}$ using a *Dionex AS5* column, which is specifically designed for the simultaneous determination of condensed phosphates. With the aid of the *AS5* column these workers were also able to quantify the percentage molar ratios of the three detected phosphates as follows: 84.1: 9.1: 5.4 (phosphate: diphosphate: tripolyphosphate) for triphenylphosphine oxide and 84.4: 8.9: 5.4 (phosphate: diphospahte: tripolyphosphate) for triphenylphosphine. Using these figures the authors went on to estimate the contribution of the enthalpy of hydrolysis of the diphosphoric and tripolyphosphoric acids to phosphoric acid, and found that the total corrections to the mean specific energy of combustion of the two substances were approximately 7.3 Jg^{-1} and 7.7 Jg^{-1} for triphenylphosphine oxide and triphenylphosphine respectively. These corrections amounted to a mere 0.02% of the total energies of combustion.

In this work, the initial analysis of the bomb solutions yielded approximately 69% of the theoretical phosphate expected for the mass of sample burnt, this figure being identical for both triphenylphosphine and triphenylphosphine oxide. In order to assess the role of the quantity of water added to the bomb prior to firing on the amount of 'recovered' orthophosphate, a larger volume of water (10 ±0.05 ml) was added to the bomb, which was also shaken vigorously twenty minutes after firing, in order to homogenize the contents as much as possible and also to promote dissolution of any phoshoric acid that may have been left 'hovering' in the bomb as a fine airborne mist.[142] Two replicate firings were carried out for both compounds and these yielded values close to 75% of the theoretical phosphate expected. In order to assess whether time also played a part in the yield of recovered orthophosphate, one more combustion of triphenylphosphine was carried out and the bomb was left unopened over the weekend, thus allowing plenty of time (approximately 63 h) for the equilibration of the system. This yielded a final recovery of 84% of the expected phosphate, equal to the percent of phosphoric acid reported by Kirklin and Domalski.[138] Titration of the same bomb solution with standard NaOH (methyl-orange) however, consistently yielded 100% of the theoretical H_3PO_4 expected and the cause for the analytical disparity could not at first be explained until the dissociation constants[29] of phosphoric and diphosphoric acids were compared:

For H_3PO_4	$Ka_1 = 1.1 \times 10^{-2}$	$pKa_1 = 1.95$
	$Ka_2 = 7.5 \times 10^{-8}$	$pKa_2 = 7.12$
	$Ka_3 = 4.8 \times 10^{-13}$	$pKa_3 = 12.32$
For $H_4P_2O_7$	$Ka_1 = 3 \times 10^{-2}$	$pKa_1 = 1.52$
	$Ka_2 = 4.4 \times 10^{-3}$	$pKa_2 = 2.32$
	$Ka_3 = 2.5 \times 10^{-7}$	$pKa_3 = 6.60$
	$Ka_4 = 5.6 \times 10^{-10}$	$pKa_4 = 9.20$

It became apparent that titrating a mixture of phosphoric (XXV in Figure 2.26) and diphosphoric acids (XXVI in Figure 2.26) (as the major components) with standard monovalent base to a methyl-orange end-point (pH interval[141] = 3-4.6) effectively titrated the first dissociation of phosphoric acid but *also* the first *two*

dissociations of diphosphoric acid (underlined for clarity above). This was thought to be the likely cause for the 'quantitative recovery' of phosphoric acid by titration alone, whereas IC did not analyse for polycondensed acid species.

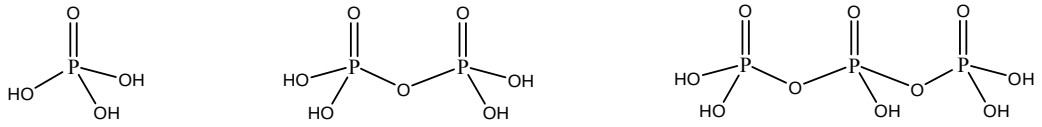

XXV orthophosphoric acid XXVI diphosphoric acid XXVII tripolyphosphoric acid

Figure 2.28 Structures of phosphoric, diphosphoric (pyrophosphoric) and tripolyphosphoric acids.

An attempt was made to determine the diphosphoric acid content in the bomb solutions by application of a rapid titrimetric method of determination of diphosphoric acid when in mixture with phosphoric acid which was found in the literature.[143] The method is based on the following reaction (Equation 30):

$$Na_2H_2P_2O_7 + 2ZnSO_4 \rightarrow Zn_2P_2O_7 + Na_2SO_4 + H_2SO_4 \qquad (30)$$

Bromophenol blue indicator was added to a known volume of diphosphate containing solution and the solution was titrated with standard 0.1 M NaOH until a faint blue coloration was obtained, at which point the disodium diphosphate would be present in solution. $ZnSO_4$ (3 times the stoichiometric amount required) was then added and the liberated sulphuric acid (which destroys the faint blue coloration) was back-titrated with the same titrant until the faint blue colour reappeared.

This method was attempted several times and although it detected the presence of pyrophosphate qualitatively when the $ZnSO_4$ was added, it actually failed to yield reproducibly quantitative results because of the very progressive colour change of the indicator in the second step of the procedure (e.g. back titration of sulphuric acid) which made the visual detection of the end-point very difficult, even with the aid of a visual comparison of the 'basic' form of the indicator.

To solve the diphosphoric acid problem, a search in the literature was successful in finding references[144,145] for the rate of hydrolysis of diphosphoric acid in

aqueous solutions at various pHs and it was shown that, at ambient temperature, the time for complete hydrolysis to phosphoric acid was very long, of the order of weeks if no hydrolytic agent (e.g. a mineral acid at high concentrations) was present and that the kinetics was (pseudo) first order. Thus the degree of hydrolysis did indeed vary with time but not significantly over the short period of a weekend. The hydrolysis reaction of diphosphoric acid follows (Equation 31):

$$H_4P_2O_7 + H_2O \rightarrow 2H_3PO_4 \qquad (31)$$

To demonstrate that the rate of hydrolysis could be responsible for the disparity observed between the quantitative determinations of orthophosphate analysed by ion chromatography and simple acidimetric titration, the bomb washings of two replicate firings for both phosphorus-containing compounds were boiled under reflux for 4 hours. Ion chromatography of these solutions yielded an average of 99.6% and 99.8% respectively of the theoretical phosphate expected, confirming that hydrolysis of diphosphate (and also of tripolyphosphate, if present) to orthophosphate had indeed occurred during the boil. Titration of aliquots of the boiled solution with standard 0.1 M NaOH gave quantitative recovery of phosphoric acid, a result practically indistinguishable from that given by the titration of aliquots of the same bomb solution carried out just minutes after a firing, when the mole fraction of diphosphate is, in theory, at its maximum. The result was later confirmed by repeating the same procedure for a commercial sample of diphosphoric acid (technical purity, Aldrich).

The difference in the quantity of orthophosphate detected by IC in the boiled solutions and in the same solutions that had not been boiled, gave an estimation of the mole fraction of diphosphate present as condensed acids. From the IC results it was also possible to compute the average mole fraction of condensed acids formed during combustion experiments with different quantities of water added to the bomb, (Table 2.21).

Volume of water added initially to the bomb prior to firing (ml ±0.05)	**Mole percent of diphosphate (within a few hours after firing)**
1.0	**31**
10.0	**25**
20.0	**20**

Table 2.21 An estimate of the average mole fraction of condensed phosphorus acids with respect to the initial volume of water added to the bomb for triphenylphosphine.

The approximate energy of hydrolysis of condensed polyphosphate anions to the orthophosphate anion amounts to only 14 kJ per mole of orthophosphate formed.[138] This would indicate an approximate correction of 8.27 Jg^{-1} for triphenylphosphine oxide and 8.29 Jg^{-1} for triphenylphosphine when a volume of 1 ml is added to the bomb, which is in good agreement with the values estimated by Kirklin and Domalsky (7.31 Jg^{-1} and 7.72 Jg^{-1} with 3 ml of water added to the bomb). These energy contributions are so small that they can be safely disregarded, especially when compared to the relatively large uncertainties associated with the measured values of the energies of combustion of these compounds.

2.2.4.4 Conclusions

When burning samples of triphenylphosphine and triphenylphosphine oxide in an oxygen bomb, phosphorus is converted mainly to phosphoric acid (approximately 70-80%) and other polycondensed phosphorus acids (20-30%). These percentages depend on the volume of water added to the bomb prior to firing, the mass of substance burnt and, within a few days, to the period of time between firing and analysis of the bomb solutions.

Ion chromatography confirmed that all phosphorus oxides formed in the combustion reaction were hydrolysed to phosphorus acids. Boiling for 4 h under reflux hydrolysed all polycondensed acids in solution to phosphoric acid.

Full qualitative and quantitative detection of the polycondensed acids formed during the combustion would have required a specific IC analytical column, but

considering the small contribution due to the energy of hydrolysis of these species to the total energy of combustion of the phosphorus-containing standards, the purchase of this column did not seem justified.

For the two phosphorus-containing secondary standards, it was shown that the Gallenkamp static bomb calorimeter was able to produce data which correlated well with published values, but was generally subject to uncertainties which were considerably greater than those found in literature studies.

2.2.5 Oxygen combustion calorimetry of organo-fluorine compounds

The combustion calorimetry of organo-fluorine compounds has received limited consideration over the last forty years. There is in fact only a handful of dated papers in the literature (late 1950s and early 1960s) and this might be due to scarce research interest in thermochemical data regarding fluorinated organic compounds. Much more work[146,147,148,149] has been carried out on chlorine-containing compounds in order to calculate quantities such as enthalpies of formation or *carbon-chlorine* bond dissociation energies, and generally because of the more common use of chlorinated precursors in preparative organic chemistry.

The combustion of fluorinated organic compounds in an oxygen vessel poses fewer problems than organo-phosphorus compounds, the only real setbacks being the highly corrosive nature of the hydrofluoric acid formed, which has imposed the use of expensive precious metals like platinum and tantalum as liners for the bomb inner surfaces and electrodes, (sometimes gold for the crucible) and also the need for a rotating bomb system in order to account for the relatively high energy of dilution of HF in water. Despite these considerations, the use of a static bomb technique was considered to be justified in this work because, as in the case for phosphoric acid, these corrections are negligible when compared to the total energy of combustion of the fluorine-containing compound.

2.2.5.1 Secondary standards for organo-fluorine compounds

As a suitable standard for the combustion of organo-fluorine compounds of *low* fluorine content, the compound 4-fluorobenzoic acid (Section 4.1.1.2) was chosen

because at least two independent values[150,151] of the standard energy of combustion were found in the literature and because the atomic ratio fluorine to hydrogen is low compared to other fluorinated substances. Many other fluorine containing substances have been thermochemically investigated, viz. hexafluorobenzene,[152] 2-fluorobenzoic acid, pentafluorobenzoic acid,[151] octafluorotoluene[153] and polytetrafluoroethylene,[154] but only one experimental value for the energy of combustion of each one of these substances was published in the literature.

2.2.5.2 Measurement of the standard internal energy of combustion of 4-fluorobenzoic acid

After five initial test firings of 4-fluorobenzoic acid there were no visible signs of corrosion on the internal walls of the bomb. A very mild discoloration of the firing electrodes was noticed but, as for the crucible, no further damage was detected. Platinum crucibles have been used in previous work with fluorine compounds and despite the chemical inertness of this metal, a mass loss up to 2 mg per firing was detected.[150] This was attributed to the formation of volatile platinum fluorides. However the energy correction for this process, coupled with the hydrolysis of the fluorides produced was shown to be negligible. In this work no mass loss of the crucible was found and this was attributed to the 'unorthodox' passivation that had occurred when previously burning the phosphorus-containing standards.

The more highly fluorinated compounds are reported[95] to be less easily combustible in pressurized oxygen and a number of expedients were developed in the past in order to ensure quantitative combustions; some workers used perforated crucibles which allowed more oxygen to come in contact with the burning compound, in some other cases a simple increase of the oxygen pressure coupled with the use of a small heat-reflector yielded significantly cleaner reactions.[95] Despite these early attempts, the technique which proved most successful for this purpose was the combustion of an auxiliary substance, usually paraffin oil,[150] thoroughly admixed with the organo-fluorine compound. Admixture of a 'kindling' hydrocarbon serves to lower the atomic ratio of fluorine

to hydrogen in the combustion charge and to reduce the formation of carbon tetrafluoride (CF_4) which in turn reduces the energy correction due to this undesirable side reaction. According to the literature,[151] mass spectrometric analysis of the gaseous products from the combustion of various organo-fluorine compounds did not detect other fluorine-containing species other than hydrogen fluoride and carbon tetrafluoride, although the accuracy of the analysis was reported to be low. Auxiliary substances have also been employed[155] to 'dilute' the deflagrative combustion typically displayed by some energetic fluorine compounds containing NF_2 groups.

In this work, a total of thirteen replicate calorimetric measurements were performed on 4-fluorobenzoic acid. The experimental results are given in Table 2.22. The combustions were found to be clean with little carbon residue being left in the crucible. This residue was not quantified. The general calorimetric method and derivation of the corrected temperature rise for the experiments has been described in Sections 2.2.2.1 and 4.1.1.2. The only difference from the combustion experiments of organo-phosphorus compounds consisted in the slow venting of the gaseous contents of the bomb into suba-sealed glass ampoules at the end of each experiment, in order to analyse the composition of the exhaust gases by GC-MS. The bomb would then be opened, the acidic solution transferred carefully to a volumetric flask and subsequently analysed by Ion Chromatography and titrimetry (Sections 2.2.5.3 and 4.1.3).

The Washburn corrections to standard states, the energy of ignition and the energy of solution of CO_2 in aqueous HF were neglected. The overall standard deviation associated with the mean energy of combustion was estimated by propagation of the uncertainties associated with the energy equivalent of the calorimeter and the standard energy of combustion of benzoic acid. Comparing the experimental value with those given in the literature (Table 2.23), it appears that there is good agreement, although the uncertainties reported by these earlier workers are, as in the case of the organo-phosphorus standards (Section 2.2.4.2), much smaller.

Combustion experiment	Mass of firing cotton (g)	Mass of sample (g)	ΔT corr (K)	**$-\Delta U_c$ (J g^{-1}) rounded to 4 signif. figures**
1	0.1000	0.2901	0.739	**21590**
2	0.0791	0.2859	0.706	**21930**
3	0.1136	1.1943	2.611	**22040**
4	0.0682	1.1453	2.430	**21970**
5	0.0846	0.6824	1.517	**21940**
6	0.0840	0.5957	1.336	**21860**
7	0.0780	0.4733	1.074	**21730**
8	0.0796	0.4795	1.108	**22150**
9	0.0653	0.4437	1.006	**22010**
10	0.0649	0.4812	1.077	**21900**
11	0.1148	0.6055	1.423	**22160**
12	0.0801	0.6419	1.423	**21860**
13	0.0893	1.1897	2.547	**21910**
Mean and SD %SD				**21930 ± 150 ± 0.7%**
After propagation of uncertainty				**$-\Delta U_c^o$= 21930 ± 200 ±0.9%**

Table 2.22 Experimental results for the standard internal energy of combustion of 4-fluorobenzoic acid.

This work	**-21930 ± 200**
Good, Scott and Waddington (rotating bomb)[150]	**-21830 ± 4**
Cox, Gundry and Head (rotating bomb)[151]	**-21862 ± 1**
Swarts (static bomb)[156]	**-22078 ± ?**

Table 2.23 Values (J g^{-1}) of the standard internal energy of combustion (ΔU_c^o) of 4-fluorobenzoic acid given in the literature.

The very small magnitude of the uncertainty intervals quoted in the literature was attributed to the high precision of the balances and thermometers used (values with six decimal places for temperature and five decimal places for weight [in air] are quoted). In addition, the samples of 4-fluorobenzoic acid used by all workers

were purified by crystallization from 50% aqueous ethanol followed by vacuum sublimation and/or zone refining,[150,151] which brought the final purity to over 99.9%. In this work the commercial sample (99.5% certified) was not purified further.

2.2.5.3 Stoichiometry of combustion reaction and product analysis

The nature of the products generated during the combustion of organo-fluorine compounds has been shown[150,151] to be critically dependant on *the atomic fluorine to hydrogen ratio* within the molecule. In the combustion of a hypothetical compound $C_aH_bO_cF_e$ in the presence of water, the reaction satisfies Equation 32 if **b>e** (the fluorine is quantitatively converted to hydrogen fluoride), but satisfies[155] Equation 33 instead, if **b≤e** (i.e. carbon tetrafluoride is also generated):

$$C_aH_bO_cF_e + \left(\frac{4a+b-2c-e}{4}\right)O_2 + \left[\frac{e(1+2n)-b}{2}\right]H_2O \longrightarrow aCO_2 + e\left[HF\,.\,nH_2O\right] \quad (32)$$

$$C_aH_bO_cF_e + \left(\frac{4a+b-2c-e}{4}\right)O_2 + \left[\frac{(e-4z)(1+2n)-b}{2}\right]H_2O \longrightarrow (a-z)CO_2 + zCF_4 + (e-4z)\left[HF\,.\,nH_2O\right] \quad (33)$$

The amount of carbon tetrafluoride arising from the combustion of an organo-fluorine compound for which b≤e was shown[151] to be greatly reduced if a hydrogen-containing substance was burned along with the fluorine compound. In the same study, it was nevertheless concluded that it was not possible to eliminate completely the formation of carbon tetrafluoride without using a very large excess of auxiliary substance, which seriously lowered the accuracy of the measured energy of combustion of the fluorine compound. The proportion of fluorine in the system that was converted to CF_4 was reported to vary between 1 and 4% when burning pentafluorobenzoic acid admixed with benzoic acid, and as much as 10 to 21% for the combustion of decafluorocyclohexane admixed with hydrocarbon oil. In this least favourable case, the correction of the energy of the reaction of Equation 33 to that of the idealized reaction of Equation 32 amounted to only 1.7% of the total measured energy change. This figure was estimated by direct alkali titration of the portion of fluorine which appeared as HF in the bomb liquid contents. A quantitative determination of the concentration of carbon tetrafluoride in the bomb gases was also attempted by mass spectrometry and, although the

results are described[150] as being "…*not very precise*", the method confirmed that no fluorine-containing gases other than carbon tetrafluoride and hydrogen fluoride were present in the bomb exhausts. It was also observed that "…*the heights of the mass peaks correlated well with the calculated mole fraction of* CF_4."

The poor precision affecting the results led the authors to assess the completeness of the reaction by gravimetric determination of carbon dioxide, following adsorption on a silica substrate coated with NaOH (Ascarite^{TM}). A scrubber containing a 0.1 M solution of sodium fluoride was interposed between the venting bomb and the adsorbent tube in order to trap residual hydrogen fluoride as the bifluoride ion, which would also be quantified by alkali titration. Recoveries of carbon dioxide of 100.00 ± 0.01% were reported after combustion of 4-fluorobenzoic acid, so that no CF_4 could have been formed when combusting this standard substance.

Although the idealized combustion reaction of 4-fluorobenzoic acid follows, by convention,[123] the stoichiometry given in Equation 34,

$$C_7H_5O_2F_{(s)} + 7O_{2(g)} + 18H_2O_{(l)} \rightarrow 7CO_{2(g)} + HF(20H_2O)_{(l)} \qquad (34)$$

the final concentration of HF in the liquid contents of the bomb depends on the volume of water that is placed in the bomb prior to firing, which in turn plays a minor role in the final energy change because the solubility and energy of solution of carbon dioxide in dilute, aqueous hydrofluoric acid solutions depends on the final acid concentration. In high precision calorimetry, the *comparison method* is normally used to rectify this problem: the energy equivalent of the calorimeter is determined by combustion of benzoic acid in the presence of an aqueous solution of HF of approximately the same concentration as that expected to be found after the combustion of the fluorine-containing sample. Alternatively, the small thermal correction may also be derived from the impressive work of Cox and Head[157] who have shown that its magnitude corresponds to only approximately 0.1% of the total energy liberated in the combustion reaction. In this work, this minute correction was disregarded.

In this work, the total amounts of hydrogen fluoride generated in the combustion experiments was analysed by alkali titration using 0.1M NaOH to a

phenolphthalein end-point after removal of carbon dioxide by boiling of the 'bomb solutions' for a few minutes, and also by Ion exchange Chromatography. The calibration plot for fluoride is shown in Figure 2.29. The line was calculated using six points, each representing the mean of four replicate runs for the same standard solution. The concentration range of 'maximum instrumental precision' for fluoride was found to lie between 2 and 5 ppm with an average response precision of ± 0.3%. The calibration line was not made to intercept the origin of the axes as a better correlation coefficient (R^2>0.999) could be obtained in this way.

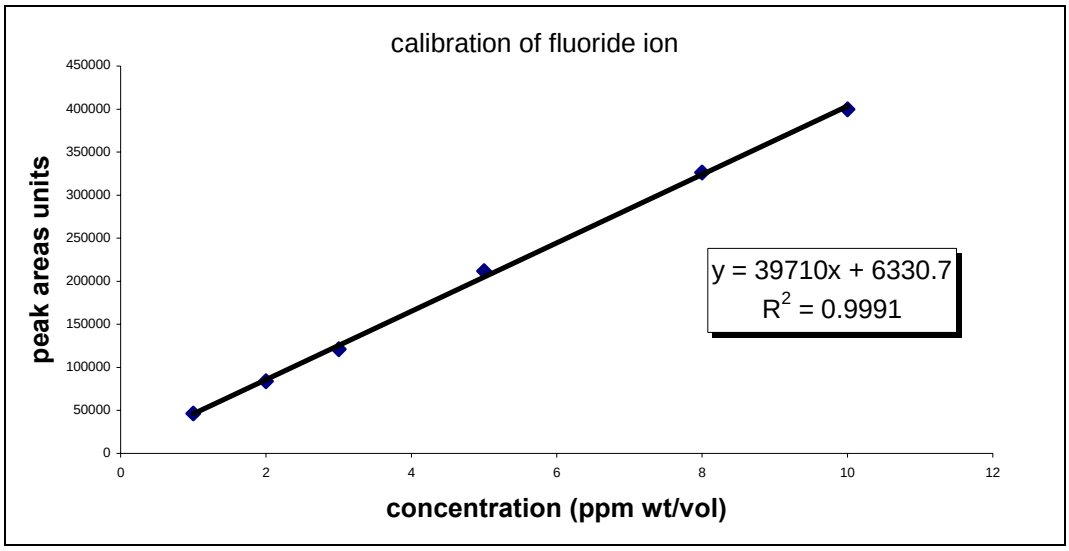

Figure 2.29 IC calibration line for fluoride, in the concentration range 1 to 10 ppm (wt/vol)

A close examination of the percentage of fluorine recovered as aqueous HF in the bomb washings from combustion experiments in which different volumes of water were added to the bomb prior to firing (Table 2.24), suggested that the presence of a relatively large volume of water shifted the equilibrium $HF_{(g)} = HF_{(aq)}$ to the right, which in turn yielded higher recoveries of hydrogen fluoride in solution. There also appeared to be an upper limit for the volume of water needed for the *maximum* recovery of HF in solution. This corresponded to the volume of water (5 ml) which totally covers the interior bottom of the bomb,

yielding the largest possible liquid-phase surface area. Prolonged manual agitation of the bomb after a firing was also attempted although no increase in the yield of hydrogen fluoride recovered in the bomb solutions was observed. These observations would tentatively suggest that most of the HF present in the gas-phase during and/or immediately after a combustion experiment, is dissolved almost immediately on contact with the water surface and that only a tiny fraction of the total HF formed remains in the gas-phase.

The exhaust gases from each combustion experiment were vented through a 0.1M solution of NaF, as suggested by Good *at al.*[150] in order to trap the residual 'gaseous' hydrogen fluoride as the bifluoride ion HF_2^- which was then quantified by titration with standard base, and also by ion chromatography. The results revealed that only up to 2% of the total expected theoretical amount of HF was 'captured' by the sodium fluoride solution trap, when residual quantities of up to 10% were expected. These results indicate that although the bomb exhaust gases were very slowly (30 min) vented through the NaF solution as a very fine stream of small bubbles to maximize the surface and time of contact with the liquid phase, most of the remaining hydrogen fluoride apparently left in the gas-phase failed to be trapped and was not detected.

In order to confirm unequivocally that hydrogen fluoride was indeed the only fluoride-containing species formed during the combustion of the standard 4-fluorobenzoic acid, the bomb gases were vented through small rubber septum-sealed glass ampoules and qualitatively analysed by GC-MS (EI, 70 eV). No carbon tetrafluoride was detected, as shown in Figure 2.30*b*, confirming that hydrogen fluoride is the only fluorine-containing species formed in the combustion of the standard compound. In order to provide a visual reference, the total-ion-current (TIC) chromatograph for a sample of exhaust gases collected from the combustion of poly(tetrafluoroethylene), PTFE (powder, Aldrich) which was shown to generate CF_4 in appreciable amounts is shown in Figure 2.30*a*. Figure 2.31 shows the electron impact (70 eV) fragmentation pattern of the detected carbon tetrafluoride compared to the MS reference library spectrum.

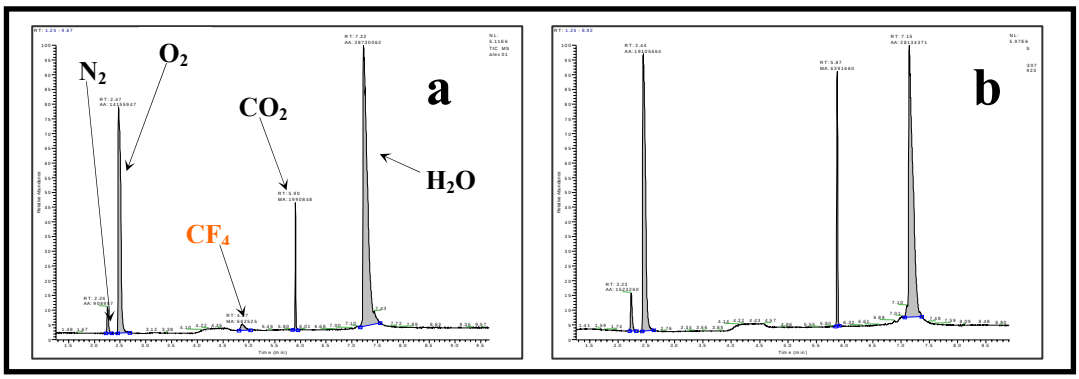

Figure 2.30 Total ion current (TIC) chromatographs of (a) a sample of gaseous exhausts from the combustion of PTFE and (b) a sample of exhaust gases from the combustion of 4-fluorobenzoic acid.

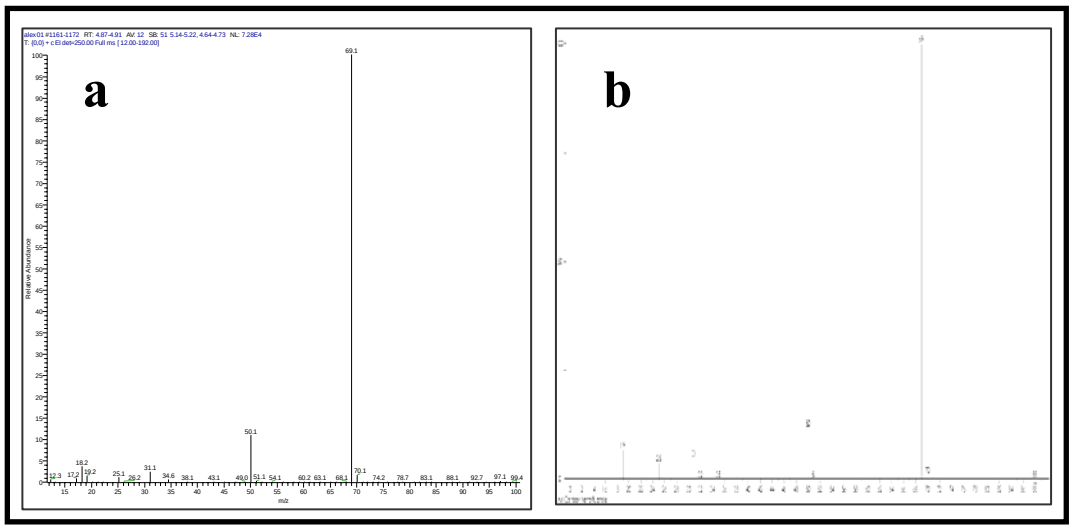

Figure 2.31 Experimental mass spectrum (EI, 70eV) of CF_4 detected in the combustion exhaust gases from PTFE (a) and the reference mass spectrum of CF_4 from the instrumental library of mass spectra (b).

In order to confirm that the presence of a 'kindling' hydrocarbon significantly reduced the amount of carbon tetrafluoride formed during the combustion of PTFE as reported in the literature, a set of two combustion experiments was also carried out in which the same mass of PTFE was burnt along *with* (Experiment A) and *without* (Experiment B) twice its weight of admixed analytical reagent

benzoic acid. Benzoic acid is reported[151] to be more effective than hydrocarbon oil at minimizing the formation of CF_4. Ion chromatography and alkali titration were employed to assess the amounts of HF present in the bomb solutions after combustion, while samples of the respective exhaust gases were analysed by GC-MS. The results confirmed that the formation of CF_4 is indeed hindered when benzoic acid is admixed with a highly fluorinated compound; 71% of the total fluorine was recovered as HF in the bomb washings of A, whereas only 21.3% was detected in the bomb washings of B, as shown in Table 2.24.

Experiment	PTFE mass (g)	Benzoic acid Mass (g)	Mole % fluorine recovered as HF in washings by IC	Mole % fluorine recovered as HF in washings by alkali titration
A	0.5330	1.1121	**71.0**	**68.1**
B	0.5334	0	**21.3**	**18.3**

Table 2.24 Experimental recovery of fluorine as HF in the bomb washings of Experiments A (PTFE + 4-fluorobenzoic acid) and B (PTFE alone).

Combustion Experiment	Sample mass (g)	Volume of H_2O added to bomb (ml) (±0.05)	Mole % of total fluorine recovered as HF by IC	Mole % of total fluorine recovered as HF by alkali titration
1	0.2901	1.0	**87.4**	**89.4**
2	1.1943	1.0	**91.0**	**91.6**
3	1.2136	5.0	**97.0**	**98.5**
4	0.2859	10.0	**98.0**	**96.0**
5	1.1453	10.0	**95.0**	**95.5**

Table 2.25 Experimental results for the percentage of fluorine recovered as aqueous HF in the bomb washings from firings of 4-fluorobenzoic acid.

2.2.5.4 Thermochemistry of CF_4

In order to estimate the contribution to the energy of combustion from the enthalpy of formation of CF_4 generated during the combustion of organo-fluorine compounds of high fluorine content, high accuracy quantitative analysis of the exhaust gases would be required. Earlier workers[151] indirectly quantified the CF_4 by gravimetric analysis of carbon dioxide, followed by subtraction of the value thus obtained from the theoretical total amount of CO_2 expected, had CF_4 not formed. In this work the amount of carbon tetrafluoride formed could only be estimated by subtracting the amount of fluorine recovered as hydrogen fluoride in the bomb washings from the total amount of fluorine present in the sample. Although this method could appear as a gross simplification, it was found that when as much as 10 ml of water were added to the bomb prior to firing samples of the standard 4-fluorobenzoic acid (Table 2.25), at least 95% of the theoretical fluorine contained in the sample ended up as HF 'recovered' in the bomb solution, with only a negligibly small residual amount being detected in the gas phase.

This statement implies that, when a relatively large volume of water is added to the bomb prior to firing, only up to 5% of the total amount of HF (in the worst case) could be left undetected. Consequently, it was assumed that the magnitude of the uncertainty affecting the estimated energy contribution for the formation of CF_4 would be very small. Gravimetric determination of carbon dioxide would have ultimately helped to reduce the error considerably, but no working procedure to accomplish this was developed. The experimental value for the standard enthalpy of hydrolysis of CF_4 to $HF_{(aq)}$ and CO_2 (ΔH°_{hyd} = -173.97 kJ mol^{-1}) may be derived from the literature[157] and applies to the Equation 35:

$$CF_{4(g)} + 82H_2O_{(l)} \rightarrow CO_{2(g)} + 4[HF \cdot 20H_2O]_{(l)} \qquad (35)$$

This value agrees reasonably well with the theoretical figure for the enthalpy of hydrolysis of CF_4 (ΔH°_{hyd} = -204.31 kJ mol^{-1}) which can be calculated by application of Hess's law to the literature enthalpies of formation[150] of the reaction products reported below:

ΔH_f° CF_4 = - 913.58 kJ mol^{-1} for $\mathbf{C_{(graphite)} + 2F_{2(g)} \rightarrow CF_{4(g)}}$

ΔH_f° CO_2 = - 393.14 kJ mol^{-1} for $\mathbf{C_{(graphite)} + O_{2(g)} \rightarrow CO_{2(g)}}$

And $\Delta H_f°$ $HF{\cdot}20H_2O$ = - 316.13 kcal mol^{-1}

The corresponding ΔU^o_{hyd} value, which *must* be identical to ΔH^o_{hyd} as the volume-work term for the hydrolysis reaction of CF_4 (Equation 34) is zero, effectively accounts for the 'missing' energy that needs to be added to the measured standard energy of combustion of the fluorine-containing compound. For fluorinated compounds that also contain hydrogen this correction is usually small because the amount of CF_4 formed from the typical half-gram weight of substance burnt during the experiment is small when compared to the relatively high oxidation energy of hydrogen. When the fluorine to hydrogen molar ratio in the molecule is greater than 5[150] however, the amount of carbon tetrafluoride formed becomes considerable, especially if no 'kindling' substance is present. In experiment B (Table 2.24) in which no admixed hydrogen-containing substance was added, as much as 79±5% of the total fluorine contained in the PTFE sample ended up as CF_4 (4.21± 0.25 mmol). This would have contributed approximately 860 J or 35% of the mean value of the energy changes observed in the calorimetric experiments (ΔU_c = -2500 J [mean value of 5 replicate firings]). Table 2.26 compares the standard internal energy of combustion of PTFE measured in this work with the only value found in the literature.[150]

In conclusion, the energy of hydrolysis of CF_4 can be an important contributor to the final value of the energy of combustion if no hydrogen is present in the sample because the fluorine has great affinity to carbon. The correction due to energy of formation of CF_4 transits from being small for hydrogen-containing compounds of low fluorine content (1< molar F/H < 5), to considerable, for highly fluorinated compounds and polymers (molar F/H > 5).

This work (without CF_4 correction)	**-5310 ± 110**
This work (with CF_4 correction)	**-6680 ± 110**
Good, Scott and Waddington[150]	**- 6725 ± 4**

Table 2.26 Experimental and literature values (J g^{-1}) for the standard internal energy of combustion of PTFE.

2.2.6 Oxygen combustion calorimetry of nitrogen-containing compounds

During combustion in an oxygen bomb, a small fraction of the total nitrogen present in a nitrogen-containing sample always oxidises to oxides of nitrogen.[158] The latter then react with the water present in the bomb until, after a period of several hours, all the nitrogen initially present in the sample exists either as elemental nitrogen or as aqueous nitric acid. This can usually be determined by titration with standard alkali[159] (using an indicator unaffected by carbon dioxide, if the latter is not removed by boiling first) or, as in this work, as nitrate anion by Ion exchange Chromatography. In the old days the determination of the nitric acid formed in the bomb was carried out by the Devarda's method,[95] in which a strongly reducing mixture of metals is used to convert the nitrate to ammonia which was then titrated with standard acid in the conventional way.

Generally it is acceptable to correct the measured energy of the bomb process for the formation of nitric acid on the assumption that this reaction is complete within the period of the calorimetric determination, but there is some evidence that this is not true. Qualitatively the presence of oxides of nitrogen is revealed by odour in a bomb opened shortly after combustion, but not in one left overnight.[77] The amount of unconverted oxides of nitrogen at the end of the calorimetric experiment is unlikely, however, to introduce a significant error into the final energy value (a reported[77] estimate is 0.02%).

The idealised combustion reaction in excess oxygen for a nitrogen-containing compound, in which only molecular nitrogen is formed, is given by Equation 36:

$$C_aH_bO_cN_d + \left(\frac{4a+b-2c}{4}\right)O_{2\,(g)} \longrightarrow aCO_{2\,(g)} + \frac{b}{2}H_2O_{\,(l)} + \frac{d}{2}N_{2\,(g)} \qquad (36)$$

In reality however, as discussed above, nitric acid is also formed according to the reaction stoichiometry given by Equation 37:

$$C_aH_bO_cN_d + \left(\frac{4a+b-2c}{4}\right)O_{2\,(g)} \longrightarrow aCO_{2\,(g)} + y\left[\ HNO_3\left\{\left(\frac{b-y}{2y}\right)H_2O\right\}\right]_{(l)} + \frac{d-y}{2}N_{2\,(g)} \qquad (37)$$

The value of *y* has been reported[77] to be such that *y/d* was found to be 0.15 (i.e. 15% of the initial molar amount of nitrogen present in the sample had converted to HNO_3), but the exact value of *y* for each experiment can only be determined by analysis of the nitric acid present in the bomb solution, after each firing. Once *y* is known accurately, it is possible to subtract the molar energy of formation of the nitric acid that has formed, from the observed energy change of the bomb process. This energy amounts[160,161] to $\Delta H^o_f\ HNO_{3(aq)}$= -59.7 kJ mol^{-1} and although this value refers to a final concentration of $[HNO_3]_{aq}$ = 0.1 M, the thermal effect of dilution to the much lower concentrations typically found in a bomb after combustion, was shown[162] to be safely negligible.

The amount of nitric acid formed in an oxygen bomb was also shown[163] to be a function of the *square root of the product* of the energy of combustion and the number of nitrogen atoms present in the molecule of the substance burned, so the hotter the flame is, the more oxides of nitrogen are formed. The same process is also known to occur within the extremely hot channels of bolts of lightning[164] (environmental nitrogen fixation) and also in the combustion chambers of diesel engines.[165]

In summary, the formation of nitric acid in a combustion bomb depends on:

- the oxygen pressure in the bomb (at pressures below 10 atm[158])
- the mass of substance burnt
- the nitrogen content in the substance burnt
- the energy of combustion of the substance burnt

2.2.6.1 Secondary standards for nitrogen-containing compounds

Several nitrogen-containing substances have been given 'official status' as reference compounds for the combustion calorimetry of nitrogen-containing

samples. Among these,[123] hippuric acid ($C_9H_9O_3N$), acetanilide (C_8H_9ON) and nicotinic acid ($C_6H_5O_2N$) are the currently recommended test materials for samples of low nitrogen content (below ≤15 wt%). 1,2,4-(1H)-Triazole ($C_2H_3N_3$) is the recommended standard for samples of medium nitrogen content (i.e. 15<N≤40 wt%) that may be combusted in excess oxygen without the need of a kindling agent. Urea (CH_4ON_2) is recommended for samples containing very high proportions of nitrogen (i.e. N > 40 wt%), so that their complete combustion in excess oxygen may be obtained only by the use of an auxiliary material (benzoic acid or paraffin oil). In this work, 1,2,4-(1H)-triazole was selected as the standard of choice (Section 3.1.1.2), as three independent experimental values for its standard energy of combustion were available in the literature.

2.2.6.2 Quantitative analysis of HNO_3 and measurement of the standard internal energy of combustion of 1,2,4-(1H)-triazole

A total of ten replicate combustion experiments were performed on 1,2,4-(1H)-triazole (Table 2.27). The combustions were all found to be surprisingly clean with no residue left in the crucible. The Washburn corrections to standard states as well as the energy of ignition and the energy of dilution of nitric acid from the value of 0.1M to the final concentration found in the bomb solutions were neglected. The general calorimetric method and derivation of the corrected temperature rise has been described in detail in Section 2.2.1.2. The ion chromatographic analysis of the diluted bomb solutions from each experiment has been described in Section 4.1.3. The calibration line for the nitrate anion (6 points) is shown in Figure 2.32. As for the orthophosphate and fluoride anions, the instrument displayed good linearity in the concentration range of calibration (0.1 to 7 ppm wt/vol). The range of 'maximum instrumental precision' for nitrate was however found to lie between 3 and 7 ppm with an average response precision of ± 0.5%. The calibration line was not made to intercept the origin of the axes as a better correlation coefficient (R^2>0.999) could be obtained in this way. Table 2.28 compares the experimentally derived value of ΔU_c^o of 1,2,4-(1H)-triazole with the values quoted in the literature. The results indicated that, on average, 4% of the

total amount of nitrogen initially present in the sample ended up as nitric acid when the bomb was pressurised to 30 atm. The thermal correction due to the formation of nitric acid amounted to approximately 0.4% of the observed energy change.

Combustion experiment	Weight of firing cotton (g)	Weight of sample (g)	Total HNO_3 formed (mmol) as detected by IC	Energy of formation HNO_3 (J)	ΔT corr (K)	**$-\Delta U_c$ (Jg^{-1}) rounded to *4 signif. figures***
1	0.1046	0.7490	1.30	77.6	1.500	**19200**
2	0.0719	0.7711	1.33	79.4	1.494	**19300**
3	0.0809	0.8711	1.51	90.2	1.673	**19120**
4	0.0887	0.8037	1.40	83.6	1.578	**19270**
5	0.0800	0.1932	0.34	20.3	0.475	**19390**
6	0.1116	0.6285	1.05	65.1	1.300	**19260**
7	0.0734	0.6041	1.09	62.7	1.194	**19250**
8	0.0791	0.6327	1.13	65.7	1.257	**19300**
9	0.1122	0.7009	1.29	72.2	1.433	**19300**
10	0.0891	0.7451	1.28	77.0	1.474	**19280**
Mean and SD %SD						**19230 ± 60 (±0.3%)**
After propagation of uncertainty						**$-\Delta U_c^o$= 19230 ± 90 (±0.5%)**

Table 2.27 Experimental results for the standard internal energy of combustion of 1,2,4-(1H)-triazole.

This work	**-19230 ± 90**
Roux, Torres and Dávalos[160]	**-19202 ± 2**
Aleksandrov, Nikina and Novikov[163]	**-19186 ± 13**
Faour and Akasheh[166]	**-19243 ± ?**

Table 2.28 Values ($J\ g^{-1}$) of the standard internal energy of combustion (ΔU_c^o) of 1,2,4-(1H)-triazole given in the literature.

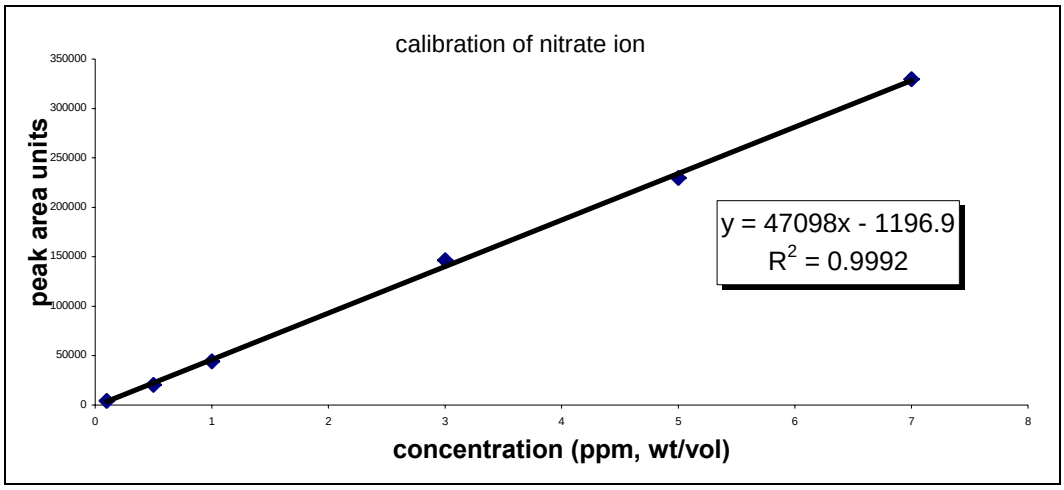

Figure 2.32 IC calibration curve for the nitrate anion in the concentration range 0.1 to 7 ppm (wt/vol).

2.2.7 General conclusions for the combustion calorimetry of the secondary standards

By performing the calorimetric experiments described in Sections 2.2.4, 2.2.5 and 2.2.6, it was concluded that the Gallenkamp static adiabatic calorimeter is capable of replicating proven work, albeit with uncertainty intervals which were estimated to fluctuate around two orders of magnitude over those quoted in the literature for the same reference standards combusted using a high-precision, rotating-bomb technique.

The products of the 'side' reactions were identified and a direct (or indirect) quantitative analytical technique for each side-product was developed. With the exception of carbon tetrafluoride, the magnitudes of the corrections to be made to the respective constant-volume energy changes, due to the formation of the non-ideal products, were assessed and found to be small, albeit not negligible, when compared to the massic energies of combustion of the reference standards.

At the time of writing, no single calorimetric reference standard material for samples containing *two* or *more* hetero-atomic species have yet been designated and calorimetrically evaluated. Nor have the gaseous and aqueous products of combustion of such compound(s) been investigated and thermochemically assessed. Although the calorimetric measurements performed on the well-

characterised secondary standards described in this chapter have undoubtedly shed light on some of the limitations of the calorimetric technique employed in this work, no information regarding the nature of the potentially complex combustion products expected to arise from samples containing multiple hetero-atomic species, like the energetic polyphosphazenes studied in this work, could be sought at this stage of the work.

It is the author's opinion that the lack of such model compounds may effectively open a whole new avenue of future research, but this would necessitate the use of high precision instrumentation.

2.2.8 Qualitative and quantitative analysis of the combustion products (excess oxygen) of linear poly [bis(2,2,2-trifluoroethoxy)phosphazene] and Polymers 1-5

2.2.8.1 Qualitative analysis of the water-soluble (and gaseous) products from linear poly[bis(2,2,2-trifluoroethoxy)phosphazene]

Upon combustion in pressurised oxygen (30 atm), the non-energetic precursor, linear poly[bis(2,2,2-trifluoroethoxy)phosphazene], (pelletized with a small hand-press), yielded, as detected by Ion exchange Chromatography (diluted bomb solutions), the water-soluble species *nitric acid*, *phosphoric acid*, *hydrogen fluoride* and also *two* unidentified species which were eluted at retention times very close to those of the nitrite (NO_2^-) and sulphate (SO_4^{2-}) anions (Figure 2.33).

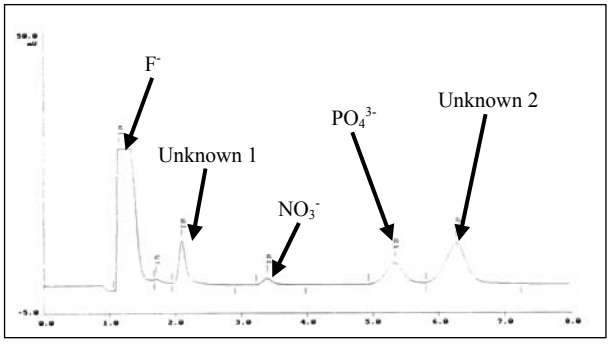

Figure 2.33 Ion chromatogram of the diluted bomb solution from the combustion of a sample of linear poly[bis(2,2,2-trifluoroethoxy)phosphazene] showing two unidentified species (retention time = min).

Spiking the dilute bomb solutions with a solution of sulphate and nitrite (both 3 ppm [wt/vol]) eliminated these as possible species. The same species were also detected, in different ratios, in the post-combustion bomb solutions of pellets of (a) *triphenylphosphine* intimately admixed with *4-fluorobenzoic acid*, and (b) *red phosphorus* intimately admixed with *PTFE* powder (Figure 2.34). These mixtures were evaluated as models for the combustion stoichiometry of the non-energetic precursor linear poly[bis(2,2,2-trifluoroethoxy)phosphazene] which was initially expected to generate small amounts of CF_4 due to its high fluorine content (molar F/P=6, molar F/H=1.5, see Section 2.2.5.3). However, GC-MS (EI, 70eV) analysis of the bomb exhaust gases from the combustion of the polymer precursor, indicated that CF_4 and other potential fluorinated carbon- and/or phosphorus-based gaseous species (Figure 2.35) had not formed, the only species detected in the bomb head-space being *nitrogen*, *carbon dioxide* (and *water* vapour). The complete oxidation of carbon was also confirmed by the absence of carbon monoxide (CO) in the exhaust gases.

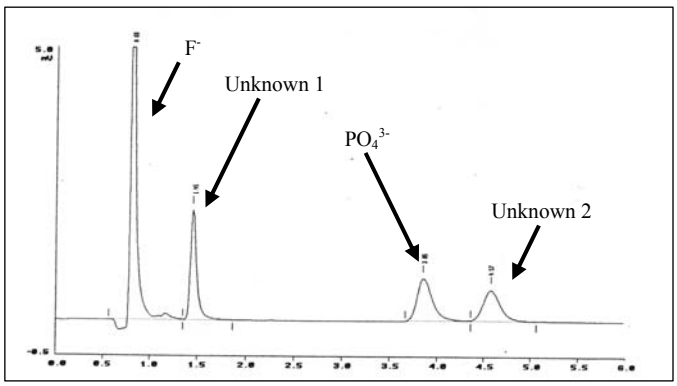

Figure 2.34 Ion chromatograph of the diluted bomb solution from the combustion of a pellet of red phosphorus admixed with PTFE powder (molar F/P=6) showing the two unidentified species (retention time = min).

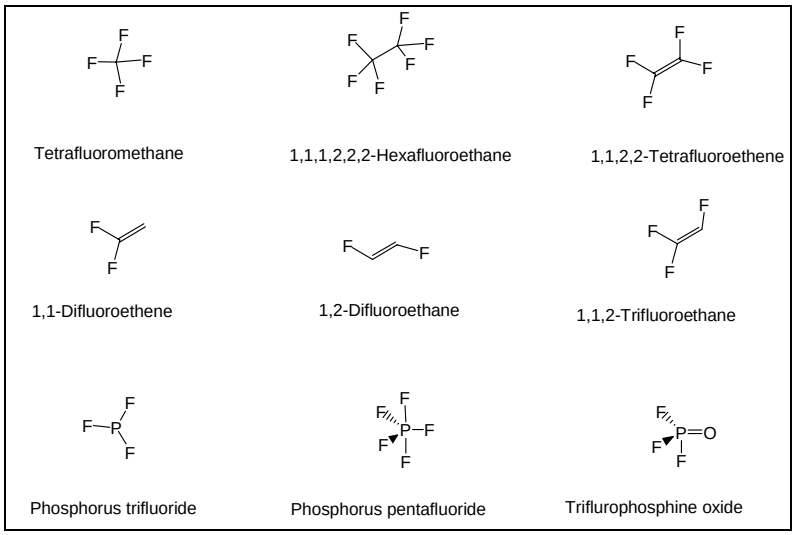

Figure 2.35 The structures of several gaseous fluorinated species that may arise during the combustion of a highly fluorinated P-containing organic compound.

Since the two unidentified water-soluble species were acidic (i.e. ionised at the IC eluent pH = 10.3) and since they were observed (by IC) to have partially hydrolysed to phosphoric acid and hydrogen fluoride over a period of 10h (Figure 2.36*a*), and completely hydrolysed within 24 h (Figure 2.36*b*), it was speculated that these species could be the known monofluoro- and difluoro-phosphoric acids, [These species are known to form when elemental phosphorus or P_2O_5 react with aqueous HF solutions[167] and also when an aqueous solution of H_3PO_4 and HF is left to equilibrate over time[168]].

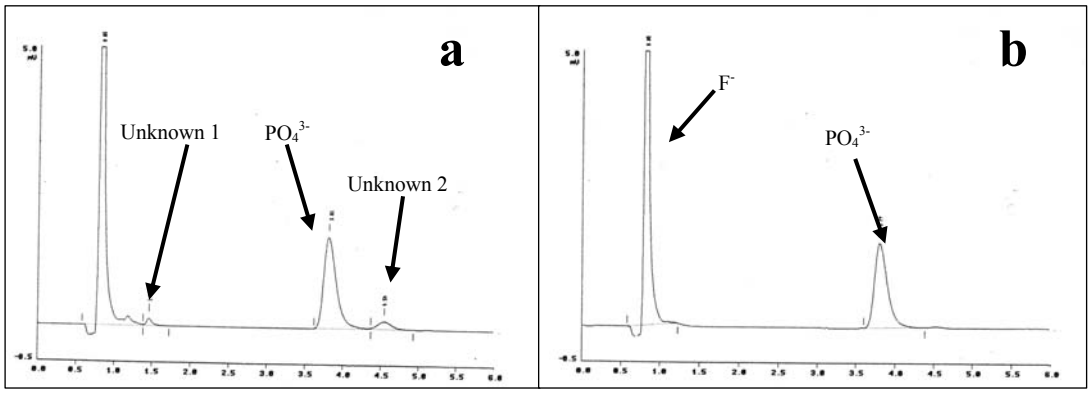

Figure 2.36 Ion chromatograph of the same solution as Figure 2.34, (a) 10 h after combustion and (b) 24 h after combustion (retention time = min).

The hydrolytic instability of the (aqueous) fluorinated phosphoric acids is well established[169,170,171] and has been extensively investigated by ^{19}F and ^{31}P NMR spectroscopy.[168,169,172] However in this study of these systems, ^{19}F-NMR offers the advantage[169,173] that only first-order doublets are observed instead of the complex multiplets observed in ^{31}P-NMR (both fluorine and phosphorus are spin-½ NMR active nuclei).

The hydrolytic instability of the two suspected fluorinated acids was also confirmed by ^{19}F-NMR which was run on samples of the undiluted bomb solutions from the combustion of a pellet (300 mg) of linear poly[bis(2,2,2-trifluoroethoxy)phosphazene], 1 and 18 h after combustion (Figures 2.37a and 2.37*b*. A reported[171] half-life value for aqueous 0.1M K_2PO_3F at pH 1 (HCl) and T=20ºC is 1.3 days). A third intense sharp doublet was also observed ('Unknown 3' in Figure 2.37*a)*, which, unlike '*Unknowns'* 1 and 2 failed to disappear over time (Figure 2.37*b*).

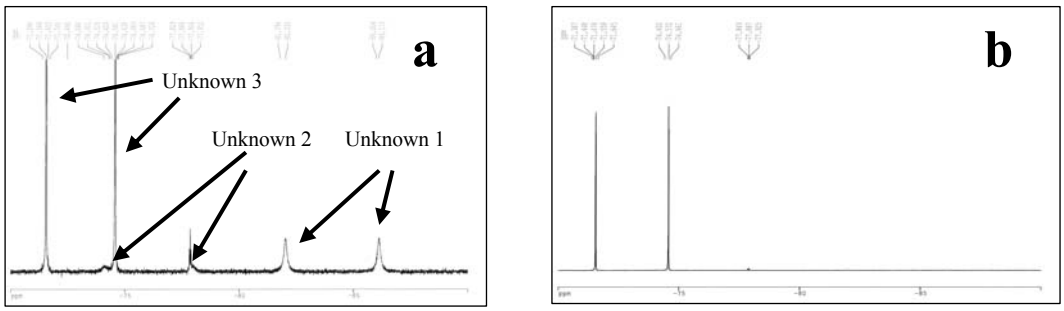

Figure 2.37 ^{19}F NMR spectrum (neat solution, acetone-d_6 internal probe) of the undiluted bomb solution from the combustion of linear poly[bis(2,2,2-trifluoroethoxy)phosphazene], (a) 1 h and (b) 18 h after combustion, confirming the stability of 'Unknown 3' towards aqueous hydrolysis.

This third species, which was not detected by Ion Chromatography, was thought to be *hexafluorophosphoric acid*, which is known to be retained indefinitely on IC and HPLC columns even when using a concentrated hydroxide eluent.[171]

In order to confirm the suggested identity of the three species observed, commercial samples of monofluorophosphoric acid (70% wt/wt in water, FluoroChem) [MFPA], difluorophosphoric acid ('technical' 95%+, Aldrich) [DFPA] and hexafluorophosphoric acid (60% wt/wt in water, Aldrich) [HFPA]

were purchased and analysed by ^{19}F-NMR spectroscopy. The chemical shifts and ^{31}P-^{19}F coupling constants observed for the three acids (in aqueous buffer, Section 2.2.8.4), corresponded to those given in the literature for the respective sodium salts (Table 2.29) and also to those of the respective (buffered) 'combustion-generated' species. ^{19}F NMR spectroscopy also confirmed the hydrolytic instability of the non-buffered monofluoro- and difluorophosphoric acids: DFPA had almost completely hydrolysed 4 h after dilution and MFPA had only half hydrolysed after the same period. The intensity of the strong doublet of HFPA had not decreased even 16 h after dilution, confirming the increased stability toward the (acid catalysed) aqueous hydrolysis of the hexafluorophosphate anion.[174]

Fluorinated phosphate	δ ^{19}F (ppm) Literature[175] value‡	δ ^{19}F (ppm) Observed value†	$^{1}J_{P-F}$ (Hz) Literature[175] value‡	$^{1}J_{P-F}$ (Hz) Observed value†
PO_3F^{2-}	-73.3	-74.5	863.0	873.2
$PO_2F_2^-$	-82.2	-84.0	960.0	962.6
PF_6^-	-71.7	-73.0	710.0	710.8

‡ $CFCl_3$ was used as the *internal* reference.

† $CFCl_3$ was the 'nominal' instrumental ^{19}F reference (Section 4.1.2)

Table 2.29 Comparison of literature and experimental values for δ (^{19}F) and J (P-F) of the three aqueous fluorinated phosphates.

The ^{19}F NMR spectrum of a dilute mixture of MFPA and HFPA yielded, surprisingly, 4 doublets (Figure 2.38).

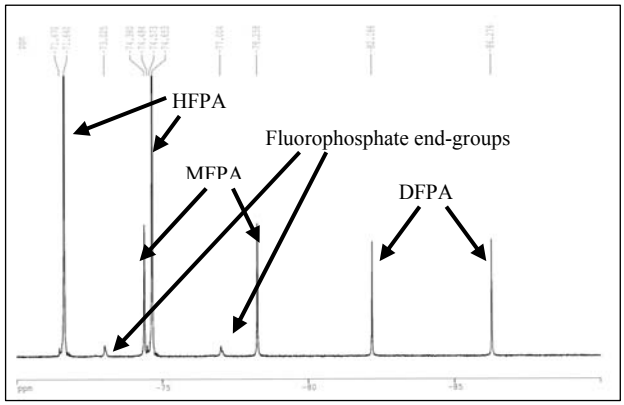

Figure 2.38 ^{19}F NMR spectrum of a mixture of HFPA and MFPA (acetone-d_6 internal probe) suggesting the likely presence of fluorinated, condensed phosphorus acids.

The fourth unexpected pair of resonances, which were both weak and broad, were at first thought to originate from *trifluorophosphine oxide*, F_3PO, but since this species is a gas at room temperature (bp: -40 ºC) this possibility was rejected in favour of either (a) the *monofluorophosphate* '*end group'*, the fluorinated phosphate residue of diphosphoric acid (XXVIII in Figure 2.39), or (b) the *monofluorophosphate* '*middle group'*, the central fluorinated residue of tripolyphosphoric acid and superior homologues (XXIX in Figure 2.39). The latter species is reported[169] to form, in small quantities, in the liquid system H_2O-HF-P_2O_5 at equilibrium. The monofluorophosphate middle group has a reported[169] ^{31}P-^{19}F coupling constant of J = 944 ± 2 Hz, which agrees reasonably well with the value observed here, (J = 937 Hz). However, the first alternative (a) would appear to be statistically more likely.

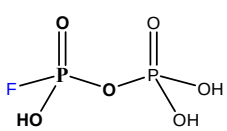

XXVIII monofluorophosphate end group

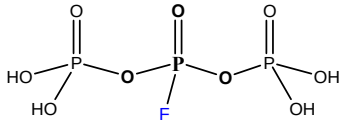

XXIX monofluorophosphate middle group

Figure 2.39 The monofluorophosphate *end*- and *middle*-groups

2.2.8.2 Qualitative analysis of the water-soluble (and gaseous) products from Polymers 1-5

^{19}F NMR spectroscopy and IC analysis of the bomb solutions from the combustion in excess oxygen of the energetic Polymers 1-5 revealed the water-soluble species *nitric acid*, *phosphoric acid*, *hydrogen fluoride, MFPA, DFPA* and also, in the case of less-substituted Polymer 2 (*ES%=31*) only, *HFPA*. In order to assess whether any condensed phosphoric acids (and/or their fluorinated analogues) had formed upon combustion of the Polymers, aqueous HCl (18.5 vol%) was added to small portions of each undiluted bomb solution was added (to pH 1) and the solution was then refluxed for 5 h. Since quantitative analysis (Section 2.2.8.4) of these hydrolysed solutions indicated that the increased molar amounts of H_3PO_4 and HF corresponded within ±2%, to the amounts of monofluoro- and difluoro-phoshoric acids which were present in the same solutions prior to hydrolysis, it was assumed that no significant amounts of condensed phosphorus species had formed. This conclusion was also supported by the absence of the ^{19}F NMR signal(s) of *monofluorophosphate 'middle groups' or 'end groups'* in the starting solutions, these being likely indicators of the presence of (fluorinated) condensed phosphoric acids in solution. Head-space GC-MS (EI, 70 eV) of the bomb gaseous exhausts from the combustions of all of the Polymers 1-5 later confirmed the *absence* of any of the P- and C-based fluorinated gaseous species (Figure 2.35) and carbon monoxide.

It was concluded that the presence of fluorine in Polymers 1-5 was responsible for the preferential formation, upon combustion in excess oxygen, of monomeric, fluorinated phosphoric acid species over the condensed species [which are observed in the absence of fluorine]. In this respect, the combustion stoichiometry of the phosphorus in Polymers 1-5 deviated significantly from that observed for the non-fluorine containing P secondary standards triphenylphosphine oxide and triphenylphosphine (Section 2.2.4.3).

2.2.8.2.1 The release of 2,2,2-trifluoroethanol during the combustion of Polymers 1-5

On a very few random occasions, the ^{19}F NMR spectra of the undiluted bomb solutions from the combustion of Polymers 1-5 showed a very weak 1-2-1 triplet signal at -77.8 ppm, which, like the signal due to hexafluorophosphoric acid, resisted hydrolysis over time. The small signal was initially obscured by part of the much stronger doublet of monofluorophosphoric acid but, after the monofluorophosphoric acid had partially hydrolysed to H_3PO_4 and HF (typically within 8-10 h), the weak triplet became visible (Figure 2.40).

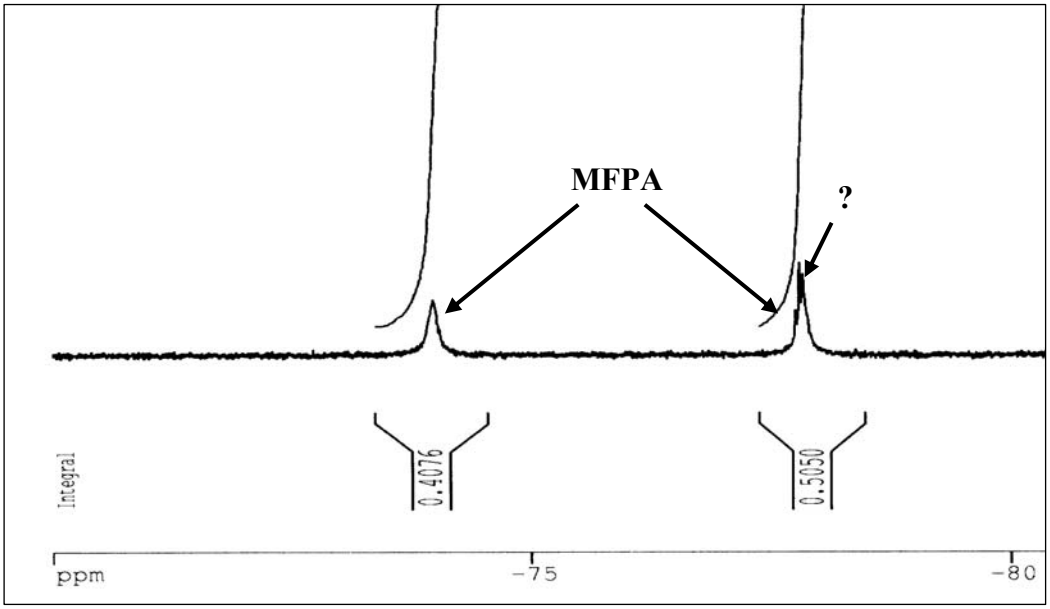

Figure 2.40 ^{19}F NMR spectrum (acetone-d_6 probe) of the undiluted bomb solution from the combustion of a sample of Polymer 5 (ES%=51), recorded 6 h after combustion.

Initially, this signal was believed to be an instrumental artefact but this explanation was soon disproved by the fact that the signal was detected in the ^{19}F spectra of 24+ h samples (when hydrolysis of monofluorophosphoric acid was complete) of the relevant bomb solutions (Figure 2.41).

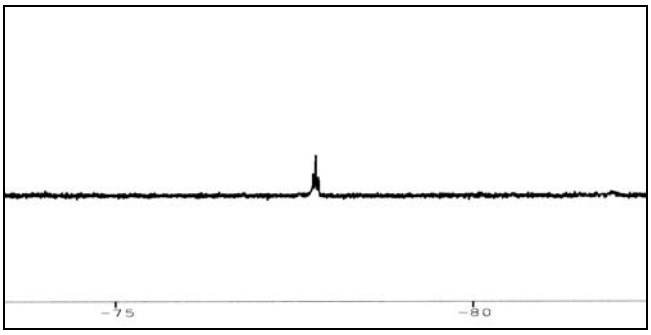

Figure 2.41 ^{19}F NMR spectrum of the same solution as Figure 2.41, recorded 72 h after combustion, showing the hydrolytically stable weak triplet signal.

This small signal was *always* observed to arise from the combustion of the precursor, linear poly[bis(2,2,2-trifluoroethoxy)phosphazene] and the less-substituted Polymer 2 (ES%=31), but *never* from the combustion of samples of red phosphorus admixed with PTFE. This peak was later assigned to free 2,2,2-trifluoroethanol, generated from the *pyrolysis* (i.e. thermal decomposition) of the burning phosphazenes in the bomb during combustion. It was speculated that after ignition in the bomb, the 'inner portions' of the burning samples must be subjected to very rapid heating when the surface is engulfed by a hot, oxygen-rich, flame envelope. GC-MS (EI, 70 eV) analysis of the bomb solutions confirmed the presence of 2,2,2-trifluoroethanol.

Free 2,2,2-trifluoroethanol was never observed in the ^{1}H NMR spectra (acetone-d_6) of Polymers 1-5, nor in those of their non-energetic precursors, as any free alcohol is eliminated after the acid-precipitation step by the repeated washing of the polymeric product with water (Section 2.1.1.1).

To gain further evidence that pyrolytic release of 2,2,2-trifluoroethanol from samples of highly fluorinated polyphosphazenes might be occurring in the bomb, a small sample of linear poly[bis(2,2,2-trifluoroethoxy)phosphazene] (150 mg) was pyrolysed in air. A 50 ml flask containing the sample was stoppered and gently passed (in an 'on and off' fashion) over the fuel-rich, 'cool' flame of a Bunsen burner. The polymer melted into a clear liquid, which, on further heating, turned light brown in colour and started to boil vigorously. With further heating copious white fumes were produced in the flask. On cooling, the white vapours condensed onto the walls of the flask as colourless transparent droplets which

were found to be miscible with water. The brown liquid re-solidified almost immediately into a hard yellow film, which was not soluble in water but slowly dissolved in acetone leaving traces of un-dissolvable carbonised material in suspension. A portion of the aqueous solution of the condensate was analysed by ^{19}F NMR spectroscopy and found to be mainly 2,2,2-trifluoroethanol (confirmed by spiking with commercial 2,2,2-trifluoroethanol). In addition, three superimposed triplets, centred at –76.7 ppm, were observed. These signals were thought to arise from water-soluble oligomeric products of *cyclisation*, which could have 'survived' upon the cooling and solidification of the polymeric mass. Linear poly[bis(2,2,2-trifluoroethoxy)phosphazene] is known[21] to undergo extensive cyclic rearrangement after melting, at temperatures between 300º and 350˚C, generating cyclic oligomers that range from 3 up to a maximum of 10 units. Since the coupling constants of the triplets were almost identical, which suggested very similar fluorine environments, it is suggested that the three triplets might be due to the first three homologous members of the cyclic oligomer series, namely the P_3-, P_4- and P_5-*bis*-(*2,2,2-trifluoroethoxy)cyclophosphazene*. Thermo-gravimetric analysis was also performed on a sample of linear poly[bis(2,2,2-trifluoroethoxy)phosphazene]. Weight loss was recorded between 350º and 450˚C, with the final weight loss amounting to 98.9%, suggesting pyrolytic releasing of 2,2,2-trifluoroethanol and volatile small-ring cyclic species.

As the minute release of 2,2,2-trifluoroethanol (corresponding to less than 0.01% of the molar amount of fluorine contained in the sample) during the bomb combustion of Polymers 1-5 of 'high' ES% (e.g. lower fluorine content) was only observed in two instances (Polymer 3, ES%=70% and Polymer 5, ES%=51%), no further precautions were taken to minimise the phenomenon.

2.2.8.3 General stoichiometric equation for the combustion in excess oxygen of Polymers 1-5.

After having ascertained the nature of the gaseous and water-soluble products of combustion, in excess oxygen, of Polymers 1-5 ($0 \leq ES\% \leq 100$) and of their non-energetic precursor linear poly[bis(2,2,2-trifluoroethoxy)phosphazene], it was

possible to derive the general stoichiometric equation (Equation 39) for the combustion reaction, with the aid of the following preliminary assumptions:

1. The molecular (unit monomer) hydrogen ends up as either H_2O or HF.
2. The water-soluble phosphoric acid species are generated by the reaction of the *corresponding anhydrides* with the water which is initially added to the bomb prior to firing, *and/or* the water formed during the combustion process. Thus H_3PO_4 originates from P_2O_5, H_2PO_3F from $P_2F_2O_4$ and HPO_2F_2 from $P_2F_4O_3$.
3. HNO_3 arises from N_2O_5.
4. When it forms, HPF_6 is generated by the reaction[176] of PF_5 with $HF_{(aq)}$.

A general combustion equation which does not yet stoichiometrically account for the moles of gaseous oxygen consumed in the process, may first be written (Equation 38):

$$C_aH_bO_cN_dF_eP_f + O_{2(g)} + \{nH_2O_{(l)}\} \xrightarrow{combustion} aCO_{2(g)} + \left[\frac{b-(e-z-2w-5s)}{2}\right]H_2O_{(l)} + yHNO_{3(aq)} + \left(\frac{d-y}{2}\right)N_{2(g)} + (e-z-2w-6s)HF_{(aq)} + (f-z-w-s)H_3PO_{4(aq)} + zH_2PO_3F_{(aq)} + wHPO_2F_{2(aq)} + sHPF_{6(aq)} \quad (38)$$

Where the number of molecules of water formed in the reaction are given by the number of H atoms present in the polymer (*b*), minus the number of F atoms which end up as HF. These, in turn, will be given by the difference between the total amount of fluorine atoms initially present (*e*) and the number of molecules of fluorinate phosphorus species formed multiplied by the number of F atoms they contain (*z-2w-5s*). Since H_2O contains two atoms of H, the latter quantity is divided by 2. From Equation 38 the number of atoms of *oxygen* (O) required for the conversion of the generic polyphosphazene of formula $\mathbf{C_aH_bO_cN_dF_eP_f}$, to the water-soluble and gaseous combustion species experimentally observed, neglecting the potential formation of *trace amounts* of condensed phosphorus acid species and their fluorinated analogues, may be calculated as:

2a *(for CO_2)* + **0.5[b-(e-z-2w-5s)]** *(for H_2O)* – **c** (internal oxygen) + **2.5y** *(for HNO_3)* + **2.5(f-z-w-s)** *(for H_3PO_4)* + **2z** *(for H_2PO_3F)* + **1.5w** *(for HPO_2F_2)*

which yields:

2a + 0.5b – c - 0.5e + 2.5f + 2.5y atoms of oxygen

From the above amount, the oxygen balanced equation (Equation 39) can finally be derived as:

$$C_aH_bO_cN_dF_eP_f + (a + 0.25b - 0.5c - 0.25e + 2.5f + 2.5y)O_{2(g)} + \{nH_2O_{(l)}\} \xrightarrow{combustion} aCO_{2(g)} + (0.5b - 0.5e + 0.5z + w + 2.5s)H_2O_{(l)} + yHNO_{3(aq)} + (0.5d - 0.5y)N_{2(g)} + (e - z - 2w - 6s)HF_{(aq)} + (f - z - w - s)H_3PO_{4(aq)} + zH_2PO_3F_{(aq)} + wHPO_2F_{2(aq)} + sHPF_{6(aq)} \quad (39)$$

Equation 39 neglects the small amounts of 2,2,2-trifluoroethanol which were observed to arise from the combustion of samples of highly fluorinated polyphospohazenes (ES% ≤ 31). The release of the fluorinated alcohol however, should not be described by Equation 39, as it does not arise as a combustion product but as a consequence of partial pyrolysis.

2.2.8.4 Quantitative analysis of the water-soluble products: stabilisation of the hydrolytically unstable species monofluoro- and difluoro-phosphoric acids

In order to obtain meaningful results from the quantitative analysis of the composition of the bomb solutions by ^{19}F NMR spectroscopy and Ion Chromatography, the hydrolytically unstable species that form during combustion of the polyphosphazenes must be ideally 'frozen', as soon as they are formed.

To accomplish this goal, it is necessary to neutralise the hydrolytically-unstable species to their corresponding salts. Although the latter are still susceptible[177] to hydrolysis in a pH-neutral aqueous solution, this occurs at a much slower rate: the rate constant of the first order hydrolysis reaction of the difluorophosphate anion in water, for example, is reported[177] to be 40 times slower at pH 4 than at pH 2, and independent of the temperature and cation. The rate of reaction decreases further as the pH increases to neutral values, when it is very slow even at relatively high temperature (> 50ºC), and it then increases again at alkaline pH values.[178] In order to complement the information found in the literature regarding the rate of hydrolysis of aqueous monofluoro- and difluoro-phosphoric acids and their salts, the approximate times for complete hydrolysis at the typical concentrations found after a combustion experiment (at room temperature) was

roughly estimated by Ion Chromatography and ^{19}F NMR spectroscopy, and was found to range from approximately 4 weeks for the salts to only a few hours (typically 8-10 h) for the corresponding acid species.

To ensure that the hydrolysis process was *slowed* to a *negligible* rate, allowing the quantitative measurement of these species *at their initial* concentrations in the bomb solution, the possibility of using a suitable buffer was explored. The buffer solution would be used in place of the small volume of distilled water added to the bomb prior to the combustion experiments in the 'chemical part' of the calorimetric investigation (Section 2.2.1), so that the hydrolysis of the emerging fluorinated phosphorus acids would be quenched immediately. The initial choice of buffering system was a 0.025 M *monohydrogenphosphate/ dihydrogenphosphate* solution (where the concentration was determined empirically as the minimum value that would yield neutral bomb solutions). Since the second acid dissociation constant of phosphoric acid ($H_2PO_4^- \rightleftharpoons HPO_4^{2-}$) is relatively low ($Ka_2 = 7.5 \times 10^{-8}$, hence $pKa_2 = 7.12$), an equimolar solution of $H_2PO_4^-$ *and* HPO_4^{2-} displays a pH of 7.12, as dictated by the *Henderson-Hasselback* equation (40).[179]

$$pH = pK_a + \log \frac{[HPO_4^{2-}]}{[H_2PO_4^-]} \qquad (40)$$

It was hoped that this buffer would minimise the alkaline hydrolysis of the fluorinated phosphoric anions due to its almost neutral pH value. In principle however, it could have also acted as an undesired source of 'added excess phosphate' which, in the presence of aqueous HF, could have generated extra amounts of fluorinated phosphorus species, according to *Le Chatelier's* principle (Figure 2.45).

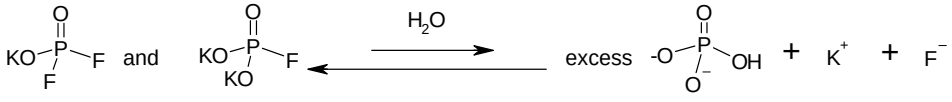

Figure 2.42 Monofluoro- and difluorophosphate anions: undesired displacement of the equilibrium induced by excess monohydrogenphosphate in the bomb solution.

Although this process may have generated small extra amounts of monofluoro- and difluoro-phosphate over long periods of time, the increase in concentration of either species was not observed by ^{19}F NMR spectroscopy over a period of three days.

The efficacy of this buffer was tested via ^{19}F NMR spectroscopy by assessing the rate of hydrolysis, if it occurred, of both monofluoro- and difluoro-phosphate anions observed in:

1. The product of neutralisation (with aqueous KOH) of commercial concentrated *difluorophosphoric acid* (composition of product given in Table 2.30, *'Salt mixture A'*, Section 4.3.1.1).
2. The product of neutralisation (with aqueous KOH) of commercial concentrated *monofluorophosphoric acid* (composition of product given in Table 2.30, *'Salt mixture B'*, Section 4.3.1.2).
3. The buffered bomb solution after combustion of a sample of *red phosphorus* intimately mixed with *PTFE* powder (F/P molar ratio =3), (from this point forward referred to as '*Mixture redP/PTFE*') which contained the same molar amounts of elemental fluorine and phosphorus that would be present in the typical combustion sample of approximately 300 mg of Polymer 3 (ES% = 61).

	Composition of salt (w/w %)				
Product of neutralisation	**K_2HPO_4**	**KPF_6**	**K_2PO_3F**	**KPO_2F_2**	**KF**
Salt Mix A	1.3	3.1	75.4	20.1	0.1
Salt Mix B	19.1	0	72.5	0	8.4

Table 2.30 Percentage mass composition of the products of neutralisation (aqueous KOH) of (A) difluorophosphoric acid and (B) monofluoro-phosphoric acid, as judged by ^{19}F NMR spectroscopy and Ion Chromatography, assuming that no hydration had occurred.

Table 2.30 shows that the direct neutralisation of commercial difluoro- and monofluoro-phosphoric acid with aqueous KOH failed to yield the desired pure fluorinated phosphate salts. *Salt mixture A* was a complex mixture containing the expected *potassium difluorophosphate* (20.1%) together with *potassium fluoride* (0.1%), *hydrogenphosphate* (1.3%), *potassium monofluorophosphate* (75.4%) and *potassium hexafluorophosphate* (3.1%). The preferential formation of *potassium monofluorophoshate* was attributed to extensive alkaline hydrolysis of *difluorophosphoric acid* during, or immediately after, neutralisation. This suggestion was reinforced by the fact that almost twice the calculated equivalents of KOH had to be used to reach neutrality, after all of the concentrated acid had been added, suggesting that the diprotic species *monofluorophosphoric acid* had been formed at this stage. The complex nature of the product of the aqueous neutralisation of *difluorophosphoric acid* explains the efforts made in the past to design new, cost-effective methods to manufacture high purity alkali difluorophosphates starting from readily available reagents.[180,181]

In conclusion, although the aqueous neutralisation of concentrated difluorophosphoric acid with alkali in water yielded predominantly *potassium monofluorophosphate*, some *potassium difluorophosphate* was still formed (20.1% w/w). This was considered to be high enough for the purpose of studying the hydrolytic behaviour of the difluorophosphate anion in the chosen buffer solution. Salt mixture B, however, was composed mainly of potassium monofluorophosphate (72.5% w/w) and contained no difluorophosphate.

2.2.8.4.1 Results and discussion

The NMR results demonstrated that the solutions (a) 10 mg of salt mixture A in 0.4 ml buffer, (b) 10 mg of salt mixture B in 0.4 ml buffer and (c) an undiluted, buffered bomb solution (from *Mixture red P/PTFE*), were essentially unchanged after 24 h. Figures 2.43a, 2.44a and 2.45a show the ^{19}F NMR spectra of solutions (a), (b) and (c) respectively, taken at the beginning of the experiments (time = 0). Figures 2.43b, 2.44b and 2.45b show the ^{19}F NMR spectra of the same solutions after 24 h. The ^{19}F NMR spectrum of solution (c), recorded three days later (Figure 2.45*c*) showed that over this longer period, the difluorophosphate anion

had slightly hydrolysed to phosphate and fluoride, the molar ratio decreasing from 22.5 to 20 %. The fluoride was also observed to have increased slightly, from 12 to 13 molar%. The monofluorophosphate anion however did not show any sign of hydrolysis (molar ratio = 66%).

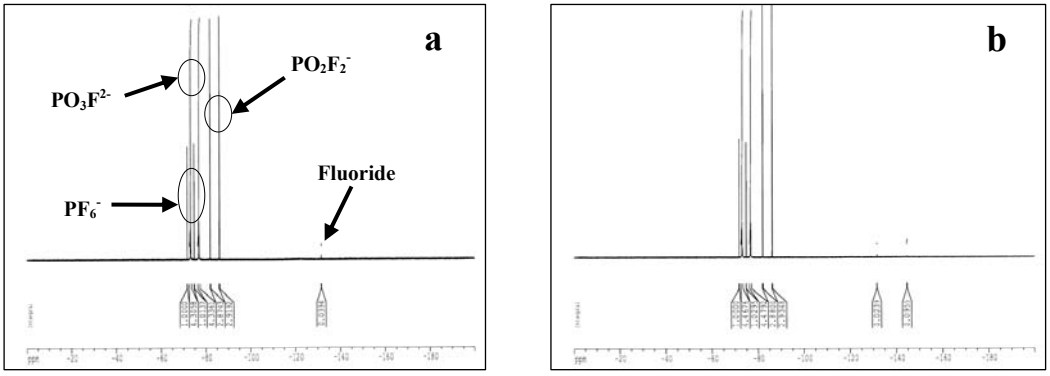

Figure 2.43 ^{19}F NMR spectrum (acetone-d_6 internal probe) of Salt Mixture A in aqueous 0.025 M $HPO_4^{2-}/H_2PO_4^-$ buffer solution (pH 7.12), recorded at time = 0 (a) and 24 h after combustion (b).

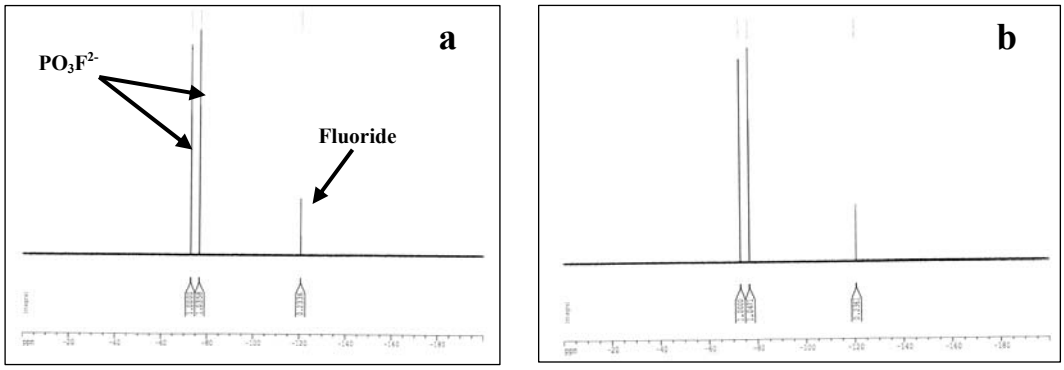

Figure 2.44 ^{19}F NMR spectrum (acetone-d_6 internal probe) of Salt Mixture B in aqueous 0.025 M $HPO_4^{2-}/H_2PO_4^-$ buffer solution (pH 7.12), recorded at time = 0 (a), and 24 h after combustion (b).

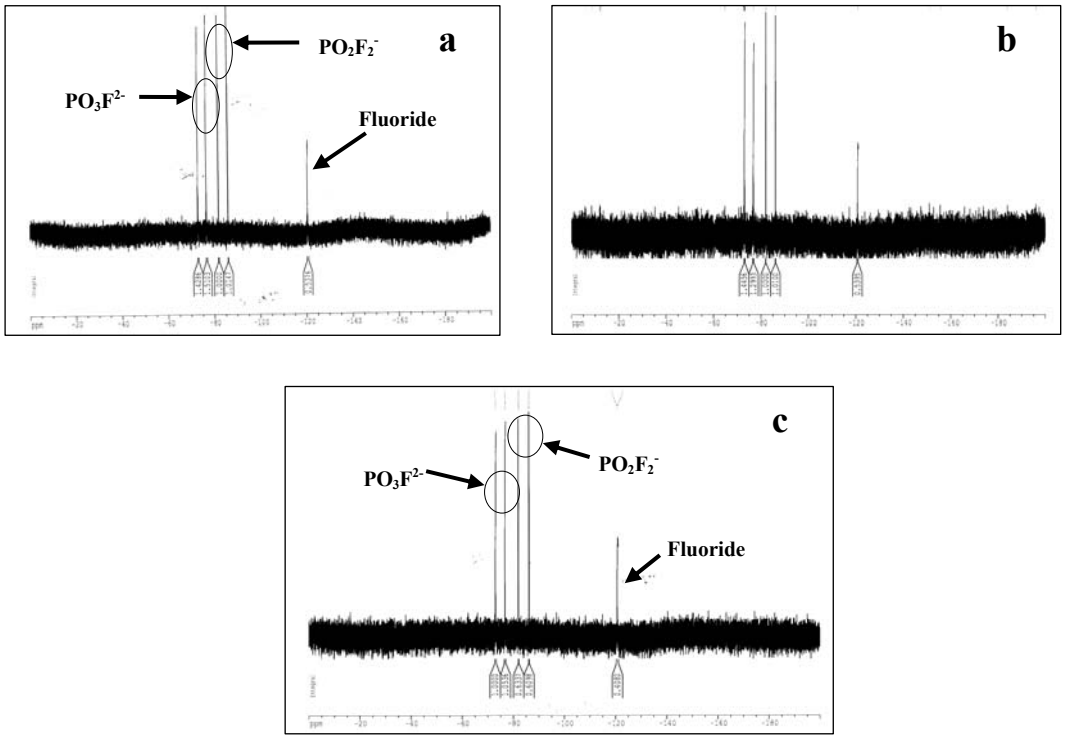

Figure 2.45 ^{19}F NMR spectrum of the buffered bomb solution (aqueous 0.025 M $HPO_4^{2-}/H_2PO_4^-$, 15 ml, pH 7.12, c) after the combustion of a sample of *Mixture red P/PTFE*, recorded at time = 0 (a) 24 h (b) and 72 h (c) after combustion.

The results indicated that the *difluorophosphate* anion was not completely stable in the 0.025 M monohydrogenphosphate/ dihydrogenphosphate buffer solution over the three days observation period. However, it was concluded that, *over the short time-span elapsing between ignition of the sample in the bomb and NMR experiment*, which is usually 10 min, the degree of hydrolysis of difluorophosphate would be negligible (approx. 0.03 molar %).

2.2.8.5 Investigation of alternative buffer systems

Although the monohydrogenphosphate/ dihydrogenphosphate buffer solution described in Section 2.2.8.4 was found to be effective at stabilising the hydrolytically unstable species monofluoro- and difluoro-phosphate over the observation period of 24 h, the system interfered seriously with the ion chromatographic quantitative analysis of the 'bomb' solutions. The small

orthophosphate anion peak arising from the combustion of the phosphorus-containing sample, would be completely obliterated by the much larger peak due to the phosphates of the buffer solution, which are both eluted as monohydrogenphosphate when using a 1.8/1.7 mM carbonate /bicarbonate eluent (pH=10.3). This large peak saturated the detector for more than 2 min, and thus also obliterating the peak due to combustion-generated monofluorophoshate anion, which, at the eluent's operative pressure, was eluted only 30 s after the orthophosphate anion. Alternative buffer systems containing no phosphate species but still capable of providing sufficient buffering capacity at neutral pH values were therefore investigated.

Aqueous buffer systems which rely on weak organic acids and their conjugate base salts i.e. acetic acid / acetate, formic acid / formate and citric acid / citrate could not be employed because the acetate, formate and citrate anions would all be eluted between 2 and 5 min, thus interfering with the nitrate and orthophosphate IC peaks of the bomb anions. Organic anions also interacted with the *IonPack AS4* IC column because the latter was designed to achieve isocratic elution of a small range of organic anionic species including acetate and formate.
A search in the literature[182] was successful in finding an alternative buffer based on the water-soluble, weak organic base *imidazole* and its conjugate acid *imidazolium chloride* (Figure 2.46), which is typically employed by biochemists working in the field of cell-culture technology. Since the pK_a of imidazole is 7.0 exactly, it follows that an equimolar solution of imidazole and its conjugate acid would generate a pH 7.0 buffer.

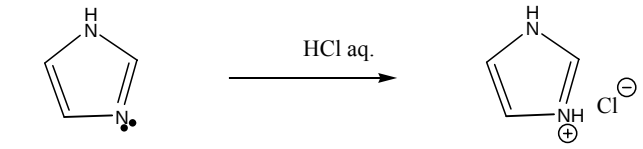

Imidazole, $C_3H_4N_2$
Mol. Wt.: 68.08
pKa= 7.0

Figure 2.46 The neutralisation of imidazole with aqueous HCl to give imidazolium chloride.

Because the chloride counter-anion of this buffer would be eluted after only 1.5 min upon injection into the ion chromatograph, thus interfering with the peaks of the fluoride and difluorophosphate anions, other inorganic and organic acids that could be used to neutralise imidazole without yielding any anionic interferents, were investigated. Orthoboric, tetrafluoroboric and perchloric acid were all found to be unsuitable for different reasons. Tetrafluoroboric acid which, in principle, could also be conveniently employed as a ^{19}F NMR internal fluorine standard, (its concentration in the buffer solution would be accurately known), was discarded after the commercial 48% aqueous solution (Aldrich) was found to be contaminated by significant amounts of HF, as judged by ^{19}F NMR spectroscopy, and would therefore interfere with the combustion-generated HF. The high isotopic abundance of the ^{10}B nucleus would also cause complications in the BF_4^- ^{19}F spectrum, due to the NMR-active multiplicity of this isotope of boron. The use of orthoboric acid was also precluded because the orthoborate anion, which eluted just after 6 min, would interfere with the monofluorophosphate anion. The perchlorate anion, from perchloric acid, is strongly retained by the *IonPack AS4* IC column and is eluted after 20 min. However, whilst this species did not interfere with any of the bomb analytes, the intensity of its broad peak only slowly 'tailed' down to zero after 50 min which rendered the use of perchloric acid impractical. Several replicate injections per day were sought.

The diprotic compound *oxalic acid,* however*,* was found to be a promising alternative for the IC interference problems. The dissociation constants of this acid ($pKa_1=1.23;\ pKa_2=4.19$), are such that at pH 10.3 (the pH value of IC carbonate/bicarbonate eluent used), the compound exists as oxalate dianion.[29] The double negative charge makes the oxalate anion interact strongly with the column stationary phase, and its retention time is consequently high (8 min), higher in fact than that of the doubly charged sulphate anion (7 min), the latter being a very strongly retained species. 8 min was sufficiently long to allow all of the bomb analytes to be eluted before the conductivity detector was 'saturated' by the passage of the oxalate species (Figure 2.47). After saturation (due to the passage of the oxalate band), the conductivity detector resumed its baseline conductivity

after only 3 min, which allowed the injection of the following sample almost immediately.

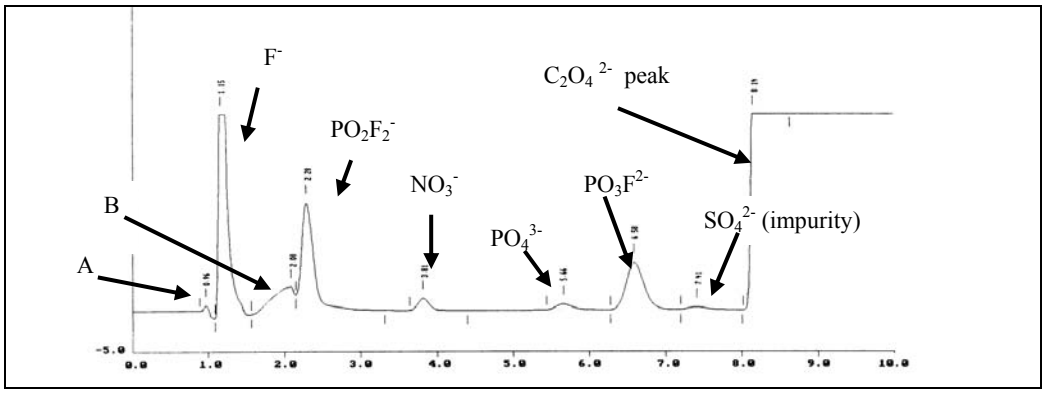

Figure 2.47 Ion chromatogram of the diluted bomb solution of the combustion of a pellet of *Mixture red P/PTFE*, using 30 ml of imidazole/ imidazolium oxalate buffer (0.8 M) in the bomb (final pH 7). The bomb was deliberately not flushed with oxygen in order to generate nitric acid.

Two unidentified peaks were observed to be eluted after 1.0 and 2.1 min (labelled A and B in Figure 2.47). It was thought that a possible explanation was that at the eluent's pH of 10.3, imidazole could, in principle, interact with the anion-exchange resin of the stationary phase of the column, due to the unprotonated lone pair on nitrogen. However, injection of an aqueous solution of imidazole at the concentration that would be found after dilution of the bomb solution (~7.2 mM), generated no visible peaks in the chromatogram. This was thought to be due to either (a) imidazole was retained indefinitely by the stationary phase of the column, as was the case for the hexafluorophosphate anion, or (b) imidazole *was* eluted from the column but could not conduct charge efficiently in the detector, this being possibly due to a low charge-to-mass ratio. A dilute solution of oxalic acid in water (25 mM) however, yielded the same two peaks (also labelled A and B in Figure 2.48) in addition to the main one expected for the oxalate anion, and also in addition to minor traces of sulphate, as an impurity (stated SO_4^{2-} content on bottle of oxalic acid $\leq$ 0.005 wt%). Lowering the pH of the injected solution caused the intensity of peak to increase sharply whilst the intensity of Peak B was only minimally affected. Although the two peaks could not be matched to any charged species, it was speculated that their origin could be due to trace amounts

of charged metal oxalate complexes, possibly arising from the (stated) trace impurities of the metals Pb, Fe and Co present in the oxalic acid sample.

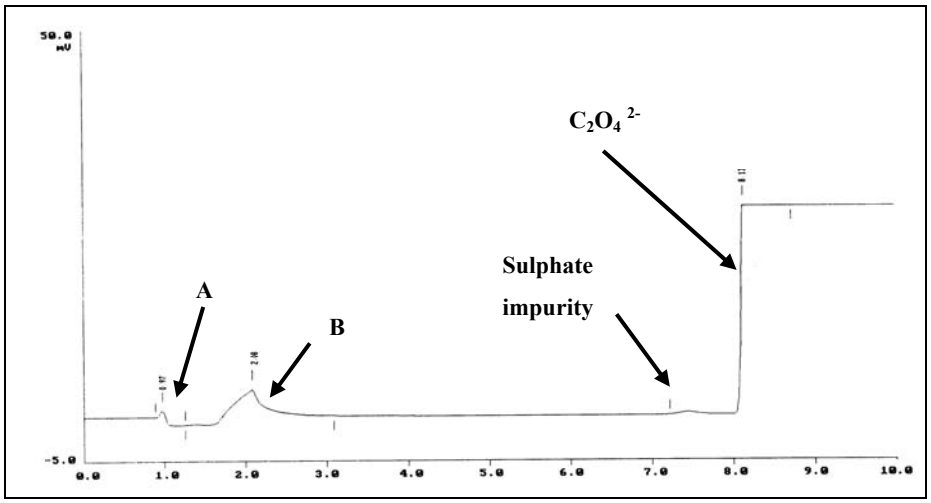

Figure 2.48 Ion chromatogram of an aqueous solution of oxalic acid (25 mM) pH 2, showing peaks A and B.

As the intensity and position of peaks A and B were such as not to cause major chromatographic interference i.e. they only *partially* overlapped with the peaks due to the difluorophoshate and fluoride anions, it was decided to re-calibrate the instrument towards these two species with standard solutions prepared with an aqueous solution of imidazole/imidazolium oxalate buffer at the same concentration that would ensue after the necessary dilutions following a typical 'buffered' combustion experiment. This expedient would hopefully minimise the magnitude of the calibration error due to peak overlap.

The optimum concentration of the buffer solution to be added to the bomb prior to combustion, was estimated empirically by determining the *minimum* concentration of a volume of 30 ml of buffer solution that would neutralise the acids arising from the combustion of pellets (300 mg) of red phosphorus / 4-fluorobenzoic acid (mixture molar F/P =3) to pH 7. The pellets contained the same molar amounts of fluorine and phosphorus that would be present in a 300 mg sample of energetic Polymer 3 (ES% =61). A minimum concentration of *0.8 M* for the imidazole / oxalic acid buffer solution was found to provide sufficient buffering capacity to neutralise to pH 7 the bomb solution after combustion.

2.2.8.6 Efficacy of the imidazole/imidazolium oxalate buffer

As for the 0.025 M HPO_4^{2-} /$H_2PO_4^-$ buffer, the efficacy of the 0.8 M imidazole/ imidazolim oxalate buffer was tested via ^{19}F NMR spectroscopy by assessing the rate of hydrolysis, if it occurred, of both the monofluoro- and difluoro-phosphate anions observed in:

(a) Salt mixture A (Table 2.30)

(b) Salt mixture B (Table 2.30)

(c) The buffered bomb solution after combustion of a sample of standard *Mixture red P/PTFE*, which contained the molar amounts of elemental fluorine and phosphorus that would be present in the typical combustion sample of approximately 300 mg of energetic polymer 3 (ES% = 61).

2.2.8.6.1 Results and discussion

The NMR results demonstrated that the solutions (a) 10 mg of salt mixture A in 0.5 ml buffer, (b) 10 mg of salt mixture B in 0.5 ml buffer and (c) undiluted buffer solution, were unchanged after 24 h. Figures 2.49*a*, 2.50*a* and 2.51*a* show the ^{19}F NMR spectra of solutions (a), (b) and (c) respectively, taken at the beginning of the experiments (time = 0). Figures 2.49*b*, 2.50*b* and 2.51*b* show the ^{19}F NMR spectra of the same solutions after 24 h. The ^{19}F NMR spectra of the same solutions recorded after 72 h confirmed the stability of both monofluoro- and difluoro-phosphate over this time period. The 0.8M imidazole / imidazolium oxalate buffer was thus found to be a better alternative to the 0.025M monohydrogen/ dihydrogenphosphate buffer that was initially evaluated.

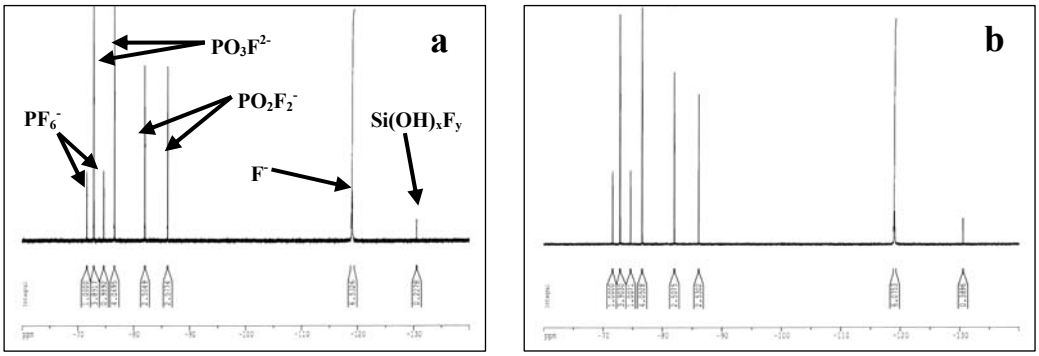

Figure 2.49 ^{19}F NMR spectrum (acetone-d_6 internal probe) of Salt Mixture A in aqueous 0.8M imidazole/imidazolium oxalate buffer solution (pH 7), recorded at time = 0 (a) and 24 h after combustion (b).

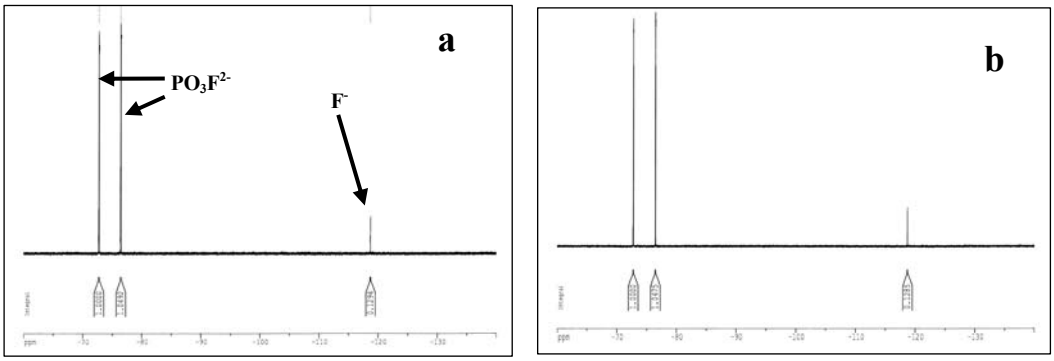

Figure 2.50 ^{19}F NMR spectrum (acetone-d_6 internal probe) of Salt Mixture B in aqueous 0.8 M imidazole/imidazolium oxalate buffer solution (pH 7), recorded at time = 0 (a), and 24 h after combustion (b).

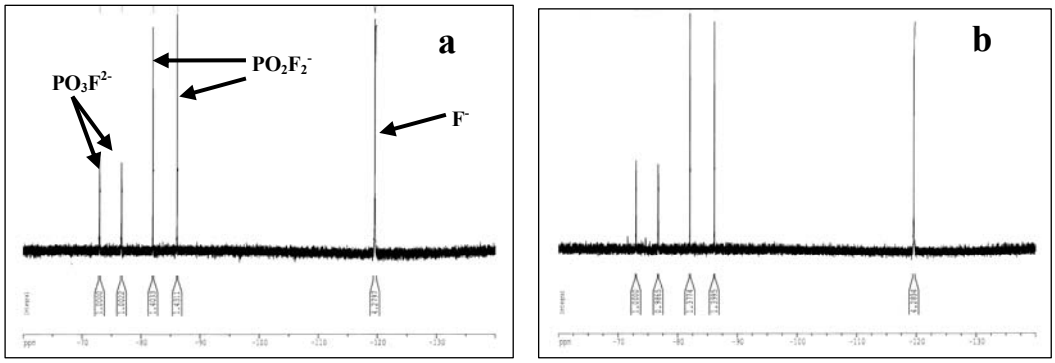

Figure 2.51 ^{19}F NMR spectrum of the buffered bomb solution (aqueous 0.8M imidazole/imidazolium oxalate, 30 ml, pH 7.0, (c) after the combustion of a sample of *Mixture red P/PTFE*, recorded at time = 0 (a) and 24 h after combustion (b).

During the evaluation stage of the imidazole-based buffer, most of the ^{19}F NMR spectra indicated the presence of an additional fluorinated species ($\delta \approx$ -130 ppm in Figure 2.49), which was initially thought to be due to difluoride anion (F_2^-) in solution. A more careful observation of this signal however, revealed the presence of significant side bands which appeared to be the result of splitting by an NMR active minor isotope. Since the coupling constant of the doublet (J = 108 Hz) was too large to be caused by ^{13}C, it was thought that the fluorine in this species must be bonded to a nucleus other than carbon, and in particular, to a species having a significant abundance of a spin ½ isotope. From the integrals of the doublet, it was possible to estimate the abundance of the splitting species to be approximately 4 molar%. A search in the literature later revealed that silicon has ^{28}Si (S=0) as the major isotope with ^{29}Si (S=½) corresponding to 4.7% isotopic abundance. This information was sufficient to suggest that the fluoride anion present in the NMR solutions had reacted with the borosilicate glass of the NMR tube forming a fluorosilicate species, whose multiplicity would be consistent with the ^{19}F signal observed. This hypothesis was reinforced by the fact that when the same NMR solutions were re-analysed 18 h later, the intensity of the signal had increased three-fold while that of the fluoride had decreased accordingly. To further prove this suggestion, a 'blank bomb solution' was prepared, containing the same amount of HF that would arise from the combustion of 300 mg of linear poly[bis(2,2,2-trifluoroethoxy)phosphazene] and the ^{19}F standard 2,2,3,3-tetrafluorobutane-1,4-diol (Section 2.2.8.8) in aqueous 0.8M imidazole/imidazolium oxalate buffer, and analysed by ^{19}F NMR spectroscopy. After only 30 min, the fluorosilicate species had already formed and its concentration kept increasing steadily over the following 18 h. A solution formed by reacting finely ground borosilicate glass (from a broken NMR tube) with HF 48%, when mixed with imidazole/imidazolium oxalate 0.8 M (15 ml), confirmed that the glass was indeed responsible for the formation of a fluorosilicate. When the same solution was basified to pH 14 by addition of aqueous NaOH however, the signal attributed to fluorosilicate was completely removed, suggesting that the latter species may be effectively hydrolysed by concentrated aqueous hydroxide,

according to Equation 41. The degree of fluorination of the fluorosilicate species remains unknown.

$$Si(OH)_xF_y + (4-x)OH^- \rightleftharpoons Si(OH)_4 + yF^- \qquad (41)$$

The assignment of the, usually small, ^{19}F signal represented a minor, yet important step, in completing the identification of the fluorinated species observable by ^{19}F NMR spectroscopy.

2.2.8.7 Calibration of the ion chromatograph towards fluoride, monofluoro- and difluoro-phosphate

In order to facilitate the quantitative analysis of the species PO_3F^{2-} and $PO_2F_2^-$ by IC *as well as* by ^{19}F NMR spectroscopy, the ion chromatograph was calibrated towards monofluoro- and difluoro-phosphate anions using 'standard solutions' prepared from salt mixture A (Table 2.30), the pure salts not being available commercially. The dilutions, from the 'sub-stock' solutions to the 'injection' solutions of these two species, and also of fluoride (starting from a 100 ppm [wt/vol] stock solution prepared from analytical reagent grade KF), were made with imidazole/imidazolium oxalate buffer in such a way as to provide the final buffer concentration as would be present in the diluted bomb solutions (7.2 mM). The pH of all of the standard solutions remained at 7, as both the imidazole and its conjugate acid would still be present in equimolar amounts after dilution. The calibration lines for the fluoride, monofluoro- and difluoro-phoshate anions in imidazole / imidazolium oxalate buffer are shown in Figures 2.52 *a*, *b* and *c* respectively. The calibrations were performed with three replicate injections for each standard. The estimated instrumental uncertainty intervals were ± 0.8% over the entire calibration range for KF, and ± 0.4% and ± 0.6% for PO_3F^{2-} and $PO_2F_2^-$ respectively.

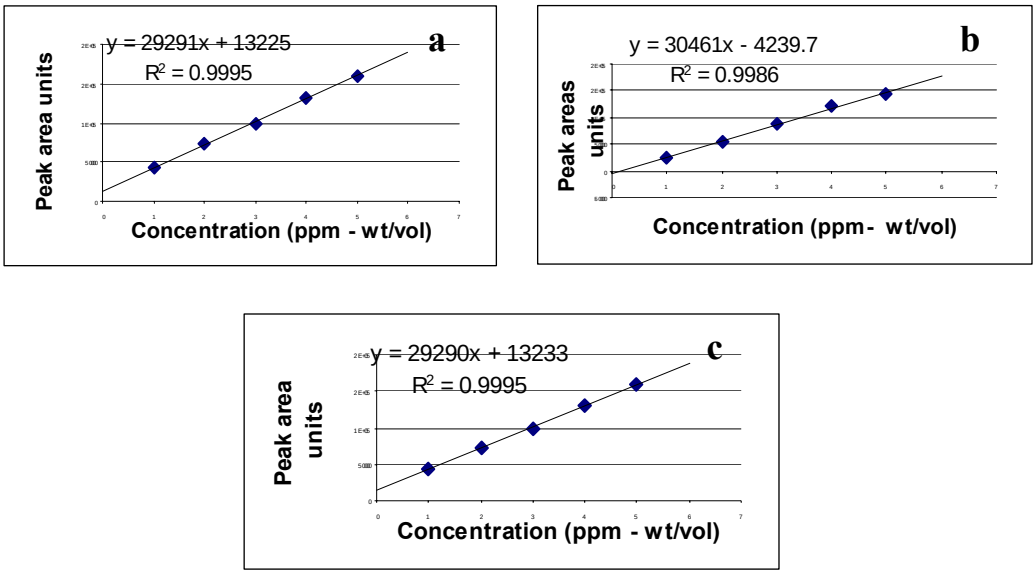

Figure 2.52 IC calibration lines for (a) fluoride (1-4 ppm wt/vol), (b) monofluorophosphate (1-5 ppm wt/vol) and (c) difluorophosphate (1-5 ppm wt/vol) in aqueous imidazole/imidazolium oxalate buffer (7.2 mM, pH 7).

2.2.8.8 Selection of a water-soluble ^{19}F NMR standard

In order to perform *quantitative* analysis by ^{19}F NMR spectroscopy of the aqueous fluorinated products arising from the combustion of the energetic polyphosphazenes, a chemically stable, water-soluble, fluorinated compound that could be used as a ^{19}F NMR internal standard had to be identified and tested. Three possible standards were evaluated, viz. *tris-2,2,2-trifluoroethyl phosphite* (a liquid, b.p. 131°C, Aldrich), *sodium 2,2,2-trifluoroacetate* and *2,2,3,3-tetrafluorobutane-1,4-diol* (both crystalline solids, Aldrich). The latter was chosen as the standard because its ^{19}F chemical shift did not interfere with those of the fluorinated combustion products that had to be analysed. In addition, this compound showed indefinite stability in water, as opposed to 2,2,2-trifluoroethylphosphite for example, which appeared to hydrolyse at a significant rate, yielding 2,2,2-trifluoroethanol. In the ^{19}F NMR spectrum, 2,2,3,3-tetrafluorobutane-1,4-diol exhibits a 1:2:1 triplet signal ($^3J_{H-F}$ = 15 Hz) due to

^{1}H-^{19}F splitting. No splitting due to the hydroxyl protons is observed in water, since, on the NMR timescale, these exchange too rapidly.

The commercial sample of 2,2,3,3-tetrafluorobutane-1,4-diol had no nominal purity specified on the label but had a melting point range (i.e. 77-82ºC). After drying, the purity of the material was estimated by ^{19}F NMR spectroscopy (using dry KPF_6, 99.9+% as an internal standard) to be 104.0%. ^{1}H NMR spectroscopy however (using dry imidazole 99.5% as an internal standard) gave 101.9%. The compound was used as such, without further purification.

2.2.8.9 Ion Chromatography versus ^{19}F NMR spectroscopy: quantitative analysis data agreement

In order to verify the agreement between the quantitative analytical data obtained by Ion Chromatography with that obtained by ^{19}F NMR spectroscopy, replicate bomb combustions of two identical pellets (A and B) of red phosphorus intimately mixed with 4-fluorobenzoic acid (containing the same molar amounts of elemental phosphorus and fluorine that would be contained in a 300 mg sample of polymer 3, ES%=61) were performed. Prior to combustion, a volume of 30 ml of imidazole / imidazolium oxalate buffer (0.8 M) was added to the bomb in order to minimise the hydrolysis of the fluorinated phosphorus acids. The combustion products of pellets A and B, as detected by ion chromatography and by ^{19}F NMR spectroscopy, were *monofluoro-, difluoro-phosphoric acids and hydrogen fluoride*. No hexafluorophosphoric acid was detected.

Since, at this stage of the research, a viable ^{19}F NMR internal standard had not been identified, the IC versus ^{19}F NMR instrumental data agreement could only be checked by comparing the *molar ratios* of the fluorinated species as detected by the two techniques. Table 2.31 compares the molar ratios of the species F^-: PO_3F^{2-} : $PO_2F_2^-$ (for the two replicate combustion experiments) as detected by ^{19}F NMR spectroscopy with those detected by Ion Chromatography. The results indicated poor agreement of the quantitative analytical data. As the concentrations of the buffered species in the NMR solution would be approximately 83 times those in

the IC injection solution, it was initially speculated that the concentration of the fluoride anion *as well as* the pH of the solution could influence the rate of hydrolysis. As considerable variation was observed in the ratios of fluorinated species formed from pellets A and B as detected by both techniques, it was also thought that perhaps the solid physical mixture employed was not reproducibly generating the fluorinated species upon combustion.

Combustion Experiment	F^-: PO_3F^{2-}: $PO_2F_2^-$ Molar ratios as detected by ^{19}F NMR spectroscopy	F^-: PO_3F^{2-}: $PO_2F_2^-$ Molar ratios as detected by Ion Chromatography
Pellet A	1 : 0.060 : 0.012	1 : 0.076 : 0.020
Pellet B	1 : 0.041 : 0.009	1 : 0.056 : 0.018

Table 2.31 Comparison of the molar ratios of the buffered combustion products F^-, PO_3F^{2-}, $PO_2F_2^-$ as detected by ^{19}F NMR spectroscopy and Ion Chromatography.

To provide further insight, following the successful identification and appraisal of 2,2,3,3-tetrafluorobutane-1,4-diol as ^{19}F NMR internal standard, the quantitative data agreement between the two techniques was assessed *indirectly* (i.e. without reliance upon IC detection of monofluoro- and difluoro-phosphate). Standard solutions of salt mixture A (product of neutralisation of HPO_2F_2 with KOH) and salt mixture B (product of neutralisation of H_2PO_3F with KOH), [Table 2.30] were analysed quantitatively by ^{19}F NMR spectroscopy (for K_2PO_3F, KPO_2F_2, KPF_6 and KF) and by ion chromatography (for KF and K_2HPO_4) and the results of the se analyses were *indirectly* compared. The ^{19}F NMR solutions were prepared by dissolving accurately weighed samples (approximately 500 mg) of salt mixtures A and B, into imidazole/imidazolium oxalate buffer solution (0.8 M, pH 7, 3.00 ml). An aqueous solution (1.00 ml) of the chosen ^{19}F internal standard 2,2,3,3-tetrafluorobutane-diol (126 mM) was then added to the solution with the aid of a precision microliter pipette. The ion chromatographic stock solutions were prepared by dissolving accurately weighed samples (approximately 500 mg) of salt mixtures A and B, into imidazole/ imidazolium oxalate buffer (0.8 M, pH 7, 20 ml) and then diluting the resulting solutions (with de-ionised water) to a final

volume of 100 ml. Small aliquots of the stock solutions were further diluted to bring the concentration of the analytes within their respective calibrated concentration range. In order to avoid any discrepancy which might arise from the presence of the buffer, a new IC calibration line for phosphate was constructed (Figure 2.53) in the concentration range 2-22 ppm (wt/vol) using standard solutions of PO_4^{3-} diluted with imidazole/imidazolium oxalate buffer at the same concentration (4.8 mM) that would result after having performed the necessary dilution of a bomb solution in a combustion experiment. The estimated average instrumental uncertainty interval associated with the line was ± 0.6% over the entire calibration range.

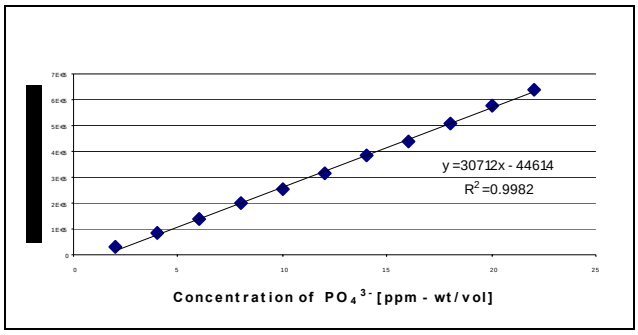

Figure 2.53 IC calibration line for PO_4^{3-} in imidazole / imidazolium oxalate buffer (4.8 mM).

By subtracting the mass corresponding to the *sum* of the molar amounts of fluorinated species that were quantified by ^{19}F NMR spectroscopy from the *mass of sample weighed* and also measuring directly K_2HPO_4 (as PO_4^{3-}) by IC alone, it was possible to ascertain the degree of agreement of the two techniques for K_2HPO_4 (Tables 2.34 and 2.35). KF could be detected by both IC *and* ^{19}F NMR spectroscopy and therefore compared directly. Tables 2.32 and 2.33 show, respectively, the composition of Salt Mixtures A and B, after analysis by the two techniques. The results also indicated that the composition of both Salt Mixtures A and B had varied substantially since the date of preparation and first analysis (14 months earlier, Cfr. Table 2.30). No significant change in composition had been observed 6 months after preparation however (Section 4.3).

Technique	Composition of salt mixture A (wt%)				
	K_2PO_3F	KPO_2F_2	KPF_6	KF	K_2HPO_4
^{19}F NMR	67.0	15.1	2.8	15.1	***nq***†
IC	*nq*†	*nq*†	*nq*†	18.2	0.5

† *nq* = not quantified.

Table 2.32 Composition (wt%) of salt mixture A as assessed by ^{19}F NMR spectroscopy and Ion Chromatography.

Technique	Composition of salt mixture B (wt%)				
	K_2PO_3F	KPO_2F_2	KPF_6	KF	K_2HPO_4
^{19}F NMR	66.2	0	0	0.9	***nq***†
IC	*nq*†	*nq*†	*nq*†	1.5	32.4

† *nq* = not quantified.

Table 2.33 Composition (wt%) of salt mixture B as assessed by ^{19}F NMR spectroscopy and Ion Chromatography.

Species observed in Salt mixture A	Mass	
	Chemical (mmol)	Physical (mg)
KF (^{19}F NMR)	**1.31**	**76.0**
KPO_2F_2 (^{19}F NMR)	**0.54**	**75.6**
K_2PO_3F (^{19}F NMR)	**1.91**	**336.5**
KPF_6 (^{19}F NMR)	**0.08**	**13.8**
Total fluorinated species	**3.84**	**501.9**
K_2HPO_4 (IC)	**0.01**	**2.5**
KF (IC)	**1.55**	**89.8**
K_2HPO_4 indirectly measured by NMR	**0.05**	**8.5**
Initial sample weight (mg)	**493.4**	
Difference between 'Initial sample weight' and 'Total species' (mg)	**-11**	

Table 2.34 Comparison of the total mass of fluorinated species quantitated by ^{19}F NMR spectroscopy in Salt Mixture A and the mass of K_2HPO_4 detected by IC with the mass of sample weighed.

Species observed in salt mixture B	Mass	
	Chemical (mmol)	Physical (mg)
KF (^{19}F NMR)	0.09	5.2
KPO_2F_2 (^{19}F NMR)	0	0
K_2PO_3F (^{19}F NMR)	2.08	366.1
KPF_6 (^{19}F NMR)	0	0
Total fluorinated species	2.17	371.3
K_2HPO_4 (IC)	1.03	179.1
KF (IC)	0.14	8.2
K_2HPO_4 indirectly measured by NMR	1.03	179.5
Initial sample weight (mg)	552.8	
Difference between 'Initial sample weight' and 'Total species' (mg)	-2.4	

Table 2.35 Comparison of the total mass of fluorinated species quantitated by ^{19}F NMR spectroscopy in Salt Mixture B and the mass of K_2HPO_4 detected by IC with the initial mass of sample weighed.

The results shown in Tables 2.34 and 2.35 suggested acceptable agreement between the amount of K_2HPO_4 *indirectly* quantitated by ^{19}F NMR (e.g. by difference between the mass of salt mixture weighed to prepare the NMR solution and the total mass of the fluorinated species observed) and the amount that was quantitated by IC analysis (especially those for Salt Mixture B, which contained an appreciable amount of K_2HPO_4, Table 2.35). For the KF species however, the quantitative data agreement was less satisfactorily. This was attributed to partial overlap, on the ion chromatogram, of one of the two peaks due to the buffer (peak B, Section 2.2.8.4.1) with the peak of the fluoride anion. Although the latter species was calibrated in buffer solution of the same concentration as would be employed in the measuring experiments (4.8 mM), the extent of overlap of the two peaks was, for unexplained reasons, not always reproducible.

Since the use of imidazole / imidazolium oxalate buffer solution was unavoidable for the ion chromatographic quantification of the orthophosphate anion and since the $PO_2F_2^-$ species also gave rise, in the ion chromatogram, to a peak which partly

overlapped with 'Peak B' of the imidazole/imidazolium oxalate buffer, it was concluded that the quantitation of all of the fluorinated phosphorus species arising from the measuring combustion experiments of Polymers 1-5 should rely on ^{19}F NMR spectroscopy alone, and that IC should only be used for the quantitation of the phosphate and the nitrate anions.

In view of the small size of the calorimetric corrections arising due to the formation of the fluorinated phosphate species observed to arise from the combustions in pressurised oxygen of Polymers 1-5, the quantitative agreement between data from IC *and* ^{19}F NMR spectroscopy was regarded as satisfactory for the specific purpose of this work.

2.2.9 Derivation of the standard enthalpy of formation (ΔH_f^o) of Polymers 1-5 and linear poly[bis(2,2,2-trifluoroethoxy) phosphazene]

2.2.9.1 Thermal contribution from the energy of solution of CO_2 in the acidic bomb solution in a 'measuring' calorimetric experiment

Prior to measuring ΔU_c of Polymers 1-5, the magnitude of the thermal contribution due to $CO_{2(g)}$ dissolving in the bomb liquid phase was investigated. Since the molar amount of gaseous carbon dioxide that dissolves at equilibrium in a given volume of water under specified conditions of pressure and temperature may vary from the amount which dissolves in the same volume of a dilute *acidic solution* at the same pressure and temperature, the energy released in the two cases by the gas dissolution process may be significantly different.[98] This implies that a small thermal discrepancy might be expected between the calibration and the measuring calorimetric experiments, if the sample burnt in the latter yields anything other than simply a water solution of carbon dioxide (which is the case for benzoic acid, in the calibration experiment).

No specific references were available in the literature regarding the values of the (standard) energy of solution of carbon dioxide in complex acidic solutions of different composition, the only related noteworthy publication being that of Cox

et al.[157] which describes the experimental measurement of the energy of dissolution of CO_2 in dilute aqueous solutions of hydrogen fluoride. This study aimed to furnish calorimetrists with a value of the solution energy of CO_2 in dilute aqueous HF solutions for the rigorous application of the corrections to *standard states* for burning samples of *highly* fluorinated compounds. Although the determination of such small amounts of heat would strictly require the use of a sensitive heat-flow calorimeter or solution micro-calorimeter, an experiment was performed with the calorimeter used in the present work to ascertain the capability of the calorimeter's thermistor digital thermometer unit to detect temperature changes associated with such low energy processes.

This was originally intended to be done by burning that weight of thermochemical standard benzoic acid which would generate, approximately, the amount of carbon dioxide that would be produced when combusting a 300 mg sample of Polymer 2 (ES%= 31), and adding a 'synthetic' acid solution to the bomb instead of distilled water. As this quantity of benzoic acid would have yielded very small *temperature increases,* accurately weighed quantities of approximately 200 mg were employed. This would generate considerably larger amounts of CO_2 than the typical sample mass of any of the energetic polymers studied in this work, but if no significant energy difference was observed between the two sets of experiments, then it would be justified to assume that any thermal discrepancy arising between the *calibration* and the *measuring* experiment of Polymers 1-5 would also be negligible.

Two sets of three replicate combustion experiments were carried out: a first set in which the 'synthetic' acidic solution (30 ml) was added to the bomb, and a second set in which distilled water (30 ml) was added. The 'synthetic' bomb solution (final pH=2) had the composition given in Table 2.36. This was prepared starting from the commercial, concentrated, aqueous solutions of the acidic species that were found to arise in the combustion of Polymer 2 (ES%=31). Since the 'mock' bomb solution was not buffered, being designed to model the real *acidic* solution arising in a 'measuring' calorimetric experiment in which water is added to the bomb, the composition of the solution was expected to change over time due to

hydrolytic instability. However, no measures were taken to accomodate for this. The results of the comparison experiments are presented in Tables 2.37 and 2.38.

Aqueous acid	H_2PO_3F	HPO_2F_2	HPF_6	H_3PO_4	HF	HNO_3
Conc. (mM)	4.32	2.16	7.20	12.6	20	7.06

Table 2.36 Composition of the 'synthetic' acidic bomb solution

Combustion experiment	Cotton Weight (g)	Benzoic Acid weight (g)	ΔT corr (K)	$-\Delta U_c$ (J g^{-1}) rounded to 4 signif. figures
1	0.0497	0.2007	0.574	26810
2	0.0430	0.1988	0.557	26710
3	0.0692	0.2203	0.652	26750
Mean and S.D. %SD				26760 ± 50 (± 0.2%)

Table 2.37 Experimental results from the combustion of benzoic acid with 'synthetic' acidic solution (30 ml) added to the bomb.

Combustion experiment	Cotton Weight (g)	Benzoic Acid weight (g)	ΔT corr (K)	$-\Delta U_c$ (Jg^{-1}) rounded to 4 signif. figures
1	0.0591	0.2114	0.613	26670
2	0.0738	0.2095	0.632	26670
3	0.0711	0.2027	0.613	26810
Mean and S.D. %SD				26720 ± 80 (± 0.3%)

Table 2.38 Experimental results from the combustion of benzoic acid with distilled water (30 ml) added to the bomb.

Although the number of replicate determinations performed in the two sets of experiments was very small, it was possible to apply a '*paired Student t*' test[129] in the attempt to verify whether the two data-sets were both part of the same

'statistical population', or, in other words, to assess whether the small difference between the two mean energy values obtained from the two sets of data was in fact *statistically significant*. A comaparison of the the calculated *t* value (0.593, with a pooled standard deviation *Sp* = 67.45) with the tabulated *t* value (2.776) for n= 4 degrees of freedom [3 + 3 (replicate observations) -2 (sets of data)] at the 95% level of confidence, indicated that there was no statistical difference between the results obtained by the two methods, and that the thermal effect of CO_2 dissolving into an acidic solution similar to those generated by the combustion of Polymers 1-5 could be safely neglected.

2.2.9.2 Calorimetric measurement of ΔU_c of Polymers 1-5

Since the general practice and theory behind the derivation of the ΔH_c^o and ΔH_f^o values of Polymers 1-5 (via calculation of ΔU_c^o), were identical for all of the specimens synthesised, a detailed description is presented here and in Section 2.2.9.5 for Polymer 2 (ES%=70, Batch 2) only, this being the first 'large scale', high ES% polymer to be synthesised. The tabulated data pertaining to the other polymers are presented in Appendix B. The units of the tabulated ΔU_c^o values (kJ mol^{-1} and Jg^{-1}), represent in these cases *kJ/mol average repeat unit*, and *J/g average repeat unit*.

The internal energy of combustion (ΔU_c) of Polymer 2 (ES%= 70, Batch 2) was measured over six replicate calorimetric experiments ('measuring' burns) as illustrated in Figure 2.54, page 168. The ΔU_c results are presented in Table 2.39 (page 168) whilst the general calorimetric procedure is described in details in Section 4.1.1.3.

The combustions of all replicate experiments of Polymer 2 (ES%=70) were found to be clean, with an average of 2 wt% of dry residue left in the alumina crucibles after combustion. No thermochemical correction was performed for the unburnt material as this was not chemically analysed. The Washburn corrections to standard states, as well as the energy of ignition were neglected. The final uncertainties associated with the mean values of ΔU_c were found to be relatively large when compared to those of the combustion experiments of the secondary standards. This was attributed to:

- The values of the energy of combustion of the secondary standards were measured over twelve or thirteen replicate experiments by burning sample masses that would generate corrected temperature increases of ~2 K. However, the calorimetric investigations of Polymer 2 (ES%= 70) used only six replicate runs and gave temperature increases of ~0.2K. This was insufficient to achieve the same precision.
- The energetic nature of Polymer 2 (ES%=70) may also have been indirectly responsible for lowering the accuracy of the calorimetric determinations. When smaller samples (100 mg) were burnt inside 70 μl alumina crucibles, smaller amounts of residue (typically 1%) were found after each combustion. The larger amounts of residue (2%) found after the combustion of the larger samples (300 mg inside 150 μl alumina crucibles) suggests that increasing the sample mass could have lead to possible heat 'quenching' inside the larger alumina crucibles. The larger amounts of water vapour formed in the latter case could condense in contact with the walls of a bigger crucible, hence cooling the flame. The latter hypothesis is reinforced by the observation that the 150 μl crucibles were found to be covered by a 'wet' film after combustion, whereas the 70 μl crucibles were apparently dry. Restricted access to oxygen in the slightly deeper vessels may also have contributed towards the increased amounts of residue. It is known[137] that the geometry and size of the crucible may affect, within small limits, the measured value of the energy of combustion of the substance burnt.

The total amounts of nitric acid and phosphoric acid formed during the combustion reactions of Polymer 2 (ES%=70) were analysed by IC of the diluted bomb solutions and the thermochemical corrections to account for the formation of aqueous HNO_3 (Section 2.2.6) and dilution of H_3PO_4 (Section 2.2.4.2) were applied at this stage. These corrections should have been applied, for consistency, during the 'chemical part' of the experiment, alongside those accounting for the energies of hydrolysis of HPO_2F_2 and H_2PO_3F. However, it was though that a more accurate graphical analysis of Polymer ΔU_c dependence on the energetic

substituent percentage (ES%) could be achieved if the source of an effectively systematic error had been eliminated.

Only one chromatogram was recorded for each bomb solution, since the uncertainty associated with the precision of the instrument over three consecutive replicate readings for both species was found to be lower than ± 0.5%. The non-ideal acidic species H_2PO_3F and HPO_2F_2 were also detected by IC in the bomb solutions, but these were quantified by ^{19}F NMR spectroscopy during the 'chemical part' of the calorimetric investigation (Section 2.2.9.5). Consequently, the thermochemical corrections to account for the energy of hydrolysis of these species to the ideal aqueous products H_3PO_4 and HF were also performed in the 'chemical part' of the investigation. Prior to combustion of Polymer 2 (ES%=70), the amounts of residual acetone in all polymer samples was estimated by ^1H NMR spectroscopy. Acetone was the solvent used to dissolve and re-concentrate all of the polymers by rotary-evaporation after synthesis. The acetone content of Polymer 3 (ES%=61, Batch 2) was found to be 0.1wt%, while the rest of the polymers were completely acetone-free. A quantity of 0.1wt% of residual acetone in Polymer 3 would have contributed approximately 11 J to the energy change when a sample of 300 mg (of which 0.3 mg was acetone) was combusted. This small thermal contribution was neglected.

Combustion Experiment Number	Cotton Weight (g)	Sample Weight (g)	ΔT corr (K)	Weight of residue in crucible (mg)	-Q (Total bomb energy change) (J)	Amount of N present in sample (mmol)	Amount of P present in sample (mmol)	HNO_3 formed as detected by IC (mmol)	H_3PO_4 formed as detected by IC (mmol)	Amount of N which converted to HNO_3 (molar%)	Amount of P which converted to H_3PO_4 (molar%)	Energy contributed by formation of HNO_3 (J)	Energy contributed by dilution of H_3PO_4 (J)	Energy contributed (as a % of the total energy bomb change)	$-\Delta U_c$ ($J\ g^{-1}$) rounded to 3 signif. figures
1	0	0.2804	0.239	7.6	2604.4	2.977	0.742	0.146	0.498	4.90	67.1	8.7	5.8	0.55	9240
2	0	0.2610	0.217	4.2	2367.9	2.771	0.690	0.136	0.473	4.91	68.5	8.1	5.5	0.57	9020
3	0	0.2745	0.238	5.2	2591.1	2.914	0.726	0.155	0.497	5.32	68.5	9.2	5.8	0.57	9380
4	0	0.3197	0.276	5.5	3005.2	3.394	0.845	0.177	0.584	5.22	69.1	10.5	6.9	0.58	9340
5	0	0.2760	0.230	5.5	2503.2	2.930	0.730	0.144	0.517	4.91	70.8	8.6	6.1	0.58	9020
6	0	0.3129	0.268	6.7	2921.9	3.322	0.828	0.163	0.563	4.90	68.0	9.7	6.6	0.56	9290
Mean and S.D. (and %SD) after propagation of error															**9220 ± 160 (± 1.7%)**

Table 2.39 Experimental measurement of the internal energy of combustion of Polymer 2 (ES% =70, Batch 2).

Figure 2.54 (a) Polymer-filled 150 µl alumina crucible (b) Polymer-filled alumina crucible with ignition wire inside bomb crucible (c) Same alumina crucible after combustion, showing traces of sooty residue. [Scale shown: cm]

2.2.9.3 Considerations regarding the ΔU_c measurement of the other Polymers

2.2.9.3.1 Preliminary calorimetric investigations

Prior to combustion of Polymer 2 (ES%= 70), preliminary calorimetric experiments were performed on smaller samples (approximately 100 mg inside 70 µl alumina crucibles) of Polymers 2 (ES%=65), 3 (ES%= 59) and 5 (ES%= 50) from the 'first' batches (Batch 1). The measured ΔU_c values for these materials are given in in Appendix B, Tables 5.4, 5.6 and 5.8 respectively. These preliminary small-scale preparations were primarily carried out to ensure the repeatability, in our laboratory, of the AWE preparation methods and also to develop suitable ^{1}H and ^{19}F NMR technique for the chemical characterisation of each one of the polymers. During the calorimetric experiments of these polymers, only three replicate 'measuring' experiments could be performed on each sample. Because of the small amounts burnt in each experiment, the corrected temperature increases, were, as expected, very small (less than 0.1K). Although no 'chemical' burns could be carried out during the preliminary experiments, the amounts of nitric and phosphoric acids formed from each replicate experiment were quantified by IC and were thermally corrected for.

2.2.9.3.2 Calorimetric measurement of ΔU_c of linear poly[bis(2,2,2-trifluoroethoxy)phopshazene] and less-substituted Polymer 2

The internal energy of combustion of the less-substituted Polymer 2 (ES% =31) and of the non-energetic precursor, linear poly[bis(2,2,2-trifluoroethoxy) phosphazene], were each measured over five replicate measurements. The corrections to account for the energy of hydrolysis of the observed aqueous species HPO_2F_2, H_2PO_3F and HPF_6 to the ideal aqueous products H_3PO_4 and HF were carried out in the respective 'chemical parts' of the calorimetric investigations (Section 2.2.9.6.1). The results are presented, respectively, in Appendix B, Tables 5.7 and 5.12 in Appendix B. Less-substituted Polymer 2 (ES%=31) burned well, leaving very little residue. Corrections were made to account for the energy of solution of H_3PO_4 and for the energy of formation of aqueous HNO_3, which were analysed by IC of the diluted bomb solutions.

The non-energetic precursor, linear poly[bis(2,2,2-trifluoroethoxy)phosphazene], on the other hand, was not easy to combust in pressurised oxygen. Although the material was a semi-crystalline powder at room temperature, 'naked' pellets of the polymer placed in direct contact with the metal crucible were found to melt partially during combustion, yielding large amounts of residue. The latter, being partially soluble in acetone and partially in water, was thought to be a mixture of unburnt (or pyrolysed) starting material (later confirmed by ^{1}H NMR spectroscopy of the resulting acetone solutions) and of inorganic ash. Presumably, the material melted upon ignition and the metallic crucible contributed to an early 'quench' by scavenging heat from the reaction spot. The problem was solved by hand-pressing the powder (using a small stainless steel dowel of 5 mm diameter) inside the same TG alumina crucibles (150 µl). These crucibles were found very effective at keeping the reaction heat localised, and retaining any molten material until it was consumed. Since attempts to sink the ignition wire directly into the solid material led consistently to failed ignitions (the material melting away from the glowing wire, presumably before reaching the ignition temperature), ignition was effected by using a cotton fuse surrounding the crucible, as shown in Figure 2.55. The cotton thread reliably ignited the sample even when not in direct physical contact. Little residue was found after all of the experiments (up to 5 mg for a 200 mg sample). Since this residue was insoluble in both acetone and water (it floated in water), it was thought to be composed mainly of carbon, although no thermochemical correction for this was performed.

Figure 2.55 Alumina crucible loaded with linear poly[bis(2,2,2-trifluoro ethoxy)phosphazene] inside the main bomb crucible, ready for combustion.

Since the cotton thread had presumably been consumed *before* igniting the sample, it was assumed that the presence of the extra source of hydrogen would not alter the ratios of formation of the fluorinated phosphoric acids. In practice though, some extra water would also form and condense onto the bomb walls. This may have had an indirect effect on the concentrations of the fluorinated species when they were dissolved in the thin aqueous film, and ultimately on their rates of hydrolysis during the time elapsed between sample ignition and the end of the calorimetric after-periods. However it was considered that this error would be much smaller than the error that would arise from partial sample combustions.

2.2.9.3.3 Calorimetric measurement of ΔU_c of Polymer 5 (ES%=68, AWE)

After receiving a sample of Polymer 5 (ES%=70) from AWE, the material was washed with diethyl ether in order to extract traces of free *hexane-1,2,6-triol trinitrate* (observed by ^{1}H NMR spectroscopy) and was then dried for 16 days in vacuo over drying agent (self-indicating silica gel). Analysis of the integral ratios of the ^{1}H NMR signals of the purified, dry material indicated that the energetic substituent percentage (ES%) of the polymer was slightly lower than originally calculated by AWE; viz. 68%. The amounts of residue found after combustion was always small with the exception of replicate experiment No. 1 of Polymer 5 (ES%=68, AWE), whose value was discarded. Thermochemical corrections were made to account for the formation of aqueous HNO_3 and for the dilution of H_3PO_4, which were analysed by IC of the diluted bomb solutions. The measured, uncorrected ΔU_c value for this polymer is presented in Appendix B, Table 5.11.

2.2.9.3.4 Calorimetric measurement of Polymer 1 (ES%=100, AWE)

The overall uncertainty affecting the calorimetric set of observations for Polymer 1 (ES%=100, AWE), was considerably larger than those found for the other energetic polymers (± 2.9% compared to approximately ± 1.5%). However, the magnitude of this interval was attributed almost entirely to Replicate 1 of the series, which furnished a considerably lower result than the other 4 replicates. By application of the 'Q-test' (Section 2.2.2.4), Replicate Experiment 1 appeared to

be on the borderline of 'rejectability' at the 90% confidence level. However, due to the small number of replicates available, Replicate Experiment 1 was retained for the estimation of the overall uncertainty interval. The results of the calorimetric measurements for this Polymer are presented in Appendix B, Table 5.2.

Another point of concern for Polymer 1 (ES%=100, AWE) was the thermal correction due to the enthalpy of solution of H_3PO_4. Since no fluorine was present in the sample, all of the phosphorus present should have converted to H_3PO_4, but since only approximately 70 molar% of the phosphorus initially present was recovered as H_3PO_4, it was speculated that either (a) some condensed phosphoric acid species had formed upon combustion, or (b) a considerable amount of H_3PO_4 (and/or P_2O_5) had been lost as 'uncondensed mist' when the bomb was vented. However, since none of the undiluted bomb solutions were refluxed to check for the presence of condensed phosphorus acid species (Section 2.2.4.3), the cause for the 'phosphorus mass loss' is unknown. For reasons of consistency with the work done with the other Polymers however, thermochemical corrections were applied only to account for the energy of solution of the amounts of H_3PO_4 actually observed.

2.2.9.4 ΔU_c dependence on % Energetic Substituent (ES%)

The measured ΔU_c values of Polymers 2, 3 and 5 (Batch 1) did not agree with those obtained for the same Polymers from Batch 2 during the 'preliminary' calorimetric investigation (Section 2.2.9.3). The differences were approximately 580, 360 and 540 J g^{-1} for Polymers 2, 3 and 5 respectively. Two possible causes for this were (a) the effect of residual solvent dissolved in the Polymers, and (b) the energy contributions due to the formation of $HNO_{3(aq)}$ and the solution of $H_3PO_{4(aq)}$. However, having checked that these did not account for the disagreement, the cause may be the *different degree of substitution of the polymers* (ES% after nitration). The origin of the different degrees of polymer side-chain substitution observed between two batches of material prepared under apparently identical conditions may be the volumes of solvent (THF) added at the

various stages of the reaction, coupled to small variations in the *NaH / Protected Alcohol* molar ratios employed during the preparation of the alkoxides. Future scale-up of the synthesis of Polymers 1-5 would require a detailed knowledge of the *limits* of variability of the degree of substitution of each Polymer, if accurate energetic predictions based on direct graphical correlation between ES% and Polymer ΔH_f^o are sought.

Since an insufficient number of corrected ΔH_c^o values for each Polymer was available, it was decided to plot the corresponding measured ΔU_c values against ES% instead. Although the values of Polymers 2, 3 and 5 (from Batch 1) measured during the 'preliminary' calorimetric investigation (Section 2.2.9.3) should not have been plotted alongside those of the same materials prepared in Batch 2 (due to the lower number of replicate observations and the smaller mass of sample burnt in those experiments), the former were retained for the construction of *tentative* correlation charts *between* ΔU_c and ES% for all of the Polymers (Figure 2.56). A summary of the results for the measured ΔU_c values of Polymers 1-5 of different ES% (yet uncorrected for the energies of hydrolysis of HPO_2F_2, HPO_3F and HPF_6) is presented in Table 2.40. Although the measured ΔU_c values were found to be dependent on Polymer ES%, the exact mathematical relationships between ΔU_c / ES% for each polymer could not be established and more data-points would be required to establish the true correlations.

Energetic Polymer	ES% (by ^{1}H NMR spectroscopy)	Measured -ΔU_c ‡ (J g^{-1})
Precursor†	0	9340 ± 210
1	76	10520 ± 180
	100	11190 ± 320
2	31	8880 ± 140
	65	8640 ± 105
	70	9220 ± 160
	78	9220 ± 230
3	59	10890 ± 160
	61	11250 ± 100
4	67	13040 ± 210
5	50	13910 ± 520
	51	14450 ± 180
	68	14440 ± 210

† non-energetic polymeric precursor: linear poly[bis(2,2,2-trifluoroethoxy)phosphazene]

‡ yet uncorrected for the energy of hydrolysis of $H_2PO_2F_2$, HPO_3F and HPF_6

Table 2.40 Measured ΔU_c values for Polymers 1-5 with different ES% values.

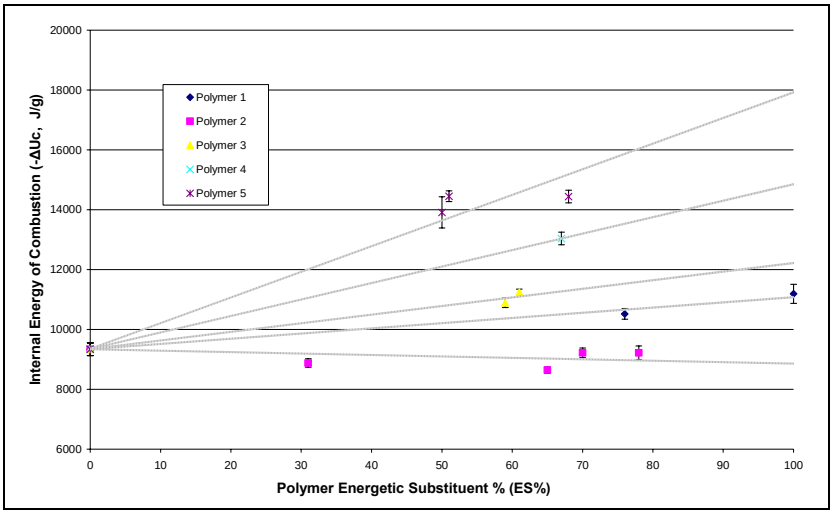

Figure 2.56 Tentative correlation chart of measured ΔU_c versus ES% value for Polymers 1-5.

However, if such relationships are assumed to be linear, as they should be in the ideal case, which neglects the potential presence of interactions between adjacent substituents on the polymers backbone (described by the use of dashed-trend lines in Figure 2.56), it is observed that the rate of increase of ΔU_c versus ES% increases (i.e. steeper slope) the bulkier the energetic substituent on the polymer.

However, this general trend is inverted when comparing Polymers 1and 2. This may be explained in terms of the high degree of self-oxidation (i.e. low oxygen balance, hence low calorific value) of the dinitratopropoxy substituent (whose ΔU_c^o value was here assumed to be close to that of *propane-1,2,3-triol-1,2-dinitrate*, ΔU_c^o = -8639 Jg^{-1})[183], which, upon exhaustive combustion, is expected to release less energy than the mononitratoethoxy substituent of Polymer 1 (whose ΔU_c^o value was here assumed to be close to that of *ethane-1,2-diol mononitrate* ΔU_c^o = -11400 Jg^{-1}, calculated via ΔH_f^o, which was estimated using the Benson *group additivity* method[184]) and only marginally more than the trifluoroethoxy substituent (whose ΔU_c^o value was here assumed to be close to that of *2,2,2-trifluoroethanol,* ΔU_c^o = -8216 Jg^{-1}).[185] Thus, as the ES% value of Polymer 2 increases, ΔU_c should also increase, albeit at a very slow rate due to the small difference in calorific output of the two substituents. However, in Figure 2.56, the ΔU_c of Polymer 2 is seen to slightly decrease. This was attributed to experimental error due to the lack of a sufficient number of data-points. The measured ΔU_c value of the non-energetic precursor, linear poly[bis(2,2,2-trifluoroethoxy) phosphazene], which is effectively Polymer 1→5 (ES%=0), is also shown in Figure 2.56, as a 'communal' ΔU_c starting point for all of the Polymers 1-5.

Since the 'tentative' trend lines shown in Figure 2.56 did not always intersect the ordinate error bars shown (the uncertainty intervals of each ΔU_c value), there were suspicions about possible sources of error associated with the determination of the Polymers ES% value via ^1H NMR spectroscopy. The averaging of successive integrations of the same spectra, coupled to the recording of multiple spectra of the same samples, are expected to reduce this uncertainty, especially for those polymer specimens for which elemental analysis is not obtained.

2.2.9.5 The 'chemical part' of the calorimetric investigation of Polymer 2 (ES%=70): derivation of ΔH_c^o and calculation of ΔH_f^o

The general procedure adopted to perform the 'chemical part' of the calorimetric investigation of Polymer 2 (ES%= 70) is described in details in Section 4.1.1.3. The combustions were all clean, leaving less than 1 wt% of residue in the alumina crucibles in which all samples were directly weighed and combusted. Tables 2.41 present the results of the Ion Chromatographic and ^{19}F NMR spectroscopic analysis of the buffered bomb solutions of the 5 replicate combustion experiments, whilst the analytical results pertaining to the 'chemical burns' of all of the other Polymers are presented in Appendix B, Tables 5.13-5.18. The only water-soluble species observed to have arisen from all 5 replicate experiments, regardless of sample mass combusted, were F^-, $PO_2F_2^-$, PO_3F^{2-} and PO_4^{3-}. However, as can be seen from Table 2.41, the recoveries of both fluorine and phosphorus in the water-soluble products were not quantitative. Since the absence of any fluorinated carbon- and phosphorus-based gases in the bomb head-space had been confirmed by GC-MS (Section 2.2.8.2), these mass defects were attributed to uncondensed mists of (fluorinated) phosphoric acids. Dense, white mists were observed on opening the depressurised bomb after each combustion experiment. Since the percentages of recovered phosphorus were a function of the amounts of *recovered fluorine* however, it was decided to scale up the latter to 100% (i.e. to the molar amounts of fluorine present in the samples) to eliminate this source of error. The revised analytical results for the 5 replicate experiments are presented in Table 2.42. Figure 2.57 shows the recovery yields of phosphorus as a function of sample mass after fluorine scale-up. Figure 2.58 shows a plot of the amounts of all of the aqueous species formed versus sample mass.

Combustion No.	Sample weight (mg)	Weight of dry residue (mg)	F^- (mmol)	$PO_2F_2^-$ (mmol)	PO_3F^{2-} (mmol)	PF_6^- (mmol)	PO_4^{3-} (mmol)	Amount of F present in sample (mmol)	Total F recovered (mmol)	Amount of P present in sample (mmol)	Total P recovered (mmol)	**F recovered (%)**	**P recovered (%)**
1	306.1	3.6	1.012	0.056	0.342	0	0.418	1.538	1.466	0.855	0.816	**95.3**	**95.4**
2	346.9	2.0	0.817	0.060	0.268	0	0.563	1.744	1.205	0.969	0.891	**69.1**	**92.0**
3	371.0	2.7	0.993	0.082	0.346	0	0.473	1.865	1.503	1.036	0.901	**80.6**	**87.0**
4	158.4	2.0	0.406	0.029	0.135	0	0.210	0.796	0.599	0.442	0.374	**75.3**	**84.6**
5	642.6	6.4	1.144	0.141	0.576	0	0.712	3.230	2.002	1.795	1.429	**62.0**	**79.6**

Table 2.41 Results of the analysis (^{19}F NMR spectroscopy and IC) of the bomb solutions from the combustion experiments of Polymer 2 (ES%=70, Batch 2).

Combustion No.	Sample weight (mg)	F^- (mmol)	$PO_2F_2^-$ (mmol)	PO_3F^{2-} (mmol)	PF_6^- (mmol)	PO_4^{3-} (mmol)	Amount of F present in sample (mmol)	Total F recovered (mmol)	Amount of P present in sample (mmol)	Total P recovered (mmol)	**F recovered (%)**	**P recovered (%)**
1	306.1	1.062	0.059	0.359	0	0.418	1.538	1.538	0.855	0.836	**100**	**97.8**
2	346.9	1.182	0.087	0.388	0	0.563	1.744	1.744	0.969	1.038	**100**	**107.1**
3	371.0	1.232	0.102	0.429	0	0.473	1.865	1.865	1.036	1.004	**100**	**96.9**
4	158.4	0.539	0.039	0.179	0	0.210	0.796	0.796	0.442	0.428	**100**	**96.8**
5	642.6	1.845	0.227	0.929	0	0.712	3.230	3.230	1.795	1.868	**100**	**104.1**

Table 2.42 Revised results of the analysis (^{19}F NMR spectroscopy and IC) of the bomb solutions from the combustion experiments of Polymer 2 (ES%= 70, Batch 2) after quantitative scale-up of the amount of fluorine recovered as water-soluble fluorinated species.

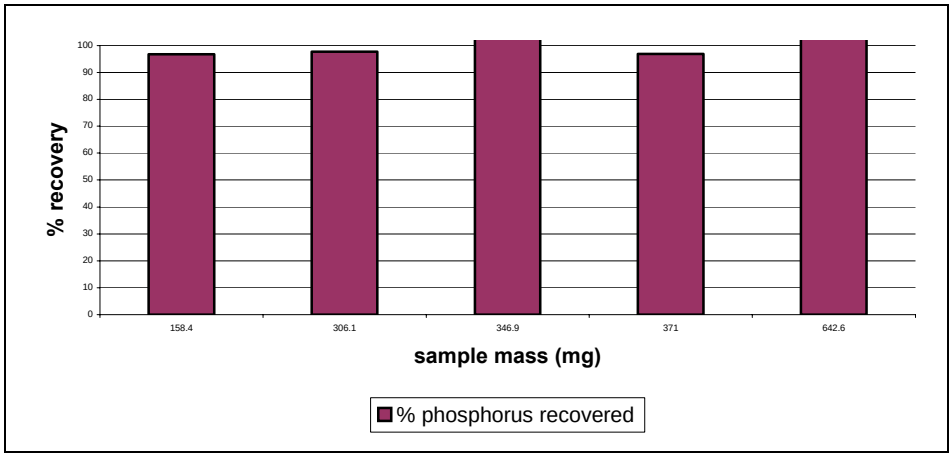

Figure 2.57 Recovery (% yield) of phosphorus as a function of sample mass of Polymer 2 (ES%=70) after scale-up of the amounts of fluorine recovered as fluorinated combustion species.

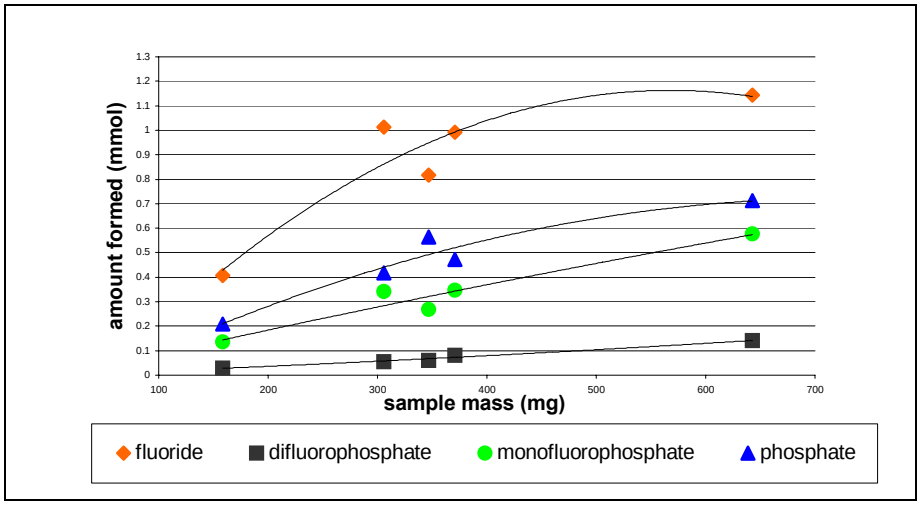

Figure 2.58 Sample mass of Polymer 2 (ES%=70) versus amounts of water-soluble combustion species formed.

As Figure 2.58 indicates, there was considerable variability in the amounts of combustion species formed between replicate experiments, even when similar sample masses were burnt. From the data available, the amounts of monofluoro- and difluoro-phosphoric acids that had formed seemed to be weakly correlated with the mass of polymer burnt. However, since the 'chemical burns' were performed in order to obtain *an estimate* of the amounts of both monofluoro- and

difluoro-phosphoric acids that would form *during the calorimetric (or measuring) part* of the investigation, the amounts of these species arising from the chemical burns had to be expressed as mean (acid formation ratio) values of the 5 replicate chemical burns. This effectively indicated the 'reproducibility of formation' of the fluorinated acid species in consecutive burns.

It is doubtful whether the reproducibility of the acid formation ratios measured using a static bomb calorimeter will ever be satisfactorily consistent. Immediately following the combustion of the sample, the products of reaction (HF and the different fluorinated phosphorus anhydrides) would immediately react and dissolve in the uniform thin layer of microscopic water droplets which condense on the inner walls of the bomb. The resulting aqueous solution may be of high concentration and very acidic. In these conditions, the rate of hydrolysis of monofluoro-, difluoro- and, to a lesser extent hexafluoro-phosphoric acid to aqueous H_3PO_4 and HF, may be very fast. Since concentration inhomogeneities due to the water-film thickness may also occur inside the bomb and since the exact time intervals between sample ignition and the subsequent manual rotation of the bomb (to homogenise the contents, Section 4.1.1.3), will seldom be identical between any replicate experiments, the observed 'acid formation ratios' may never be reproducible. The use of a rotating bomb calorimeter, coupled with a constant time interval between sample ignition and the commencement of mechanical rotation of the bomb, may provide a significant improvement.

By multiplying each value of the 'acid formation ratios' (mmol/ mg sample), which are presented in Table 2.43, by 1000 to get *the unit mass* (1.000 g) for each member of the polymer series, it was possible to obtain an *estimate* of the molar amounts of both hydrolytically unstable fluorinated species that would arise from the calorimetric experiment of 1.000 g of Polymer 2 (ES%=70). These estimates are required in order to perform the thermochemical corrections that 'bring back' to the ideal combustion behaviour, and to correct the measured ΔU_c value to the corresponding standard value, ΔU_c°.

Combustion No.	$PO_2F_2^-$ (mmol) / sample mass (mg) [$x10^{-4}$]	$PO_3F_2^-$ (mmol) / sample mass (mg) [$x10^{-3}$]	$-\Delta U_c$ ($J\ g^{-1}$)
1	1.927	1.173	9240.7
2	2.507	1.118	9240.6
3	2.749	1.156	9241.6
4	2.462	1.130	9240.8
5	3.532	1.445	9247.1
Mean and S.D. %S.D.	2.635± 0.584 (± 22.2%)	1.204± 0.136 (± 11.3%)	9242.2 ± 2.3 (±0.03%)

Table 2.43 Ratios of the amounts (mmol) of monofluoro- and difluoro-phosphoric acids formed and the mass of sample burnt (mg) for Polymer 2 (ES%=70, Batch 2) and corrected values of the measured internal energy of combustion (column 4).

The small amounts of monofluoro- and difluoro-phosphoric acids that were assumed to have also formed during the calorimetric experiments, were multiplied by their reported *standard enthalpies of hydrolysis* to phosphoric acid and hydrogen fluoride, viz. ΔH_{hyd}^{o} $H_2PO_3F_{(aq)}$ = -15.3 kJ mol^{-1}, ΔH_{hyd}^{o} $HPO_2F_{2(aq)}$ = -14.1 kJ mol^{-1} respectively.[186] The ΔU_{hyd}^{o} values are expected to be almost identical to the ΔH_{hyd}^{o} values since the hydrolysis reactions occur in aqueous solution. The literature values were obtained from the equilibrium constants (K_{hyd}) at various temperatures for the respective acid-catalysed, aqueous hydrolysis reactions, as measured by ^{31}P NMR spectroscopy. The thermochemical corrections *add* the thermal energy evolved by the hydrolysis of H_2PO_3F and HPO_2F_2 to HF and H_3PO_4, (the latter two *would have formed* in the ideal combustion processes of each polymer), to the measured values of internal energy of combustion (which had been already corrected for the formation of HNO_3 and for the dilution of H_3PO_4).

Whilst the transfer of thermochemical corrections based on the acid formation ratios of the 'chemical burns' *to* the mean ΔU_c result of the calorimetric burns would not be strictly justified from a pure thermochemical point of view, this may be the only option available when using a static bomb calorimeter.

As can be seen from Appendix B, Tables 5.13-5.18, only a limited number of chemical burns could be carried out for the other Polymers. Only one successful experiment for Polymer 5 (ES%=51, Batch 2, Appendix B, Table 5.18) was possible due to the small amount of this material that was left over from the calorimetric experiments. In addition, the thermochemical corrections for the formation of monofluoro- and difluoro-phosphoric acids which were carried out on the calorimetric data of Polymer 2 (ES%=70, Batch 2) could not be applied to the uncorrected calorimetric data obtained for the same Polymer from the previous batch (Polymer 2, ES%=65, Batch 1) since the different ES% values of these materials would produce different combustion stoichiometries. The same applied to the other Polymers that were prepared in two consecutive batches i.e.Polymers 3 and 5. In order to estimate the magnitude of the error affecting the corrected values of ΔU_c, the main calorimetric uncertainties were propagated to the error arising from the estimation of the amounts of the acids formed during the calorimetric burns, [for Polymer 2 (ES%=70) see Table 2.43, column 4]. For Polymer 5 (ES%=51, Batch 2), for which only one 'chemical burn' was carried out, the estimated error was obtained by propagating the main calorimetric error (Appendix B, Table 5.10) to the largest 'chemical error' observed for the other polymers i.e. ±2.3% (Polymer 2, ES%=70, Table 2.43). Table 2.44 presents the results of these thermochemical corrections for Polymer 2 (ES%=70, Batch 2) and for Polymers 1-5, with the exception of less-substituted Polymer 2 (ES%=31) and the precursor linear poly[bis(2,2,2-trifluoroethoxy)phosphazene], which both generated some hexafluorophosphoric acid. These two polymers will be discussed in the next section (2.2.9.6).

Polymer (ES%)	**Measured value of $-\Delta U_c$ ($J\ g^{-1}$)**	HPO_2F Formed (mmol) from 1 g sample	H_2PO_3F Formed (mmol) from 1g sample	Energy contributed by hydrolysis of HPO_2F_2 to be added (J)	Energy contributed by hydrolysis of H_2PO_3F to be added (J)	Total energy correction applied to measured $-\Delta U_c$ value (J)	**$-\Delta U°_c$ ($J\ g^{-1}$)**
1 (ES%=76)	**10520**	**0.291**	**1.611**	**4.1**	**24.7**	**28.8**	**10550**
2 (ES%=70)	**9220**	**0.264**	**1.204**	**3.7**	**18.4**	**22.1**	**9240**
2 (ES%=78)	**9220**	**0.178**	**0.718**	**2.5**	**11.0**	**13.5**	**9230**
3 (ES%=61)	**11250**	**0.167**	**1.014**	**2.4**	**15.5**	**17.9**	**11270**
4 (ES%= 67)	**13040**	**0.241**	**0.844**	**3.4**	**12.9**	**16.3**	**13060**
5 (ES%=51)	**14450**	**0.195**	**1.126**	**2.8**	**17.2**	**20.0**	**14470**
5 (ES%=68)	**14440**	**0.104**	**0.600**	**1.5**	**9.2**	**10.7**	**14450**

Table 2.44 Thermochemical corrections for the hydrolysis of monofluoro- and difluoro-phosphoric acids applied to the measured ΔU_c values of selected Polymers.

The results presented in Table 2.44 indicate that the average magnitude of the corrections is very small indeed (less than 0.3%). This is a positive conclusion, in light of the fact that the amounts of monofluoro- and difluoro-phosphoric acids that had formed during the calorimetric burns of each polymer, could only be *estimated* by extrapolation of the results obtained from the chemical part of the investigations.

Since the corrections were additive amounts, the propagation of error was estimated by application of Equation 42,[129] which is applicable to addition and substraction.

$$S_a = \sqrt{S_b^{\,2} + S_c^{\,2}} \qquad (42)$$

where S_b and S_c are the standard deviations associated with the figures which are added or subtracted and S_a is the standard deviation affecting the resulting value for the operation $a = b \pm c$. The results of error propagation for 4 selected Polymers is presented in Table 2.45. At the truncation level used, the overall, final uncertainties were essentially unchanged, suggesting that the propagation of the

error associated with the thermochemical corrections, as shown in Table 2.44, to the main calorimetric uncertainties were effectively negligible.

Polymer (ES%)	$-\Delta U°_c$ calculated using mean values of 'acid formation ratios' ± main calorimetric uncertainty (± %SD) ($J\ g^{-1}$)	± SD of the mean $\Delta U°_c$ values obtained using the individual 'acid formation ratios' (± %SD) (J)	$-\Delta U°_c$ after propagation of error to main calorimetric uncertainty (± %SD) ($J\ g^{-1}$)
1 (ES%=76)	10550 ± 180 (± 1.7%)	1.0 (0.01)	10550 ± 180 (± 1.7%)
2 (ES%=70)	9240 ± 160 (± 1.7%)	2.3 (0.03)	9240 ± 160 (± 1.7%)
3 (ES%=61)	11270 ± 100 (± 0.9%)	1.7 (0.01)	11270 ± 100 (± 0.9%)
5 (ES%=51)	14470± 180 (± 1.2%)	2.3 (0.02)	14470± 180 (± 1.2%)

Table 2.45 Propagation of the error associated with the estimation of the amounts of the monofluoro- and difluoro-phosphoric acids formed in the calorimetric burns of selected Polymers to the respective main calorimetric uncertainties.

2.2.9.5.1 Derivation of $\Delta H_c°$ and calculation of $\Delta H_f°$ of Polymer 2 (ES%=70)

As the unit monomer empirical formula of Polymer 2 (ES%=70) is known (Section 2.1.6), the balanced ideal combustion reaction of this polymer i.e. that does not take into consideration the formation of nitric acid, monofluoro- and difluoro-phosphoric acids, which have already been corrected for during the evaluation of the standard internal energy of combustion, may be described as follows:

$$\mathbf{C_{5.40}H_{8.20}N_{3.80}O_{10.40}F_{1.80}P_{1.00} + 3.05O_2 + (nH_2O) \rightarrow 5.40CO_{2(g)} + 3.20H_2O_{(l)} + + 1.90N_{2(g)} + 0.5\ P_2O_{5\ (cr)}\ (\rightarrow 1.00\ H_3PO_{4(aq)}) + 1.80HF_{(aq)}}$$

$\Delta H_c°$ is thus derived from $\Delta U_c°$ by application of Equation 2 (Section 1.4, $\Delta H^\circ_c = \Delta U^\circ_c + \Delta nRT$)

Where:

$\Delta n = + 5.40 + 1.90 - 3.05 =$ **+ 4.25 mol**

And $\Delta nRT = (+ 4.25)(mol) \times 8.314 (J\ mol^{-1}\ K^{-1}) \times 298.15 (K) =$ **+ 10.5 kJ**

From bomb calorimetry, the standard internal energy of combustion is

$\mathbf{\Delta U^{\circ}_c = - 9240 \pm 160\ J\ g^{-1}} = \mathbf{- 3307 \pm 57\ kJ\ mol^{-1}}$ (monomer unit MW= 357.91)

Hence

$\mathbf{\Delta H^{\circ}_c = - 3307 + (+ 10.5) = - 3296 \pm 57\ kJ\ mol^{-1} = -9209 \pm 160\ J\ g^{-1}}$

Where the units of both ΔH_c° and ΔH_f° (kJ mol^{-1} and J g^{-1}), represent in this case (and those that follow) *kJ/ mol average repeat unit* and *J/ g average repeat unit*.

Finally, from the latest CODATA values[187] for the standard enthalpies of formation of the ideal products of reaction (after secondary reaction with water), which are:

$\Delta H^{\circ}_f\ CO_{2\ (g)\ (298.15\ K)}$	$= -393.51 \pm 0.13$	kJ mol^{-1}
$\Delta H^{\circ}_f\ H_2O_{\ (l)\ (298.15\ K)}$	$= -285.83 \pm 0.04$	kJ mol^{-1}
$\Delta H^{\circ}_f\ N_{2\ (g)\ (298.15\ K)}$	$= 0$	kJ mol^{-1}
$\Delta H^{\circ}_f\ H_3PO_{4\ (aq)(298.15\ K)}$	$= -1299.0 \pm 1.5$	kJ mol^{-1}
$\Delta H^{\circ}_f\ HF_{\ (aq)\ (298.15\ K)}$	$= -335.35 \pm 0.65$	kJ mol^{-1}

$\Delta H^{\circ}_{f\ Polymer\ 2(ES\%=70)}$ can therefore be calculated as follows:

$\mathbf{\Delta H^{\circ}_{f\ Polymer\ 2\ (ES\%=70)}} = |\ \mathbf{\Sigma \Delta H^{\circ}_{f\ (products)} - \Delta H^{\circ}_{c\ Polymer\ 2\ (ES\%\ =70)}}\ | =$

$- \{(5.40 \times 393.51) + (3.20 \times 285.83) + (1.90 \times 0) + (1.80 \times 335.35) + (1.00 \times 1299.0)\} - (- 3296) = -4942.2 + 3292 =$ **-1650 kJ mol^{-1} = -4610 J g^{-1}**

The propagation of the uncertainties associated with the ΔH°_f values of the products of reaction to the main uncertainty associated with the $\mathbf{\Delta H^{\circ}_c}$ value of Polymer 2 (ES%=70) can be shown to be negligible by application of Equation 42 to the standard enthalpy terms summated, where $\delta\ \Delta H_f^{\circ}\ x$ is the absolute standard deviation associated to the value $\Delta H_f^{\circ}\ x$:

$$\delta\left(\Delta H_f^{\circ}{}_{Polymer\ 2}\right) = \left[\left(\delta\ \Delta H_f^{\circ}{}_{CO_2}\right)^2 + \left(\delta\ \Delta H_f^{\circ}{}_{H_2O}\right)^2 + \left(\delta\ \Delta H_f^{\circ}{}_{H_3PO_4}\right)^2 + \left(\delta\ \Delta H_f^{\circ}{}_{HF}\right)^2 + \left(\delta\ \Delta H_c^{\circ}{}_{Polymer\ 2}\right)^2\right]^{0.5}$$

$= 57.02 \approx 57$ kJ mol^{-1}

In conclusion, the value of ΔH°_{f} for Polymer 2 (ES%=70, Batch 2) may be expressed as:

$$\Delta H^{\circ}_{f\ Polymer\ 2\ (ES\%=70)} = -1650 \pm 57\ kJ\ mol^{-1} = -4610 \pm 160\ J\ g^{-1}$$

The standard enthalpies of combustion (ΔH_c º) and formation (ΔH_f º) of the other Polymers were derived in the same manner. The results for these materials, with the exception of less-substituted Polymer 2 (ES%=31) and of linear poly[bis(2,2,2-trifluoroethoxy)phosphazene], which are discussed separately (Section 2.2.9.6), are summarised in Table 2.46, alongside the literature ΔH_f º values[121] of the carbon-based energetic binders PolyGLYN, PolyNIMMO and GAP (Section 1.1).

Energetic Polymer	ES%	ΔH_c ° ($J\ g^{-1}$)	ΔH_c ° ($kJ\ mol^{-1}$)	ΔH_f ° ($J\ g^{-1}$)	ΔH_f ° ($kJ\ mol^{-1}$)
1	76	-10530 ± 180	-2672 ± 46	-5849 ± 180	-1484 ± 46
	100	-11170 ± 320	-2871 ± 82	-4453 ± 320	-1145 ± 82
2	70	-9209 ± 160	-3296 ± 57	-4610 ± 160	-1650 ± 57
	78	-9201 ± 230	-3415 ± 85	-4219 ± 230	-1566 ± 85
3	61	-11250 ± 100	-4052 ± 36	-4627 ± 100	-1667 ± 36
4	67	-13040 ± 210	-4821 ± 82	-5213 ± 210	-1927 ± 82
5	51	-14460 ± 180	-5345 ± 66	-4282 ± 180	-1583 ± 66
	68	-14440 ± 210	-5946 ± 86	-4268 ± 210	-1758 ± 86
PolyGLYN				-2710	-323
PolyNIMMO				-2290	-337
GAP				-1150	-114

Table 2.46 Standard enthalpy of combustion (ΔH_c °) and standard enthalpy of formation (ΔH_f °) of energetic polymers 1-5 and corresponding literature values for PolyGLYN, PolyNIMMO and GAP.

Table 2.46 shows that the $\Delta H_f°$ values of Polymers 1-5 are considerably more *negative* than those of the carbon-based energetic polymers listed. This may, at first, appear as detrimental for the achievement of high detonation enthalpies. However, it must be remembered that the magnitude of the latter quantity is dictated, by virtue of Hess's Law, by the difference between the sum of the enthalpies of formation of the detonation products and the enthalpy of formation of the energetic binder. The carbon-based energetic binders are thus expected to yield, upon detonation, a complex mixture of products which are not particularly exothermic, such as CO ($\Delta H_f° \approx -110$ kJ mol^{-1}), CO_2 ($\Delta H_f° \approx -393$ kJ mol^{-1}), H_2 ($\Delta H_f° = 0$ kJ mol^{-1}), H_2O ($\Delta H_f° \approx -285$ kJ mol^{-1}) and amorphous carbon ($\Delta H_f° \approx 0$ kJ mol^{-1}). Polymers 1-5 however, would generate, in addition to the above and HF, highly exothermic (fluorinated) phosphoric anhydrides. The highly negative $\Delta H_f°$ of the latter products is expected to contribute towards the release, upon detonation, of additional thermal energy.

2.2.9.6 The 'chemical part' of the calorimetric investigations of less-substituted Polymer 2 (ES%=31) and of linear poly[bis(2,2,2-trifluoroethoxy)-phosphazene]: derivation of $\Delta H_c°$ and calculation of $\Delta H_f°$

2.2.9.6.1 Less-substituted Polymer 2 (ES%=31)

Due to the small amounts of material left over from the calorimetric experiments only two chemical burns were carried out for this polymer. ^{19}F NMR spectroscopic analysis of the buffered, undiluted bomb solutions revealed that HPF_6 and 2,2,2-trifluoroethanol had been formed (see Figure 2.59). No thermochemical corrections due to these two products were applied to the measured ΔU_c value, due to the very small amounts detected (Table 2.47).

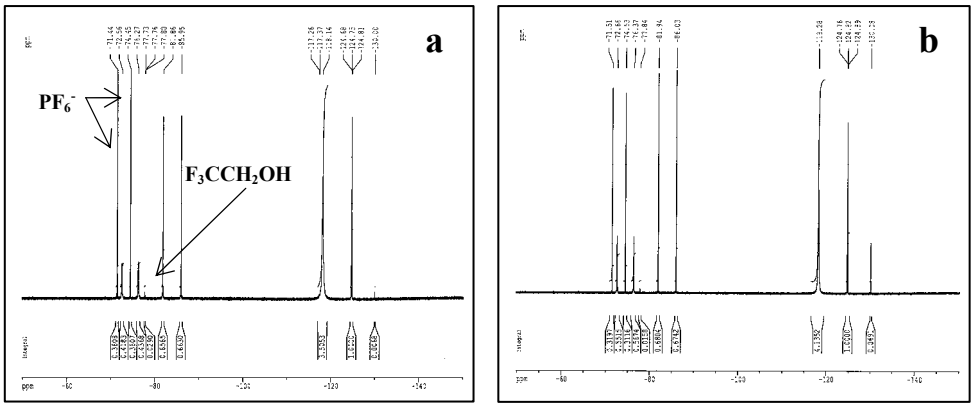

Figure 2.59 ^{19}F NMR spectra (acetone-d_6 internal probe) of the undiluted, buffered bomb solutions (imidazole / imidazolium oxalate 0.8M, pH=7) of (a) Chemical Burn 1 and (b) Chemical Burn 2, of Polymer 2 (ES%=31).

Tables 2.47 *a* and *b* present the results of the quantitative phosphorus and fluorine analysis (^{19}F NMR and IC) of the bomb solutions from the chemical burns. The amounts of phosphorus recovered as water-soluble species exceeded (by approximately 17.5%) the theoretical amounts of the element that was contained in the samples. Elemental analysis of Polymer 2 (ES%=31) was unfortunately not measured, and the cause of this inconsistency remains unclear. Table 2.48 shows the mean formation ratios of the acidic species. As observed for the Polymer 2 (ES%=70), there was poor consistency for both species.

Combustion No.	Sample weight (mg)	Weight of dry residue (mg)	F^- (mmol)	$PO_2F_2^-$ (mmol)	PO_3F^{2-} (mmol)	PF_6^- (mmol)	F_3CCH_2OH (mmol x10^{-3})	PO_4^{3-} (mmol)
1	245.4	3.0	1.772	0.334	0.432	0.064	4.93	0.156
2	287.0	4.5	2.091	0.342	0.566	0.053	2.65	0.182

Combustion No.	Amount of F present in sample (mmol)	Total F recovered (mmol)	Amount of P present in sample (mmol)	Total P recovered (mmol)	**F recovered (%)**	**P recovered (%)**
1	3.456	3.271	0.835	0.986	**94.6**	**118.1**
2	4.042	3.667	0.976	1.143	**90.7**	**117.1**

Table 2.47(a) top and (b) bottom. Results of the quantitative analysis (^{19}F NMR and IC) of the buffered bomb solutions from the chemical burns of Polymer 2 (ES%=31).

Combustion No.	$PO_2F_2^-$ (mmol) / sample mass (mg) [$x10^{-3}$]	PO_3F^{2-} (mmol) / sample mass (mg) [$x10^{-3}$]	PF_6^- (mmol) / sample mass (mg) [$x10^{-3}$]	Corrected $-\Delta U_c$ ($J\ g^{-1}$)
1	1.361	1.760	0.261	8917.7
2	1.192	1.972	0.185	8921.0
Mean and S.D %S.D.	1.277 ± 0.12 (± 9.4%)	1.866 ± 0.15 (± 8%)	0.223 ± 0.05 (± 24.1%)	8819.4 ± 2.33 (± 0.03%)

Table 2.48 Ratios of the amounts (mmol) of monofluoro-, difluoro- and hexafluoro-phosphoric acids formed and the mass of sample burnt (mg) for Polymer 2 (ES%=31) and corrected values of ΔU_c.

The low and high values of these ratios were used to estimate the uncertainty associated with the predicted amounts of fluorinated acid species that would form in the calorimetric burn, per unit mass of the material. Upon propagation to the main calorimetric uncertainty, this error was negligible, as explained in Section 2.2.9.5. Table 2.49 corrects the measured ΔU_c (Table 5.3, Appendix B) for the formation of the three fluorinated species.

Measured value of $-\Delta U_c$ ($J\ g^{-1}$)	HPO_2F_2 Formed (mmol) from 1 g sample	H_2PO_3F Formed (mmol) from 1g sample	HPF_6 Formed (mmol) from 1g sample	Energy ($-\Delta H° \approx -\Delta U°$) contributed by hydrolysis of HPO_2F_2 (J)	Energy ($-\Delta H° \approx -\Delta U°$) contributed by hydrolysis of H_2PO_3F (J)	Energy ($+\Delta H° \approx +\Delta U°$) contributed by hydrolysis of HPF_6 (J)	Total energy correction applied to measured $-\Delta U_c$ value (J)	Final corrected value of $-\Delta U°_c$ rounded to 3 signif. figures ($J\ g^{-1}$)
8880	1.280	1.870	0.220	18.0	28.5	7.2	39.3	8920

Table 2.49 Thermochemical corrections to account for the aqueous hydrolysis of monofluoro-, difluoro- and hexafluoro-phosphoric acids, applied to the measured ΔU_c value of Polymer 2 (ES%=31).

The literature ΔH_{hyd} values of monofluoro- and difluoro-phosphoric acids, as mentioned in Section 2.2.9.5, were again used, but a literature value for HPF_6 was not available. The ΔH_{hyd} value of $HPF_{6(aq)}$ was estimated by application of Hess's Law to the standard enthalpies of formation of the reactants and products of its hydrolysis reaction. Aqueous HPF_6 exists as the solvated ionic species $H_3O^+\ PF_6^-$. The standard enthalpy of formation of the H_3O^+ species is $-\Delta H°_{f\ (298.15K)}\ H_3O^+ = 0$ kJ mol^{-1} (by definition), whereas that of the PF_6^- anion is reported to be $-\Delta H°_{f\ (298.15K)}\ PF_6^- = -2200$ kJ mol^{-1} (a recommended experimental value[188]).

Hexafluoro-phosphoric acid	**1 $HPF_{6(aq)}$** + **4 $H_2O_{(l)}$** → **1 $H_3PO_{4(aq)}$** + **6 $HF_{(aq)}$**			
$-\Delta H°_f$ (298K) (kJ mol^{-1})	2200	1143.3	1299.0	2012.1

Hess's Law Estimated $\Delta H°_{hyd}$ HPF_6^- = +32.2 kJ mol^{-1}

The standard enthalpies of hydrolysis of monofluoro- and difluoro-phosphoric acids were also calculated in the same way and these values compared with the experimental $\Delta H°_{hyd}$ values quoted in the literature:

Monofluoro-phosphoric acid	**1 $H_2PO_3F_{(aq)}$** + **1 $H_2O_{(l)}$** → **1 $H_3PO_{4(aq)}$** + **1 $HF_{(aq)}$**			
$-\Delta H°_f$ (298K) (kJ mol^{-1})	1307.30[186]	285.83	1299.0	335.35

Hess's Law Estimated $\Delta H°_{hyd}$ H_2PO_3F = -41.22 kJ mol^{-1}; Lit. value = -15.3 kJ mol^{-1}. (Δ: - 25.9 kJ mol^{-1})

Difluoro-phosphoric acid	**1 $HPO_2F_{2(aq)}$** + **2 $H_2O_{(l)}$** → **1 $H_3PO_{4(aq)}$** + **2 $HF_{(aq)}$**			
$-\Delta H°_f$ (298K) (kJ mol^{-1})	1327.60[186]	571.66	1299.0	670.7

Hess's Law Estimated $\Delta H°_{hyd}$ HPO_2F_2 = -70.44 kJ mol^{-1}; Lit. value = -14.1 kJ mol^{-1}. (Δ: - 56.3 kJ mol^{-1})

As can be seen, the $\Delta H°_{hyd}$ values estimated by application of Hess's Law do not agree with the experimental $\Delta H°_{hyd}$ values quoted in the literature. However, after consultation with workers of the Thermodynamics Modelling Group at NPL Teddington, who were able to verify the estimated figures, it was speculated that the values reported in the literature could be affected by a significant source of error, as the authors also stated. The use of the (possibly inaccurate) experimental, literature values for H_2PO_3F and HPO_2F_2, and of the $\Delta H°_{hyd}$ value for HPF_6 however, may be permissible in view of the very small amounts of these species that are formed. These require thermal corrections that are always much smaller than the overall calorimetric uncertainty.

The standard enthalpies of combustion (ΔH_c^o) and formation (ΔH_f^o) of Polymer 2 (ES%=31, unit monomer MW= 293.91) were derived in the same manner as for

the other polymers, as described in Section 2.2.9.5. The idealised, oxygen-balanced combustion equation is:

$$\mathbf{C_{4.62}H_{5.86}N_{2.24}O_{5.72}F_{4.14}P_{1.00} + 3.44O_2 + (nH_2O) \rightarrow 4.62CO_{2(g)} + 0.86H_2O_{(l)} + + 1.12N_{2(g)} + 0.5\ P_2O_{5\ (cr)}\ (\rightarrow 1.00\ H_3PO_{4(aq)}) + 4.14HF_{(aq)}}$$

From this equation, the difference between the number of moles of gaseous products and reactants is $\Delta n = +2.30$ mol and $\Delta nRT = +5.70$ kJ. It follows that

$\mathbf{\Delta H_c^o}_{\text{Polymer 2(ES\%=31)}} = \Delta U_c^o + \Delta nRT = -2622 + (+5.70) =$

$\mathbf{-2616 \pm 41\ kJ\ mol^{-1} = -8901 \pm 140\ J\ g^{-1}}$

Hence $\mathbf{\Delta H_f^o}_{\text{Polymer 2(ES\%=31)}} = \mathbf{- 2135 \pm 41\ kJ\ mol^{-1} = - 7264\ kJ\ g^{-1}}$

2.2.9.6.2 Linear poly[bis(2,2,2-trifluoroethoxy)phosphazene]

Three chemical burns were carried out for the homopolymeric precursor to Polymers 1-5. A new procedure was used to initiate the material that would not require the use of cotton thread. This procedure is described in Section 4.1.1.3. Tables 2.50 *a* and *b* present the results of the quantitative analysis (^{19}F NMR and IC) of the buffered (imidazole / imidazolium oxalate, 0.8 M, pH =7) solutions. As in the case of the less-substituted Polymer 2 (ES%=31), hexafluorophosphate and 2,2,2-trifluoroethanol were detected in the bomb solutions, alongside phosphate, monofluoro- and difluoro-phosphate. GC-MS of the bomb exhausts from all three experiments indicated that CF_4, and other fluorinated carbon- and/or phosphorus-based gases had not formed.

Combustion No.	Sample weight (mg)	Weight of dry residue (mg)	F^- (mmol)	$PO_2F_2^-$ (mmol)	PO_3F^{2-} (mmol)	PF_6^- (mmol)	F_3CCH_2OH (mmol x10^{-3})	PO_4^{3-} (mmol)
1	296.6	6.0	2.808	0.317	0.338	0.196	7.28	0.062
2	301.5	5.3	3.041	0.305	0.319	0.140	9.21	0.107
3	324.0	7.5	3.269	0.360	0.507	0.141	11.5	0.143

Combustion No.	Amount of F present in sample (mmol)	Total F recovered (mmol)	Amount of P present in sample (mmol)	Total P recovered (mmol)	**F recovered (%)**	**P recovered (%)**
1	7.320	4.963	1.220	0.913	**67.8**	**74.8**
2	7.443	4.820	1.241	0.871	**64.8**	**70.1**
3	8.000	5.354	1.333	1.151	**66.9**	**86.3**

Table 2.50 (a) top and (b) bottom. Results of the analysis (^{19}F NMR and IC) of the bomb solutions of the chemical burns of linear poly[bis(2,2,2-trifluoroethoxy)phosphazene].

As can be seen from Table 2.50, the recoveries of fluorine and phosphorus as water-soluble species were low. The halogen-like smelling fumes that were observed on opening the bomb were much 'denser' and more persistent than those observed after the combustion of Polymer 2 (ES%=31). The occurrence of these uncondensed mists (suspended fluorinated anhydrides ?) were thought to be the major cause for the mass loss (see below). Table 2.51 presents the 'acid formation ratios' for the three chemical burns, while Table 2.52 applies the thermochemical corrections to the measured ΔU_c value to account for the formation of the non ideal, fluorinated phosphoric acids. The energies of hydrolysis used are those mentioned in Section 2.2.9.6.1.

Combustion No.	$PO_2F_2^-$ (mmol) / sample mass (mg) [x10^{-3}]	PO_3F^{2-} (mmol) / sample mass (mg) [x10^{-3}]	PF_6^- (mmol) / sample mass (mg) [x10^{-3}]
1	1.068	1.140	0.661
2	1.011	1.058	0.464
3	1.111	1.565	0.435
Mean and S.D %S.D.	1.063 ± 0.05 (± 4.7%)	1.254 ± 0.27 (± 21.7%)	0.520 ± 0.12 (± 23.7%)

Table 2.51 Ratios of the amounts (mmol) of monofluoro-, difluoro- and hexafluoro-phosphoric acids formed and the mass of sample burnt (mg) for linear poly[bis(2,2,2-trifluoroethoxy)phosphazene].

Measured value of $-\Delta U_c$ ($J\ g^{-1}$)	HPO_2F_2 Formed (mmol) from 1 g sample	H_2PO_3F Formed (mmol) from 1g sample	HPF_6 Formed (mmol) from 1g sample	Energy ($-\Delta H° \approx -\Delta U°$) contributed by hydrolysis of HPO_2F_2 (J)	Energy ($-\Delta H° \approx -\Delta U°$) contributed by hydrolyseis of H_2PO_3F (J)	Energy ($+\Delta H° \approx +\Delta U°$) contributed by hydrolysis of HPF_6 (J)	Total energy correction ($-\Delta H°$) applied to measured $-\Delta U_c$ value (J)	Final corrected value of $-\Delta U°_c$ rounded to 3 signif. figures ($J\ g^{-1}$)
9340	1.063	1.254	0.520	15.0	19.2	16.7	17.3	9360

Table 2.52 Thermochemical corrections to account for the hydrolysis of monofluoro-, difluoro- and hexafluoro-phosphoric acids, applied to the measured ΔU_c values of linear poly[bis(2,2,2-trifluoroethoxy)phosphazene].

In order to prove that the uncondensed white mists were the cause of the observed mass defects, an extra chemical burn was performed and the post-combustion exhaust gases were vented slowly, as a fine mist of bubbles, through a tall scrubber containing deionised water (200 ml). The resulting solution was qualitatively analysed by IC for any fluorinated species. The analysis confirmed the presence of fluoride and difluorophosphate, in addition to traces of phosphate and monofluoro-phosphate. Hexafluorophosphate would not be observed by IC, due to its affinity for the column stationary phase. No ^{19}F NMR spectroscopic analysis was performed on this solution, due to the low concentration of the analytes. Since a considerable portion of the white smoke was still observed to escape the scrubber when the bubbles broke the surface, IC quantitative analysis of the scrubbing water was also not attempted.

The balanced idealised combustion reaction in excess oxygen gas of linear poly[bis(2,2,2-trifluoroethoxy)phosphazene], {Polymers 1-5 (ES%=0)}, $C_{4.00}H_{4.00}N_{1.00}O_{2.00}F_{6.00}P_{1.00}$, (monomer unit MW: 243.04) is difficult to conceive without involvement, in the reaction, of the water physically added to the bomb prior to performing the combustion experiment. There are in fact only four hydrogen atoms available to form HF in the monomer unit empirical formula, leaving an excess of two fluorine atoms, which, in theory, may contribute to the formation of the various fluorinated carbon- and/or phosphorus-based gaseous species that were envisaged as possible 'side-reaction' by-products, and the formation of which would have to be thermochemically corrected for.

In order to gain more insight into the stoichiometry of the combustion reaction of this polymer, a 300 mg sample was combusted (30 atm oxygen) in the total absence of water in the bomb ('dry bomb' conditions). During this experiment the sample was successfully ignited without the use of cotton thread, by direct contact of the material (which was pressed inside a 150 µl alumina crucible) with the glowing fuse wire. The exhaust gases from the latter experiment were qualitatively analysed by GC-MS for the presence of the above-mentioned fluorinated gaseous species and also for elemental fluorine gas, which is reported to form during the combustion in excess oxygen of highly-fluorinated compounds which do *not* contain hydrogen e.g. hexafluorobenzene[152] and octafluorotoluene,[153] in the absence of water vapour ('dry bomb' conditions[189]). However none of these gases were detected. Due to its extreme reactivity, fluorine gas reacts with liquid water (or water vapour) to form oxygen and aqueous HF, and since water vapour was indeed detected by GC-MS in the exhausts of Experiment B, it is feasible to envisage that (a) any F_2 that may have formed during the combustion of the sample would have immediately reacted with this water to yield HF (not observed by GC-MS), (b) it quantitatively reacted with the glass of the glass crimp-top vial which was used to sample the exhaust gases, to form a stable fluorosilicate, or (c) it may have reacted with the column film of the VARIAN CP-PoraPLOT GC capillary column, possibly generating fluorinated species which may have been retained indefinetely. This has been known[190] to occur with this column for other reactive gaseous species e.g. NO_2.

On depressurising the bomb, a very dense white smoke was observed to issue from the release valve. The remarkable 'density' of this smoke re-inforced the view that, in the absence of a liquid phase in the bomb, the fluorinated gaseous species generated by the combustion of a highly fluorinated, phosphorus containing organic material, cannot interact (solubilise in or react with) with water and hence remain, to a large extent, suspended as an uncondensed smoke.

In view of the latter results, during the combustion of linear poly[bis(2,2,2-trifluoroethoxy)phosphazene] in the presence of a liquid phase in the bomb (as in

the 'calorimetric burns' for this material), it was reasoned that (a) the formation of any gaseous fluorinated carbon and / or phosphorus species does not occur, (b) some of the hydrogen in the monomer unit is converted to water, (c) some of the fluorine in the monomer unit is initially converted to $F_{2(g)}$, which then reacts with the water formed in the reaction and / or with the water added to the bomb to give $HF_{(aq)}$ and $O_{2(g)}$. In the least favourable case in which all of the fluorine present was initially converted to $F_{2(g)}$, 3 moles of fluorine gas would liberate, by reacting with water, 1.5 moles of $O_{2(g)}$ which would contribute towards the total volume increase of the bomb process and hence upon the final calculation of Δn.

$C_{4.00}H_{4.00}N_{1.00}O_{2.00}F_{6.00}P_{1.00} + 6O_2 + nH_2O \rightarrow 4.00CO_{2(g)} + 0.5N_{2(g)} + 2H_2O_{(l)} + 0.5\ P_2O_5(s)\ (\rightarrow 1.00H_3PO_{4\ (aq)}) + 6HF_{(aq)} + 1.5O_{2(g)}$

$\Delta n = + 4.00 + 0.5 + 1.5 - 6.0 =$ **0 mol**

$\Delta nRT =$ (0)(mol) x 8.314 (J mol^{-1} K^{-1}) x 298 (K) = **0 kJ**

From bomb calorimetry, the corrected $\mathbf{\Delta U^{\circ}_c = -9360 \pm 210\ J\ g^{-1}}$

$\mathbf{= -2275 \pm 51\ kJ\ mol^{-1}}$

and hence

$\mathbf{\Delta H^{\circ}_c = -2275 \pm 51\ kJ\ mol^{-1} \approx -9360 \pm 210\ J\ g^{-1}}$

Finally,

$\mathbf{\Delta H^{\circ}_{f\ linear\ poly[bis(2,2,2\text{-}trifluoroethoxy)phosphazene],\ (298.15\ K)}}$ = - {(4.00 x 393.51) + (2.00 x 285.83) + (0.5 x 0) + (1.5 x 0) + (6.00 x 335.35) + (1.00 x 1299.0)} – (- 2275) =

-5456.8 + 2275 = $\mathbf{-3182 \pm 51\ kJ\ mol^{-1} = -13090 \pm 210\ J\ g^{-1}}$

In order to estimate the magnitude of the thermal discrepancy that would arise from conducting the calorimetric burns of linear poly[bis(2,2,2-trifluoroethoxy)phosphazene] under dry bomb conditions i.e. no liquid phase added to the bomb, five more replicate calorimetric burns were performed, in which the samples were ignited without using cotton thread. Table 2.53 presents the results of these experiments.

Combustion Experiment	Sample Weight (g)	ΔTcorr (K)	Weight of residue in crucible (mg)	$-\Delta U_c$ (Jg^{-1}) rounded to 3 signif. figures
1	0.2810	0.209	2.5	8110
2	0.2698	0.210	4.8	8460
3	0.3267	0.226	6.1	7520
4	0.3946	0.305	1.5	8420
5	0.3134	0.223	3.9	7750
Mean and S.D. after propagation of error				8050 ± 410 (± 5.1%)

Table 2.53 Experimental measurement of ΔU_c of linear poly[bis(2,2,2-trifluoroethoxy)phosphazene] under dry bomb conditions.

Since the small variation in heat capacity of the system, due to the absence of the liquid phase in the bomb, could not have been responsible for the large discrepancy ($\Delta\Delta E_c \approx 1.3$ kJ g^{-1}), it was thought that a significant proportion of the (constant volume) energy that would normally be released upon combustion in the presence of a liquid phase in the bomb i.e. mainly due to reaction of the various phosphoric anhydrides with water and their subsequent dilution, cannot be released and, consequently, the measured, mean ΔU_c value will be lower.

2.2.9.7 Polymer ΔH_c^o and ΔH_f^o dependence upon ES% value

Just as the tentative correlation chart between ΔU_c and Polymer ES% values indicated that there was an energy trend for each member of the Polymer series, an analogous chart was drawn to correlate Polymer ΔH_c^o and hence ΔH_f^o with ES% value, albeit for Polymer 2 only, for which the highest number of samples of different ES% values were synthesised and combusted. The ΔH_c^o and ΔH_f^o values of Polymer 2 (ES%= 65, Batch 1) were calculated from the uncorrected value of ΔU_c, as no 'chemical burns' were performed on this sample. This may be justified however, in view of the very small magnitude of the corrections due to the hydrolysis of monofluoro- and difluoro-phophoric acids. Table 2.54 presents a summary of the ΔU_c-derived ΔH_c^o and ΔH_f^o values for Polymer 2 at different ES% values, while Figure 2.60 shows a plot of ΔH_c^o and ΔH_f^o against the polymer ES% value.

ES%	$-\Delta H_c^o$ (kJ mol^{-1})	$-\Delta H_c^o$ (J g^{-1})	$-\Delta H_f^o$ (kJ mol^{-1})	$-\Delta H_f^o$ (J g^{-1})
0	2275 ± 51	9360 ± 210	3182 ± 51	13090 ± 210
31	2616 ± 41	8871 ± 140	2135 ± 41	7277 ± 140
65	3018 ± 37	8630 ± 105	1900 ± 37	5433 ± 105
70	3296 ± 57	9209 ± 160	1650 ± 57	4610 ± 160
78	3415 ± 85	9201 ± 230	1566 ± 85	4219 ± 230

Table 2.54 ΔH_c^o and ΔH_f^o of Polymer 2 for different ES% values.

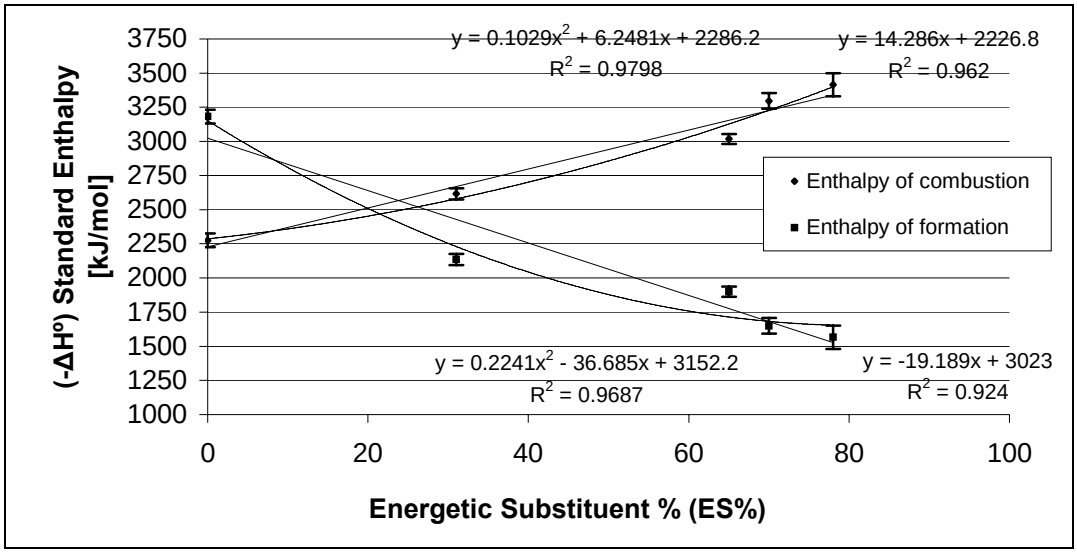

Figure 2.60 Tentative plot of ΔH_c^o and ΔH_f^o of Polymer 2 versus Polymer ES% value.

The trends shown in Figure 2.60, which, as in the case of the tentative ΔU_c / ES% plots, should be linear in the ideal cases, would appear to better fit polynomial relationships. The 'accurate' or 'true' experimental trends may, in fact, be low-order polynomials by virtue of the possible 'thermal' effect imparted by specific interactions between different adjacent substituent groups on the polymers. In this respect, the polynomial trends should be used for the purpose of detonation enthalpies predictions.

As can be seen from Figure 2.60, only the data-points pertaining to Polymer 2 (ES%=65) would appear to be significantly 'outside' the observed trends. However, this value should be used with due consideration, in the light of the small number of replicate calorimetric experiments, the small masses of sample burnt and the absence of any 'chemical burn' data for this material. It would also appear that higher Polymer ES% values would generally lead to increased combustion enthalpies and more positive (less exothermic) enthalpies of formation. More positive values of ΔH_f^o would indeed be desirable in the detonation thermochemical cycles in order to achieve higher enthalpies of detonation.

Although the number of available data-points was doubtless insufficient for the unambiguous definition of the true mathematical relationships between ΔH_c^o and ΔH_f^o of Polymer 2 and its ES% value, Figure 2.60 is believed to give a preliminary approximated view of the nature of the observed trends, for Polymer 2. The latter may only be verified or amended when more samples of intermediate ES% values have been synthesised and combusted.

2.2.10 Calorimetric investigations carried out under nitrogen

2.2.10.1 Preliminary observations on the initiation of Polymers 2 and 5

As was discussed in Section 1.3, a semi-empirical derivation of the standard enthalpies of detonation of Polymers 1-5 requires the 'modelling' of the detonation reaction of each polymer i.e. self-oxidation under inert atmosphere, and the quantitative analysis of the reaction products. However, the energy output and product distribution observed following the anaerobic initiation in a closed bomb of any of the Polymers 1-5, can only be a crude approximation of the thermochemical behaviour that these materials would display during a 'real' detonation of a PBX containing them. The thermochemistry of the real detonation reaction may be expected to depend on (a) the oxygen content of the explosive filler and plasticizer(s) and (b) the complex gas equilibria expected to be present at the extremely high temperatures and pressures behind the shock-front, and, to a lesser extent, the atmospheric conditions i.e. T, P and relative humidity.

Notwithstanding the above limitations, the feasibility of ignition and propagation under inert atmospheres of the energetic polyphosphazenes was investigated prior to performing any 'closed bomb' anaerobic experiment. This was investigated by electrically initiating small samples (100 mg inside 70 μl alumina crucibles) of Polymer 2 (ES%=70, Batch 2) and Polymer 5 (ES%=51, Batch 2) under nitrogen gas (P≈1 atm), inside the purpose built device shown in Figure 2.61. The improvised 'combustion bomb' was built using a glass desiccator, enclosed inside a metallic cage for extra safety. A glass container was chosen to allow direct visual observation of the experiments. Nitrogen gas was left to flow through the vessel for at least 10 min prior to ignition of the samples in order to displace the air. A nichrome fuse wire was connected to an external variable power supply and brought into contact with the polymer. The ignition of a sample of PolyGLYN under identical conditions was also attempted, since this polymer displays an oxygen balance (-60.5) similar to that of Polymer 5 (ES%=51, OB= -67.8).

All three polymers promptly ignited and successfully propagated, via flameless combustion, generating white smoke and leaving behind some black residue. In particular, Polymer 5 (ES%=51) was found to generate a black, voluminous spongy residue which could not be re-initiated even under oxygen at 30 atm using an ignition promoter (cotton thread).

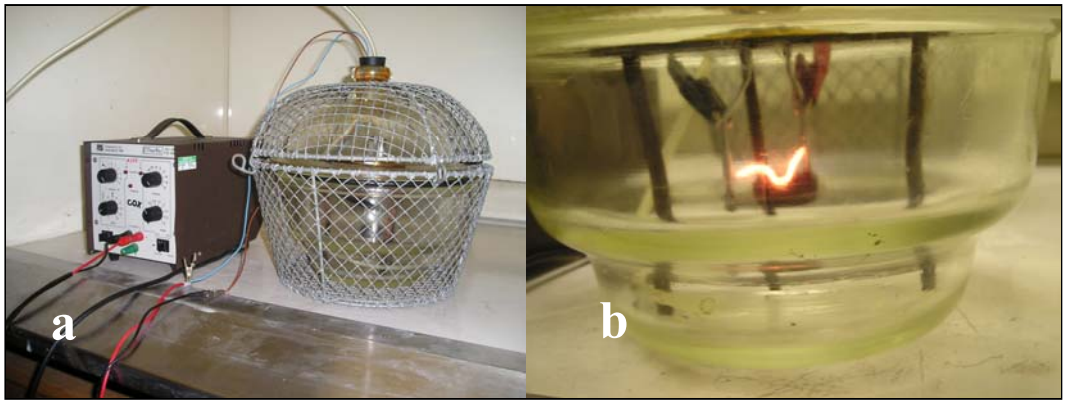

Figure 2.61 (a) The improvised 'glass bomb' with ignition leads and nitrogen line (b) Glowing nichrome wire (diameter 0.1 mm, length 25 mm, 0.5 A, 12 V DC).

2.2.10.2 Calorimetric measurement of the energy released upon initiation of Polymer 2(ES%=64)

After having ascertained that the energetic polyphosphazene will initiate under anaerobic conditions, a small batch of Polymer 2 was prepared and characterised for the specific purpose of conducting calorimetric studies of this material under nitrogen. The material, which had an estimated ES%=64, was free from contaminants, as judged by ^{1}H and ^{19}F NMR spectroscopy (unit monomer empirical formula: $C_{5.28}H_{7.85}N_{3.57}O_{9.71}F_{2.15}P_{1.00}$, estimated MW: 348.45, OB= -35.4). Polymer 2 was chosen as the first material to be investigated calorimetrically under anaerobic conditions since it was *more* oxygen balanced than the higher homologous members of the polymer series. In addition, during the preliminary 'glass bomb' experiments, it was noticed that Polymer 2 generated smaller amounts of residue. The general procedure adopted to perform the calorimetric and chemical burns under nitrogen was the same adopted for the oxygen experiments and is described in Section 4.1.1.4. Three calorimetric experiments in addition to two 'chemical' burns (P= 30±1 atm) were performed. Table 2.55 presents the results of the 'calorimetric' experiments, whilst Tables 2.57 *a* and *b* show the analytical results of the chemical burns.

In order to estimate the energy difference arising between the combustion of the polymer under nitrogen and oxygen, three more replicate calorimetric measurements and two chemical burns were also performed under oxygen (P= 30±1 atm). No corrections to standard states were performed. Table 2.56 presents the results of the oxygen calorimetric experiments, whilst Table 2.57 shows the results of the corresponding chemical burns. Finally, Table 2.58 shows the formation ratios for the water-soluble species detected in the bomb solutions of the chemical burns performed under nitrogen and oxygen. A massic energy difference of approximately 5.45 kJ g^{-1} was observed. However, the mean ΔE_c value was affected by a larger uncertainty than the mean ΔU_c value possibly due to the fact that, for the combustion under nitrogen (a) the net temperature increases (per sample mass unit) were considerably less than the oxygen case, and (b) much larger amounts of residue were left behind (cf. Tables 2.55 and 2.56).

Combustion Experiment	Sample Weight (g)	ΔTcorr (K)	Weight of residue in crucible (mg)	$-\Delta E_c$ (J g^{-1}) rounded to 3 signif. figures
1	0.2351	0.080	9.5	3720
2	0.2316	0.071	14.9	3340
3	0.2483	0.079	12.1	3460
Mean and S.D. after propagation of error (±%SD)				3510 ± 200 (± 5.5%)

Table 2.55 Experimental measurement of the energy released (at constant volume) by combustion under N_2 (30 atm) of Polymer 2 (ES%=64).

Combustion Experiment	Sample Weight (g)	ΔTcorr (K)	Weight of residue in crucible (mg)	$-\Delta U_c$ (J g^{-1}) rounded to 3 signif. figures
1	0.2557	0.214	2.5	9110
2	0.2531	0.212	1.7	9110
3	0.2734	0.217	3.0	8660
Mean and S.D. after propagation of error (±%SD)				8960 ± 260 (± 2.9%)

Table 2.56 Experimental measurement of the energy released (at constant volume, ΔU_c) by combustion under O_2 (30 atm) of Polymer 2 (ES%=64).

Bomb Gas (P = 30 atm)	Sample weight (mg)	Weight of dry residue (mg)	F^- (mmol)	$PO_2F_2^-$ (mmol)	PO_3F^{2-} (mmol)	PF_6^- (mmol)	CF_3CH_2OH (mmol)	PO_4^{3-} (mmol)
N_2 (a)	0.2351	16.3	0.923	0.039	0.103	0.003	0.127	0.488
N_2 (b)	0.2862	21.0	0.869	0.080	0.198	0.002	0.056	0.485
O_2 (a)	0.2557	3.5	0.910	0.045	0.253	0	0	0.329
O_2 (b)	0.2664	2.3	0.985	0.099	0.388	0	0	0.341

Bomb Gas (P = 30 atm)	Amount of F present in sample (mmol)	Total F actually recovered (mmol)	Amount of P present in sample (mmol)	Total P actually recovered (mmol)	Total P recovered after F-recovery normalisation (mmol)	**Scaled P recovered (%)** †	NO_3^- (mmol)
N_2 (a)	1.451	1.503	0.675	0.633	0.628	**93.0**	traces
N_2 (b)	1.766	1.407	0.821	0.765	0.836	**101.8**	0
O_2 (a)	1.577	1.253	0.734	0.627	0.704	**95.9**	0.093
O_2 (b)	1.645	1.571	0.765	0.828	0.851	**111.2**	0.141

† after fluorine recovery normalisation to 100%

Table 2.57 (a) top and (b) bottom. Results of the analysis (^{19}F NMR spectroscopy and IC) of the buffered (imidazole/imidazolium oxalate 0.8M, pH 7) bomb solution from the chemical burns of Polymer 2 (ES%=64) initiated under nitrogen and oxygen.

Bomb Gas (P= 30 atm)	F^- (mmol) / sample mass (mg) [$x10^{-3}$]	$PO_2F_2^-$ (mmol)/ sample mass (mg) [$x10^{-3}$]	PO_3F^{2-} (mmol) / sample mass (mg) [$x10^{-3}$]	PF_6^- (mmol) / sample mass (mg) [$x10^{-5}$]	PO_4^{3-} (mmol) / sample mass (mg) [$x10^{-3}$]
N_2 (a)	4.849	0.204	0.540	1.57	2.076
N_2 (b)	3.809	0.349	0.867	0.87	1.694
O_2 (a)	4.478	0.223	1.244	0	1.287
O_2 (b)	3.870	0.390	1.524	0	1.280

Table 2.58 Ratios of the amount (mmol) of each combustion species observed (after fluorine recovery normalisation to 100%) and the mass of sample burnt (mg) for the chemical burns of Polymer 2 (ES%=64) performed under N_2 and O_2.

The effect of bomb pressure upon the energy released under anaerobic conditions was also investigated by carrying out three replicate combustion at a nominal pressure of 1 atm (Section 4.1.1.4). The results, presented in Table 2.59, indicated that the energy released by the polymer under these conditions was considerably lower than when the bomb was pressurised to 30 atm. Since the amounts of residue left in the crucible were larger than the amounts left behind at higher pressure, the observed decrease in energy was attributed to a less efficient combustion process. Slower reaction rates would cause low temperatures and hence increased pyrolysis and charring. The rate of combustion reactions (ordinary fuel-external oxidiser types and pyrotechnic systems alike) is well known to be pressure-dependant.[191,192,193]

Combustion Experiment Number	Sample Weight (g)	ΔTcorr (K)	Weight of residue in crucible (mg)	$-\Delta E$ ($J\ g^{-1}$) rounded to 3 signif. figures
1	0.3297	0.068	45.0	2240
2	0.2706	0.053	52.6	2130
3	0.2790	0.058	39.4	2270
Mean and S.D. after propagation of error (±%SD)				2210 ± 70 (± 3.2%)

Table 2.59 Experimental measurement of the energy released (at constant volume, ΔE_c) by combustion under N_2 (1 atm) of Polymer 2 (ES%=64).

Figure 2.62 shows the appearance of the residue left behind after combustion of Polymers 2 (ES%=64) and 5 (ES%=51) under oxygen (30 atm) and nitrogen (1 and 30 atm). As can be seen from the photographs, only pressurised oxygen furnished complete combustions. Figure 2.62 shows: (a) an empty 150 µl alumina crucible (b) a crucible loaded with 250 mg of Polymer 5 (ES%=51) ready for combustion, (c) the typical residue (2-6 mg) left behind after combustion (all

Polymers) in oxygen at 30 atm, (d) the residue left behind (15-20 mg) by Polymer 2 (ES% 64) after combustion under nitrogen (30 atm), (e) as (d) but at 1 atm, and (f) the residue (70-90 mg) left by Polymer 5 (ES%=51) after combustion under nitrogen (30 atm), and (g) as (f) but at 1 atm.

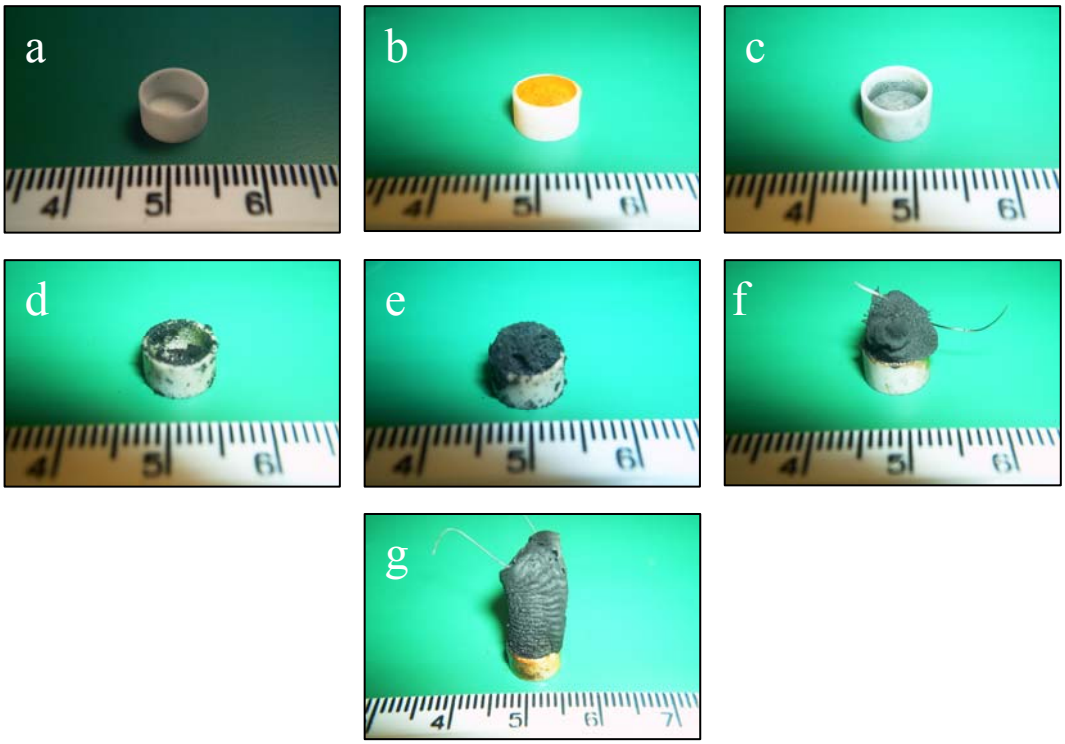

Figure 2.62 Appearance of residue left behind from the combustion of Polymers 2 (ES%=64) and 5 (ES%=51) initiated under oxygen and nitrogen at different pressure [scale shown: cm].

The analytical results shown in Table 2.57 indicated that the amounts of water-soluble products obtained from the chemical burns performed under pressurised nitrogen were qualitatively and quantitatively similar to those that had been obtained under pressurised oxygen. Since the recoveries of phosphorus for the nitrogen experiments were above 90% of the initial molar amounts contained in the sample, it was reasoned that the phosphorus had acted as an efficient 'oxygen scavenger' upon anaerobic initiation of the oxygen-deficient polymer, leaving the limited remaining oxygen available for the oxidation of some of the carbon and hydrogen. As the fluorine recoveries were also above 90%, it was reasoned that

the balance of the fluorine had reacted with hydrogen to give HF. This result should be regarded as an important step in the study of the products formed upon the initiation of this class of polymers under inert atmospheres, as it implies that, once all the phosphorus has been converted to phosphate and/or its fluorinated analogues (in reality the corresponding oxides, which then react with water to furnish the corresponding acid species) and the remaining fluorine has been converted to HF, carbon and hydrogen may only then 'compete' to react with the remaining oxygen mimicking the chemistry followed, upon detonation, by common oxygen-deficient explosives.

The final products of a detonation reaction may be predicted, with a reasonable level of confidence, by one of three sets of empirical 'rules'[8] which were developed during World-War II in order to predict the products of detonation of common explosive compounds. These rules, which take the name of *Kistiakowsky-Wilson* (K-W), *modified Kistiakowsky-Wilson* (mod. K-W) and *Springall-Roberts* (S-R), after the name of the developers, apply to materials of different oxygen balance and are stated later. The K-W rules are used for explosive materials with an oxygen balance less negative than –40% (e.g. NG, EGDN, PETN, RDX and HMX), whereas the mod. K-W and S-R rules are typically employed for explosives that are less oxygen balanced i.e. more negative than -40% (e.g. picric acid, TATB, HNS and TNT). These rules have been applied to model the detonation reaction stoichiometries of the carbon-based energetic binders polyGLYN and polyNIMMO.[194]

In order to compare the experimentally determined energy difference between the combustion of Polymer 2 (ES%= 64) in oxygen and nitrogen ($\Delta\Delta E_{exp} \approx 5.45$ kJ mol^{-1}) with the corresponding calculated value, six hypothetical 'detonation' stoichiometric reactions were written following each 'rule' and using the molar amounts of polymer and of the corresponding amounts of water-soluble products that were detected from Chemical Burns *a* and *b* carried out under oxygen and nitrogen. The calculated energy difference is given, by *the difference between the sum of the standard enthalpies of formation of the products of combustion in excess oxygen and the sum of the enthalpies of formation of the products of combustion obtained by initiating the polymer in pressurised nitrogen*. The sum of

the enthalpies of formation of the products of the reactions were thus calculated and the energy difference was calculated for the six different possibilities. This was carried out in order to define which 'detonation reaction stoichiometry model' was closest to that actually followed by the anaerobic combustion reaction of Polymer 2. No GC-MS analysis of the bomb exhausts from the anaerobic initiation experiments was performed and the formation of fluorinated P- and C-based gases was assumed to be negligible. Since the polymer oxygen balance was –35% i.e. on the borderline between the applicability range of the K-W and mod. K-W (or S-R) rules, it was thought that all three sets of rules would model the experimental result equally well, albeit approaching it from 'opposite' sides.

The exhaustive combustion reactions (O_2, 30 atm) were written first, using the ion chromatographic and ^{19}F NMR spectroscopic analysis of the water-soluble products from oxygen Chemical Burns *a* and *b* (Table 2.57). It was assumed that the 'missing' amounts of fluorine and phosphorus had converted to phosphoric acid and hydrogen fluoride:

Combustion in O_2 (a)

$$\mathbf{0.734\ C_{5.28}H_{7.85}N_{3.57}O_{9.71}F_{2.15}P_{1.00(l)} + excess\ O_{2(g)} + H_2O_{(l)} \rightarrow 0.057HPO_2F_{2(aq)} + 0.318\ H_2PO_3F_{(aq)} + 0.329\ H_3PO_{4(aq)} + 1.145\ HF_{(aq)} + 2.309\ H_2O_{(l)} + 0.093\ HNO_{3(aq)} + 1.264\ N_{2(g)} + 3.876\ CO_{2(g)}}$$

The *sum of the standard enthalpies of formation* ($\Sigma\Delta H^\circ_f$) of all of the products of reaction was calculated as:

$$\mathbf{\Sigma\Delta H^\circ_{f\ (comb.\ products\ in\ excess\ oxygen)} =}$$

$$\mathbf{-[(0.057 \times 1327.60) + (0.318 \times 1307.30) + (0.329 \times 1299.0) + (1.145 \times 335.35) + (2.309 \times 285.83) + (0.093 \times 59.70) + (3.876 \times 393.51)] =}$$

$$\mathbf{= = -3493.5\ J(0.734mmol\ polymer)^{-1} = -4759.6\ J\ mmol^{-1} = -13659\ J\ g^{-1}}$$

Combustion in O_2 (b)

$0.765\ C_{5.28}H_{7.85}N_{3.57}O_{9.71}F_{2.15}P_{1.00(l)}$ + excess $O_{2(g)}$ + $H_2O_{(l)}$ → $0.104HPO_2F_{2(aq)}$ + $0.406\ H_2PO_3F_{(aq)}$ + $0.341\ H_3PO_{4(aq)}$ + $1.031\ HF_{(aq)}$ + $2.490\ H_2O_{(l)}$ + $0.141\ HNO_{3(aq)}$ + $1.295\ N_{2(g)}$ + $4.040\ CO_{2(g)}$

The *sum of the standard enthalpies of formation* ($\Sigma\Delta H^\circ_f$) of all of the products of reaction was calculated as:

$\Sigma\Delta H^\circ_{f\ (comb.\ products\ in\ excess\ oxygen)}$=

-[(0.104 x 1327.60) + (0.406 x 1307.30) + (0.341 x 1299.0) + (1.031 x 335.35) + (2.490 x 285.83) + (0.141 x 59.70) + (4.040 x 393.51)] =

= -3767.5 J(0.765mmol polymer)$^{-1}$ = - 4924.8 J mmol^{-1}= -14133 J g^{-1}

The 'detonation' stoichiometric reactions (N_2, 30 atm) were written on the basis of the ion chromatographic and ^{19}F NMR spectroscopic analysis of the water-soluble products from nitrogen Chemical Burns *a* and *b* (Table 2.57), according to each rule viz. *mod. K-W, K-W and S-R rules*. As for the oxygen combustions, it was assumed that the 'missing' amounts of fluorine and phosphorus had converted to phosphoric acid and hydrogen fluoride. The standard enthalpies of formation of the water-soluble and gaseous 'detonation reaction' products are given in Section 2.2.9.5.1. The value of ΔH_f^o of $CO_{(g)}$ is the latest reported CODATA value (ΔH_f^o = -110.53 kJmol^{-1}), whereas the ΔH^o_f value of 2,2,2-trifluoroethanol, which was formed during the nitrogen combustions, was taken as = -931.7 kJ mol^{-1}. [185]

Combustion in N_2 (a) mod. K-W

The modified K-W rules can be summarised as follows:

1. Hydrogen is first converted to water
2. Carbon is then converted to carbon monoxide
3. If oxygen is still available, CO is then oxidised to CO_2
4. Any nitrogen is converted to $N_{2(g)}$

According to the above criteria the detonation reaction of Chemical Burn *a* (N_2, 30 atm) was written as:

0.675 $C_{5.28}H_{7.85}N_{3.57}O_{9.71}F_{2.15}P_{1.00(l)}$ + $H_2O_{(l)}$ → 0.038$HPO_2F_{2(aq)}$ + 0.099$H_2PO_3F_{(aq)}$ + 0.0029 $HPF_{6(aq)}$ + 0.488 $H_3PO_{4(aq)}$ + 0.891$HF_{(aq)}$ 2.203$H_2O_{(l)}$ + 0.123 2,2,2-trifluoroethanol$_{(aq)}$ + 2.026$CO_{(g)}$ + 1.538 $C_{(s, amorph)}$ + 1.205 $N_{2(g)}$

The *sum of the standard enthalpies of formation* ($\Sigma\Delta H^\circ_f$) of all of the products of the 'detonation' reaction was calculated as:

$\Sigma\Delta H^\circ_{f\ (anaerobic\ comb.\ products)}$ mod. K-W=

-[(0.038 x 1327.60) + (0.099 x 1307.30) + (0.0029 x 2200) + (0.488 x 1299.0) + (0.891 x 335.35) + (2.203 x 285.83) + (0.123 x 931.7) + (2.026 x 110.53)] =

= -2087.2 J(0.675mmol polymer)$^{-1}$ = -3092 J mmol^{-1} = -8874 Jg^{-1}

<u>Combustion in N_2 (b) mod. K-W</u>

0.821 $C_{5.28}H_{7.85}N_{3.57}O_{9.71}F_{2.15}P_{1.00(l)}$ + $H_2O_{(l)}$ → 0.100$HPO_2F_{2(aq)}$ + 0.248$H_2PO_3F_{(aq)}$ + 0.0025 $HPF_{6(aq)}$ + 0.485 $H_3PO_{4(aq)}$ + 1.090$HF_{(aq)}$ 2.676$H_2O_{(l)}$ + 0.070 2,2,2-trifluoroethanol$_{(aq)}$ + 2.412$CO_{(g)}$ + 1.923 $C_{(s, amorph)}$ + 1.465 $N_{2(g)}$

The *sum of the standard enthalpies of formation* ($\Sigma\Delta H^\circ_f$) of all of the products of the 'detonation' reaction was calculated as:

$\Sigma\Delta H^\circ_{f\ (anaerobic\ comb.\ products)}$ mod. K-W=

-[(0.100 x 1327.60) + (0.248 x 1307.30) + (0.0025 x 2200) + (0.485 x 1299.0) + (1.090 x 335.35) + (2.676 x 285.83) + (0.070 x 931.7) + (2.412 x 110.53)] =

= -2554.7 J(0.821mmol polymer)$^{-1}$ = -3112 J mmol^{-1} = -8931 J g^{-1}

Combustion N_2 (a) K-W

The (unmodified) K-W rules can be summarised as follows:

1. Carbon is converted to CO
2. Hydrogen is then oxidised to H_2O
3. Any remaining oxygen will convert CO into CO_2
4. All nitrogen converts to $N_{2(g)}$

According to the above criteria the detonation reaction of Chemical Burn *a* (N_2, 30 atm) was written as:

$0.675\ C_{5.28}H_{7.85}N_{3.57}O_{9.71}F_{2.15}P_{1.00(l)} + H_2O_{(l)} \rightarrow 0.038HPO_2F_{2(aq)} + 0.099H_2PO_3F_{(aq)} + 0.0029\ HPF_{6(aq)} + 0.488\ H_3PO_{4(aq)} + 0.891HF_{(aq)} + 0.123$ 2,2,2-trifluoroethanol$_{(aq)} + 3.564\ CO_{(g)} + 0.665\ H_2O_{(l)} + 1.538\ H_{2(g)} + 1.205\ N_{2(g)}$

$\Sigma\Delta H^{\circ}_{f\ (anaerobic\ comb.\ products)}$ K-W =

-[(0.038 x 1327.60) + (0.099 x 1307.30) + (0.0029 x 2200) + (0.488 x 1299.0) + (0.891 x 335.35) + (0.123 x 931.7) + (3.564 x 110.53) + (0.665 x 285.83)] =

= -1817.6 J(0.675mmol polymer)$^{-1}$ = -2693 Jmmol^{-1} = -7729 J g^{-1}

Combustion N_2 (b) K-W

$0.821\ C_{5.28}H_{7.85}N_{3.57}O_{9.71}F_{2.15}P_{1.00(l)} + H_2O_{(l)} \rightarrow 0.100HPO_2F_{2(aq)} + 0.248H_2PO_3F_{(aq)} + 0.0025\ HPF_{6(aq)} + 0.485\ H_3PO_{4(aq)} + 1.090HF_{(aq)} + 0.070$ 2,2,2-trifluoroethanol$_{(aq)} + 4.335\ CO_{(g)} + 0.753\ H_2O_{(l)} + 2.687\ H_{2(g)} + 1.466\ N_{2(g)}$

$\Sigma\Delta H^{\circ}_{f\ (anaerobic\ comb.\ products)}$ K-W =

-[(0.100 x 1327.60) + (0.248 x 1307.30) + (0.0025 x 2200) + (0.485 x 1299.0) + (1.090 x 335.35) + (0.070 x 931.7) + (4.335 x 110.53) + (0.753 x 285.83)] =

= -2217.2 J(0.821mmol polymer)$^{-1}$ = -2701 Jmmol^{-1} = -7751 Jg^{-1}

Combustion in N_2 (a) S-R

The S-R rules, a variation of the K-W rules, can be summarised as follows:

1. Carbon is converted to CO
2. Hydrogen is then oxidised to water
3. CO is oxidised to CO_2
4. One third of the CO formed in converted to carbon *and* CO_2
5. One sixth of the original amount of CO is converted to carbon and H_2O if H is available.

According to the above criteria the detonation reaction of Chemical Burn *a* (N_2**,** 30 atm) was written as:

$0.675\ C_{5.28}H_{7.85}N_{3.57}O_{9.71}F_{2.15}P_{1.00(l)} + H_2O_{(l)} \rightarrow 0.038HPO_2F_{2(aq)} + 0.099H_2PO_3F_{(aq)} + 0.0029\ HPF_{6(aq)} + 0.488\ H_3PO_{4(aq)} + 0.891HF_{(aq)} + 0.123$ 2,2,2-trifluoroethanol$_{(aq)} + 1.782\ CO_{(g)} + 0.962H_2O_{(l)} + 1.241H_{2(g)} + 1.188\ C_{(s,\ amorph)} + 1.205\ N_{2(g)} + 0.594\ CO_{2(g)}$

$\Sigma\Delta H^{\circ}_{f\ (anaerobic\ comb.\ products)}$ S-R =

-[(0.038 x 1327.60) + (0.099 x 1307.30) + (0.0029 x 2200) + (0.488 x 1299.0) + (0.891 x 335.35) +(0.123 x 931.7) + (1.782 x 110.53) + (0.962 x 285.83) + (0.594 x 393.51)] =

= -1939.6 J(0.675mmol polymer)$^{-1}$ = -2873 Jmmol^{-1} = -8245 J g^{-1}

Combustion in N_2 (b) S-R

$0.821\ C_{5.28}H_{7.85}N_{3.57}O_{9.71}F_{2.15}P_{1.00(l)} + H_2O_{(l)} \rightarrow 0.100\ HPO_2F_{2(aq)} + 0.248\ H_2PO_3F_{(aq)} + 0.0025\ HPF_{6(aq)} + 0.485\ H_3PO_{4(aq)} + 1.090HF_{(aq)} + 0.070$ 2,2,2-trifluoroethanol$_{(aq)} + 2.166\ CO_{(g)} + 1.476\ H_2O_{(l)} + 1.200\ H_{2(g)} + 1.446\ C_{(s,\ amorph)} + 1.466\ N_{2(g)} + 0.723\ CO_{2(g)}$

$\Sigma\Delta H^{\circ}_{f\,(anaerobic\ comb.\ products)}$ S-R =

-[(0.100 x 1327.60) + (0.248 x 1307.30) + (0.0025 x 2200) + (0.485 x 1299.0) + (1.090 x 335.35) + (0.070 x 931.7) + (2.166 x 110.53) + (1.476 x 285.83) + (0.723 x 393.51)] =

= -2469.2 J(0.821mmol polymer)$^{-1}$ = -3008 Jmmol^{-1} = -8633 J g^{-1}

Table 2.60 shows a summary of the values of the calculated $\Sigma\Delta H^{\circ}_{f\,(products)}$ values for Chemical Burns *a* and *b* performed under oxygen and nitrogen respectively, whilst Table 2.61 shows the values of the difference between $\Sigma\Delta H^{\circ}_{f\,(oxygen\ combustion\ products)}$ and $\Sigma\Delta H^{\circ}_{f\,(nitrogen\ combustion\ products)}$ for the various possible permutations arising from the duplicate chemical burns.

Bomb Atmosphere	Modelling stoichiometry	Calculated $-\Sigma\Delta H^{\circ}_{f\,(comb.products)}$ (J g^{-1})
O_2 30 atm (Burn *a*)	*Exhaustive combustion*	13659
O_2 30 atm (Burn *b*)	*Exhaustive combustion*	14133
N_2 30 atm (Burn *a*)	*Modified K-W*	8874
	Unmodified K-W	7729
	S-R	8245
N_2 30 atm (Burn *b*)	*Modified K-W*	8931
	Unmodified K-W	7751
	S-R	8633

Table 2.60 Summary of $\Sigma\Delta H^{\circ}_{f\,(products)}$ calculated for Chemical Burns *a* and *b* performed under oxygen and nitrogen.

Oxygen Chemical Burn	Nitrogen Chemical Burn and Modelling Stoichiometry	$-\Delta\Delta E_{(oxygen\ burn - nitrogen\ burn)}$ ($J\ g^{-1}$)	Δ (experimental-calculated)
a	(a) Mod K-W	**4785**	**-665**
	(b) Mod K-W	**4728**	**-722**
	(a) K-W	**5930**	**+450**
	(b) K-W	**5908**	**+458**
	(a) S-R	**5414**	**-36**
	(b) S-R	**5026**	**-424**
b	(a) Mod K-W	**5259**	**-191**
	(b) Mod K-W	**5202**	**-248**
	(a) K-W	**6404**	**+954**
	(b) K-W	**6382**	**+932**
	(a) S-R	**5888**	**+438**
	(b) S-R	**5500**	**+50**
Experimental $\Delta\Delta E_c$ value after propagation of uncertainty		**5450**	**±320**

Table 2.61 Values of the calculated difference between $\Sigma\Delta H^{\circ}_{f\ (oxygen\ combustion\ products)}$ and $\Sigma\Delta H^{\circ}_{f\ (nitrogen\ combustion\ products)}$ for all of the permutations arising from the duplicate chemical burns under oxygen and nitrogen.

From the results shown in Table 2.61, it would appear that the *S-R* and the *modified K-W rules* are capable of describing the measured thermochemistry (experimental figures) of the anaerobic combustion reaction of Polymer 2 (ES%=64) more accurately than the *unmodified K-W rules* (2 calculated figures out of 4 for both the S-R and the mod. K-W rules are within the uncertainty of the experimental figure). Since the S-R rules predict the self-oxidation stoichiometry of energetic systems that are typically less oxygen balanced (more negative) than -40%, the degree of agreement between the measured and the calculated energy difference value may suggest that Polymer 2 behaves, upon initiation under inert atmospheres, as a much less oxygen-balanced material than its calculated,

nominal value of -35%, which may be a consequence of the 'early' scavenging of oxygen by phosphorus and hydrogen by fluorine which was discussed above. The ability to accurately predict the likely detonation products without having to rely on experimental analysis would prove advantageous for the graphical correlation of the enthalpies of detonation of each member of the polymer series and their enthalpies of formation. However, experimental analysis (GC-MS) of the gases formed upon anaerobic initiation would be essential for the validation of the predicted values. Such gaseous product mixtures are also expected to contain minor components which are known to form upon simulated detonation (anaerobic initiation) of a variety of CHNO explosives and the formation of which is neglected by the well established 'stoichiometry prediction' rules mentioned above. These components include NH_3, CH_4, HCN, C_2H_6, H_2CO_2 and HCOH.[84]

The very high amounts of sintered ash that were left behind by Polymer 5 (ES%=51), would suggest that not all members of the polymer series behave in the same manner upon anaerobic initiation, despite their structural similarity. Unfortunately, elemental analysis was carried out only for a sample of ash from Polymer 2 (ES%=64) and this yielded the unexpected result C 24%, H 3.5% and N 12%. The low carbon content indicated that the stoichiometry of reaction may have been more complex than that predicted by S-R or mod. K-W rules. However, the relatively small amounts of residue left behind after each anaerobic Chemical Burn may justify the use of the model. Elemental analysis of the residue left behind by the other members of the series would be expected to throw more light onto the anaerobic combustion stoichiometry of the whole class of materials.

In conclusion it must be emphasized that the general observations and energy values obtained from the anaerobic initiation experiments described above are only *preliminary*, due to the very limited amount of data collected.

3 CONCLUSIONS AND RECOMMENDATIONS FOR FURTHER WORK

3.1 THE KEY FINDINGS OF THE RESEARCH

The work described in this thesis has been successful on several fronts: initial efforts contributed to the automation of the existing calorimetric system and proved that the latter was capable, under controlled temperature conditions, to replicate published work (for secondary standards for nitrogen, phosphorus and fluorine) which were carried out using accurate rotating bomb instruments. The degrees of accuracy and precision obtainable after automation of the system and the development of a suitable technique for the derivation of the corrected temperature rise, were regarded as acceptable.

Concurrently with the calorimeter appraisal, the synthesis and characterisation of samples of Polymers 2, 3 and 5 in quantities sufficient to allow accurate calorimetric work, were accomplished following the AWE procedures. In addition, two novel systems, Polymers 1 and 4, were successfully synthesised and characterised, thus extending the pre-existing polyphoshazenes series.

However, the key contributions of this research to the existing calorimetry theory remain the successful identification of the previously unreported, water-soluble, fluorinated phosphoric acid species that arise from the combustion of Polymers 1-5, and an estimation of the small magnitudes (< 0.3%) of the thermal corrections to 'standard states' required to account for the formation of these non-ideal products. The formation of the same compounds is expected to arise also during the calorimetric study of a potentially large number of compounds and polymers containing both phosphorus *and* fluorine. The analytical techniques required to qualify and quantify these products, two of which were identified as hydrolytically unstable, was successfully developed. This was a synergic combination of ^{19}F NMR spectroscopy and Ion exchange Chromatography of the appropriately buffered, post-combustion bomb solutions.

Calorimetric measurements performed under pressurised oxygen of selected batches of Polymers 1-5 allowed the first tentative graphical correlations between Polymer Energetic Substituent % (ES%) and ΔU_c, and (for Polymer 2 only) ΔH_f^o to be drawn. The internal energies of combustion and thus enthalpies of formation of the polymers were shown to depend, ideally via linear relationships, on (a) the polymer ES% values and (b) the energy of combustion of the substituent groups.

As a preliminary step towards estimating ΔH_d^o of the energetic polymers, initial calorimetric investigations of Polymer 2 (ES%=64) and 5 (ES%=51) under nitrogen were carried out. These experiments confirmed that under an inert atmosphere the polymers could be (a) initiated and (b) that the combustion would propagate. Analysis of the resulting bomb solutions from samples of Polymer 2 (ES%=64) revealed a distribution of water-soluble products which was similar to that obtained when the same polymer was combusted in an oxygen atmosphere. This suggested that, in the absence of external oxygen, the preferred processes are conversion of F and P to HF, P_2O_5 (H_3PO_4) and fluorinated analogues. Any surplus oxygen would then be distributed between the oxidation of carbon and any remaining hydrogen, mimicking the detonation chemistry of a conventional CHNO explosive of low (< -40%) OB.

Overall, a sound and practical calorimetric technique for the thermochemical evaluation of a wide range of compounds (energetic and conventional systems alike) containing the hetero-atomic species nitrogen, fluorine and phosphorus has been successfully developed and appraised.

3.2 CRITICAL EVALUATION OF THE WORK (LIMITATIONS)

This research is also affected by several limitations, amongst which is the limited chemical characterisation of the polymers. Since the thermochemical contributions of the 'end-groups' of each polymer were neglected, it would have been advantageous to *accurately* determine the *polydisperisities* of each sample and therefore to modify the estimated empirical formulas of the unit monomers in order to account for the contributions of the end-groups.

In addition to this, multiple signal integration of the same ^{1}H NMR spectrum of each polymer, coupled to the recording of several spectra for each sample, could have lead to an increase in the accuracy of the estimated degrees of side-chain substitution (leading to ES%) and ultimately, of the empirical formulas.

Regarding the synthesis of Polymers 1-5, the painstaking, multi-step synthetic and purification procedures meant that an insufficient number of specimens with intermediate ES% values, have been prepared. This inevitably led to a limited amount of 'middle range' calorimetric data (all of which were also obtained with a great deal of patience) and consequently, to the impossibility of accurately establishing the true nature of the (non-ideal) relationships between polymer ΔU_c, and hence ΔH_c^o, with ES% value.

Regarding the calorimetric data that *was* obtained, the main criticism would most likely be addressed to the relatively large uncertainty intervals associated with the measured energy values of all of the polymer specimens. Due to the small scale of the batches that were prepared, only small sample masses could be combusted in order to maximise the number of calorimetric and chemical burns obtainable from each batch. The small sample mass, coupled to the energetic nature of the polymers, may have contributed to the loss in precision that was observed when compared to the results obtained for the more calorific secondary standards. Combusting larger samples would be expected to yield a significant improvement.

As a direct consequence of the large uncertainty intervals, another major flaw affecting the available calorimetric data involved the magnitude of the corrections accounting for the formation of the water-soluble, fluorinated phosphoric acid species. The magnitude of these were shown to amount to a mere 0.3% of the massic energy values. For consistency reasons, these small contributions may have been neglected, as were the Washburn corrections to standard states, since they may have been safely included within the main, much larger, calorimetric uncertainty limits. However, in order to develop a robust method which would quantify the magnitude of these corrections and allow future appraisal of other compounds which might generate, upon combustion, higher proportions of fluorinated phosphoric acids, the application of the corrections to the measured

combustion energies was, indeed, carried out. To use a good metaphorical analogy, the author would describe this practice as an attempt to 'wax polish a muddy tractor'. The 'tractor' may well need a basic water-wash before the wax polish can be applied, and the 'basic water-wash' would be the use of a more sensitive calorimetric system (i.e. a rotating bomb design which monitors T to μK accuracies), coupled to larger samples, combusted over an increased number of replicate observations. These ameliorations would doubtless render the application of the above mentioned corrections more 'justified' from a 'practical' point of view.

The preliminary combustion studies carried out under nitrogen were also flawed by (a) a limited number of replicate calorimetric observations, and (b) the over-simplistic approach taken whilst using models designed to predict the detonation stoichiometry of CHNO explosives only.

3.3 RECOMMENDATIONS FOR FURTHER WORK

In the light of what was stated in the last two sections and in view of the overall aim of the project i.e. the graphical correlation of polymer ΔH_d^o with ES% values, any further work on this project should primarily focus on the experimental chemical analysis of the 'simulated detonation' reactions, carried out, perhaps, under He or Ar, to allow quantification of the nitrogen gas formed. Before these investigations can commence however, it would be necessary to synthesise, on an appropriate scale, new batches of Polymers 1-5 with uniform ES% values. To achieve this, some insight into effect of Li- or Na-based alkoxides on the synthetic mechanisms, would be necessary. At present there is large variability in the degree of polymer side-chain substitution. The proposed relationships between ΔU_c and ΔH_c^o versus ES% value, that are tentatively described in this thesis, need to be verified. However this might require a superior calorimetric system, as mentioned Section 3.2.

4 EXPERIMENTAL

4.1 INSTRUMENTAL METHODS

4.1.1 Bomb Calorimetry

All calorimetric measurements were carried out using a Gallenkamp 'Autobomb CBA-305' static adiabatic calorimeter, fitted with a Parr 1108-Cl halogen-resistant twin-valve combustion bomb. Ignition of all samples was effected by passing a DC current (4.5 A) through a 35 mm length of 'nichrome' wire (diameter 0.19 mm, specific resistance 50Ω/m). The temperature increases inside the bomb, both before and after ignition, were monitored by a Gallenkamp F25 platinum-resistance-probe precision digital thermometer, accurate to $\pm 10^{-3}$K, interfaced to an external PC which allowed on-line recording of temperature data (sampling interval 3 s). The starting temperatures of all calibrating and measuring experiments were equilibrated to 300 ± 0.5K by means of a 60 L thermostatic water bath unit, in which both the water-filled calorimetric bucket (containing 2123 ± 0.5g of distilled water) and the charged, pressurised bomb were left immersed for 20 min. The cooling coil of the calorimeter's adiabatic jacket was fed with distilled water at 290 ± 0.1K (flow rate: 10 L/min), which was supplied by a GRANT LTD-6G low-temperature bath/circulator unit.

The calorimeter was calibrated using Parr *thermochemical standard* grade benzoic acid (Parr Cat. No. 3415, with a quoted standard internal energy of combustion of ΔU_c° = -26454 ± 3 Jg^{-1}), ignited by the combustion of a pre-weighed length of cotton (pure cellulose fuse, Parr, 845DD, which had a standard internal energy of combustion, ΔU_c° = -17520 ± 180 Jg^{-1}). Both the cotton thread and the benzoic acid had been permanently stored in a dessicator over drying agent prior to use. All calibrating and measuring calorimetric experiments were performed under nitrogen-free oxygen of 99.95% certified purity (BOC Gases), at a nominal pressure of 30±1 atm, unless otherwise specified in the relevant section in 'Results and Discussion'.

4.1.1.1 Procedure for the calibration of the calorimeter with thermochemical standard benzoic acid

Before carrying out any calibrating experiments, the calorimeter, the digital thermometer unit, the water bath and the cooling coil thermostatted circulator were left switched on for at least 1h to ensure temperature equilibration. Dry benzoic acid (1g approximately) was compacted into a pellet using a manual press. The formed pellet was weighed (±0.0001g) and placed inside the bomb crucible. The nichrome wire was threaded between the bomb electrodes and a weighed (±0.0001g) length of dry cotton fuse (approximately 60 mm) was tied to the wire and led into the crucible, in contact with the benzoic acid pellet. A volume of distilled water (15 ± 0.1 ml) was added to the bomb before sealing it. The closed bomb was flushed three times with oxygen before final pressurisation to 30 atm. The calorimetric bucket was filled with distilled water fed by the custom-made glass funnel. A slow flow rate from the funnel (approximately 200 ml/min) ensured that no significant amounts of water would be left adhering to the glass walls of the funnel. The water-filled bucket, along with the charged bomb, were immersed in the thermostatted water-bath (300±0.5 K) for 20 min. The outside surfaces of the calorimetric bucket were then dried and it was lowered into the adiabatic jacket of the calorimeter. The dried bomb was placed inside it, taking care not to lose any water from the bucket.

After sealing the lid of the calorimeter and checking for continuity of the firing circuit, the temperature of the calorimetric system was left to re-equilibrate and stabilise for 10 min, after which time the logging of the temperature was started on the PC and was continued for 40 min before the bomb was fired. After firing, the logging of the temperature was continued for another 50 min. At the end of the calorimetric experiment the bomb was depressurised, and its interior walls and the crucible were visually checked for signs of incomplete combustion, i.e. unburnt material and/or substantial sooty deposits. The presence of these would invalidate the experiment. A total of nine consecutive calibrating experiments in which the temperature was recorded ‘automatically’ were performed. The heat capacity of the calorimeter was calculated from the mean of the nine replicate calibrating experiments. The results of each experiment were obtained by spreadsheet

analysis of the calorimetric thermographs, as explained in 'Results and Discussion'.

Prior to interfacing the digital thermometer unit to a PC, the temperature of the system could only be logged *manually* at intervals of 30 s. A set of 20 replicate calibration experiments were performed in this way whilst following the general procedure described above. The calorimetric *fore*- and *after*-periods however were taken to be only 10 min in duration. The results of both the 'manual' and 'automated' calibrations of the calorimeter are presented in Section 2.2.1.2.

4.1.1.2 Calorimetric combustion experiments of the secondary thermochemical standards triphenylphosphine, triphenylphosphine oxide, 4-fluoro-benzoic acid and 1,2,4-(1H)-triazole.

Triphenylphosphine, triphenylphosphine oxide, 4-fluorobenzoic acid and 1,2,4-(1H)-triazole were purchased from Acros Organics, (99.5%, 99%, 99.5% and 99.5% respectively). The materials were stored in a vacuum desiccator and were used without further purification. The compounds were pressed into pellets and weighed as quickly as possible to avoid absorption of moisture, the average pellet weighing 550 mg.

The general procedure adopted for the *calorimetric part* of the experiments of all the secondary standards was the same as that employed for the 'automated' calibration of the calorimeter using benzoic acid (Section 2.2.1.2). 1,2,4-Triazole however, did not required to be consolidated into pellets, due to the hard, 'solid drop'-like nature of the sample, which was weighed directly inside the bomb crucible.

In the *chemical part* of the investigations, after a time of 2 min after firing, the bomb was removed from the calorimeter and agitated manually for 5 min to homogenise the final solution inside. On opening the bomb, the aqueous solution was carefully transferred to a 250 ml volumetric flask. The empty bomb and lid were rinsed (3 x 20 ml) with distilled water and the washings pooled with the bomb solution. These were analysed by Ion Chromatography as described in Section 4.1.3.

4.1.1.3 Calorimetric experiments of the energetic polyphosphazenes 1-5 and of linear poly[bis(2,2,2-trifluoroethoxy)phosphazene].

The general procedure adopted to perform the *calorimetric part* of the combustion experiments of all of the five energetic polyphosphazenes and of their precursor, linear poly[bis(2,2,2-trifluoroethoxy)phosphazene], was the same as that employed for the 'automated' calibration of the calorimeter using benzoic acid (Section 4.1.1.1), but with the exception that the viscous, liquid polymers were loaded and weighed (approximately 300 mg, ±0.0001g) inside a 150 µl Al_2O_3 crucible (Mettler-Toledo, thermo-gravimetric crucibles, ME-24124). After loading with polymer, the latter was placed *inside* the bomb crucible. The ignition nichrome wire was 'sunk' directly inside the viscous polymer and thus no cotton fuse was used. This was done to aid the accuracy of the measurements. In the case of linear poly[bis(2,2,2-trifluoroethoxy)phosphazene] however, the nichrome wire was weighed and placed in the alumina crucible first, followed, on top, by the powdery precursor, which was gently consolidated in the alumina crucible by hand, using a small steel dowel (5 mm diameter).

In the *chemical part* of the calorimetric investigations, aqueous imidazole/imidazolium oxalate buffer (0.8M, pH 7, 30 ml) was added to the bomb instead of distilled water. After a time of 2 min after firing, the bomb was removed from the calorimeter and manually agitated for 2 min to ensure homogenisation of the final solution. On opening the vessel, the ^{19}F NMR standard, aqueous 2,2,3,3-tetrafluorobutane-1,4-diol (0.125 mM, 1.00 ml) was added to the solution; the bomb was re-sealed and manually agitated for 5 min. An aliquot of the resulting final solution (0.5 ml) was analysed by ^{19}F NMR spectroscopy (neat, acetone-d_6 probe). The remainder of the solution was analysed by Ion Chromatography, as described in Section 4.1.3.

4.1.1.4 Calorimetric investigations of the energetic polyphosphazene 2 under a nitrogen atmosphere

The general procedure adopted to perform the *calorimetric part* of the calorimetric investigations of the energetic polyphosphazene 2 under a nitrogen atmosphere was the same as that employed for the 'automated' combustion

experiment in oxygen i.e. the temperature was logged automatically (Section 4.1.1.3). The bomb was flushed three times to displace the atmospheric oxygen before being pressurised with oxygen-free nitrogen (BOC Gases) to a pressure of 30±1 atm. For the calorimetric investigation carried out under low pressure (*approximately* 1 atm), the charged bomb was, initially, pressurised to 10 atm and then slowly depressurised to a nominal gauge reading of 1 atm.

The *chemical part* of the calorimetric investigations was performed in the same manner as that of all of the energetic polyphosphazenes in oxygen (Section 4.1.1.3).

4.1.2 NMR Spectrometry

All NMR spectra were recorded at 300K on a Bruker DPX-250 spectrometer. The chemical shifts are quoted in parts per million (ppm) with reference to tetramethylsilane (TMS) for ^{1}H and ^{13}C spectra recorded in acetone-d_6 and chloroform-d or sodium trimethylsilylpropanesulphonate (TMSPS) for spectra recorded in D_2O, and to an instrumental internal reference (nominally $CFCl_3$) for ^{19}F spectra. The latter had been checked using internal $CFCl_3$.

4.1.3 Ion Chromatography

The ion chromatograms of the diluted bomb solutions were recorded on a Dionex *Qic* ion chromatograph fitted with a Dionex IONPAC AS4A® analytical column (4x 250 mm) packed with anion exchange latex resin. The eluent was an 18/17 mM sodium carbonate/bicarbonate buffer in de-ionised water (pH=10.3), which was pumped through the IONPAC column at a flow rate of 2 ml min^{-1}. The ion chromatograph was equipped with a conductivity detector and an Anion Micro Membrane (eluent conductivity) Suppressor (AMMS-II) which required a 0.05 mol kg^{-1} regenerant solution of H_2SO_4 in de-ionised water at a flow rate of 4 ml min^{-1}.

Prior to sample injection, the bomb washings of all experiments were filtered twice through 0.45μm nitrocellulose filter discs (Whatman) and diluted to 500 ml in a volumetric flask. Aliquots of this stock solution were further diluted as required and injected into the sampling port with a hypodermic syringe.

4.1.4 GC-MS

The instrument used was a *ThermoQuest* Trace GC gas chromatograph (GC) hyphenated to a *Fisons MD800* mass spectrometer (MS). Both the GC and MS were controlled via a PC running *Xcalibur* software.

The analyses of 1,2,5-triacetoxypentane and pentane-1,2,5-triol (in CH_2Cl_2) were both performed using a VARIAN CP-Sil 5 CB-Low Bleed GC fused silica capillary column (internal diameter 0.25 mm, length 15 m, film thickness 0.25μm, dimethylpolysiloxane, carrier: He). GC oven temperature conditions: 50ºC (1 min) → 250ºC at 20 $Kmin^{-1}$ → 250 ºC (5 min).

The headspace analysis of the bomb exhausts was performed by venting (3 min) via a length of PTFE tubing with SwageLock couplings, the gases from the pressurised bomb, into 10 cm^3 glass vials (Chromacol 10-CV) sealed with aluminium crimp caps and butyl rubber/PTFE septa. The headspace analyser was a *ThermoQuest HS 2000* instrument. The vials were placed in the headspace analyser and maintained at 50ºC. Volumes of 0.05 ml were automatically injected into the GC-MS. Gas separation was achieved using a VARIAN CP PoraPlot Q (internal diameter 0.25 mm, length 25 m, film thickness 8μm, carrier: He). GC oven temperature conditions: -80ºC (3 min) → 150ºC at 60 $Kmin^{-1}$ 150 ºC (13 min). The MS was set to scan from m/z 10 to m/z 250 (EI, 70 eV).

4.1.5 IR Spectroscopy

IR spectra of the reaction mixture from the preparation of *tris*-*P*-(2,2,2-trifluoroethoxy)-N-(trimethylsilyl)phosphoranimine were recorded in dry $CHCl_3$ solution in an IR liquid sample cell (optical path length = 0.15 mm, background: dry $CHCl_3$), on a *Bruker Vector 22* FT-IR spectrophotometer, interfaced to an external PC running OPUS software (version 1.02).

4.1.6 Differential Scanning Calorimetry and Thermogravimetric Analysis

The differential scanning calorimetric plots of the energetic polyphosphazenes and the thermogravimetric plot of the precursor linear poly[*bis*(2,2,2-trifluoroethoxy)phosphazene] were recorded on a Mettler TA4000 DSC/TG calorimeter.

4.1.7 Polymer Elemental Analysis

The CHN elemental analyses of Polymers 1, 2, 3 and 5 were determined by Butterworth Laboratories Ltd, while that of Polymer 4 was determined by the Chemistry Department of Bath University.

4.2 POLYMER SYNTHESIS

4.2.1 Preparation of linear poly[bis(2,2,2-trifluoroethoxy)-phosphazene]

4.2.1.1 *Preparation of tris-P-(2,2,2-trifluoroethoxy)-N-(trimethylsilyl)-phosphoranimine*

Tris-2,2,2-trifluoroethylphosphite [Aldrich, 99%] (26.9g, 82.1 mmol) was reacted with a two-fold molar excess of trimethylsilylazide, TMSA [Aldrich, 97%] (28.9g, 251 mmol) under reflux at 110ºC for a period of 90 h (Section 4.2.1.1.1), after which time the reaction mixture was allowed to cool to room temperature and the excess azide was removed by rotary-evaporation at 35ºC under reduced pressure (30 mm Hg). The mixture was then analysed by ^{1}H and ^{19}F NMR spectroscopy (neat liquid; external acetone-d_6/TMS probe). The integral ratio of the proton signals 9:6.8 (methyls vs. methylene in product) observed in the ^{1}H NMR spectrum indicated that tris-2,2,2-trifluoroethylphosphite had reacted (to 85%) with trimethylsilylazide to yield the desired phosphoranimine. The pure phosphoranimine was distilled under reduced pressure (main fraction collected at b.p. 23ºC, 0.05 mmHg) from the crude mixture, to yield a colourless, mobile but dense liquid. Yield: 29.2 g (86%). NMR (Appendix A, Figures 5.3-5.4): ^{1}H (neat

liquid, external acetone-d_6/TMS probe): -0.60 ppm [s, 9.00H, $(CH_3)_3Si$] and 3.49-3.62 [m, 6.18H, $(F_3CCH_2O)_3P{=}N$] and 3.62-3.69 ppm [m, 0.53H, unreacted $(F_3CCH_2O)_3P$ and possibly also impurities in the starting material]. ^{19}F: - 78.21 (t, 1.00F, $^3J_{H\text{-}F}$ = 8.00 Hz, $(F_3CCH_2O)_3P{=}N$-) and –78.45 ppm (t, 0.09F, $^3J_{H\text{-}F}$ = 8.0 Hz, unidentified impurity).

4.2.1.1.1 Optimisation of reaction yields

Prior to attempting the synthesis of the first 'large' batch of phosphoranimine monomer, the reaction of trimethylsilylazide and tris(2,2,2-trifluoroethyl) phosphite was performed in three consecutive, small scale trials, in which the progress of the reaction was carefully monitored by ^1H and ^{19}F NMR spectroscopy and IR spectroscopy. The latter technique allowed the reduction in intensity of the 2140 cm^{-1} IR absorption, assigned to the asymmetric stretch of the N=N azide bond, to be observed over time. These small scale trial reactions were carried out in order to investigate the possibility of increasing the yield when adopting the AWE reaction conditions (Section 1.2.2.1), and also to explore the dramatic reduction in reaction time (3 h only at 80ºC) reported in a recent Japanese patent,[195] in which dimethylformamide (DMF) was added to the reagents as a catalyst. During these trials, no attempts were made to isolate the product, due to the small scale employed.

Although the addition of DMF to the reaction mixture caused a noticeable increase in the rate of reaction at 80ºC, the yield of the desired product, as estimated by ^1H NMR spectroscopy after 20 h (40%), did not match the yields reported in the Japanese patent under the same conditions, viz. 60% after 3h. In addition, it was observed that the reaction, in the presence of DMF, led to the extensive formation of fluorinated by-products, which complicated the analysis of both ^1H and ^{19}F NMR spectra. When the AWE reaction conditions were employed however (i.e. using a two-fold excess of trimethylsilylazide, no DMF, reflux at 110ºC), partial product degradation occurred between 88 and 150 h. Since the estimated product yield after 88h, as judged by ^1H NMR spectroscopy, was satisfactorily (85%), it was concluded that the most advantageous reaction conditions for the synthesis of P-tris(2,2,2-trifluoroethoxy)-N-(trimethylsilyl)

phosphoranimine would be those employed by AWE, albeit extending the reaction time from 72 to 90 h, which increases the yield of product by approximately 10%.

4.2.1.2 Polymerisation of tris-P-(2,2,2-trifluoroethoxy)-N-(trimethylsilyl)-phosphoranimine

To a stirred solution of freshly distilled tris-P-(2,2,2-trifluoroethoxy)-*N*-(trimethylsilyl)phosphoranimine (29.2g, 70.4 mmol) in anhydrous diglyme (35 ml) was added 1-methyimidazole (150 µl, ~1mol %) as anionic initiator. The mixture was heated at 125ºC for 8 h to yield a clear, yellow liquid. The liquid was decanted into a flask containing $CHCl_3$ (120 ml) that had been previously cooled to its freezing point (-63.5ºC) in a solid CO_2/ethanol bath. The polyphosphazene product precipitated immediately as a white solid. This was filtered off immediately and washed with $CHCl_3$ (6 x 60 ml), before drying in vacuo overnight. Yield: 13.4g (78%). NMR (acetone-d_6), [Appendix A, Figures 5.5-5.6]: ^{1}H: 4.55 ppm (broad d, $^3J_{H-P}$ = 7.6 Hz, P-O-C*H*$_2$CF$_3$) ^{19}F: -76.47 ppm (broad asymmetric t, $^3J_{H-F}$ = 8.0Hz, P-O-CH$_2$C*F*$_3$). Size exclusion chromatographic data (SEC) expressed as the mean value of 3 replicate runs: M_n = 10794, M_w = 13574, PDI = 1.26; sample concentration: 2 mg/ml, solvent: THF, calibration standards: polystyrene in THF).

4.2.2 General synthetic procedure for the preparation of the energetic polyphosphazenes 1-5, (random linear poly[P-(di)nitratoalkoxy/P-2,2,2-trifluoroethoxyphosphazene])

4.2.2.1 Preparation of the protected sodium alkoxide

The reaction was carried out under a nitrogen atmosphere. Sodium hydride [as 60% w/w dispersion in protecting mineral oil, Aldrich, 116 mmol of NaH] was freed from oil by washing with dry hexane (3 x 30ml) and then suspended in dry THF (Aldrich, 100 ml). The protected alcohol (116 mmol) in dry THF (75 ml) was added slowly via a pressure equalising funnel and the mixture vigorously stirred at room temperature for 3 h, during which time hydrogen evolution was

observed and the product, sodium alkoxide, formed as a light brown suspension in the THF.

4.2.2.2 Preparation of random linear poly[P-alkoxy/P-2,2,2-trifluoroethoxy phosphazene]

The reaction was carried out under a nitrogen atmosphere. Linear poly[bis(2,2,2-trifluoroethoxy)phosphazene] (23.1 mmol, 0.2 equivalents) dissolved in dry THF (110 ml) was added to the alkoxide suspension prepared in the previous step via a pressure equalizing funnel. The reaction mixture was refluxed for 24 h and then cooled to room temperature. The solvent was evaporated and the residual red, waxy product was vigorously stirred in water (900 ml) at room temperature until completely dissolved. Complete dissolution was achieved in approx. 1h. The polymeric product was then re-precipitated by adding 12.1M HCl (20.0 ml) to pH 2 in a separating funnel and then directly re-dissolved it in $CHCl_3$ (500 ml). The acidic aqueous layer was further extracted with $CHCl_3$ (3 x 200 ml). The $CHCl_3$ solutions were then pooled and repeatedly washed with water (10 x 1000 ml) and brine (1 x 200 ml) in order to eliminate as much free alcohol as possible. The dried solution ($MgSO_4$), was rotary-evaporated to constant weight.

4.2.2.3 Preparation of random linear poly[P-(di)nitratoalkoxy/ P-2,2,2-trifluoroethoxyphosphazene]

Nitric acid 95% (175 ml, 4.13 mol) at 0 ˚C was added with vigorous stirring to *random linear poly[P-alkoxy/P-2,2,2-trifluoroethoxyphosphazene]* (21.6mmol) thinly dispersed on the walls of a 1000 ml round bottomed flask immersed in an ice-bath. After 15 min the reaction solution was quenched by drop-wise addition to ice-cold distilled water (800 ml). The resulting suspension was mechanically stirred for 1 h, during which time the polymer particles coalesced onto the walls of the beaker and the stirrer. The light yellow, highly viscous liquid was washed (on the beaker walls) several times with distilled water to a final pH of 6, dried in vacuo at 40ºC for 4 h and then overnight in a vacuum desiccator over drying agent. The dry polymer was re-dissolved in acetone (20 ml) and then re-concentrated by rotary-evaporation inside a 50 ml pear-shaped flask to constant weight.

4.2.3 Synthesis of energetic polymer 1 (random linear poly[P-2-nitratoethoxy/P-2,2,2-trifluoroethoxyphosphazene])

4.2.3.1 Preparation of random linear poly[P-2-t-butoxyethoxy/P-2,2,2-trifluoroethoxyphosphazene]: reaction of linear poly[bis(2,2,2-trifluoroethoxy)phosphazene] with sodium 2-t-butoxyethoxide.

The reaction was carried out as, and scaled to the general procedure described in Sections 4.2.2.1 and 4.2.2.2. 2-t-Butoxyethanol (99%) was purchased from ABCR GmbH, Karlshrue, Germany, and was used without further purification. The degree of 2,2,2-trifluoroethoxy group substitution, as estimated by ^{1}H NMR was 76%. Yield: 5.62g (94%). NMR (acetone-d_6), [Appendix A, Figures 5.7-5.8]: ^{1}H: 1.17 (s, 0.59H, *Me*$_3$C residual 2-t-butoxyethanol), 1.21 (br s, 9.00H, *Me*$_3$C), 3.49 (br s, 2.42H, C-1 C*H*$_2$), 4.12 (br s, 2.11H, C-2 C*H*$_2$), 4.53 (br s, 0.68H C*H*$_2$, trifluoroethoxy); ^{19}F: -75.35 ppm (br s, trifluoroethoxy).

4.2.3.2 Preparation of random linear poly[P-2-nitratoethoxy/P-2,2,2-trifluoroethoxyphosphazene]: nitration of random linear poly[P-2-t-butoxyethoxy/ P-2,2,2-trifluoroethoxyphosphazene with excess nitric acid.

The reaction was carried out as, and scaled to the general procedure described in Section 4.2.2.3. Since the presence of non-polymeric contaminants was confirmed by ^{1}H NMR spectroscopy, the product, random linear *poly*[P-2-nitratoethoxy/P-2,2,2-trifluoroethoxyphosphazene] (5.67 g), was re-dissolved in acetone (30 ml) and rotary evaporated to form a thin film (high surface area) inside a 1000 ml round bottomed flask. Diethyl ether (300 ml) was then added to the flask which was rotated for 20h. The polymer swelled visibly within 30 min but did not dissolve in the solvent. The extraction solvent was then decanted and the polymer 'dried' in vacuo at 40ºC for 3 h. As judged by ^{1}H NMR spectroscopy, the contaminants had been completely eliminated to yield a clean nitrated polymer. Yield: 4.64g. (85%). Overall yield: 79%. NMR (acetone-d_6), [Appendix A, Figures 5.9-5.12]: ^{1}H: 4.28 (br s, 2.61H, C-1 P-O-C*H*$_2$ + P-O-C*H*$_2$CF$_3$) and 4.84 ppm (br s, 2.00H, C*H*$_2$ONO$_2$); ^{19}F: -76.03 ppm (br s, trifluoroethoxy). The

extraction solvent was rotary evaporated to leave an oily yellow liquid which was analysed by ^{1}H NMR spectroscopy (acetone-d_6). It was probably mainly the nitrated derivatives of t-butyl alcohol and 2-t-butoxyethanol. No further work was undertaken to positively identify these species.

4.2.4 Synthesis of energetic polymer 2 (random linear poly[P-2,3-dinitratoprop-1-oxy/P-2,2,2- trifluoroethoxyphosphazene])

4.2.4.1 Preparation of random linear poly[P-(2',2'-dimethyl-1',3'-dioxolan- 4'-yl)methoxy/P-2,2,2-trifluoroethoxyphosphazene]: reaction of linear poly [bis(2,2,2-trifluoroethoxy)phosphazene] with sodium (2',2'-dimethyl-1',3'-dioxolan-4'-yl)methoxide.

The reaction was carried out as and scaled to the general procedure described in Sections 4.2.2.1 and 4.2.2.1. 2,2-Dimethyl-4-hydroxymethyl-1,3-dioxolan (98%) was purchased from Aldrich and used without further purification. The degree of 2,2,2-trifluoroethoxy group substitution, as estimated by ^{1}H NMR, was 64%. Yield: 8.28g (88%). NMR (acetone-d_6), [Appendix A, Figure 5.13]: ^{1}H: 1.32 (br s, 3.00H, CH_3), 1.40 (br s, 3.00H, CH_3), 3.86-4.54 ppm (br m, 6.11H, C-2' CH_2, C-4' CH, C-1 CH_2, C-1 CH_2 and CH_2 trifluoroethoxy); ^{19}F: -75.73 ppm (br s, trifluoroethoxy).

4.2.4.2 Preparation of random linear poly[P-(2,3-dinitratoprop-1-oxy)/P-2,2,2-trifluoroethoxyphosphazene]: Nitration of random linear poly[[P-(2',2'-dimethyl-1',3'-dioxolan- 4'-yl)methoxy/P-2,2,2-trifluoroethoxyphosphazene].

The reaction was carried out as, and scaled to the general procedure described in Section 4.2.2.3. Yield: 6.25g (61%). Overall yield: 55%. NMR (acetone-d_6), [Appendix A, Figures 5.14-5.15]: ^{1}H: 4.54-5.10 (br m, 7.22H, C-5' CH_2, C-1 CH and CH_2 trifluoroethoxy) and 5.77 ppm (br s, 1.00H, C-4' CH). ^{19}F: -75.43 ppm (br s, trifluoroethoxy). Hereafter this product is referred to as Batch 4. Three earlier preparations (Batches 1, 2 and 3) had degrees of 2,2,2-trifluoroethoxy group substitution of 65%, 70% and 78% respectively. Batch 1 yield: 810 mg.

Overall yield: 70%. Batch 2 yield: 5.30g. Overall yield: 67%. Batch 3 yield: 3.63g. Overall yield: 68%.

4.2.5 Synthesis of less-substituted energetic polymer 2 (random linear poly[P-2,3-dinitratoprop-1-oxy/P-2,2,2-trifluoroethoxyphosphazene])

4.2.5.1 Preparation of less-substituted random linear poly[P-(2',2'-dimethyl-1',3'-dioxolan- 4'-yl)methoxy/P-2,2,2-trifluoroethoxyphosphazene]: reaction of linear poly[bis(2,2,2-trifluoroethoxy)phosphazene] with sodium (2',2'-dimethyl-1',3'-dioxolan-4'-yl)methoxide.

The reaction was carried out following the general procedure described in Sections 4.2.2.1 and 4.2.2.1, however, sodium (2',2'-dimethyl-1',3'-dioxolan-4'-yl)methoxide and linear poly[bis(2,2,2-trifluoroethoxy)phosphazene] were reacted in a 1:1 molar ratio, instead of the usual 5:1 molar ratio, and for a reaction time of 6h only. Estimated degree of 2,2,2-trifluoroethoxy group substitution, as judged by ^{1}H NMR: 31%. Yield: 3.15g (73%). NMR (acetone-d_6), [Appendix A, Figures 5.16-5.17]: ^{1}H: 1.31 (br s, 3.00H, CH_3), 1.38 (br s, 3.00H, CH_3) and 3.83-4.54 ppm (br m, 9.41H, C-2' CH_2, C-4' CH, C-1 CH_2, C-1 CH_2 and CH_2 trifluoroethoxy); ^{19}F: -76.15 ppm (br s, trifluoroethoxy).

4.2.5.2 Preparation of less-substituted random linear poly[P-(2,3-dinitratoprop-1-oxy)/P-2,2,2-trifluoroethoxyphosphazene]: Nitration of random linear poly[[P-(2',2'-dimethyl-1',3'-dioxolan- 4'-yl)methoxy/P-2,2,2-trifluoroethoxyphosphazene].

The reaction was carried out as, and scaled to the general procedure described in Section 4.2.2.3. The resultant dried polymer was re-dissolved in acetone (10 ml), rotary-evaporated to form a thin film (high surface area) inside a 100 ml round bottomed flask and washed with diethyl ether (50 ml) for 5 h to extract the last traces of mineral oil. Yield: 2.53g (76%). Overall yield: 56%. NMR (acetone-d_6), [Appendix A, Figures 5.18-5.21]: ^{1}H: 4.56-5.08 (br m, 13.17H, C-5' CH_2, C-1 CH

and C*H*$_2$ trifluoroethoxy) and 5.76 ppm (br s, 1.00H, C-4' C*H*). ^{19}F: -76.26 ppm (br s, trifluoroethoxy).

4.2.6 Synthesis of energetic polymer 3 (random linear poly[P-3,4-dinitratobut-1-oxy/P-2,2,2-trifluoroethoxyphosphazene])

4.2.6.1 Preparation of 4-(2'-hydroxyethyl)-2,2-dimethyl-1,3-dioxolan: reaction of butane-1,2,4- triol with acetone

Butane-1,2,4-triol (24.04 g, 227 mmol, 96%, Acros) was added to a 10-fold molar excess of acetone (200 ml, 2.72 mol) with vigorous stirring. Dichloromethane (200 ml) was added after all the triol had dissolved. Dried $MgSO_4$ (200 g) was added to scavenge the water formed during the condensation reaction. The catalyst *p*-toluenesulphonic acid monohydrate (0.520 g, 2.73 mmol) was added and the reaction mixture was stirred at room temperature for 24 h. The $MgSO_4$ was then filtered off and the clear filtrate was washed with saturated $NaHCO_3$ (50 ml) and brine. The pooled aqueous phases were extracted with fresh CH_2Cl_2 (4 x 50 ml). The final combined CH_2Cl_2 solution was dried over $MgSO_4$, filtered and rotary-evaporated to constant weight. Yield: 32.31g (98%). NMR (acetone-d_6), [Appendix A, Figures 5.22-5.26]: ^{1}H: 1.27 (s, 3.00H, CH_3), 1.32 (s, 3.00H, CH_3), 1.64-1.85 (m, 2.03H, C-1' C*H*$_2$), 3.27-3.55 (m, 1.93H, C-5 C*H*H), 3.64 (broad s, 1.98H, C-2' C*H*$_2$), 4.00-4.06 (m, 1.02H, C-5 CH*H*) and 4.13-4.23 ppm (m, 0.99H, C-4 C*H*); ^{13}C (main component only; minor isomeric by-product not reported): 26.05 (CH_3), 27.28 (CH_3), 37.53 (C-1' *C*H_2), 59.52 (C-2' *C*H_2), 70.18 (C-5 *C*H_2), 74.72 (C-4 *C*H) and 108.76 ppm (C-2 *C*). ^{1}H-^{1}H correlation (COSY45): 1.64-1.85 coupled to 3.64 (C-2' C*H*$_2$) and 4.13-4.23 (C-4 C*H*), 3.27-3.55 coupled to 4.00-4.06 (C-5 CH*H*) and 4.13-4.23 (C-4 C*H*). ^{1}H-^{13}C correlation: 1.64-1.85 correlated to 37.53 (C-1'), 3.27-3.55 correlated to 70.18 (C-5), 3.64 correlated to 59.52 (C-2'), 4.00-4.06 correlated to 70.18 (C-5) and 4.13-4.23 ppm correlated to 74.72 (C-4).

4.2.6.2 Preparation of random linear poly[P-2-(2',2'-dimethyl-1',3'-dioxolan-4'-yl)ethoxy/P-2,2,2-trifluoroethoxyphosphazene]: reaction of linear poly[bis(2,2,2-trifluoroethoxy)phosphazene] with sodium 2-(2',2'-dimethyl-1',3'-dioxolan-4'-yl)ethoxide

The reaction was carried out as, and scaled to the general procedure described in Sections 4.2.2.1 and 4.2.2.2. Estimated degree of 2,2,2-trifluoroethoxy group substitution, as judged by ^{1}H NMR: 61%. Yield: 3.16g (86%). NMR (acetone-d_6), [Appendix A, Figures 5.27-5.28]: ^{1}H: 1.28 (br s, 3.00H, CH_3), 1.37 (br s, 3.00H, CH_3), 1.97 (br s, 2.25H, C-1 C*H*$_2$), 3.60-4.20 ppm (br m, 5.61H, C-2' CH_2, C-4 C*H*) and 4.49 ppm (br s, 0.72H, C*H*$_2$ trifluoroethoxy; ^{19}F: - 75.53 ppm (br s, trifluoroethoxy).

4.2.6.3 Preparation of random linear poly[P-3,4-dinitratobut-1-oxy/P-2,2,2-trifluoroethoxyphosphazene]: nitration of random linear poly[P-2-(2',2'-dimethyl-1,3-dioxolan-4'-yl)ethoxy/P-trifluoroethoxy phosphazene] with excess nitric acid

The reaction was carried out as, and scaled to the general procedure described in Section 4.2.2.3. Yield: 3.09g (76%). Overall yield 71%. NMR (acetone-d_6), [Appendix A, Figures 5.29-5.30]: ^{1}H: 2.29 (br s, 2.07H, C-1'C*H*$_2$), 4.28-5.08 (br m, 5.21H, C-2' C*H*$_2$, C-5 C*H*$_2$, C-4 C*H*) and 5.67 ppm (br s, 1.00H, C*H*$_2$ trifluoroethoxy); ^{19}F: -75.81 ppm (br s, trifluoroethoxy). Hereafter this product is referred to as Batch 2. An earlier preparation (Batch 1) had an estimated degree of 2,2,2-trifluoroethoxy substitution of 59%. Yield: 531 mg. Overall yield: 62%.

4.2.7 Synthesis of energetic polymer 4 (random linear poly[P-4,5-dinitratopent-1-oxy/P-2,2,2-trifluoroethoxyphosphazene])

4.2.7.1 Preparation of 1,2,5-triacetoxypentane

Acetic anhydride (244 g, 2.8mol) was added to crushed $ZnCl_2$ (5.7g). The mixture was heated to boiling point and tetrahydrofurfuryl alcohol (71.4g, 0.7mol) was added drop-wise during 30 min. When the addition of the alcohol was complete, the reaction mixture was refluxed for 24 h. After the zinc salts had been filtered

off, the filtrate was distilled under vacuum (excess acetic acid/ anhydride collected at b.p. 24ºC, 4 mmHg). When the distillation had ceased and the vapour-temperature dropped, the pressure was lowered and the product, 1,2,5-triacetoxypentane, distilled very slowly (main fraction collected at b.p. 100-107ºC, 0.05 mmHg). After 9h the distillation was discontinued and the dark, syrupy residue was retained for later distillation of the remaining product. Yield: 66g (39%). NMR ($CDCl_3$), [Appendix A, Figures 5.31-5.33]: ^{1}H: 1.63-1.84 (m, 3.68H, C-4 C*H*$_2$ and C-5 C*H*$_2$), 1.81 (m, 0.65H, unidentified impurity), 2.05-2.15 (m, 9.56H, (OCOC*H*$_3$)$_3$), 2.14 (s, 0.43H C*H*$_3$COOH), 3.53-3.58 (m, 0.29H, unidentified impurity), 4.00-4.08 (m, 2.99H, C-1 C*H*$_2$ and C-3 C*H*H), 4.21-4.27 (m, 1.07H, C-3 CH*H*) and 5.08-5.12 ppm (m, 1.0H, C-2 C*H*). ^{13}C (main component only): 20.74, 20,91 and 21.01 ((OCO*CH*$_3$)$_3$), 24.48 (C-4), 27.39 (C-5), 63.87 (C-1), 64.93 (C-3), 71.03 (C-2), and (170.53, 170.71, 171.05) ppm (O*C*OCH$_3$)$_3$). ^{1}H-^{1}H correlation (COSY45): 1.63-1.84 coupled to 4.00-4.08 and to 5.08-5.12, (unidentified impurity: 1.81 coupled to 3.53-3.58), 4.00-4.08 coupled to 5.08-5.12, 4.21-4.27 coupled to 5.08-5.12 ppm.

4.2.7.2 Further distillation of 1,2,5-triacetoxypentane from the residual mother liquor

The distillation of the dark, oily residue that was left over from the first attempted distillation of 1,2,5-triacetoxypentane (Section 4.2.6.1) was resumed 6 months later. The product distilled over only 50 min, (main fraction collected at b.p. 100-104, 0.05 mmHg). Yield: 35g, (21%). NMR ($CDCl_3$), [Appendix A, Figures 5.34-5.35]: ^{1}H: 1.66-1.68 (m, 4.02H, C-4 C*H*$_2$ and C-5 C*H*$_2$), 2.05-2.09 (m, 9.43H, (OCOC*H*$_3$)$_3$), 4.00-4.10 (m, 3.03H, C-1 CH_2 and C-3 C*H*H), 4.21-4.27 (m, 1.04H, C-3 CH*H*) and 5.09-5.10 ppm (m, 1.0H, C-2 C*H*). ^{13}C: 20.75, 20,93 and 21.02 ((OCO*CH*$_3$)$_3$), 24.48 (C-4), 27.40 (C-5), 63.87 (C-1), 64.92 (C-3), 71.02 (C-2), and 170.51, 170.70, 171.03 ppm ((O*C*OCH$_3$)$_3$).

4.2.7.3 Preparation of an authentical sample of tetrahydrofurfuryl acetate

Acetyl chloride (230 mg, 2.9 mmol) was added to tetrahydrofurfuryl alcohol (200 mg, 1.9 mmol) in diethyl ether (1.0 ml) and the resulting solution was stirred at room temperature for 16h, after which time the solvent, excess acetyl chloride (and HCl) were rotary evaporated off to leave a colourless oily liquid with a pleasant fruity odour. Yield: 255 mg (93%). NMR ($CDCl_3$), [Appendix A, Figures 5.36-5.37]: ^{1}H: 1.56-1.64 (m, 1.01H, C-3 C*H*H), 1.87-2.05 (br m, 3.05H C-3 CH*H* and C-4 CH_2), 2.09 (s, 3.00H, CH_3) and 3.79-4.19 ppm (m, 5.07H, C-2 C*H*, C-5 CH_2 and C-6 CH_2). ^{13}C: 20.92 (CH_3), 26.08 (C-4), 28.01 (C-3), 66.59 (C-6), 68.45 (C-5), 76.52 (C-2) and 171.02 ppm (carbonyl); (^{1}H and ^{13}C shifts identical to those published in the literature[196]).

4.2.7.4 Preparation of pentane-1,2,5-triol: acid hydrolysis of 1,2,5-triacetoxypentane

1,2,5-Triacetoxypentane (66g, 0.27 mol) was refluxed with aqueous H_2SO_4 (approx. 1% wt/vol, 50 ml) for 30 min, after which time the two layers had become homogeneous. This was then steam-distilled until approximately 1000 ml of water/acetic acid distillate had been collected. The resulting distillation residue was left to cool and was subsequently neutralised by adding $Ca(OH)_2$ (1.2 g) to pH 10. The precipitate, $CaSO_4$, was filtered off and the basified filtrate was distilled under moderate vacuum (water-pump) to drive off most of the remaining water. This yielded a red oil which was distilled under high vacuum to obtain the desired product as a colourless, odourless, viscous oil (main fraction distilled at b.p. 103-132 ºC, 0.01 mmHg). Yield: 11.3g (35%). The residual red wax, possibly a complex mixture of oligomerisation products, was discarded. NMR (acetone-d_6), [Appendix A, Figures 5.38-5.42]: ^{1}H: 1.32-1.68 (m, 4.0H, C-3 CH_2 and C-4 CH_2), 2.25 (s, 0.20H, possibly OCOCH_3 of monoacetoxy and diacetoxy by-products) and 3.39-4.00 ppm (m, 7.79H, C-1 CH_2, C-2 C*H*, C-5 CH_2, (O*H*)$_3$); ^{13}C (main peaks only): 29.95 (C-4), 31.03 (C-3), 62.73 (C-5), 67.37 (C-1) and 72.67 (C-2). ^{1}H-^{1}H correlation (COSY45): 1.32-1.68 (C-4 CH_2) coupled to 3.39-4.00 ppm (C-5 CH_2). ^{1}H-^{13}C correlation: 1.32-1.68 (C-4 CH_2) correlated to 29.95 (C-

4), 1.32-1.68 (C-3 CH_2) correlated to 31.03 (C-3), 3.39-4.00 ppm (C-5 CH_2) correlated to 62.73 (C-5), 3.39-4.00 ppm (C-1 CH_2) correlated to 67.37 (C-1), 3.39-4.00 ppm (C-2 CH_2) correlated to 72.67 ppm (C-2).

4.2.7.5 Acid hydrolysis of the second fraction of 1,2,5-triacetoxypentane

The reaction was scaled to the procedure described in Section 3.2.7.4, starting from 1,2,5-triacetoxypentane (25g, 0.10 mol). The product was collected over a slightly narrower temperature interval (main fraction distilled at b.p. 105-125 ºC, 0.01 mmHg). Yield: 9.5g (78%). The residual light-brown wax was discarded. NMR (acetone-d_6), [Appendix A, Figures 5.43-5.44]: ^{1}H: 1.40-1.68 (m, 4.0H, C-3 CH_2 and C-4 CH_2) and 3.39-3.98 ppm (m, 7.82H, C-1 CH_2, C-2 CH, C-5 CH_2, (OH)$_3$); ^{13}C: 30.95 (C-4), 31.03 (C-3), 62.71 (C-5), 67.33 (C-1) and 72.36 ppm (C-2).

4.2.7.6 Preparation of 4-(3'-hydroxypropyl)-2,2-dimethyl-1,3-dioxolan: reaction of pentane-1,2,5-triol with acetone

The reaction was carried out as and scaled to the procedure described in Section 4.2.6.1 starting from pentane-1,2,5-triol (8g, 66.8 mmol). Yield: 9.05 g (85%). Product physical appearance: colourless, mobile oil. NMR (acetone-d_6), [Appendix A, Figures 5.45-5.46]: ^{1}H: 1.27 (s, 3.00H, CH_3), 1.32 (s, 3.00H, CH_3), 1.47-1.66 (m, 4.01H, C-1' CH_2 and C-2' CH_2), 3.43-3.57 (m, 3.06H, C-5 CHH, C-1'CH_2) and 4.01-4.30 ppm (m, 1.87H, C-4 CH and C-5 CHH); ^{13}C: 26.00 (CH_3), 27.28 (CH_3), 29.86 (C-2'), 30.90 (C-3'), 62.27 (C-1'), 69.93 (C-5) and 76.69 ppm (C-4) and 108.98 (C-2).

4.2.7.7 Preparation of random linear poly[P-3-(2',2'-dimethyl-1',3'-dioxolan-4'-yl)prop-1-oxy/P-2,2,2-trifluoroethoxyphosphazene]: reaction of linear poly[bis(2,2,2-trifluoroethoxy)phosphazene] with sodium 3-(2',2'-dimethyl-1',3'-dioxolan-4'-yl)propoxide.

The reaction was carried out as, and scaled to the general procedure described in Sections 4.2.2.1 and 4.2.2.2. Estimated degree of 2,2,2-trifluoroethoxy group substitution, as judged by ^{1}H NMR spectroscopy: 67%. Yield: 3.40g (93%). NMR (acetone-d_6), [Appendix A, Figures 5.47-5.48]: ^{1}H: 1.30 (br s, 3.00H, CH_3), 1.36 (br s, 3.00H, CH_3), 1.69-1.82 (br m, 4.18H, C-2' C*H*$_2$ and C-3' C*H*$_2$), 3.51-3.63 (br m, 1.31H, C-5 C*H*H,), 4.07-4.12 (br m, 3.50H, C-4 C*H*, C-5 CH*H,* C-1' C*H*$_2$) and 4.46-4.49 ppm (br m, 0.78H, C*H*$_2$ trifluoroethoxy); ^{19}F: -75.66 ppm (br s, trifluoroethoxy). The integral value (1.31) of the ^{1}H NMR signals at δ = 3.51-3.63 would suggest that both C-5 protons experience a slightly different chemical environment, which may be due to conformational isomerism of the polymer backbone.

4.2.7.8 Preparation of random linear poly[P-(4,5-dinitratopent-1-oxy)/P-2,2,2-trifluoroethoxyphosphazene]: nitration of random linear poly[P-3-(2',2'-dimethyl-1',3'-dioxolan-4'-yl)prop-1-oxy/ P-2,2,2-trifluoroethoxyphosphazene].

The reaction was carried out as, and scaled to the general procedure described in Section 4.2.2.3. Yield: 2.3 g (56%). Overall yield: 52%. NMR (acetone-d_6), [Appendix A, Figures 5.49-5.52]: ^{1}H: 1.95 (br s, ~3.58H, C-2 C*H*$_2$ and C-3 C*H*$_2$), 4.16-5.02 (br m, 5.05H, C-1 C*H*$_2$, C-5 C*H*$_2$, C*H*$_2$ trifluoroethoxy) and 5.52 ppm (br s, 1.00H, C-4 C*H*); ^{19}F: -75.81 ppm (br s, trifluoroethoxy).

4.2.8 Synthesis of energetic polymer 5 (random linear poly[P-5,6-dinitratohex-1-oxy/P-2,2,2-trifluoroethoxyphosphazene])

4.2.8.1 Preparation of 4-(4'-hydroxybutyl)-2,2-dimethyl-1,3-dioxolan: reaction of hexane-1,2,6-triol with acetone

The reaction was carried out, and scaled to the procedure described in Section 4.2.6.1 starting from hexane-1,2,6-triol (17.72g, 132.1mmol, 96%, Aldrich). Yield: 15.16g (66%). Product physical appearance: light yellow, mobile oil. NMR (acetone-d_6), [Appendix A, Figures 5.53-5.55]: 1.27 (s, 3.00H, CH_3), 1.31 (s, 3.00H, CH_3), 1.35-1.59 (m, 6.27H, C-1' C*H*$_2$, C-2' C*H*$_2$ and C-3' C*H*$_2$), 3.42-3.55 (m, 3.91H, C-5 C*H*H, C-4 C*H*, C-4' C*H*$_2$) and 3.97-4.09 ppm (m, 1.95H, C-5 CH*H*, O*H*). ^{13}C: 22.92 (C-2'), 25.99 (CH_3), 27.28 (CH_3), 33.31 (C-1'), 34.20 (C-3'), 62.22 (C-4'), 69.95 (C-5), 77.00 (C-4) and 108.85 ppm (C-2).

4.2.8.2 Preparation of random linear poly[P-4-(2',2'-dimethyl-1',3'-dioxolan-4'-yl)butoxy/P-2,2,2-trifluoroethoxyphosphazene]: reaction of linear poly[bis(2,2,2-trifluoroethoxy)phosphazene] with sodium 4-(2',2'-dimethyl-1',3'-dioxolan-4'-yl)butoxide.

The reaction was carried out as, and scaled to the general procedure described in Sections 4.2.2.1 and 4.2.2.2. Estimated degree of 2,2,2-trifluoroethoxy group substitution, as judged by ^{1}H NMR: 51%. Yield: 3.03g (79%). NMR (acetone-d_6), [Appendix A, Figures 5.56-5.58]: ^{1}H: 1.30 (br s, 3.00H, CH_3), 1.35 (br s, 3.00H, CH_3), 1.41-1.75 ppm (br m, 6.05H, C-1' C*H*$_2$, C-2' C*H*$_2$, C-3' C*H*$_2$), 3.48 (br s, 1.91H, C-5 C*H*H), 4.06 (br s, 3.98H, C-4 C*H*, C-4' C*H*$_2$, C-5 CH*H*), 4.46-4.49 ppm (br m, C*H*$_2$ trifluoroethoxy); ^{1}H-^{1}H correlation (COSY45): 1.41-1.75 (C-1' C*H*$_2$, C-3' C*H*$_2$) coupled to 4.06 (C-4 C*H,* C-4' C*H*$_2$), 3.48 (C-5 C*H*H) coupled to 4.06 ppm (C-5 CH*H*). ^{19}F: -75.65 ppm (br s, trifluoroethoxy).

4.2.8.3 Preparation of random linear poly[P-(5,6-dinitratohex-1-oxy)/ P-2,2,2-trifluoroethoxyphosphazene]: Nitration of random linear poly[[P-4-(2',2'-dimethyl-1',3'-dioxolan- 4'-yl)butoxy/P-2,2,2-trifluoroethoxy-phosphazene].

The reaction was carried out as, and scaled to the general procedure described in Section 4.2.2.3. The dry polymer was re-dissolved in acetone (20 ml) and rotary evaporated in a 50 ml pear-shaped flask. The polymer was then washed with diethyl ether for 20h to eliminate the remaining traces of free hexane-1,2,6-triol trinitrate. Yield: 3.28g (93%). Overall yield: 72%. NMR (acetone-d_6), [Appendix A, Figures 5.59-5.63]: ^{1}H: 1.51-1.91 (br m, 6.00H, C-3 C*H*$_2$, C-4 C*H*$_2$ and C-5 C*H*$_2$), 4.10-5.02 (br m, 4.83H, C-1 C*H*$_2$, C-6 C*H*$_2$ and OC*H*$_2$ CF_3) and 5.50 ppm (br s, 0.91H, C-2 C*H*). ^{1}H-^{1}H correlation (COSY45): 1.51-1.91 (C-5 C*H*$_2$, C-3 C*H*$_2$) coupled to 4.10-5.02 (C-6 C*H*$_2$) and to 5.50 (C-2 C*H*). ^{19}F: -75.81 ppm (br s, trifluoroethoxy). Hereafter this product is referred to as Batch 2. An earlier preparation (Batch 1) had an estimated degree of 2,2,2-trifluoroethoxy group substitution of 50%. Yield: 395 mg. Overall Yield: 51%.

4.2.8.4 Preparation of a sample of hexane-1,2,6-triol trinitrate

4-(4'-Hydroxybutyl)-2,2-dimethyl-1,3-dioxolan (1.8g, 10.2 mmol) was added drop-wise to 95% HNO_3 (12.5 ml, 283 mmol) with vigorous stirring in an ice-bath. After 15 min the reaction mixture was added to cold distilled water (80 ml) and the product was extracted with $CHCl_3$ (3 x 40 ml). The chloroform solutions were pooled together, repeatedly washed with distilled water to pH 6, dried ($MgSO_4$) and rotary-evaporated to leave the product, a light yellow, mobile oil. Yield: 2.60g (94%). NMR (acetone-d_6), [Appendix A, Figures 5.64-5.68]: ^{1}H: 1.61-1.96 (m, 6.52H, C-3 C*H*$_2$, C-4 C*H*$_2$, C-5 C*H*$_2$), 4.58 (t, $^3J_{H\text{-}H}$ = 6.3 Hz, 2.1H, C-6 C*H*$_2$), 4.68-4.76 (dd, $^2J_{H\text{-}H}$ = 13.0Hz, $^3J_{H\text{-}H}$ = 6.3 Hz, 1.11H, C-1 C*H*H), 4.97-5.03 (dd, $^2J_{H\text{-}H}$ = 13.0Hz, $^3J_{H\text{-}H}$ = 2.71 Hz, 1.03H, C-1 CH*H*) and 5.48-5.55 ppm (m, 1.00H, C-2 C*H*). ^{13}C: 21.97 (C-4), 27.00 (C-5), 29.24 (C-3), 72. 63 (C-1), 74.01 (C-6) and 80.74 ppm (C-2). ^{1}H-^{1}H correlation (COSY 45): 1.61-1.96 (C-5 C*H*$_2$ and C-3 C*H*$_2$) coupled to 4.58 (C-6 C*H*$_2$) and to 5.48-5.55 (C-2 C*H*). ^{1}H-^{13}C correlation: 21.97 (C-4), 27.00 (C-5) and 29.24 (C-3) correlated to 1.61-1.96 (C-3

CH_2, C-4 CH_2 and C-5 CH_2), 72.63 (C-1) correlated to 4.68-4.76 (C-1 C*H*H) and to 4.97-5.03 (C-1 CH*H*), 80.74 (C-2) correlated to 5.48-5.55 ppm (C-2 C*H*)

4.2.9 Investigation of alternative nitration methods (Polymer 2)

4.2.9.1 Two-phase nitration using $HNO_3/CHCl_3$

Polymer 2, random linear poly[P-2,3-dinitratoprop-1-oxy/P-2,2,2-trifluoroethoxy phosphazene] (Batch 1, 105 mg, 0.37 mmol) in $CHCl_3$ (1 ml) was added drop-wise to a pre-cooled suspension of 95% nitric acid (2.5 ml, 57 mmol) in $CHCl_3$ (4 ml) with gentle stirring in a round-bottomed flask immersed in a ice-bath. The temperature was monitored during the addition but no exotherm was observed. Aliquots (0.5 ml) of the acid phase were removed from the reaction mixture after 15, 30, 60 and 120 min and immediately quenched in cold distilled water (4 ml) in a test-tube. The sticky, solid product, which adhered to the walls of the tube, was washed several times with distilled water to pH 6 and dried in vacuo at 45ºC for 1h. The ^{1}H NMR spectra of the product obtained after 15, 30, 60 and 120 min showed no major differences. The final yield was not recorded. NMR (acetone-d_6, 120 min aliquot) [Appendix A, Figure 5.69]: ^{1}H: 3.50-5.12 (br m, 10.44H, C-1 C*H*$_2$, C-3 C*H*$_2$, C*H*$_2$ trifluoroethoxy plus an unidentified, possibly polymeric impurity) and 5.78ppm (br s, 1.00H, C-2 C*H*).

4.2.9.2 Attempted nitration using N_2O_5

Nitration 1. Polymer 2, random linear poly[P-2,3-dinitratoprop-1-oxy/P-2,2,2-trifluoroethoxy phoshazene] (Batch 1, 106 mg, 0.37 mmol) in CH_2Cl_2 (20 ml) was pre-cooled to 0ºC and added to a solution of N_2O_5 (2.7 ml, 1.29 mol/l, 3.5 mmol, ~10 equivalents) in CH_2Cl_2 with gentle stirring. The solution turned hazy after 45 min and became turbid-white after 1.5 h, suggesting the possible formation of reaction by-products. The progress of the reaction was monitored by ^{1}H-NMR spectroscopy of samples removed at 15 min and 2h. These aliquots of the reaction mixture (5 ml) were removed with a Pasteur pipette and quenched in cold distilled water (20 ml). The sticky, solid precipitate was washed with distilled water to pH 6 and dried in vacuo at 45ºC for 1h. Comparison of the complex ^{1}H NMR spectra (acetone-d_6) of the samples isolated at 15 min and 2 h with that of an authentic

sample of nitrated Polymer 2 (Batch 1, nitrated using HNO_3 95%), confirmed that the desired product had not formed and also suggested that extensive degradation of the starting material had occurred.

Nitration 2. Polymer 2, random linear poly[P-2,3-dinitratoprop-1-oxy/P-2,2,2-trifluoroethoxy phoshazene], (Batch 1, 103 mg, 0.36 mmol) was weighed directly into a 25 ml round-bottomed flask and pre-cooled in an ice-bath. N_2O_5 in CH_2Cl_2 (1.29 mol/l, 2.7 ml, 3.5 mmol) was directly added to the polyphosphazene and the reaction mixture was stirred vigorously for 2 h in an ice-bath. After 10 min a precipitate formed. The liquid, decanted from the solid product, was added to crushed ice (1.7 g), to yield a sticky, white solid. This was washed with distilled water to pH 6 and dried in vacuo at 45ºC for 2h. Yield: 35 mg, (28%). NMR (acetone-d_6), [Appendix A, Figure 5.70]: ^{1}H: 4.32-5.64 ppm (br m, C-1 C*H*$_2$, C-2 C*H*, C-3 C*H*$_2$, C*H*$_2$ trifluoroethoxy, in addition to traces of *H*$_2$O and C*H*$_2$Cl$_2$).

Nitration 3. The procedure adopted for 'Nitration 2' was repeated adding N_2O_5 in CH_2Cl_2 solution (1.35 ml, 1.75 mmol) to Polymer 2, random linear poly[P-2,3-dinitratoprop-1-oxy/P-2,2,2-trifluoroethoxyphoshazene], (Batch 1, 113 mg, 0.40 mmol). After only 5 min a white precipitate formed. After 15 min the liquid was decanted and added to crushed ice (1.4g) yielding a white sticky solid. This was washed with distilled water to pH 6 and dried in vacuo at 45ºC for 2h. ^{1}H NMR spectroscopy of a sample of the dry material did not yield any signals attributable to the desired product and suggested extensive degradation of the starting material.

Nitration 4. To Polymer 2, random linear poly[P-2,3-dinitratoprop-1-oxy/P-2,2,2-trifluoroethoxyphoshazene] (Batch 1, 120 mg, 0.42 mmol) in a 25 ml round-bottomed flask pre-cooled in an ice-bath, was added a solution of N_2O_5 in CH_3CN (1.56 mol/l, 2.2 ml, 3.5 mmol) with vigorous stirring. The reaction mixture was left stirring for 2h. A white opalescence appeared after 10 min and disappeared after 30 min. The reaction mixture was added to cold distilled water (20 ml). The solid product was washed to pH 6 and dried in vacuo at 45ºC for 1h. ^{1}H NMR spectroscopy of the dried material showed that extensive degradation of the

starting material had occurred and that the desired product had not formed [Appendix A, Figure 5.71].

4.3 PREPARATION OF "SALT MIXTURES" A AND B

4.3.1.1 Salt mixture A: the product of neutralization of concentrated difluorophosphoric acid with aqueous KOH

HPO_2F_2 (FluoroChem, 90%, d= 1.667g/ml, 9.7 ml, 143 mmol) was added drop-wise and with vigorous stirring to aqueous KOH (0.95 M, 150ml, 143 mmol) in a 250 ml round-bottomed flask immersed in an ice-bath. Since the pH of the final solution was still acidic (pH 2), suggesting that the acid had partially hydrolysed to the diprotic species monofluorophosphoric acid, small aliquots of aqueous KOH 3 M were added until the pH of the solution rose to 8 (total volume added: 62 ml, 186 mmol KOH). After rotary-evaporation of the water, the residue, a white powder, was dried in vacuo over drying agent to a constant weight. Yield: 20.2 g. NMR (acetone-d_6 probe), [Appendix A, Figure 5.72]: ^{19}F: aqueous 2,2,3,3-tetrafluorobutane-1,4-diol (126.1 mM, 1.00ml) was added to the aqueous buffered solution [imidazole/imidazolium oxalate 0.8 M, pH 7, 3.00 ml] of the salt mixture (493.4 mg) to allow quantitative analysis of the fluorinated species: -124.90 (t, $^2J_{H-F}$ = 16.5 Hz, 1.00F, $(CH_2F_2)_2$ standard), -123.44 (br s, 2.60F, F^-), -87.90 (d, $^1J_{P-F}$ = 940 Hz, 2.16F, KPO_2F_2), -74.92 (d, $^1J_{P-F}$ = 864 Hz, 3.79F, K_2PO_3F) and -73.35 ppm (d, $^1J_{P-F}$ = 708 Hz, 0.90F, KPF_6). *Ion chromatography*: salt mixture A (395.4 mg) in aqueous imidazole / imidazolium oxalate buffer (0.8 M, pH 7, 20.0 ml) was diluted to 100.0 ml and quantitatively analysed for orthophosphate using the instrumental settings and general method described in Section 3.1.3. The composition (wt%) of the dry salt mixture, assuming no hydration of the (fluoro)phosphate species was present in the sample, was thus calculated to be: 1.3 (K_2HPO_4), 3.1 (KPF_6), 75.4 (K_2PO_3F), 20.1 (KPO_2F_2) and 0.1 (KF). The composition of the dry salt mixture, as analysed by ion chromatography and ^{19}F NMR spectroscopy was found to be unchanged after a period of 6 months.

4.3.1.2 Salt mixture B: the product of neutralization of concentrated monofluorophosphoric acid with aqueous KOH

H_2PO_3F (FluoroChem, 70%, d= 1.818g/ml, 8.92 ml, 114 mmol) was added drop-wise and with vigorous stirring to aqueous KOH (0.95 M, 240 ml, 228 mmol) in a 250 ml round-bottomed flask immersed in an ice-bath. The final pH of the solution was 8. The water was removed by rotary-evaporation and the residue, a white powder, was dried in vacuo over drying agent to constant weight. Yield: 24.5 g. NMR (acetone-d_6 probe), [Appendix A, Figure 5.73]: ^{19}F: aqueous 2,2,3,3-tetrafluorobutane-1,4-diol (126.1 mM, 1.00ml) was added to the aqueous buffered solution [imidazole/imidazolium oxalate 0.8 M, pH 7, 3.00 ml] of the salt mixture (552.8 mg) to allow quantitative analysis of the fluorinated species: -124.84 (t, $^2J_{H\text{-}F}$ = 16.5 Hz, 1.00F, $(CH_2F_2)_2$ standard), -119.29 (s, 0.18F, F^-), and -74.59 (d, $^1J_{P\text{-}F}$ = 866 Hz, 4.12F, K_2PO_3F). *Ion chromatography*: the salt mixture (322.9 mg) in aqueous imidazole/imidazolium oxalate buffer (0.8 M, pH 7, 20.0 ml) was diluted to 100.0 ml and quantitatively analysed for orthophosphate using the instrumental settings and general method described in Section 3.1.3. The composition (wt%) of the dry salt mixture, assuming no hydration of the (fluoro)phosphate species was present in the sample, was thus calculated as: 19.1 (K_2HPO_4), 72.5 (K_2PO_3F) and 8.4 (KF). The composition of the dry salt mixture was found to be unchanged after a period of 6 months.

5 REFERENCES

1. Sikder A.K. and Sikder N., *J. Haz. Mat.*, 2004, **A112**, 1-15.
2. Geetha M., Nair U.R., Sarwade D.B.; Gore G.M., Ashtana S.N. and Singh H., *J. Therm. Anal. and Calorimetry*, 2003, **73**, 913-22.
3. Chavez D.E., Hiskey A. and Naud D.L., *Propellants, Explosives, Pyrotechnics*, 2004, **29(4)**, 209-15.
4. Bailey A. and Murray S.G., *Explosives, Propellants & Pyrotechnics*, Brassey's, London, 1989.
5. Wild R. and Maasberg W., Energetic Materials for Insensitive Munitions, Paper presented at the 5th Seminar: *New Trends in Research of Energetic Materials*, Pardubice University, Czech Republic, 24-25 Apr. 2002, 383-398.
6. Isler J., *Propellants, Explosives, Pyrotechnics*, 1998, **23(6)**, 283-91.
7. Burrows, K.S., New Explosives for Insensitive Munitions: A Comparative Evaluation, Paper presented at the Insensitive Munitions and Energetic Materials Symposium, Bordeaux, France, 8-11 Oct. 2001, **1**, 230-238.
8. Akhavan J., *The Chemistry of Explosives*, RSC Paperbacks, Cambridge, 1998.
9. Govindan G. and Athithan, S.K., *Propellants, Explosives, Pyrotechnics*, 1994, **19(5)**, 240-4.
10. Lu Y.C. and Kuo K.K., *Therm. Acta*, 1996, **275(2)**, 181-91.
11. Desai H., Cunliffe A.V., Stewart M.J. and Amass A.J., *Polymer*, 1993, **34(3)**, 642-47.
12. Desai H.J., Cunliffe A.V., Hamid J., Honey P.J., Stewart M.J. and Amass A.J., *Polymer*, 1996, **37(15)**, 3461-69.
13. Bala K. and Golding P., The Influence of Molecular Weight on Explosive Hazard, Paper presented at the Insensitive Munitions & Energetic Materials Technology Symposium, San Francisco, 2004.
14. Frankel M.B. and Flanagan J.E., US Patent No. *4268450*, 1981.

15. Miller R. S.*, Research on New Energetic Materials***,** Materials Research Society Symposium Proceedings, (Decomposition, Combustion, and Detonation Chemistry of Energetic Materials), 1996, **418**, 3-14.
16. Jin R.C., Young G.C., Jin S.K., Hyun S.K. and Hyung S.K., A New Energetic Prepolymer, M-PGN and its Undegradable Elastomer; Paper presented at the Insensitive Munitions & Energetic Materials Technology Symposium, San Francisco, 2004.
17. Simmons R.L., Thermochemistry of NENAs Plasticizers, Paper presented at the 25th International Annual Conference of ICT, Karlshrue, Germany. 1994, 10/1-10/10.
18. Christiansen M. and Johansen O.H., The development of a two-step batch-synthesis to a two-step continuous synthesis, Paper presented at the 33rd International Annual Conference of ICT, 2002, Karlshrue, Germany.
19. Golding P. and Trussell S.J., Energetic Polyphsophazenes – A New category of Binders for Energetic Formulations; Paper presented at the Insensitive Munitions & Energetic Materials Technology Symposium, San Francisco, 2004.
20. Provatas A., *J. Energetic Materials*, 2003, **21(4)**, 237-45.
21. Allcock H.R., *Chemistry and Applications of Polyphosphazenes*, Wiley-Interscience, Hoboken, New Jersey, 2003.
22. Allcock H.R., *Phosphorus-Nitrogen Compounds*, Academic Publishing, New York, 1972.
23. Billmeyer F.W., *Textbook of Polymer Science*, Wiley Interscience, New York, 1984.
24. Wang B., Rivard E. and Manners I., *Inorg. Chem.*, 2002, **41(7)**, 1690-91.
25. Matyjaszewski K., Lindenberg M.S., Moore M.K. and White M.L., *J. Polymer Science*, 1994, **32**, 465-73.
26. Allcock H.R., Chester A.C., Morrissey C.T., Nelson J.M. and Reeves S.D., *Macromolecules*, 1996, **29**, 7740-47.
27. Allcock H.R., Powell E.S., Maher A.E., Prange R.L. and Denus C.R., *Macromolecules*, 2004, **37**, 3635-41.

28. Allcock H.R., Reeves S.D., Nelson J.M. and Crane C.A., *Macromolecules*, 1997, **30**, 2213-15.
29. Greenwood N.N. and Earnshaw A., *Chemistry of the Elements*, Pergamon Press, Oxford, 1984.
30. Liebig J., *Ann. Chem*., 1834, 11, 139-49.
31. Rose H., *Ann. Chem.*, 1834, **11**, 131-50.
32. Gladstone J.H. and Holmes J.D., *J. Chem. Soc.*, 1864, **17**, 225-37.
33. Stokes H.N., *Am. Chem. J.*, 1895, **17**, 275-90.
34. Neilson R.H. and Wisian-Neilson P., *Chem. Rev.*, 1988, **88**, 541-562.
35. Gleria M., Bertani R. and De Jaeger R., *J. Inorg. and Organomet. Polymers*, 2004, **14(1)**, 1-28.
36. Allcock, H.R., Pucher, S.R., Fitzpatrick, R.J. and Rashid, K., *Biomaterials*, 1992, **13(12)**, 857-62.
37. Allcock, H.R. and Kim, C., *Macromolecules*, 1991, **24(10)**, 2846-51.
38. Frech, R.; York, S.; Allcock, H.and Kellam, C., *Macromolecules*, 2004, **37(23)**, 8699-8702.
39. Paulsdorf, J.; Burjanadze, M.; Hagelschur, K., Wiemhoefer, H.D.; *Solid State Ionics,* 2004, **169**, 25-33.
40. llen, G.; Lewis, C. J. and Todd, S. M.; *Polymer*, 1970, **11(1)**, 44-60.
41. Allen, C. W.and Hernandez-Rubio, D.; *Phosphazenes*, 2004, 485-503.
42. Zhang, Teng; Cai, Qing; Wu, De-Zhen; Jin, Ri-Guang., *J. Applied Polymer Science*, 2005, **95(4)**, 880-889.
43. Pintauro, P.N. and Wycisk, R., *Phosphazenes*, 2004, 591-620.
44. Grolleman, C. W. J., De Visser, A. C.; Wolke, J. G. C., Van der Goot, H. and Timmerman, H., *J. Controlled Release*, 1986, **4(2)**, 119-31.
45. Laurencin C. T., Koh H J; Neenan T. X. Allcock H. R. and Langer R., *J. Biomedical Materials Research*, 1987, **21(10)**, 1231-46.
46. Gaeta, S. N., Zhang, H., Drioli, E. and Basile, A., *Desalination*, 1991, **80(2-3)**, 181-92.
47. Dave P.R., Forohar F., Axenrod T., Bedford C.D., Chaykovsky M., Gilardi R., Anderson F. and George C., Preparation of Cyclotriphosphazene Polynitramines, Paper presented at the Joint International Symposium on

Energetic Materials, American Defence Preparedness Association, New Orleans, 1992.

48. Colclough M.E., Studies on the Synthesis of Energetic Phosphazenes, Paper presented at the International Symposium on Energetic Materials Technology, Phoenix, 1995, 33-38.
49. Chapman R.D., Welker M.F. and Kreutzberger C.B., *J. Inorganic and Organomet. Polymers*, 1996, **6(3)**, 267-275.
50. Allcock H.R., Maher A.E. and Ambler C.M., *Macromolecules*, 2003, **36**, 5566-72.
51. Allcock, H.R. and Kim Y.B., *Macromolecules*, 1994, **27**, 3933-42.
52. Gabler D.G. and Haw, J.F, *Macromolecules,* **24(14)**, 1991, 4218-20.
53. AWE Aldermaston, unpublished work.
54. Flindt, E.P. and Rose H., *Z. anorg. Chem.*, 1977, **430**, 155-60.
55. Staudinger H., *Helv. Chim. Acta*, 1919, **2**, 635-41.
56. Allcock, H.R., *Chem. Rev.*, 1972, **72(4)**, 315-56.
57. Private conversation with Dr S. Trussell, Polymer Synthesis Group, AWE Aldermaston.
58. Lora S, Palma G., Bozio R., Caliceti P. and Pezzin G., *Biomaterials*, 1993, **14(6)**, 430-6.
59. Tur, D.R., Korshak, V.V., Vinogradova S.V., Dobrova N.B., Novikova S.P., Ll'ina M.B. and Sidorenko E.S., *A. Polymerica*, 1985, **36(11)**, 627-31.
60. Nakamura H., Masuko T., Kojima M. and Magill J.H., *Macromol. Chem. and Phys.*, 1999, **200(11)**, 2519-24.
61. McCaffrey R.R., McAtee, R.E., Grey A.E., Allen C.A., Cummings D.G., Apelhans A.D., Wright R.B. and Jolley J.G., *Separation Sci. and Tech.*, 1987, **22(2)**, 873-87.
62. Flindt E.P. and Rose H., *Z. anorg. Chem.*, 1977, **428**, 204-8.
63. Montague R.A., Green J.B. and Matyjaszewski K., *J. Macromol. Sci., Pure and Applied Chemistry*, 1995, **A32**, 1497-1519.
64. Matyjaszewski K., Moore M.M. and White, M.L., *Macromolecules*, 1993, **26(25)**, 6741-48.

65. Matyjaszewski K., Lindberg, M.S., Moore M.M. and White M.L., *J. Pol. Sci., Series A*, 1994, **32**, 465-73.
66. Moore, W.J., *Physical Chemistry*, Longman, London, 1972.
67. Warn J.R.W. and Peters A.P.H., *Concise Chemical Thermodyna*mics, Stanley Thornes Publishers, Cheltenham, 1999.
68. IUPAC Compendium of Chemical Terminology, 2nd Edition, 1997.
69. Freeman, R.D., *J. Chem. Eduation.*, 1985, **62(8)**, 681-6.
70. Atkins, P.W., *Physical Chemistry*, 5th edn, Oxford University Press, 1999.
71. Barrow, G.M., *Physical Chemistry*, McGraw-Hill, New York, 1972.
72. Schmidt R.D. and Manser G.E., *Heats of Formation of Energetic Oxetane Monomers and Polymers*; Paper presented at the 32nd International Conference of ICT, Karlshrue, Germany, 2001, 140/1-140/8.
73. Bourasseau S., *J. Energ. Mat.,*, **8(5)**, 1990, 416-441.
74. Volk F., *Philosophical Transactions of the Royal Society. A*, **339**, 335-343.
75. Ornellas D.L., *Propellants, Explosives, Pyrotechnics*, 1989, **14**, 122-3.
76. Cox J., *J. Chem. Thermodynamics*, 1978, **10(10)**, 903-6.
77. Cox J.D. and Pilcher G., *Thermochemistry of Organic and Organometallic Compounds, Academic Press*, London, 1970.
78. Feng-qi Z., Chen P., Hu R.Z., Luo Y., Zhang Z.Z., Zhou Y.S., Yang X.W., Gao Y., Gao S.L. and Shi Q.Z., *J. Haz. Mat.*, 2004, **A113**, 67-71.
79. Desai H.J., Cunliffe A.V., Lewis T., Millar R.W. Paul N.C., Stewart M.J. and Amass A.J., *Polymer*, 1996, **37(15)**, 3471-76.
80. McGuire R.R., Ornellas D.L. and Akst I.B., *Propellants and Explosives*, 1979, **4**, 23-6.
81. Taylor J., *Detonation in condensed explosives*, Monographs on the Physics and Chemistry of Materials, Oxford University Press, Oxford, 1952.
82. Ornellas D.L., Carpenter J.H. and Gunn S. R., *Rev. Sci. Instr.*, 1966, **37(7)**, 907-912.
83. Cudzilo S., Trębinsky R., Trzcinky W., Waldemar A. and Wolanski P., Comparison of Heat Effects on Combustion and Detonation of Explosives in a Calorimetric Bomb, Paper presented at the 29th International Annual Conference of ICT, Karlshrue, Germany, 1998, 150/1-150/8.

84. Ornellas D.L., *J. Phys. Chem.*, 1968, **72(7)**, 2390-95.
85. Volk F. and Schedlbauer F., *Khim. Fiz.*, 2001, **20(8)**, 43-49.
86. Keshauarz M.H. and Pouretedal H.R., *T. Acta*, 2004, **414**, 203-208.
87. Chen, P.C., Wu J.C. and Chen S.C., *Computers and Chemistry*, 2001, **25**, 439-445.
88. Muthurajan H., Sivabalan R., Talawar M.B. and Ashtana S.N., Computer Code for Qualitative Prediction of Heat of Formation of High Energetic Materials- Part I; Proceedings of the 7th Seminar 'New Trends in Research of Energetic Materials', Pardubice University, Czech Republic, Apr. 2004, 1, 203-24.
89. Mathieu D. and Simonetti P., *T. Acta,* 2002, **384**, 369-375.
90. Duchowicz P., Castro E.A. and Chen P.C., *J. Korean Chem. Soc.*, 2003, **47(2)**, 89-91.
91. Benson S.W., *Thermochemical Kinetics, Methods for the Estimation of Thermochemical Data and Rate Parameters*, John Wiley, New York, 1968.
92. Walters, N.R., Hackett, S.M. and Lyon R.E., *Fire and Materials*, 2000, **24**, 245-52.
93. Babrauskas, V., *Heat Release in Fires*, Elsevier, London, 1992.
94. Pasquetto S. and Patrone L., *Chimica Fisica, Termodinamica Chimica, Elettrochimica*, Vol. 3, Masson Editori, Milan, 1992.
95. Sunner S. and Månsson M., *Combustion Calorimetry, Experimental Chemical Thermodynamics*, IUPAC Series, Pergamon Press, Oxford, 1979.
96. Bradford H.R., *J. Min. Eng.*, 1957, **9**, 78-9.
97. Haines P.J. (Editor), *Principles of Thermal Analysis and Calorimetry*, RSC Paperbacks, London, 1999.
98. Rossini F.D. (Editor), *Experimental Thermochemistry*, Interscience Publishers, New York, 1956.
99. Rojas A. and Valdes A., *J. Chem. Therm.*, 2003, **35**, 1309-19.
100. Rojas-Aguilar A., *J. Chem. Therm.*, 2002, **34**, 1729-43.
101. Sakiyama M. and Kiyobayashi T., *J. Chem. Therm.*, 2000, **32**, 269-79.

102. Private telephone conversation with Dr Hugh Davies, Thermodynamics Modelling Team, National Physical Laboratory, Teddington.
103. Hubbard W.N., Katz C. and Waddington G., *J. Phys. Chem.*, 1954, **58**, 142-52.
104. Matthews G.P., *Experimental Physical Chemistry*, Clarendon Press, Oxford, 1985.
105. Washburn E.W., *J. Res. Nat. Bur. Stand.*, 1933, **10**, 525-58.
106. Siegel B. and Schieler L., *Energetics of Propellant Chemistry*, John Wiley & Sons, New York, 1964.
107. Gallazzi M.C., Freddi G., Sanvito G. And Viscardi G., *J. Inorg. Organomet. Pol.*, 1996, **6(4)**, 277-300.
108. Taber D.F., Xu M. and Hartnett J.C., *J. Am. Chem. Soc.*, 2002, **124**, 13121-6.
109. Meyers A.I. and Lawson J.P., *Tetrahedron Letters*, 1982, **47**, 4883-6.
110. Marton D., Stivanello D. and Tagliavini G., *Gazzetta*, 1994, **124**, 265-70.
111. Michael A. and Carlson G.H., *J. Am. Chem. Soc.*, 1935, **57**, 1268-76.
112. Strazzolini P. and Runcio A., *Europ. J. Org. Chem.*, 2003, **3**, 526-36.
113. Strazzolini P., Dall'Arche M.G. and Giumanini A.G., *Tetrahedron Letters*, 1998, **39**, 9255-58.
114. Grummit O. and stearns J.A., *Org. Synth.,* 1949, **29**, 89-91.
115. Brimble M.A., Park J.H. and Taylor C.M., *Tetrahedron*, 2003, **59(31)**, 5861-68.
116. Kuehnert S.M. and Maier M.E*., Org. Lett.*, 2002, **4(4)**, 643-46.
117. Manners I., Wang B. and Rivard E., *Inorg. Chem.*, 2002, **41(7)**, 1690-91.
118. Pinciroli V., Biancardi R., Visentin G. And Rizzo V., *Organic Process Research & Development*, 2004, **8**, 381-84.
119. IUPAC Commission on Atomic Weights and Isotopic Abundances, *J. Phys. Chem. Ref. Data*, 1995, **24(4)**, 1561-76.
120. Sanping C., Gang X., Guang F., Shengli G. and Qizhen S., *J. Chem. Therm.*, 2005, **37**, 397-404.
121. Diaz E., Brousseau P., Ampleman G. and Prud'Homme R.E., *Propellants, Explosives, Pyrotechnics*, 2003, **28(3)**, 101-106.

122. Sanden, R., *Determination of the Heat of Formation of Poly(dimethylsiloxane)*; Internationale Jahrestagung - Fraunhofer-Institut fuer Treib- und Explosivstoffe, 17th ICT Meeting , 1986, 65/1-65/13.
123. Sabbah T., Xu-Wu A., Chickos J.S., Planas Leitão M.S., Roux M.V. and Torres L.A., *T. Acta*, 1999, **331**, 93-204.
124. Brimblecombe P., *Air Composition and Chemistry*, Cambridge University Press, 1995.
125. *Operating Instructions for the 1341 Oxygen Bomb Calorimeter, Manual No. 204M,* Parr, Inc.
126. '*The Enthalpy of Formation of Camphor by Bomb Calorimetry'*, Colby University's Chemistry Department. Work published on the WWW: http://www.colby.edu/chemistry/PChem/lab/Enthalpyof Formation.pdf
127. H.W.Salzberg, J.I. Morrow and M.E. Green., *Physical Chemistry Laboratory: Principles and Experiments*, Macmillan, New York, 1978.
128. Wadso I, *Sci. Tools*, 1966, **13(3)**, 33-39.
129. Christian G.C., *Analytical Chemistry*, J. Wiley and Son, Oxford, 1994.
130. Garner W.E. and Abernethy C.L., *Proc. Roy. Soc.*, A, **99**, 1921, 213, cited in Urbanski T., *Chemistry and Technology of Explosives*, Vol. 1, Pergamon Press, Oxford, 1986.
131. Urbanski T., *Chemistry and Technology of Explosives*, Vol. 2, Pergamon Press, Oxford, 1986.
132. Federoff, B.T., *Encyclopedia of Explosives and Related Items*, Vol. 2, Picatinny Arsenal, Dover, NJ, 1960.
133. Gibbs T.R. and Popolato A., (Editors), *LASL Explosive Property Data*, University of California Press, Berkeley, 1980.
134. Bugaut F., Performances des Noveaux Explosifs Insensibles, Cas du NTO, Deuxiemens Journeés Scientifiques, Paul Vielle, Brest, 16-18 Oct. 1991.
135. Finch A., Gardner, P.J., Head A.J. and Majdi H.S., *J.Chem. Therm.*, 1991, **23**, 1169-73.
136. Harrop D. and Head A.J., *J. Chem. Therm.*, 1977, **9**, 1067-76.
137. Bedford A.F. and Mortimer C.T., *J. Chem. Soc.*, 1960, 1622-25.
138. Kirklin D.R. and Domalski E.S., *J. Chem. Therm.*, 1988, **20**, 743-54.

139. Holmes W.S., *Trans. Faraday Soc.*, 1962, **58**, 1916-25.
140. Wagenaar W., *J. Chem. Soc.*, 1912, **100(II)**, 931.
141. Belcher R., *Quantitative Inorganic Analysis*, Butterworth Scientific Publications, London, 1955.
142. *'1108Cl Halogen-resistant bomb';* Instruction and Manteinance Manual, Parr Inc.
143. Britske E.V. and Dragunov S.S., *J. Chem. Ind.*, 1927, **4**, 49-51.
144. Chess W.B. and Bernhart D.N., *Analyt. Chem.*, 1959, **31**, 1116-19
145. Altynikova P.M., Kharakoz A.E., Osipova T.P. and Bleshinskii S.V., *Ser. Fiz. Mat. Estet. Nauk*, 1950, **3**, 63-7.
146. Smith N.K., Scott D.W. and McCullough J.P., *J. Phys. Chem.*, 1964, **68(4)**, 934-39.
147. Hajiev S.N. and Agarunov M.J., *J. Organomet. Chem.*, 1970, **22**, 305-311.
148. Hu, A.T. and Sinke G.C*., J. Chem. Therm.*, 1969, **1**, 507-13.
149. Hubbard W.N., Knowlton J.W. and Hugh, M.H., *J. Phys. Chem.*, 1954, **58**, 396-402.
150. Good W.D., Scott D.W. and Waddington G., *J. Phys. Chem.*, 1956, **60**, 1080-89.
151. Cox J.D., Gundry H.A. and Head A.J., *Trans. Faraday Soc.*, 1964, **60**, 653-65.
152. Krech M., Price S.J.W. and Yared W.F., *Canad. J. Chem.*, 1972, **50(18)**, 2935-38.
153. Krech M.J., Price S.J.W and Yared W.F., *Canad. J. Chem.*, 1973, **51(22)**, 3662-64.
154. Domalski E.S. and Armstrong, G.T., *J. Res.Nat. Bur. Stand., A: Physics and Chemistry*, 1967, **71(2)**, 105-18.
155. Good W.D., Douslin D.R. and McCullough J.P, *J. Physical Chemistry*, 1963, **67**, 1312-14.
156. Swarts F.; *J. Chim. Phys.*, 1919, **17**, 3-70.
157. Cox J.D. and Head A.J., *Trans. Faraday Soc.*, 1962, **58**, 1839-45.
158. Peters H., Tappe E. and Urbanczik M., *Monatsberichte zu Berlin*, 1967, **9**, 703-14.

159. Williams M.M., McEwan W.S. and Henry R.A., *J. Phys. Chem.*, 1957, **61**, 261-7.
160. Roux M.V., Torres L.A. and Davalos J.Z., *J. Chem. Therm.*, 2000, **33**, 949-57.
161. Jiménez P., Roux M.V. and Turrión C., *J. Chem. Therm.*, 1992, **24**, 1145-49.
162. Becker, G. and Roth W.A., *Zhurnal Physik. Chem*., 1935, **174**, 104-14.
163. Aleksandrov Y., Mikina V.D. and Novikov G.A., *Trudy Metrolog. Insitutov SSSR*, 1969, **111**, 95-102.
164. Uman, M.A., *The lightning discharge*, Academic Press, New York, 2000.
165. Harris G.W., McKay G.I., Iguchi T., Schiff H.I., Harold I. and Schuetzle D.; *Env. Sci. and Tech.*, 1987, **21(3)**, 299-304.
166. Faour M. and Akasheh T.S., *J. Chem. Soc., Perkin Trans. 2: Phys. Org. Chem.*, 1985, **6**, 811-13.
167. Kongpricha S. and Jache A.W., *J. Fluorine Chem.*, 1971, **72**, 79-84.
168. Plakhotnik V.N., Shamakhova N.N., Tul'chinskii B.V. and Ll'in E.G., *Z. Neorgan. Khim.*, 1985, **30(11)**, 2773-77.
169. Ames D.P., Ohashi S., Callis C.F., Van Wazer J.R., *J. Am. Che. Soc.*, 1959, **81**, 6350-57.
170. Larson J.W. and Su B., *J. Chem. & Eng. Data*, 1994, **39**, 36-38.
171. Yoza N., Nakashima S., Ueda N., Miyajima T., Nakamura T. and Vast P., *J. Chromatography A*, 1994, **664**, 111-16.
172. Vast P., Semmoud A., Addou A. and Palavit G., *J. Fluorine Chem.* 1985, **27(3)**, 319-325.
173. Nixon J.F. and Schmutzler R.S., *Spectrochim. Acta*, 1964, **20(12)**, 1835-42.
174. Gebala A.E. and Jones M.M., J. *Inorg. & Nuc. Chem.*, 1969, **31**, 771-76.
175. Reddy G.S. and Schmutzler R., *Z. Naturforsch., B (Anorg. Chem.)*, 1970, **25(11)**, 1199-1214.
176. Lindahl C.B., *Fluorine Compounds of Inorganic Phosphorus*, Kirk-Othmer Encyclopedia of Chemical Technology (3rd edn.), Wiley, New York.

177. Pelletier P. and Durant J.L., *Z. anorg. Chem.*, 1990, **581**, 190-98.
178. Ryss, I.G. and Tul'chinskii, V.B., *Zhur. neorg. Khim.*, 1962, **7**, 1313-15.
179. Skoog D.A. and West D.M., *Fundamentals of Analytical Chemistry*, Holt, Rinehart and Winston Publishing, New York, 1976.
180. Vast P., Semmoud A., Addou A. and Plavit G., *J. Fluorine Chem.*, 1985, **27**, 319-25.
181. Addou A., and Vast P., *J. Fluo. Chem.*, 1979, **14**, 163-69.
182. Gaudiano A. and Gaudiano G., *Vademecum di Chimica per Chimici, Biochimici e Farmacisti*, Masson Italia Editori, Milan, 1982.
183. Kazakov A.I., *Bull. Acad. Sci. USSR, Division Chemical Sciences*, 1990, 1565-70.
184. Benson S.W. and Cohen N., *Che. Rev.*, 1993, **93**, 2419-38.
185. Kolesov V.P., *Russian J. Phys. Chem.* (English translation), 1971, **45**, 303-5. Cited as reference in the ICT Thermochemical Code, ICT, Karslruhe, Germany.
186. Larson J.W. and Su B., *J. Chem. Eng. Data*, 1994, **39**, 36-38.
187. Cox, J.D., Wagman, D.D. and Medvedev, V.A., *CODATA Key Values for Thermodynamics*, Hemisphere Publishing Corporation, New York, 1989.
188. Lau, J.K. and Li, W., *J. Mol. Structure (Theochem)*, 2002, **578**, 221-28.
189. Miroshnichenko E.A., Lebedev V.P., Kostikova, L.M., Vorob'eva V.P., Voro'ev A.B. and Inozemtcev J.O., Enthalpy characteristics of nitro- and fluorine-nitro derivatives heterocyclic compounds, Paper presented at the 34th International Conference of ICT, Karshrue, Germany, 2003, 122/1-122/7.
190. Private conversation with Dr P. Gill, DEOS, Cranfield University at the Defence Academy of the United Kingdon.
191. Deepak D., Sridharan P. and Padmanbhan M.S., *J. Propl. and Power*, 1998, **14(3)**, 290-94.
192. Milyokhin Y.M., Klyuchnikov A.N., Fedorychev A.V. Gunin S.V. and Serushkin V.V., Identification of experimental dependences of propellant burning rate on pressure; Paper presented at the 34th International Conference of ICT, Karshrue, Germany, 2003, 142/1-142/11.

193. Siegel B. and Schieler L., *Energetics of Propellant Chemistry*, John Wiley & Sons, New York, 1964.
194. Desai H.J., Cunliffe A.V., Lewis T., Millar R.W., Paul N.C. and Stewart M.J., *Polymer*, 1996, **37(15)**, 3471-76.
195. Suzuki, H. and Okada, F., Japanese Patent No. ***JP 04134086***, 1992.
196. Ranu B.C. and Hajra A., *J. Chem. Soc, Perkin Trans. 1*, 2001, 2262-65.

APPENDIX A SPECTROSCOPIC EVIDENCE

Relating to Section 4.2.1.1.

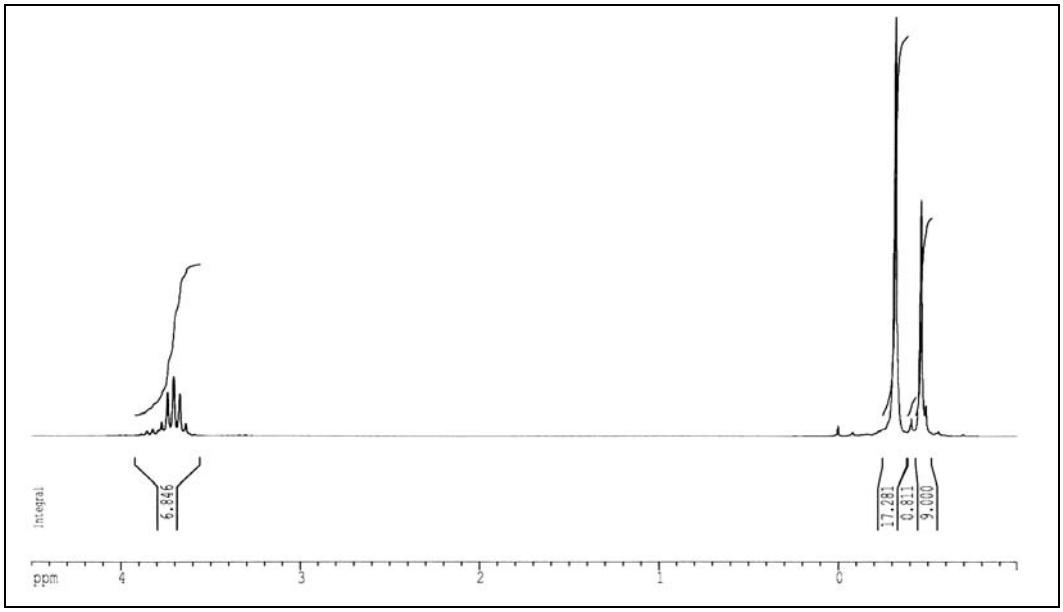

Figure 5.1 ^{1}H NMR spectrum (acetone-d_6 /TMS probe) of the crude reaction mixture after 90 h at 110ºC.

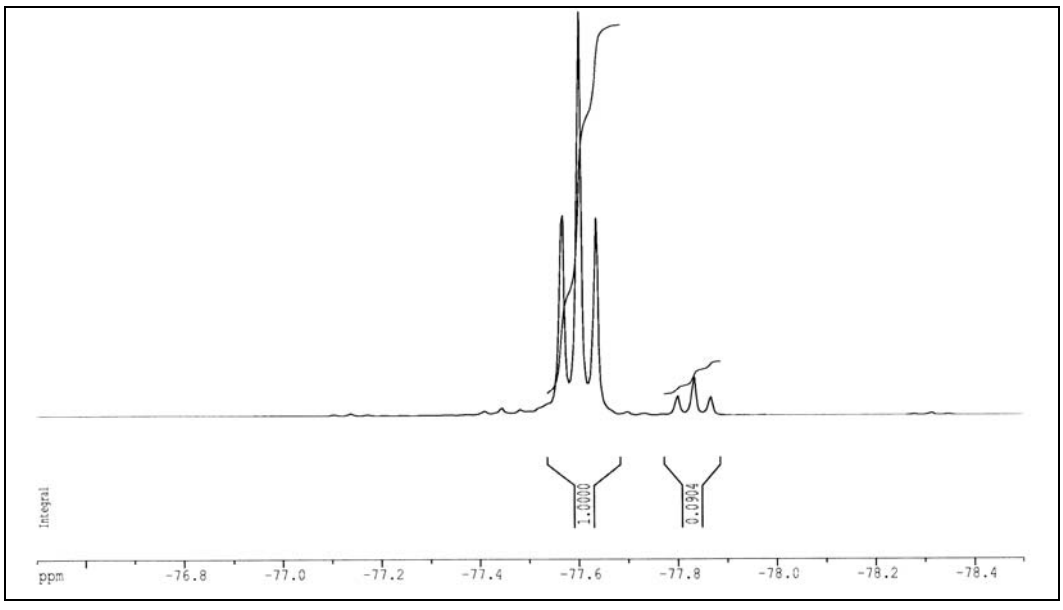

Figure 5.2 ^{19}F NMR spectrum (acetone-d_6 /TMS probe) of crude reaction mixture after 90 h at 110ºC.

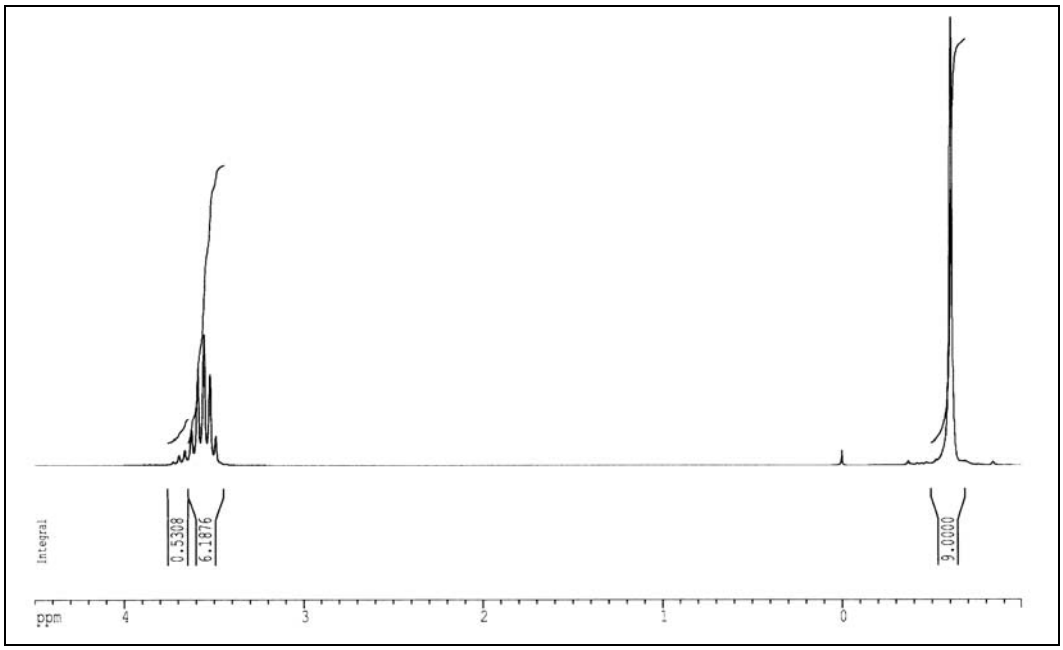

Figure 5.3 ^{1}H NMR spectrum (acetone-d_6 /TMS probe) of the distilled phosphoranimine product.

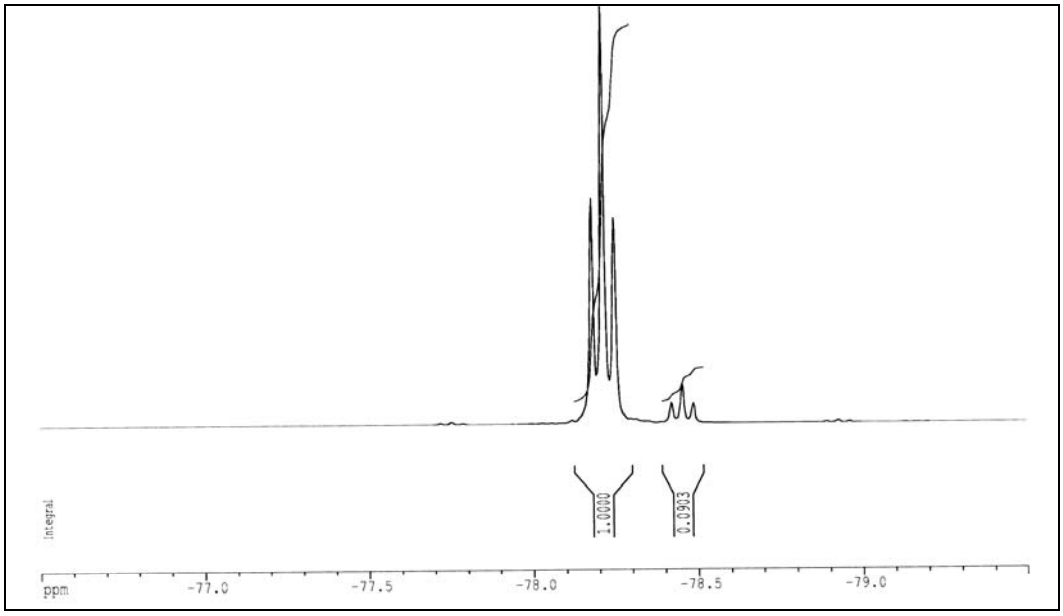

Figure 5.4 ^{19}F NMR spectrum (acetone-d_6 /TMS probe) of the distilled phosphoranimine product.

Relating to Section 4.2.1.2.

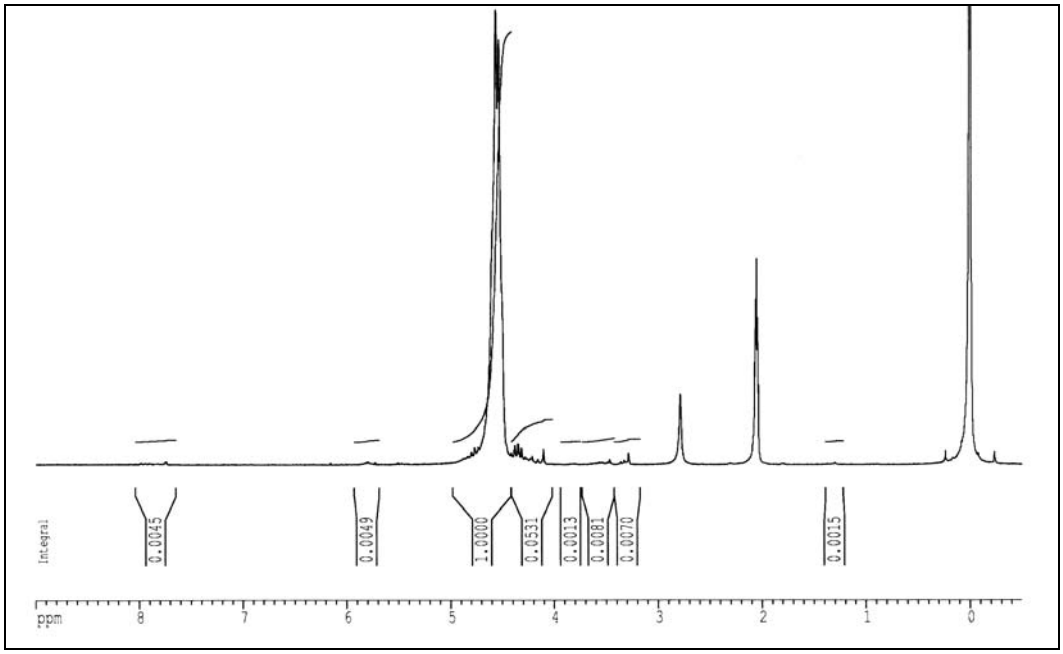

Figure 5.5 ^{1}H NMR spectrum (acetone-d_6) of linear poly[bis(2,2,2-trifluoroethoxy)phosphazene].

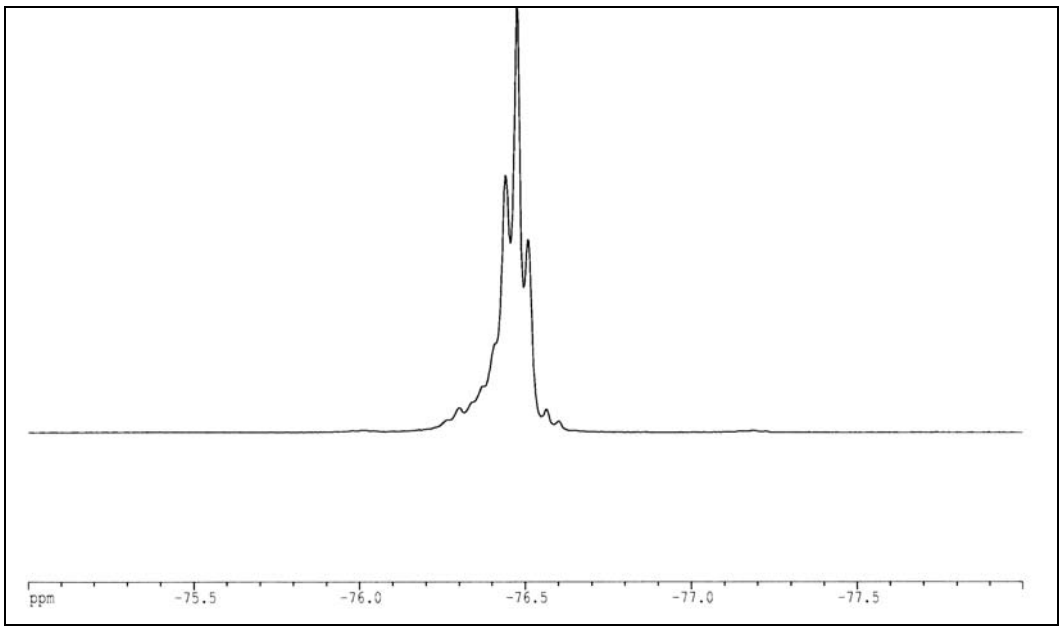

Figure 5.6 ^{19}F NMR spectrum (acetone-d_6) of linear poly[bis(2,2,2-trifluoroethoxy)phosphazene].

Relating to Section 4.2.3.1

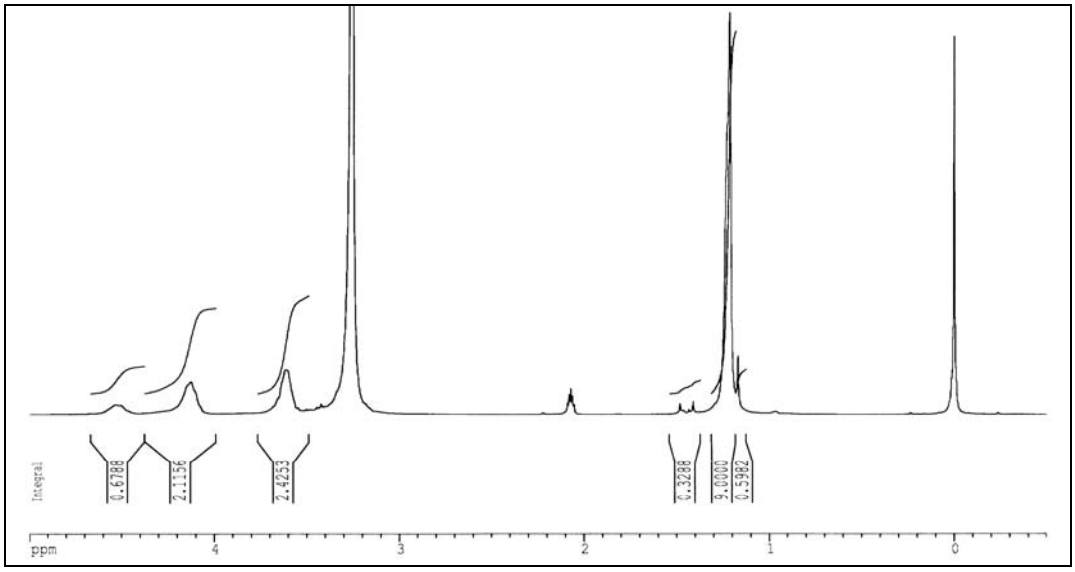

Figure 5.7 ^{1}H NMR spectrum (acetone-d_6 + H_2O) of random linear poly[P-2-t-butoxyethoxy/P-2,2,2-trifluoroethoxyphosphazene].

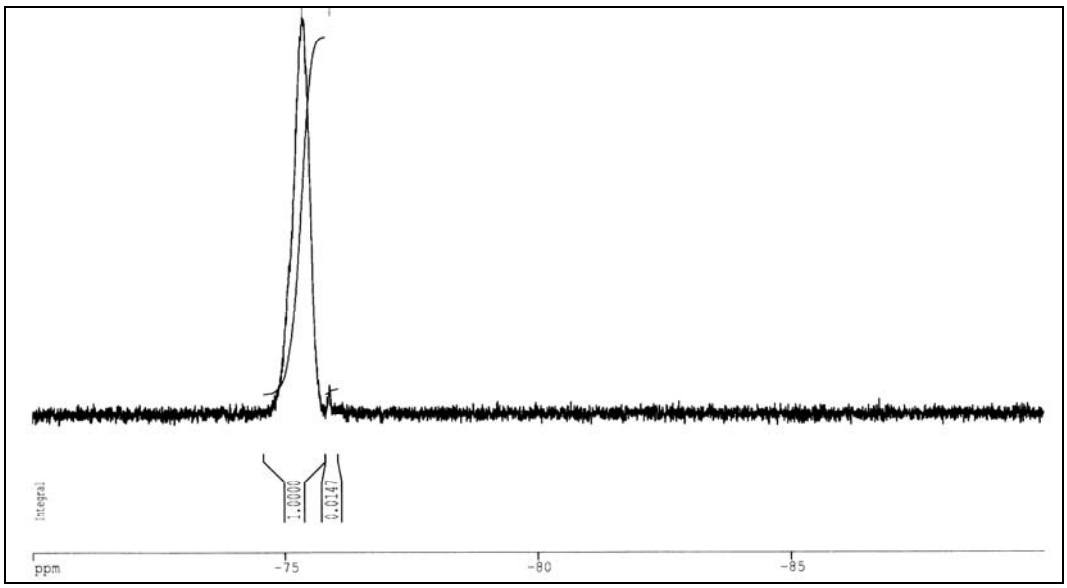

Figure 5.8 ^{19}F NMR spectrum (acetone-d_6) of random linear poly[P-2-t-butoxyethoxy/ P-2,2,2-trifluoroethoxyphosphazene].

Relating to Section 4.2.3.2

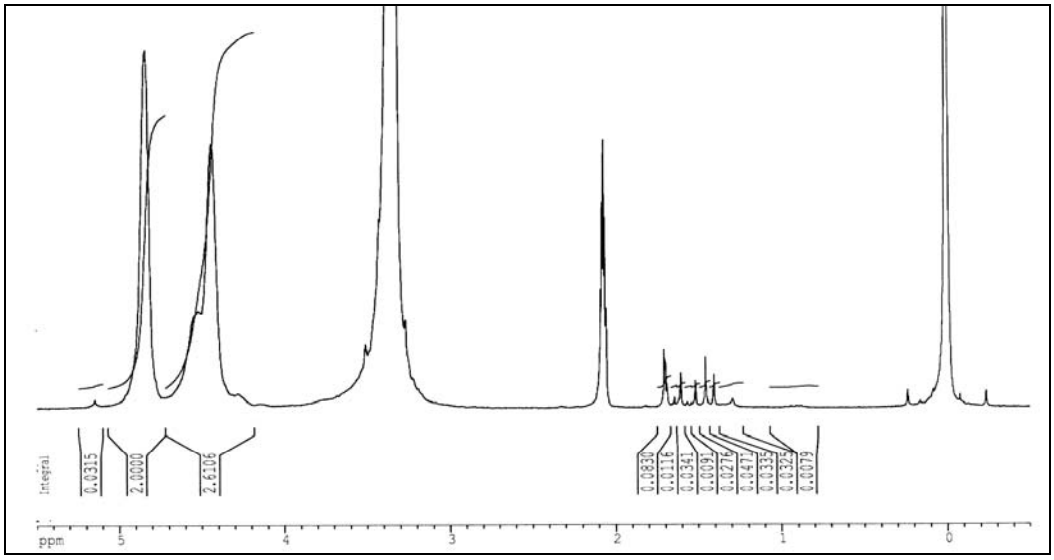

Figure 5.9 ^{1}H NMR spectrum (acetone-d_6 + H_2O) of random linear poly[P-2-nitratoethoxy/P-2,2,2-trifluoroethoxyphosphazene], showing non-polymeric contamination.

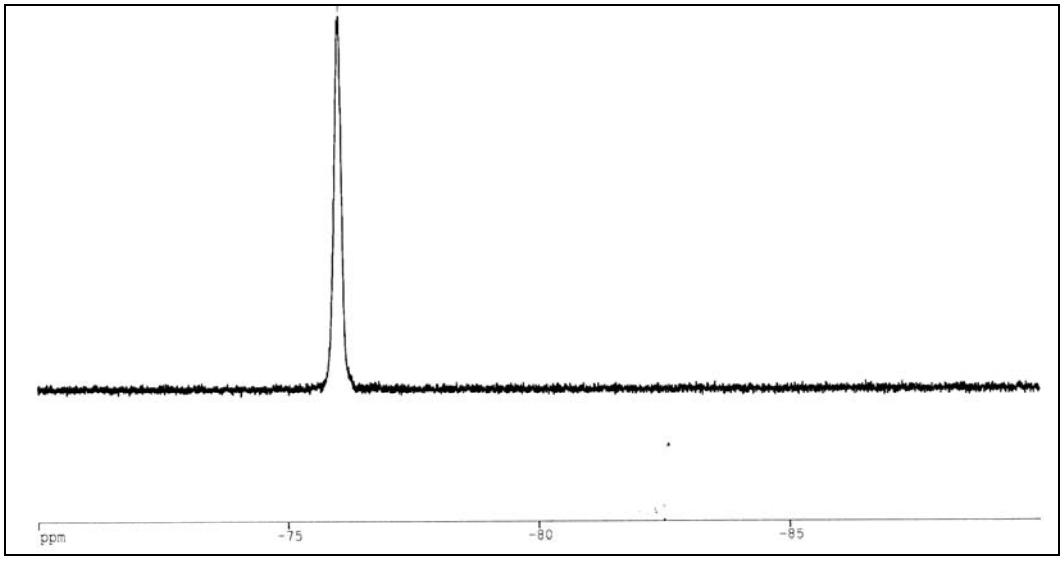

Figure 5.10 ^{19}F NMR spectrum (acetone-d_6) of random linear poly[P-2-nitratoethoxy/P-2,2,2-trifluoroethoxyphosphazene].

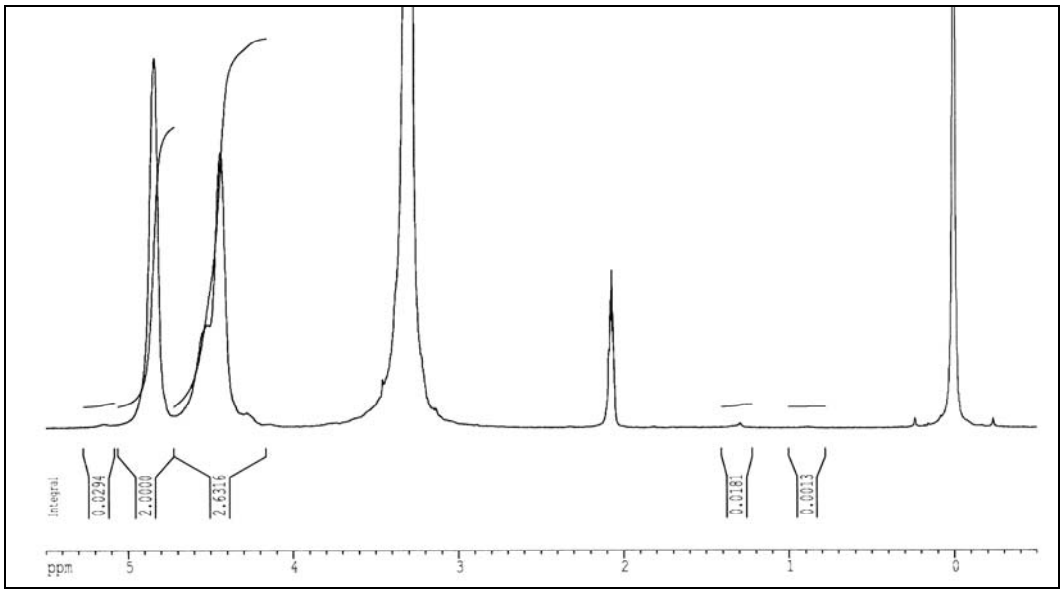

Figure 5.11 ^{1}H NMR spectrum (acetone-d_6 + H_2O) of random linear poly[P-2-nitratoethoxy/P-2,2,2-trifluoroethoxyphosphazene] after washing the polymer with Et_2O for 20 h.

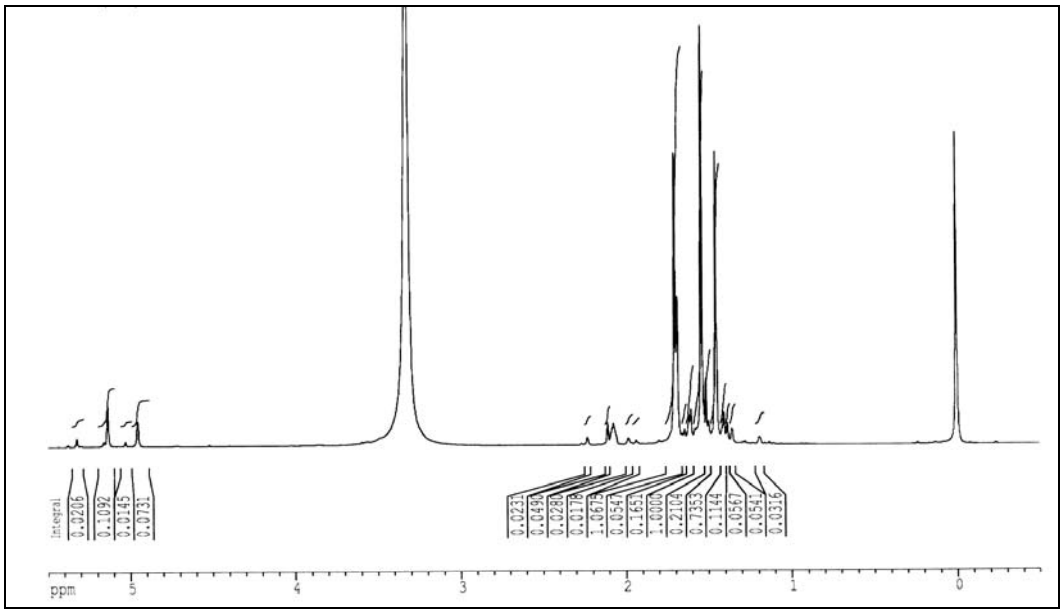

Figure 5.12 ^{1}H NMR spectrum (acetone-d_6+ H_2O) of the Et_2O extract, showing the signals due to the extracted contaminants.

Relating to Section 4.2.4.1.

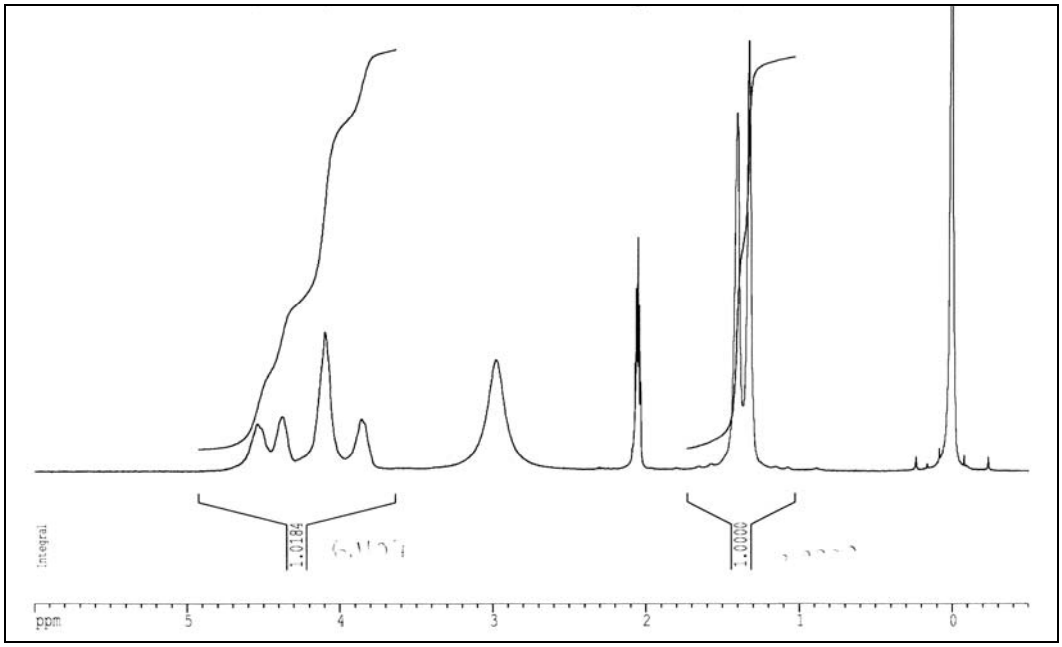

Figure 5.13 ^{1}H NMR spectrum (acetone-d_6 + H_2O) of random linear poly[P-(2',2'-dimethyl-1',3'-dioxolan-4'-yl)methoxy/P-2,2,2-trifluoroethoxy-phosphazene].

Relating to Section 4.2.4.2.

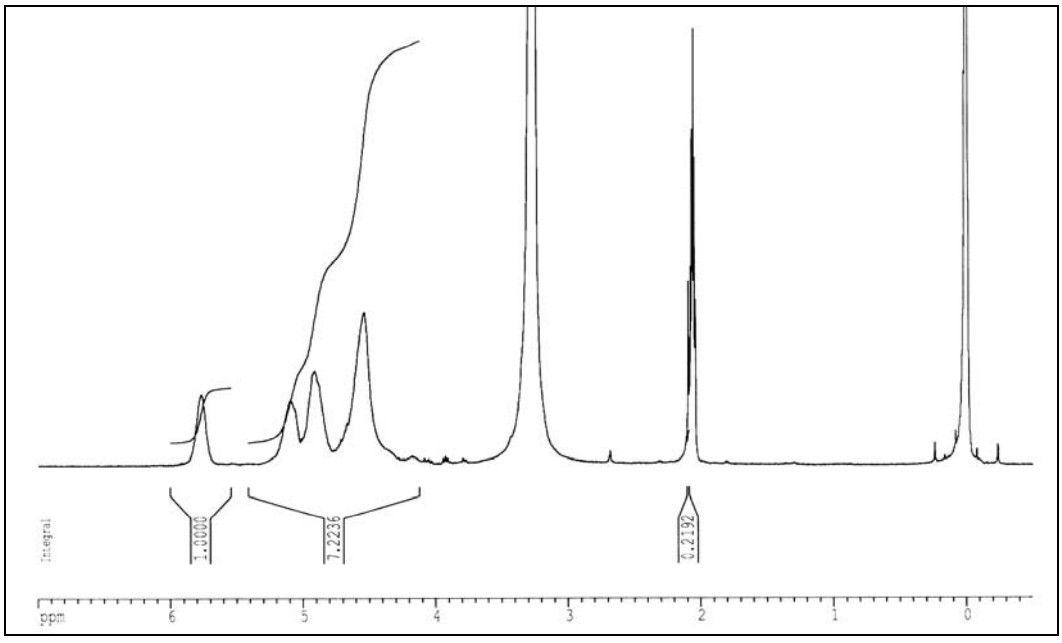

Figure 5.14 ^{1}H NMR spectrum (acetone-d_6 + H_2O) of random linear poly[P-2,3-dinitratopropoxy/P-2,2,2-trifluoroethoxyphosphazene].

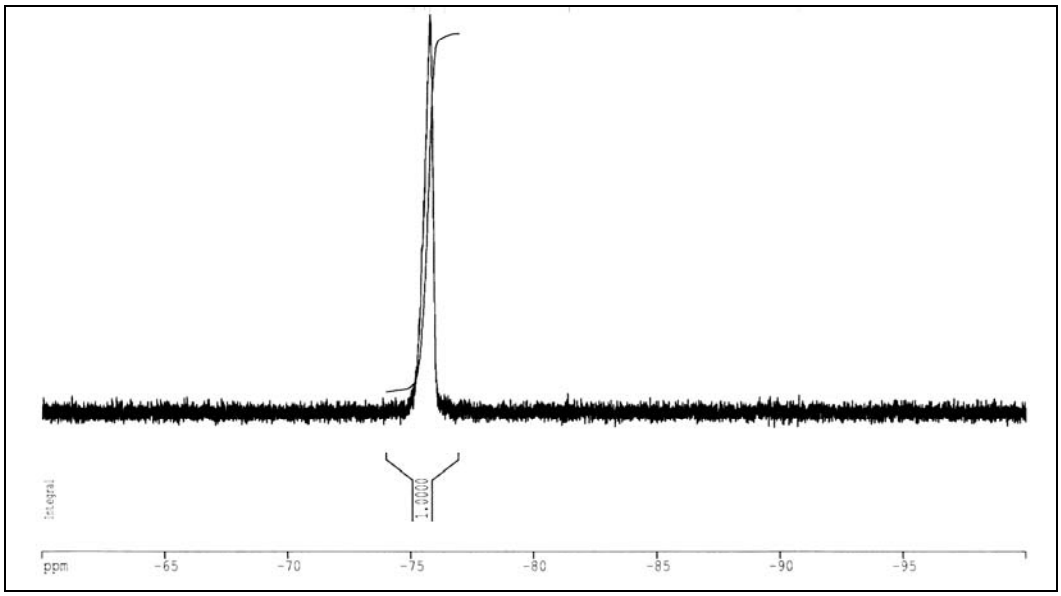

Figure 5.15 ^{19}F NMR spectrum (acetone-d_6) of random linear poly[P-2,3-dinitratopropoxy/P-2,2,2-trifluoroethoxyphosphazene].

Relating to Section 4.2.5.1.

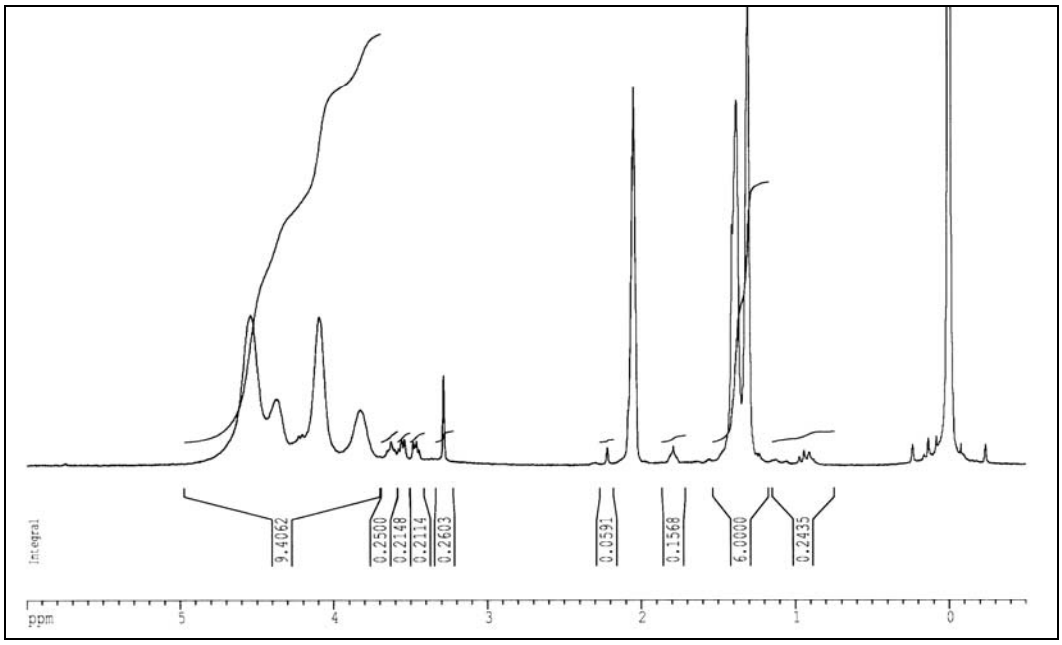

Figure 5.16 ^{1}H NMR spectrum (acetone-d_6) of less-substituted, random linear poly[P-(2',2'-dimethyl-1',3'-dioxolan-4'-yl)methoxy/P-2,2,2-trifluoroethoxy phosphazene].

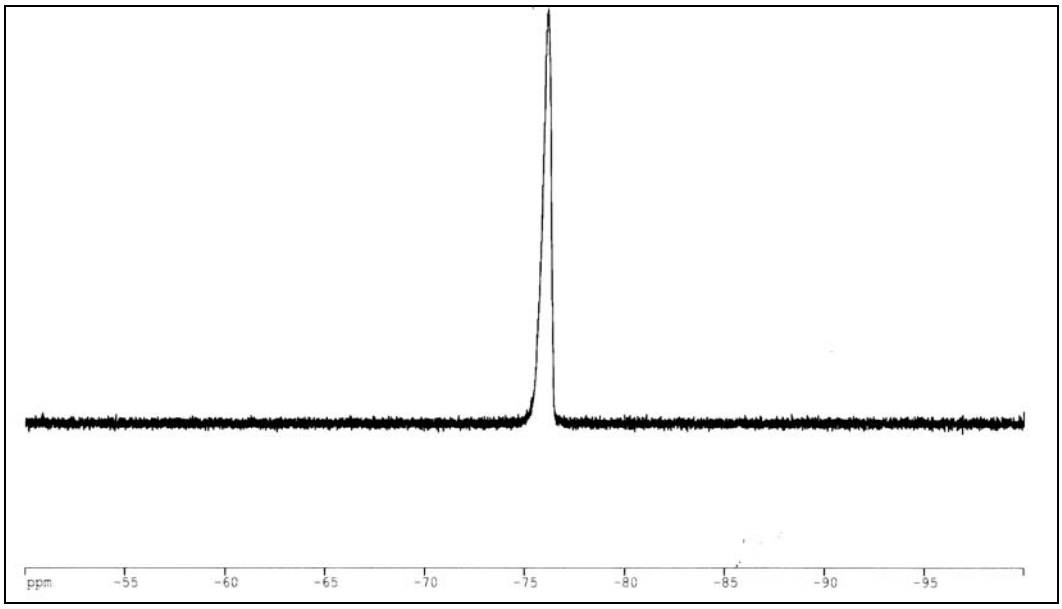

Figure 5.17 ^{19}F NMR spectrum (acetone-d_6) of less-substituted, random linear poly[P-(2',2'-dimethyl-1',3'-dioxolan-4'-yl)methoxy/P-2,2,2-trifluoroethoxy phosphazene].

Relating to Section 4.2.5.2.

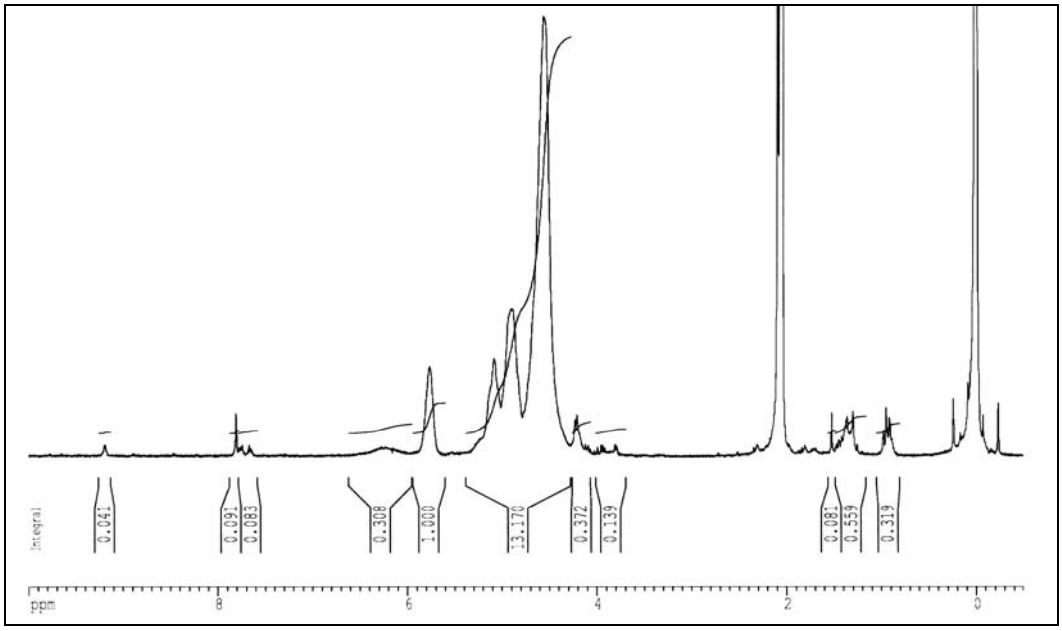

Figure 5.18 ^{1}H NMR spectrum (acetone-d_6) of less-substituted random linear poly[P-2,3-dinitratopropoxy/P-2,2,2-trifluoroethoxyphosphazene] before washing with Et_2O.

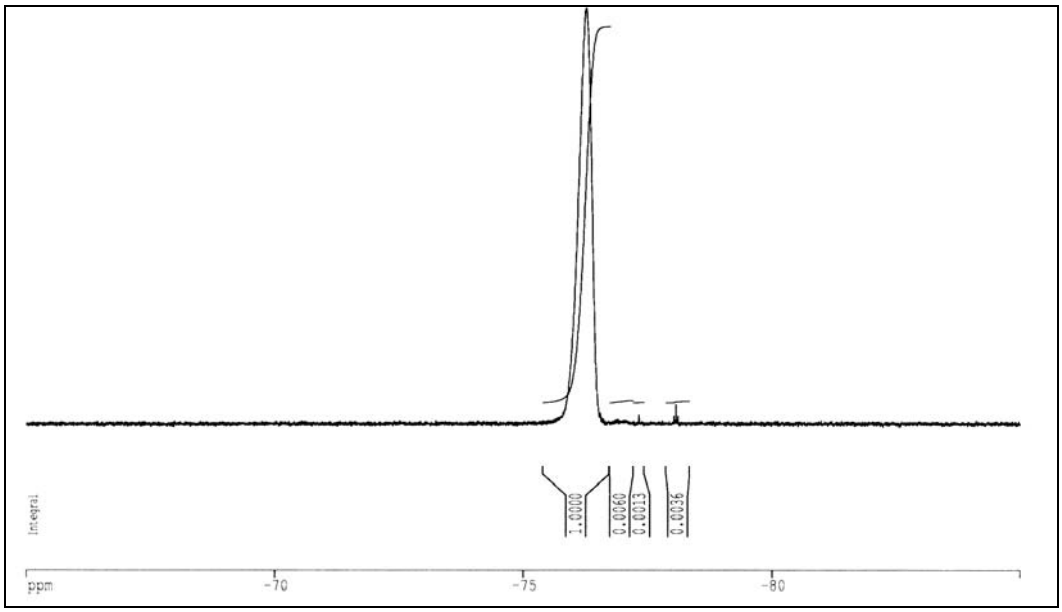

Figure 5.19 ^{19}F NMR spectrum (acetone-d_6) of less-substituted random linear poly[P-2,3-dinitratopropoxy/P-2,2,2-trifluoroethoxyphosphazene] before washing with Et_2O.

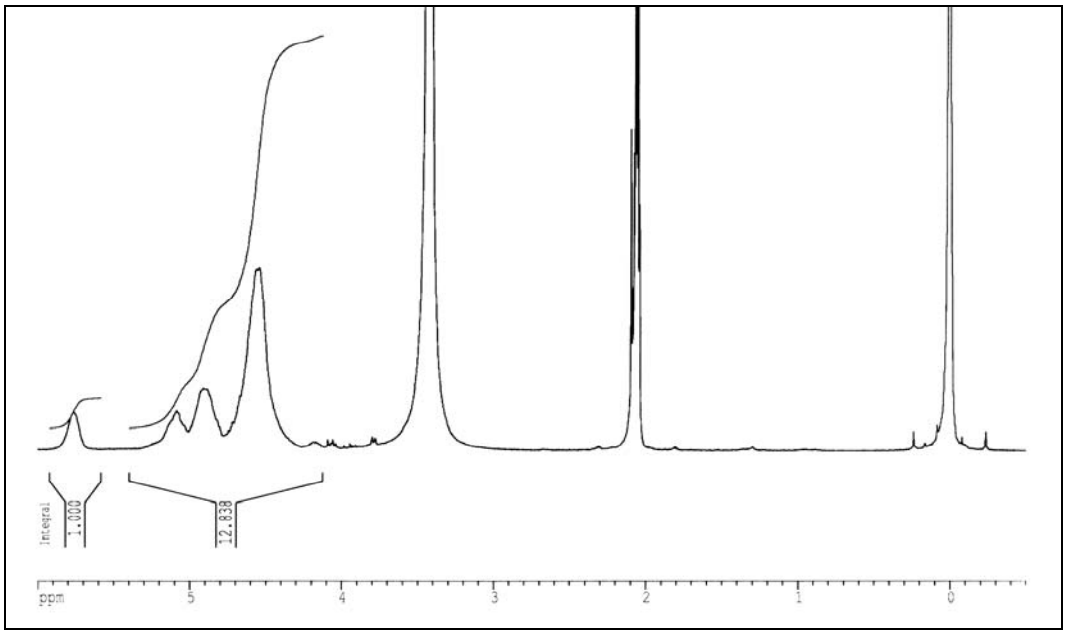

Figure 5.20 ^{1}H NMR spectrum (acetone-d_6 + H_2O) of less-substituted random linear poly[P-2,3-dinitratopropoxy/P-2,2,2-trifluoroethoxyphosphazene] after washing with Et_2O.

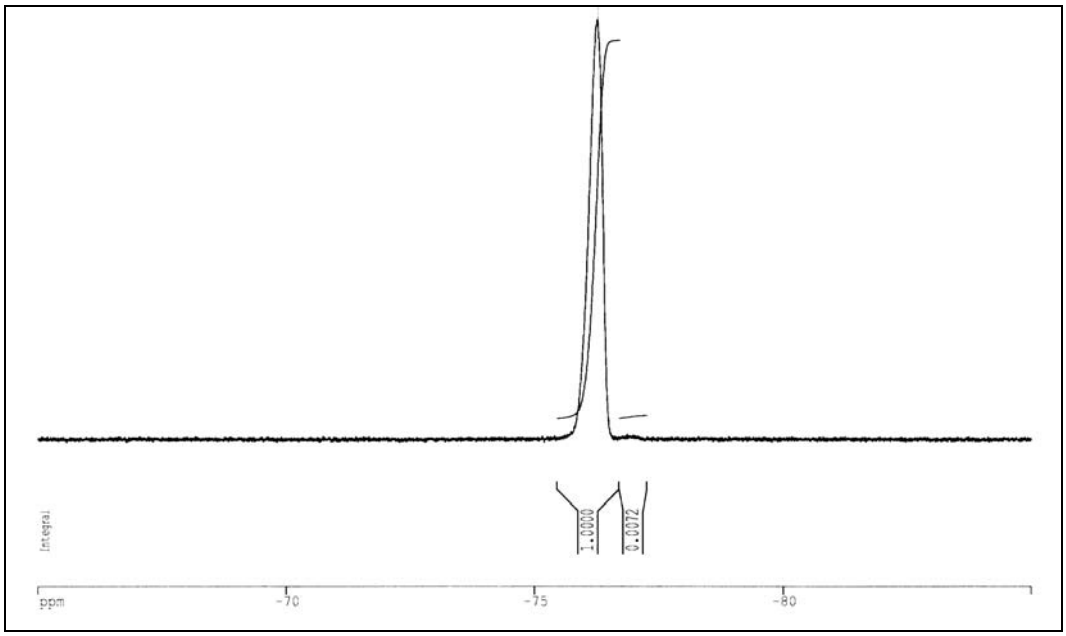

Figure 5.21 ^{19}F NMR spectrum (acetone-d_6) of less-substituted random linear poly[P-2,3-dinitratopropoxy/P-2,2,2-trifluoroethoxyphosphazene] after washing with Et_2O.

<u>Relating to Section 4.2.6.1.</u>

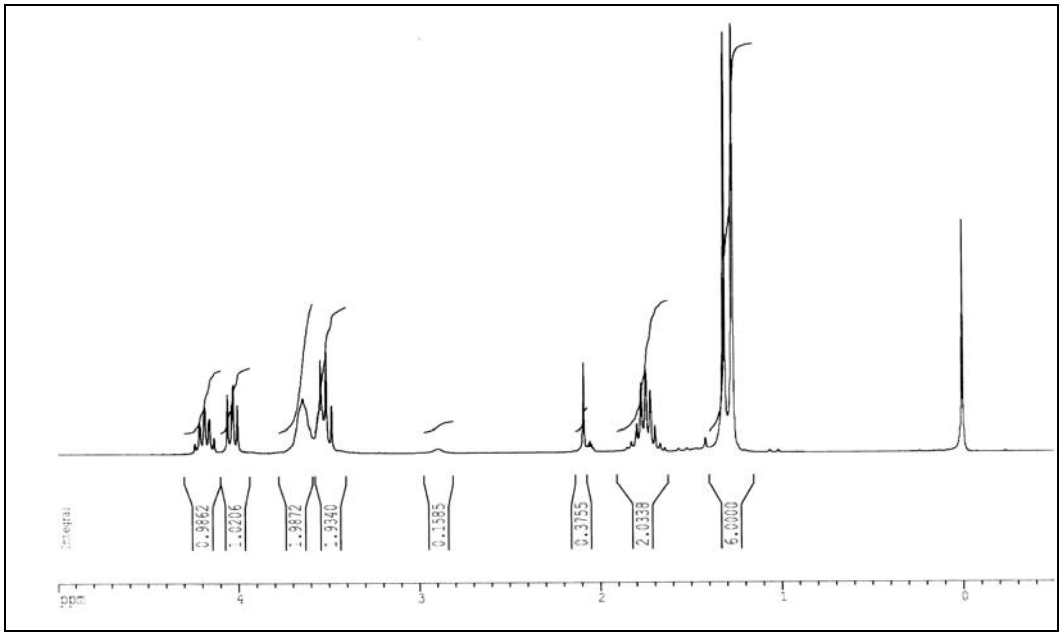

Figure 5.22 ^{1}H NMR spectrum (acetone-d_6) of 4-(2'-hydroxyethyl)-2,2-dimethyl-1,3-dioxolan.

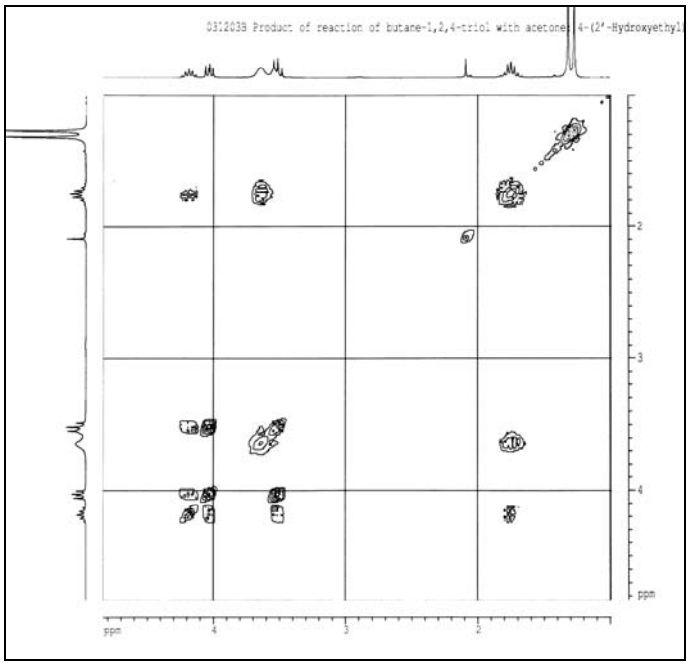

Figure 5.23 ^{1}H-^{1}H correlation spectrum (COSY45), (acetone-d_6) of 4-(2'-hydroxyethyl)-2,2-dimethyl-1,3-dioxolan.

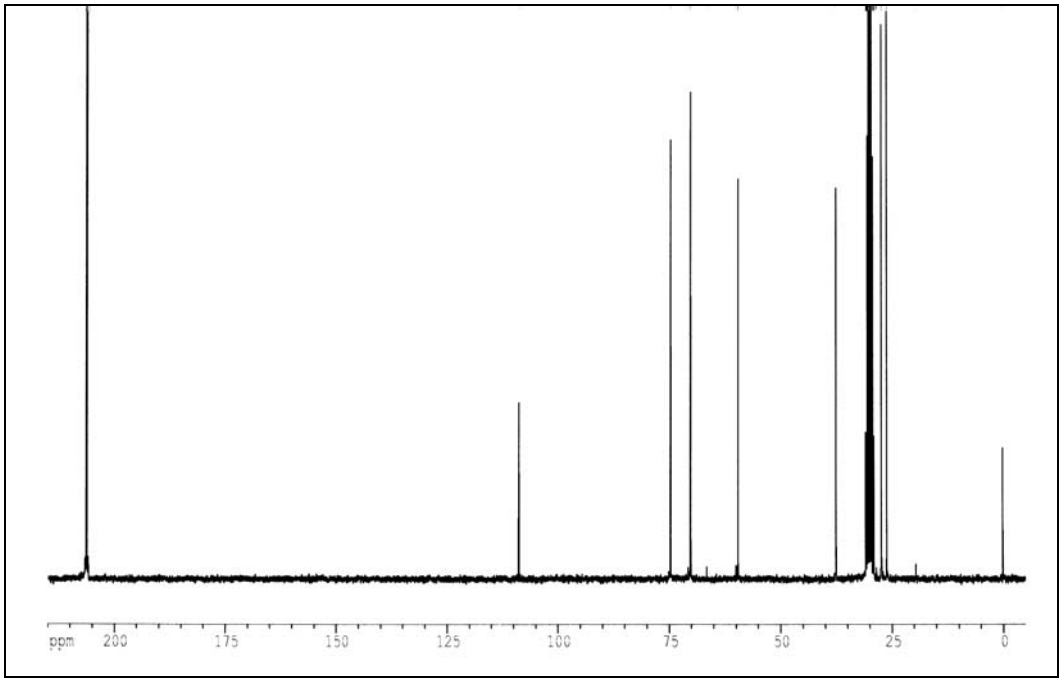

Figure 5.24 ^{13}C NMR spectrum (acetone-d_6) of 4-(2'-hydroxyethyl)-2,2-dimethyl-1,3-dioxolan.

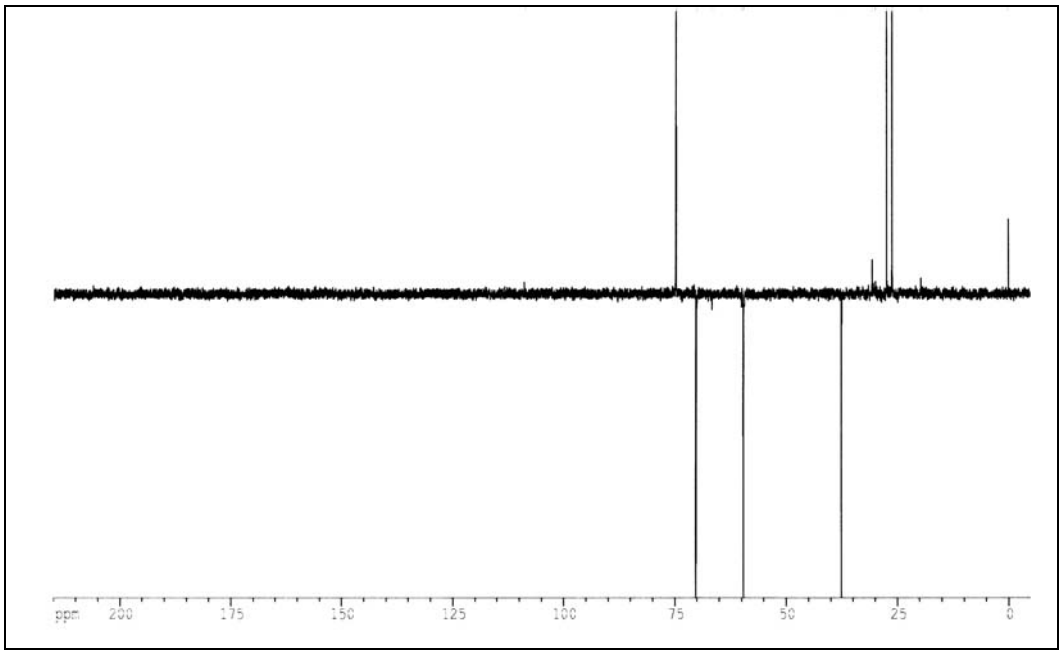

Figure 5.25 ^{13}C DEPT135 spectrum (acetone-d_6) of 4-(2'-hydroxyethyl)-2,2-dimethyl-1,3-dioxolan.

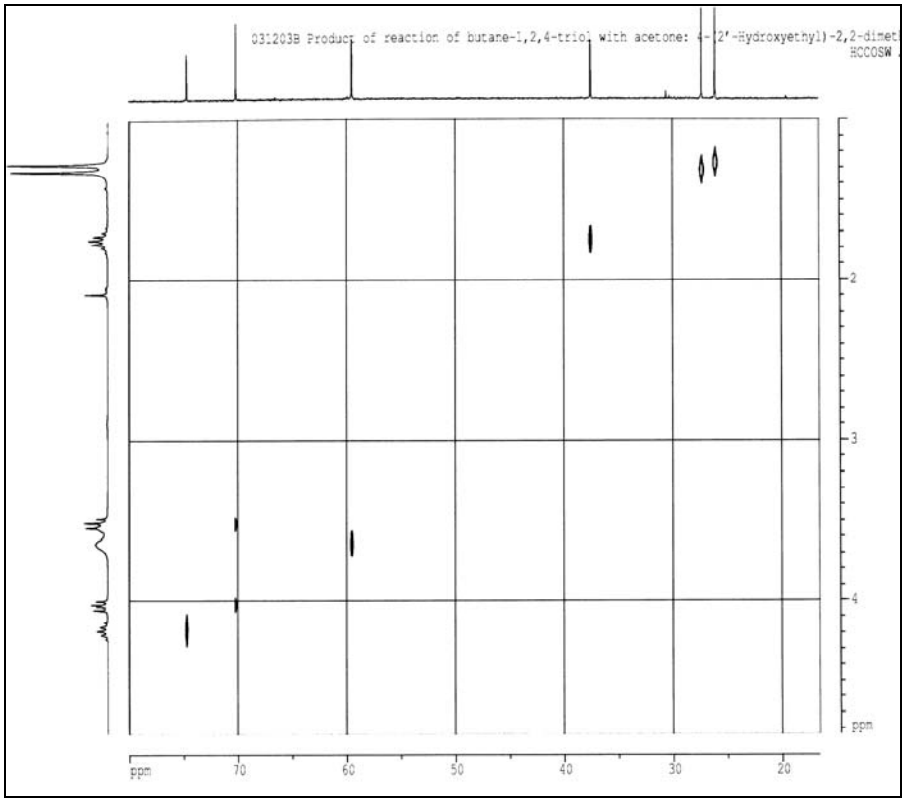

Figure 5.26 ^{1}H-^{13}C correlation spectrum (acetone-d_6) of 4-(2'-hydroxyethyl)-2,2-dimethyl-1,3-dioxolan.

Relating to Section 4.2.6.2.

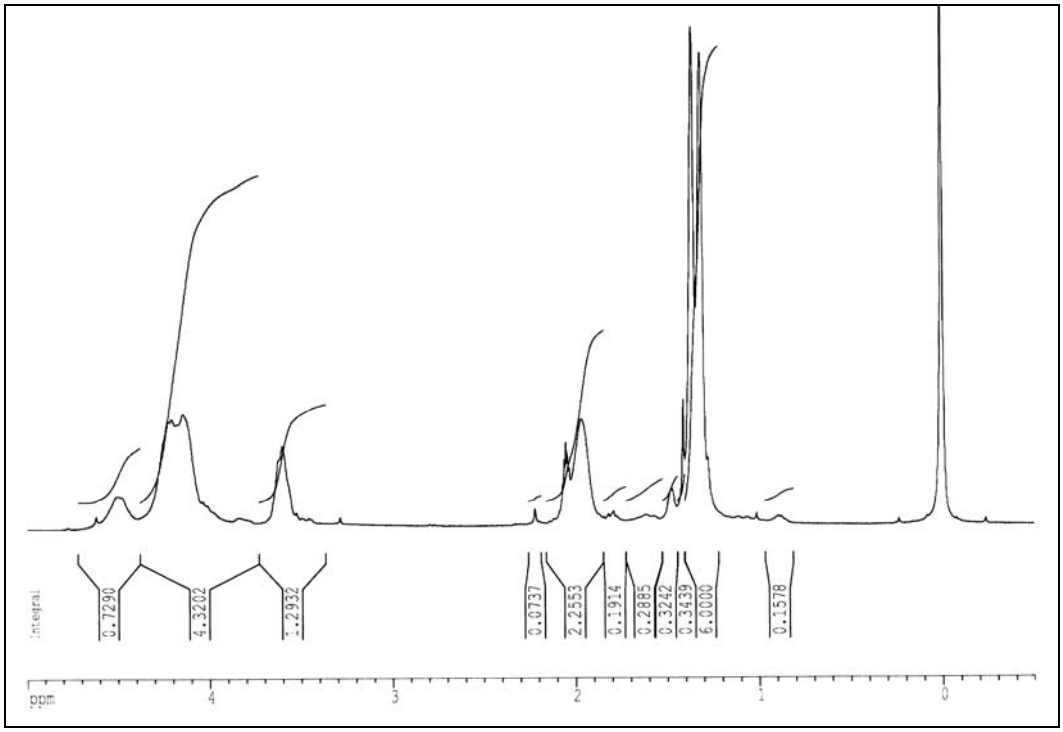

Figure 5.27 ^{1}H NMR spectrum (acetone-d_6) of random linear poly[P-2-(2',2'-dimethyl-1',3'-dioxolan-4'-yl)ethoxy/P-2,2,2-trifluoroethoxyphosphazene].

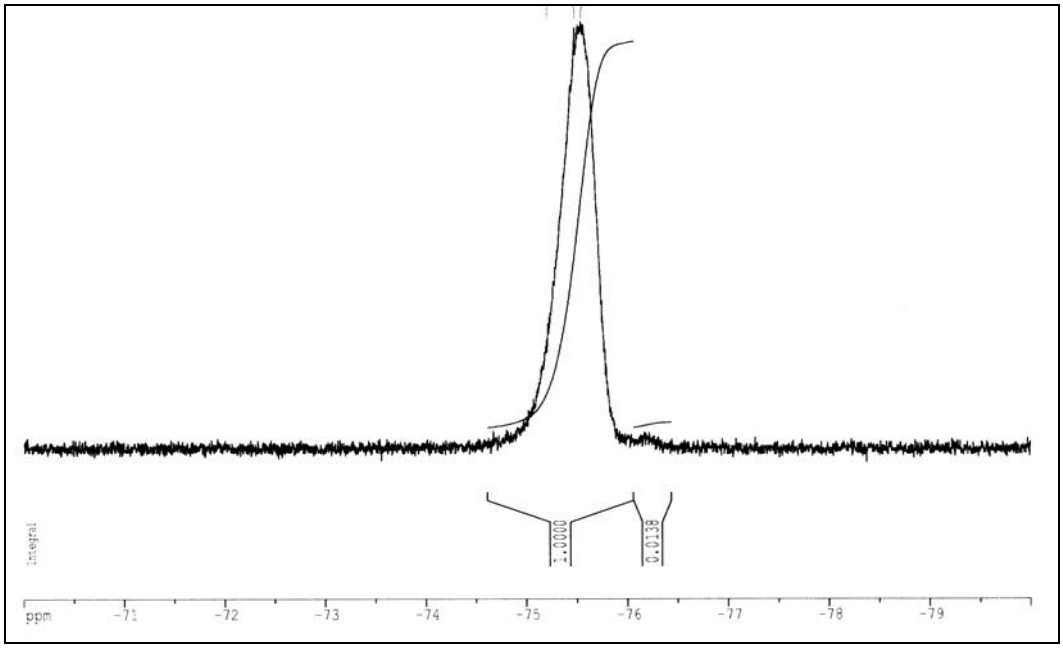

Figure 5.28 ^{19}F NMR spectrum (acetone-d_6) of random linear poly[P-2-(2',2'-dimethyl-1',3'-dioxolan-4'-yl)ethoxy/P-2,2,2-trifluoroethoxyphosphazene].

Relating to Section 4.2.6.3.

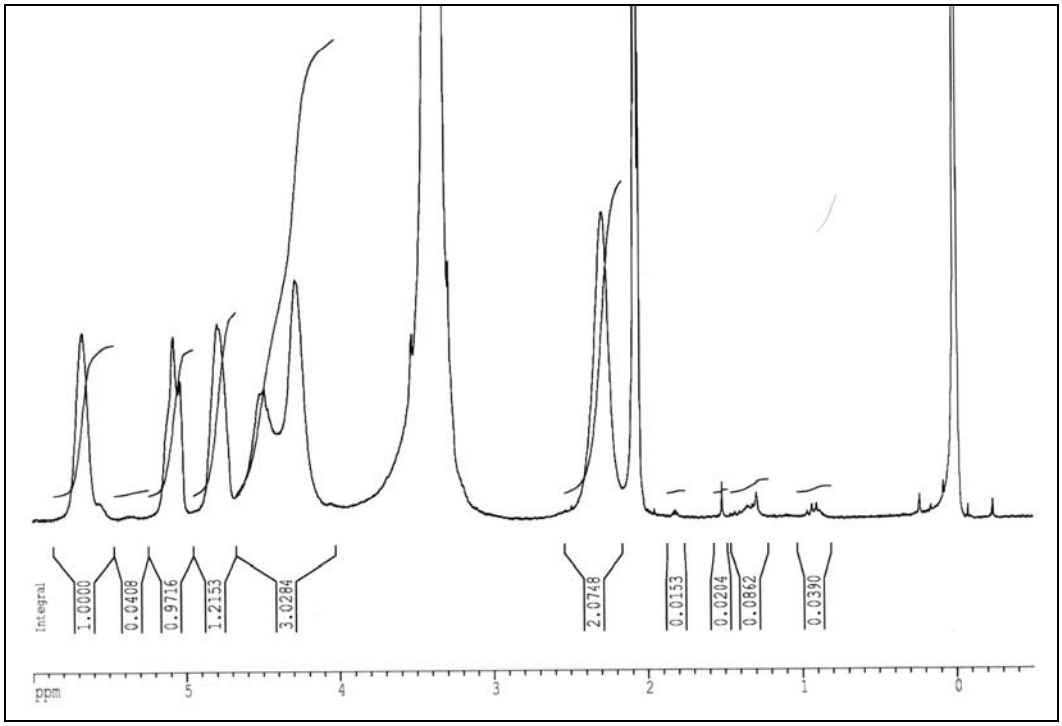

Figure 5.29 ^{1}H NMR spectrum (acetone-d_6 + H_2O) of random linear poly[P-3,4-dinitratobut-1-oxy/P-2,2,2-trifluoroethoxyphosphazene].

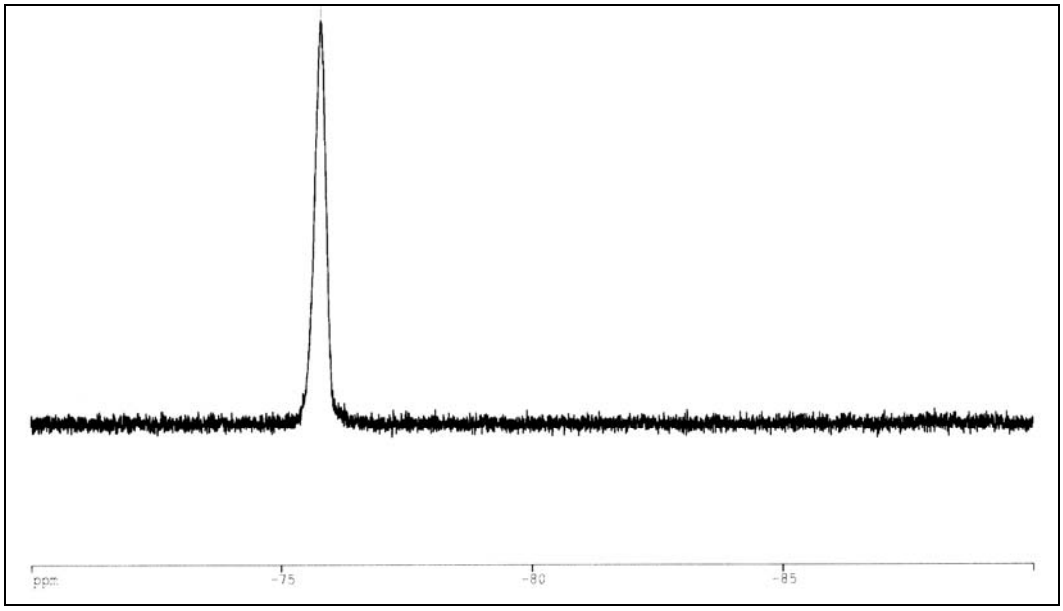

Figure 5.30 ^{19}F NMR spectrum (acetone-d_6) of random linear poly[P-3,4-dinitratobut-1-oxy/ P-2,2,2-trifluoroethoxyphosphazene].

Relating to Section 4.2.7.1.

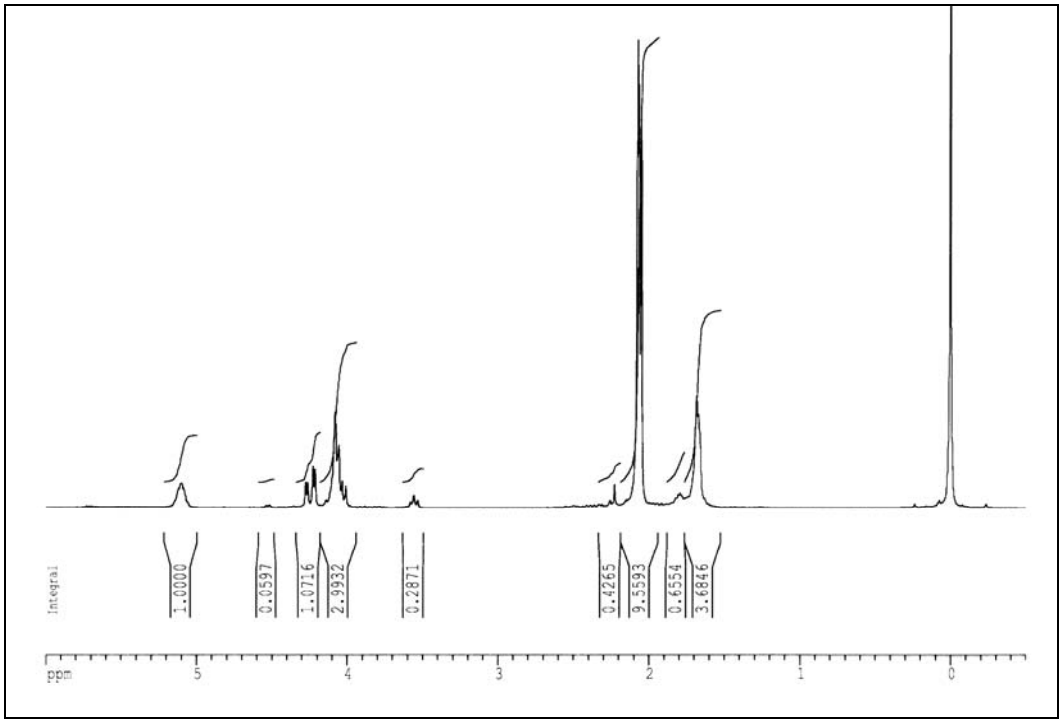

Figure 5.31 ^{1}H NMR spectrum ($CDCl_3$) of the main distillation fraction from the preparation of 1,2,5-triacetoxypentane (first attempted distillation).

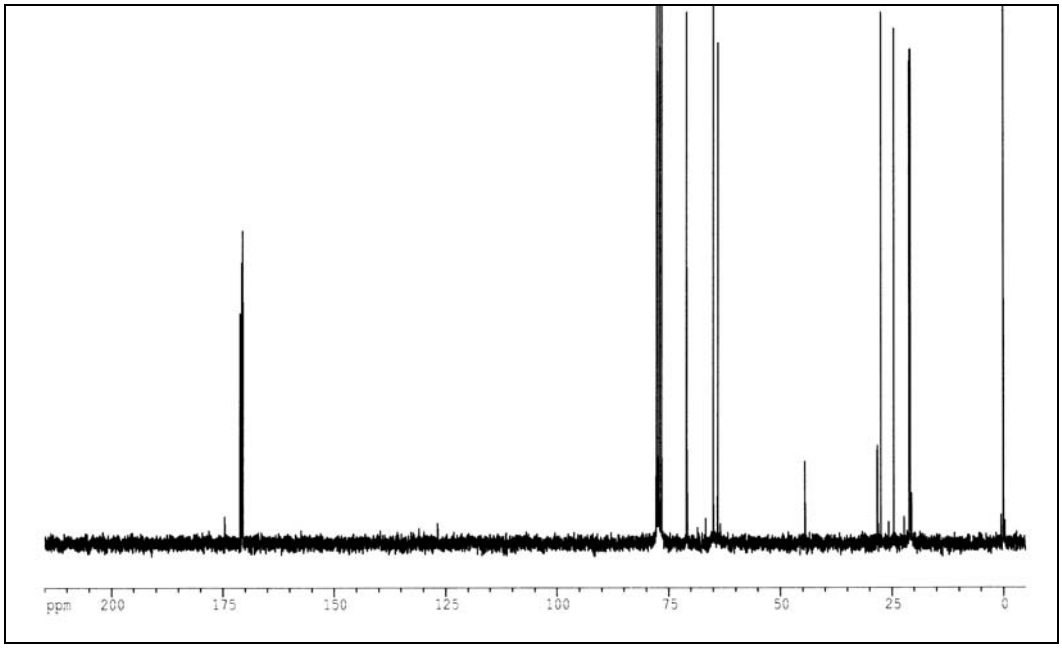

Figure 5.32 ^{13}C NMR spectrum ($CDCl_3$) of the main distillation fraction from the preparation of 1,2,5-triacetoxypentane (first attempted distillation).

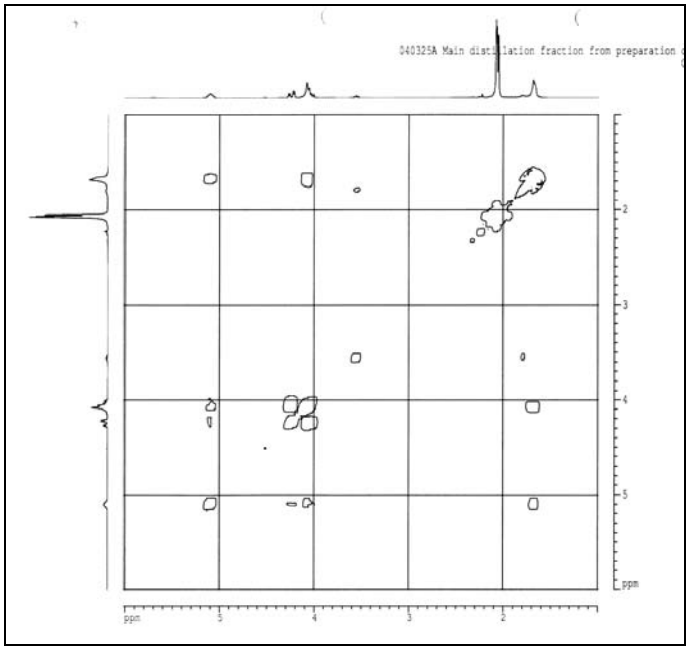

Figure 5.33 ^{1}H-^{1}H correlation (COSY 45) NMR spectrum ($CDCl_3$) of the main distillation fraction from the preparation of 1,2,5-triacetoxypentane (first attempted distillation).

<u>Relating to Section 4.2.7.2.</u>

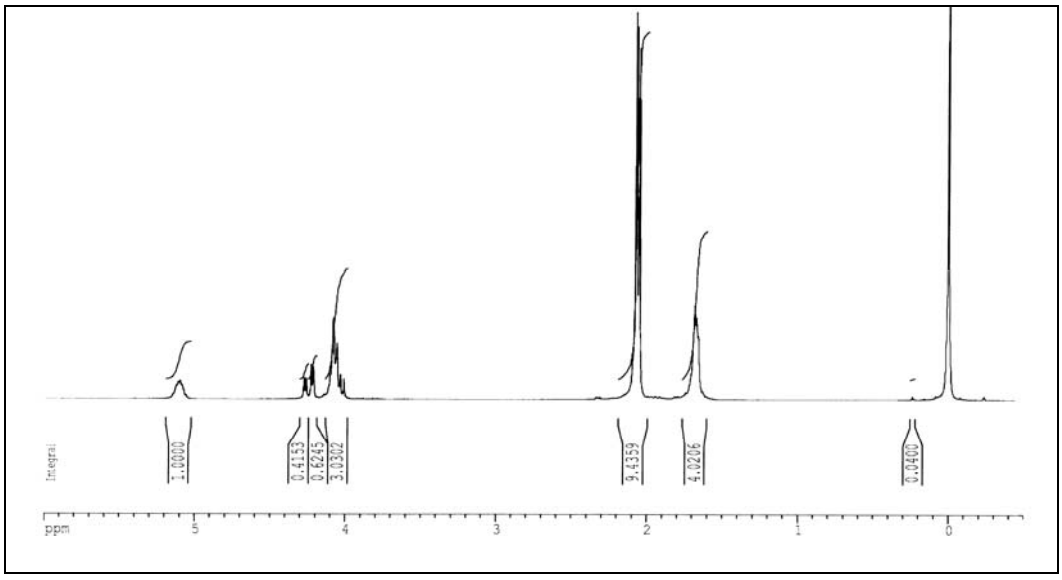

Figure 5.34 ^{1}H NMR spectrum ($CDCl_3$) of the main distillation fraction from preparation of 1,2,5-triacetoxypentane (second attempted distillation of residual dark residue, 6 months later).

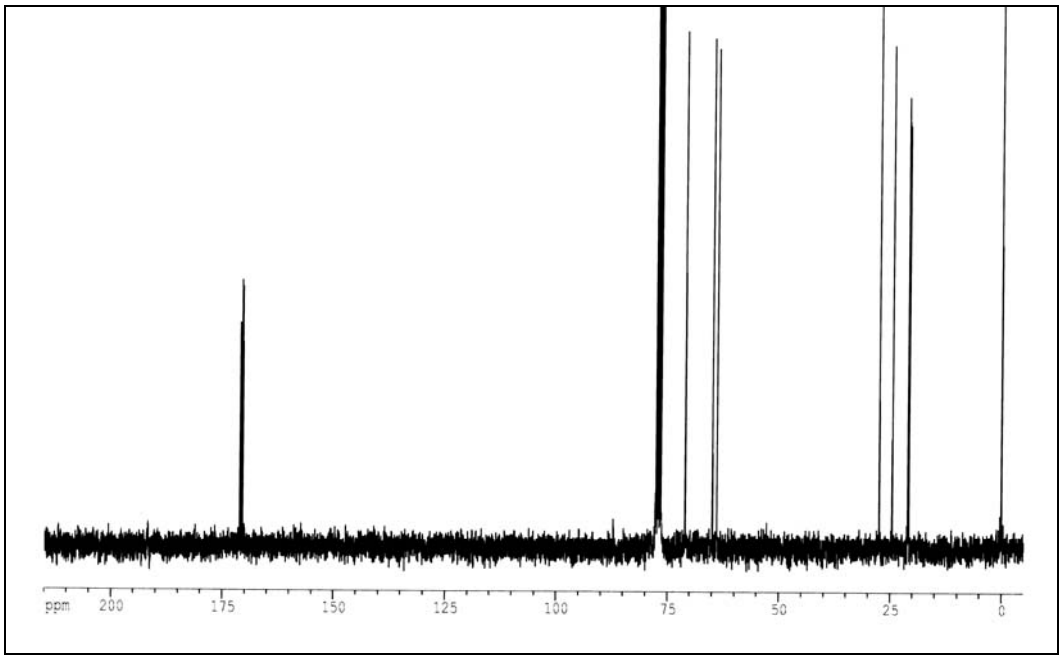

Figure 5.35 ^{13}C NMR spectrum ($CDCl_3$) of the main distillation fraction from preparation of 1,2,5-triacetoxypentane (second attempted distillation of residual dark residue, 6 months later).

Relating to Section 4.2.7.3.

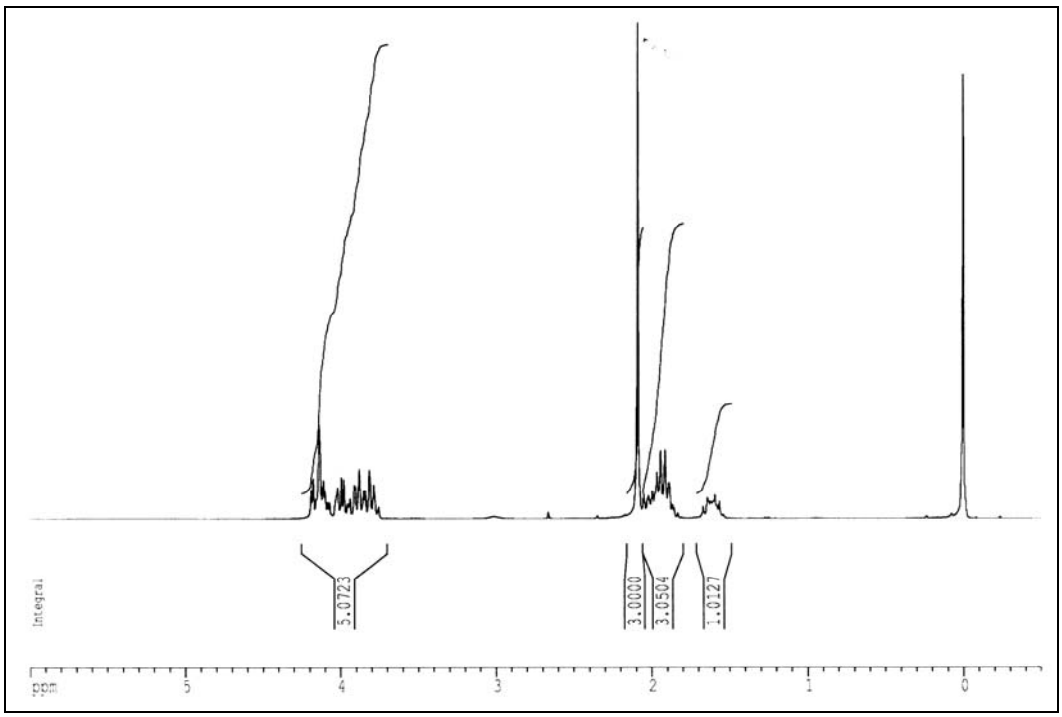

Figure 5.36 ^{1}H NMR spectrum ($CDCl_3$) of tetrahydrofurfuryl acetate.

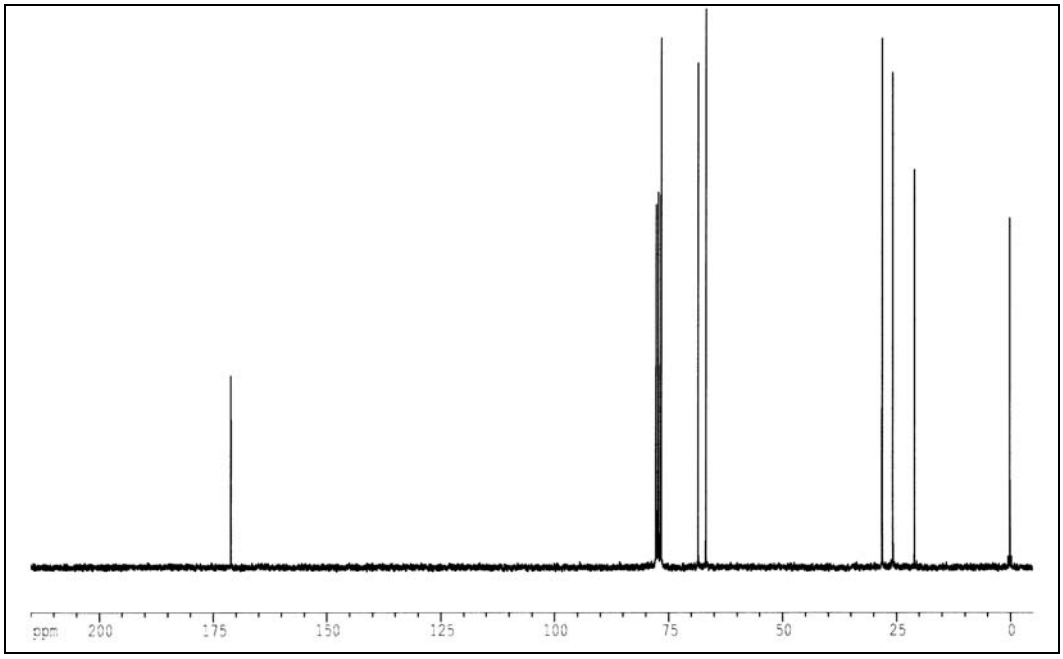

Figure 5.37 ^{13}C NMR spectrum ($CDCl_3$) of tetrahydrofurfuryl acetate.

Relating to Section 4.2.7.4.

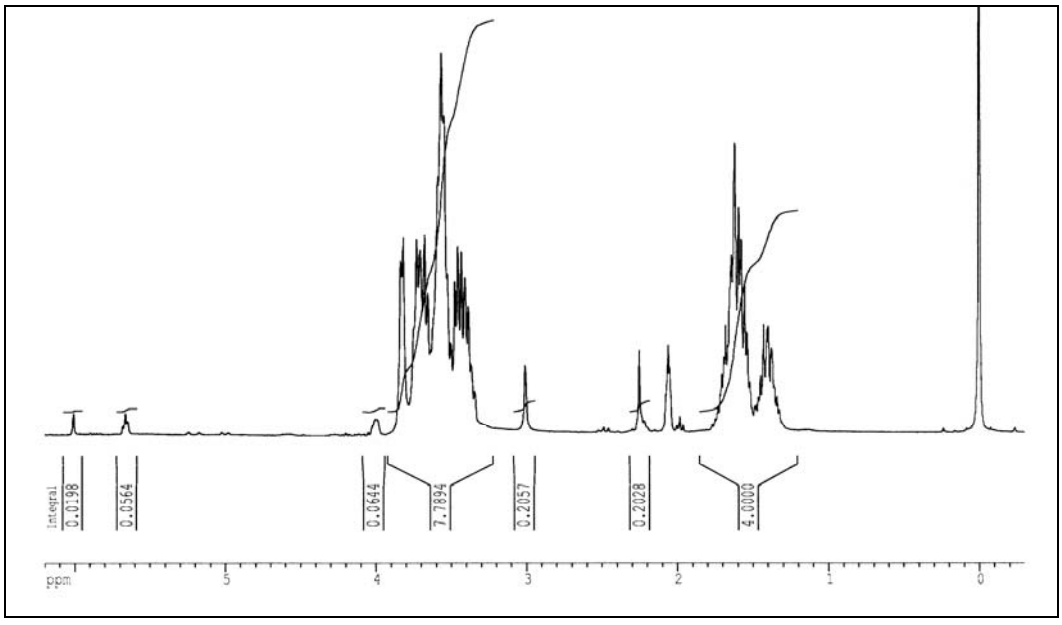

Figure 5.38 ^{1}H NMR spectrum (acetone-d_6) of pentane-1,2,5-triol (from first attempted distillation).

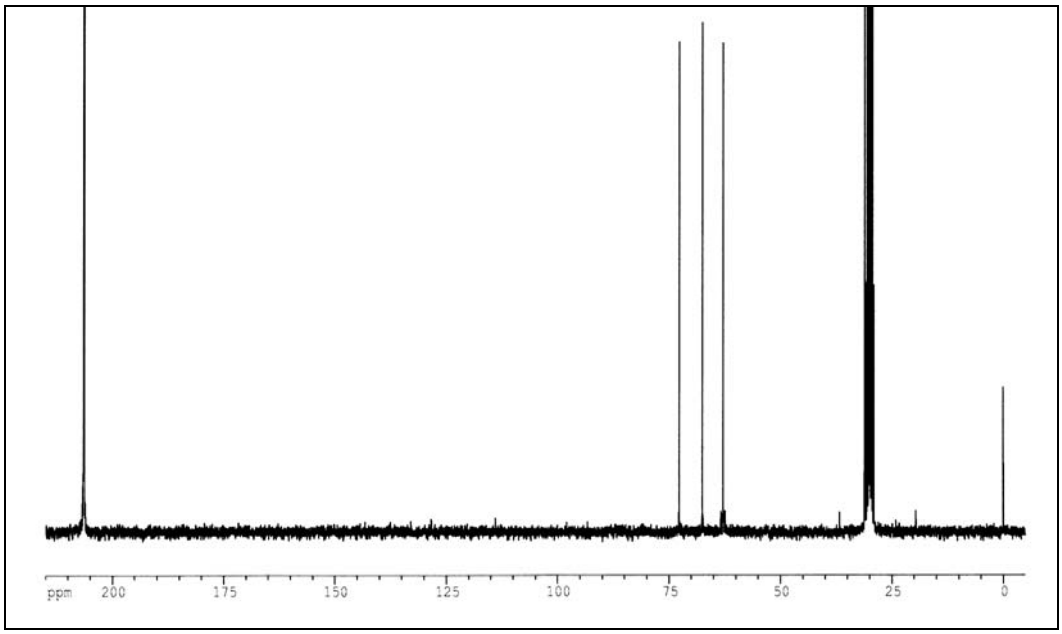

Figure 5.39 ^{13}C NMR spectrum (acetone-d$_6$) of the sample of pentane-1,2,5-triol (from first attempted distillation).

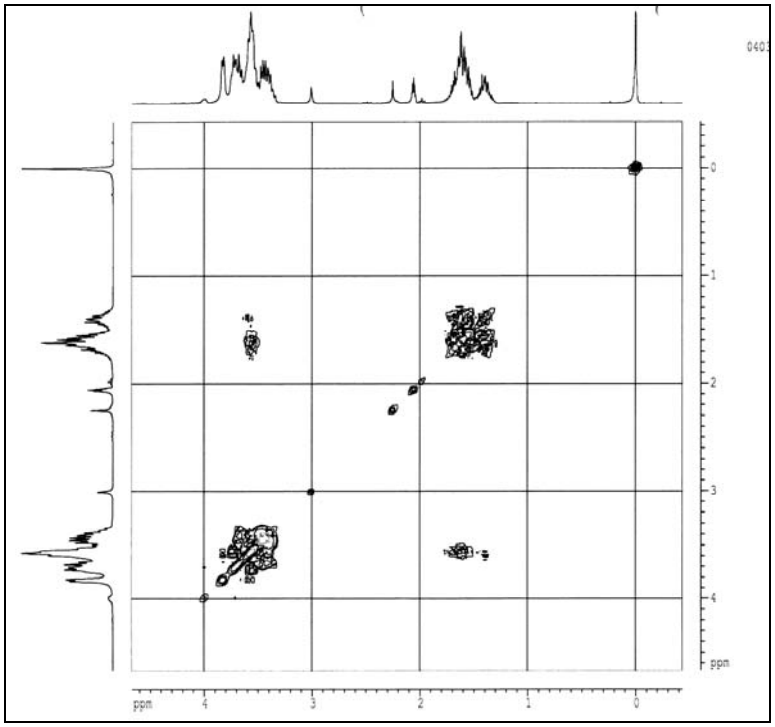

Figure 5.40 ^{1}H-^{1}H correlation (COSY45) NMR spectrum (acetone-d$_6$) of pentane-1,2,5-triol (from first attempted distillation).

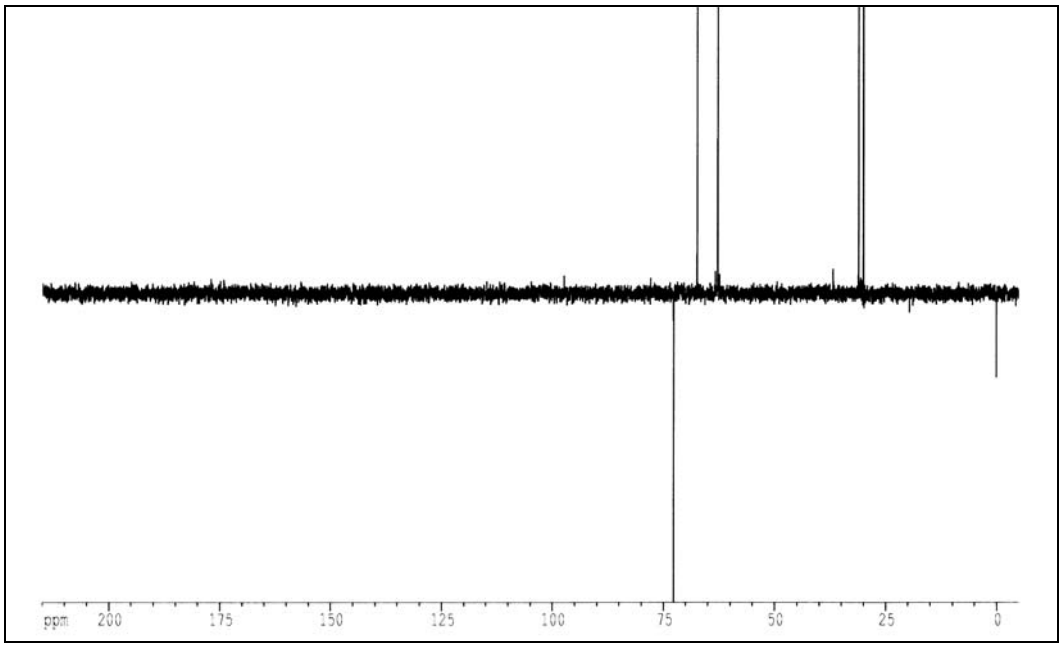

Figure 5.41 ^{13}C DEPT135 NMR spectrum (acetone-d_6) of pentane-1,2,5-triol (from first attempted distillation).

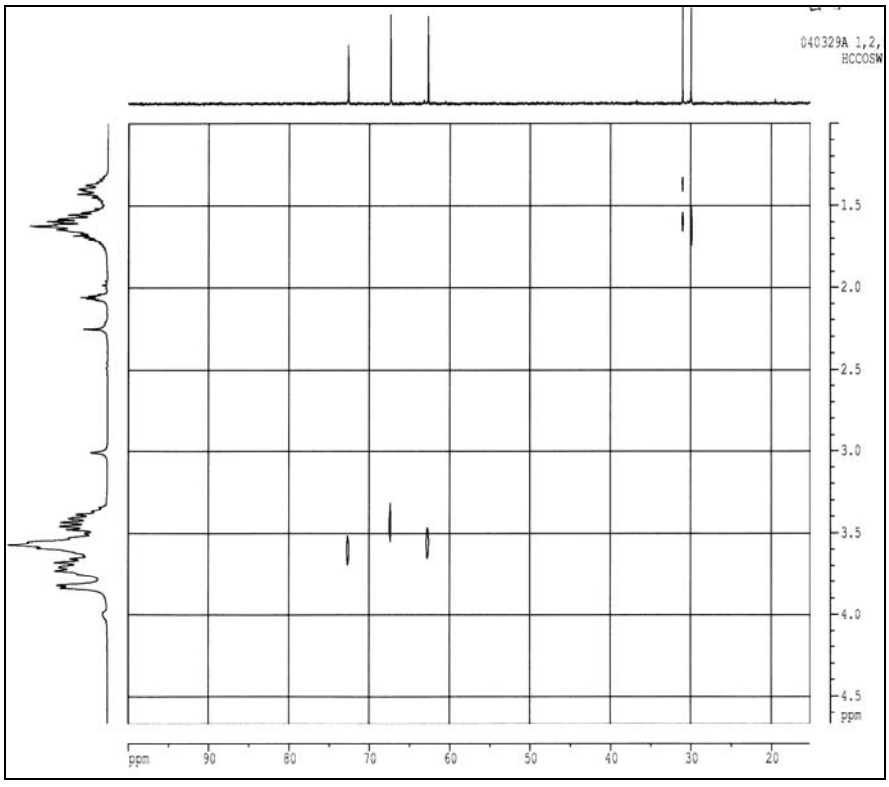

Figure 5.42 ^{1}H-^{13}C correlation NMR spectrum (acetone-d_6) of pentane-1,2,5-triol (from first attempted distillation).

Relating to Section 4.2.7.5.

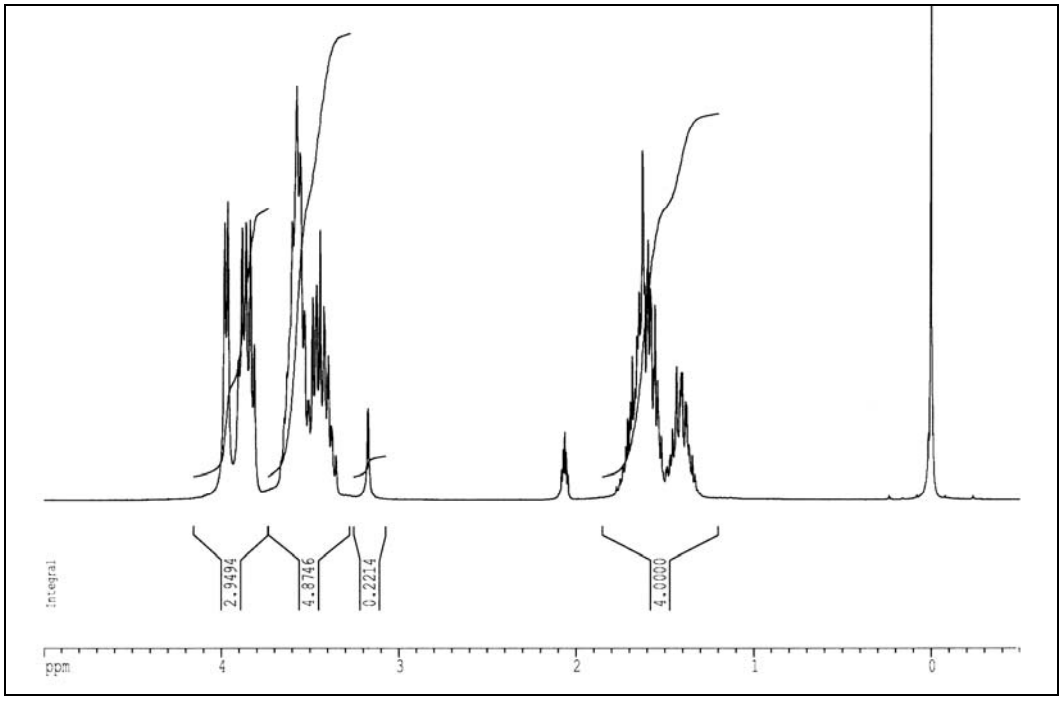

Figure 5.43 ^{1}H NMR spectrum (acetone-d_6) of pentane-1,2,5-triol (from second distillation, 6 months later).

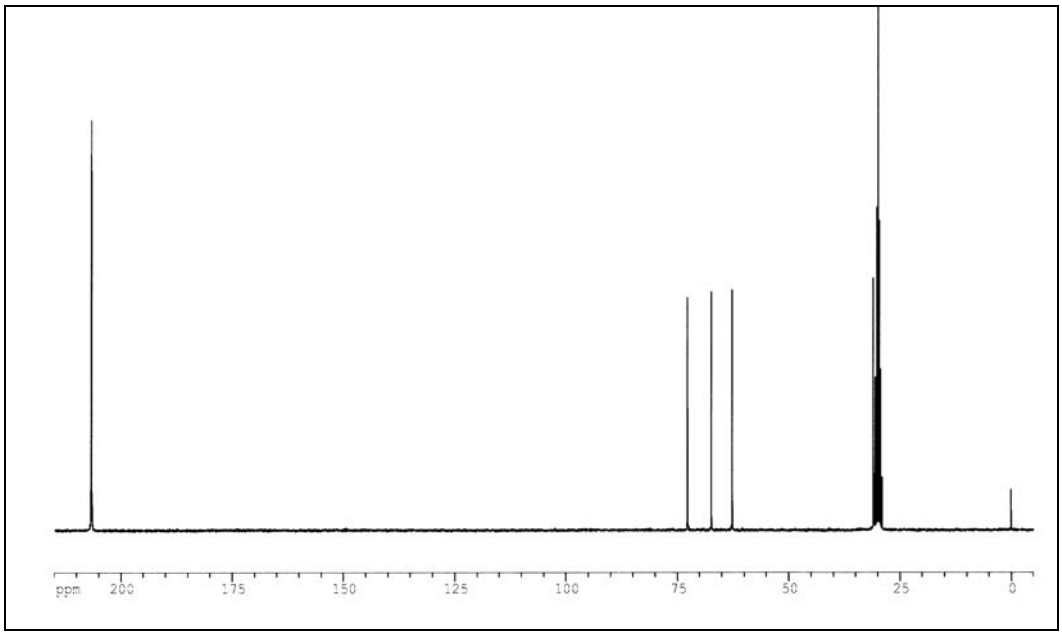

Figure 5.44 ^{13}C NMR spectrum (acetone-d_6) of pentane-1,2,5-triol (from second distillation, 6 months later).

Relating to Section 4.2.7.6.

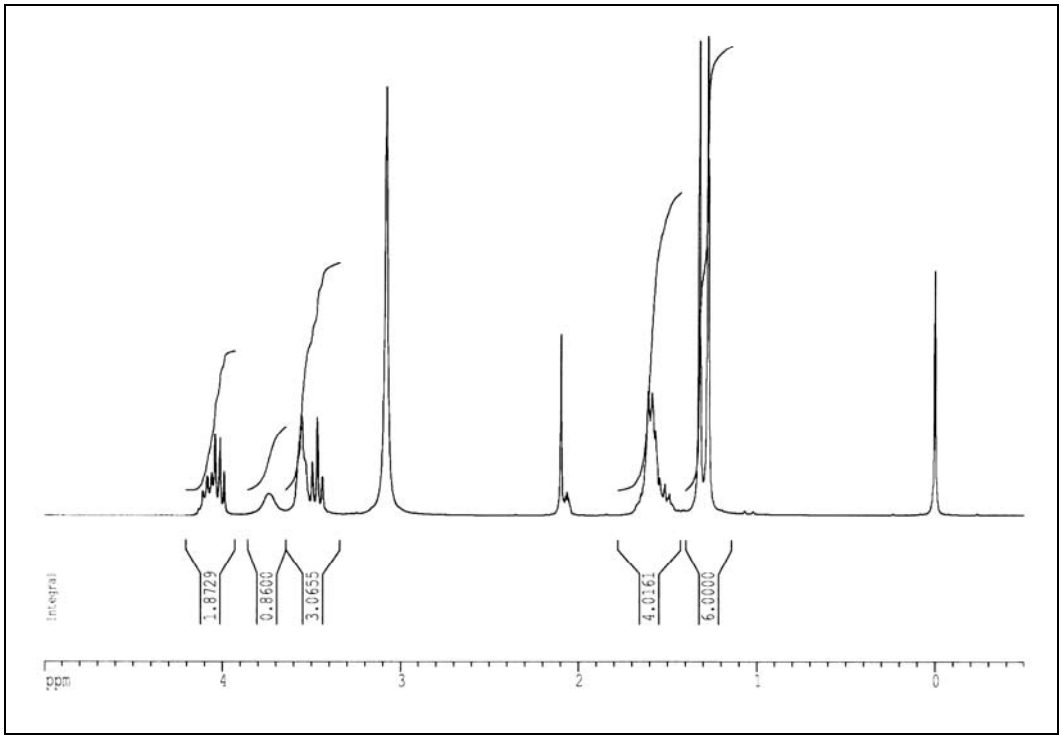

Figure 5.45 ^{1}H NMR spectrum (acetone-d_6 + H_2O) of the product of reaction between pentane-1,2,5-triol and excess acetone.

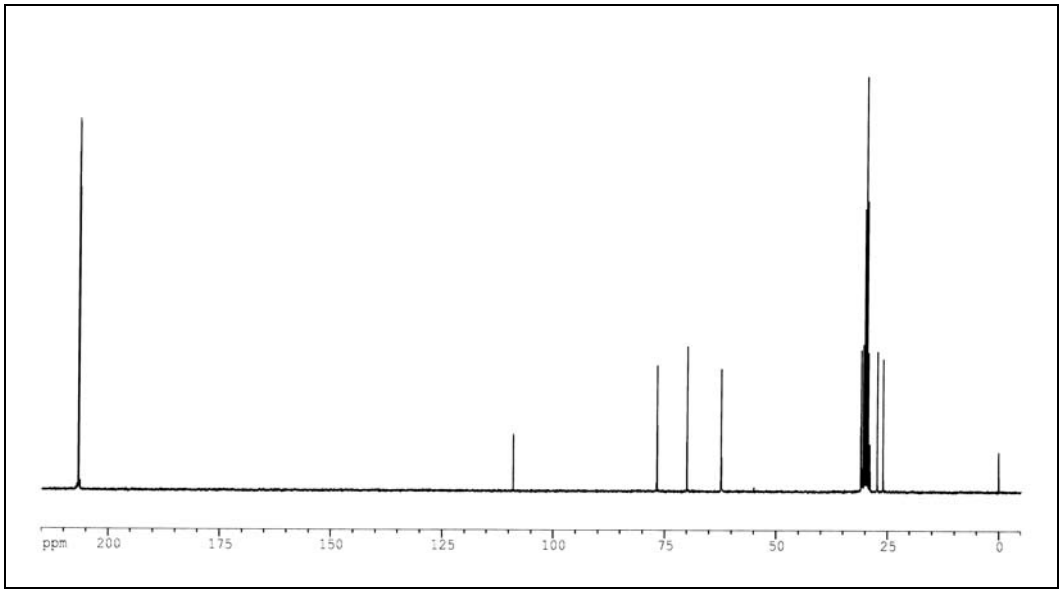

Figure 5.46 ^{13}C NMR spectrum (acetone-d_6) of the product of reaction between pentane-1,2,5-triol and excess acetone.

Relating to Section 4.2.7.7.

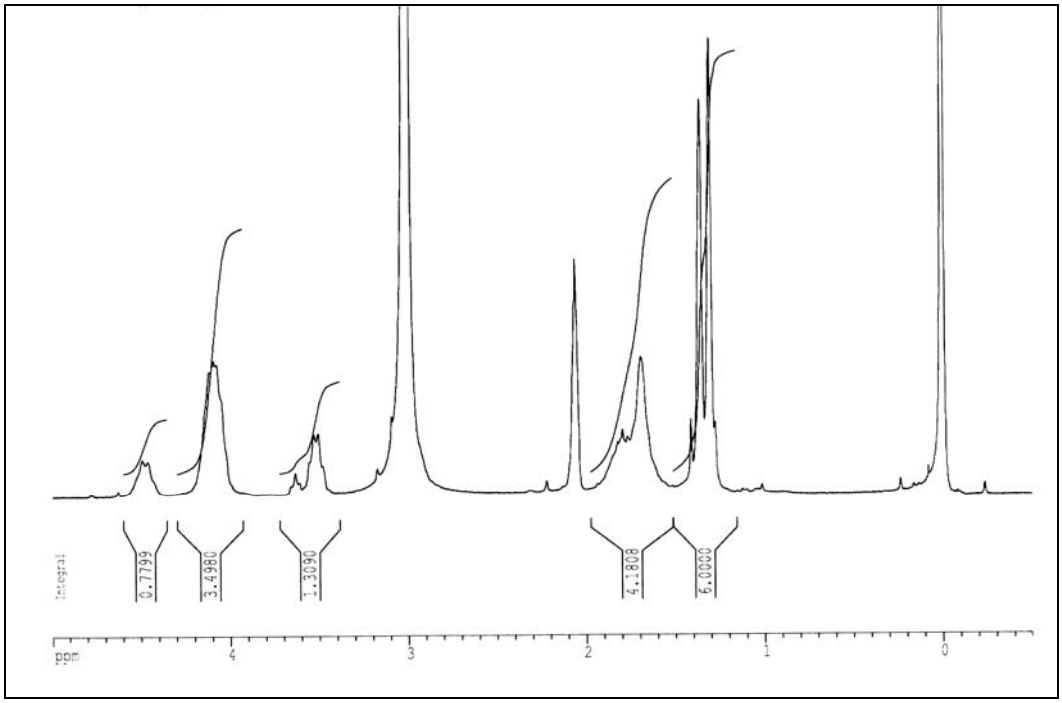

Figure 5.47 ^{1}H NMR spectrum (acetone-d_6 + H_2O) of random linear poly[P-3-(2',2'-dimethyl-1',3'-dioxolan-4'-yl)prop-1-oxy/P-2,2,2-trifluoroethoxy-phosphazene].

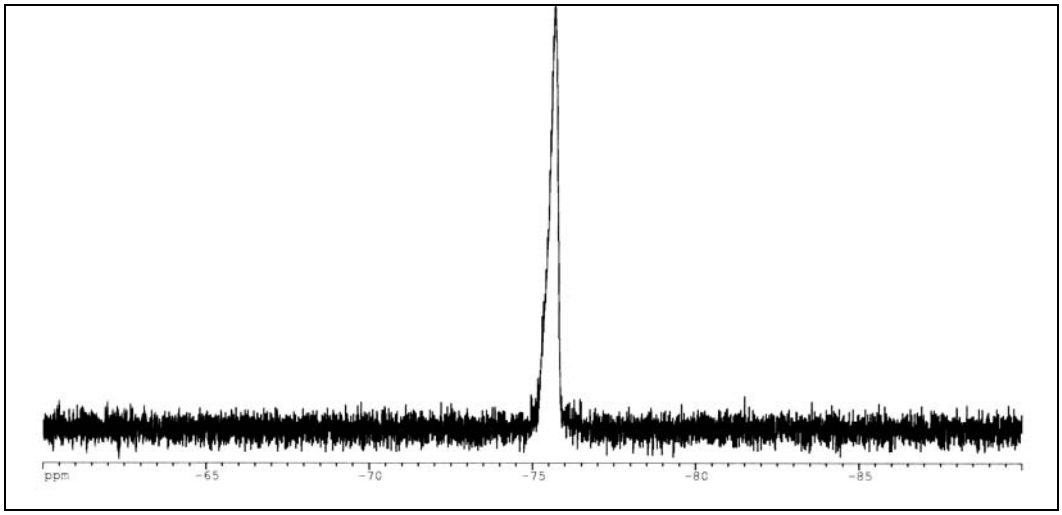

Figure 5.48 ^{19}F NMR spectrum (acetone-d_6) of random linear poly[P-3-(2',2'-dimethyl-1',3'-dioxolan-4'-yl)prop-1-oxy/P-2,2,2 trifluoroethoxy phosphazene].

Relating to Section 4.2.7.8.

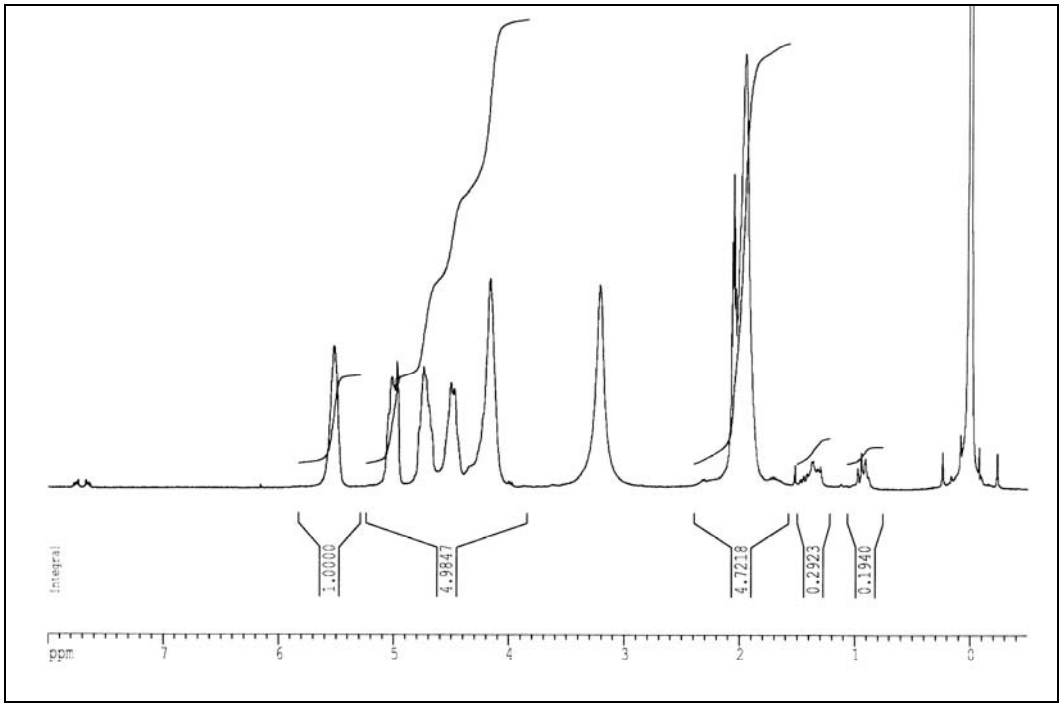

Figure 5.49 ^{1}H NMR spectrum (acetone-d_6 + H_2O) of random linear poly[P-4,5-dinitratopent-1-oxy/P-2,2,2-trifluoroethoxyphosphazene].

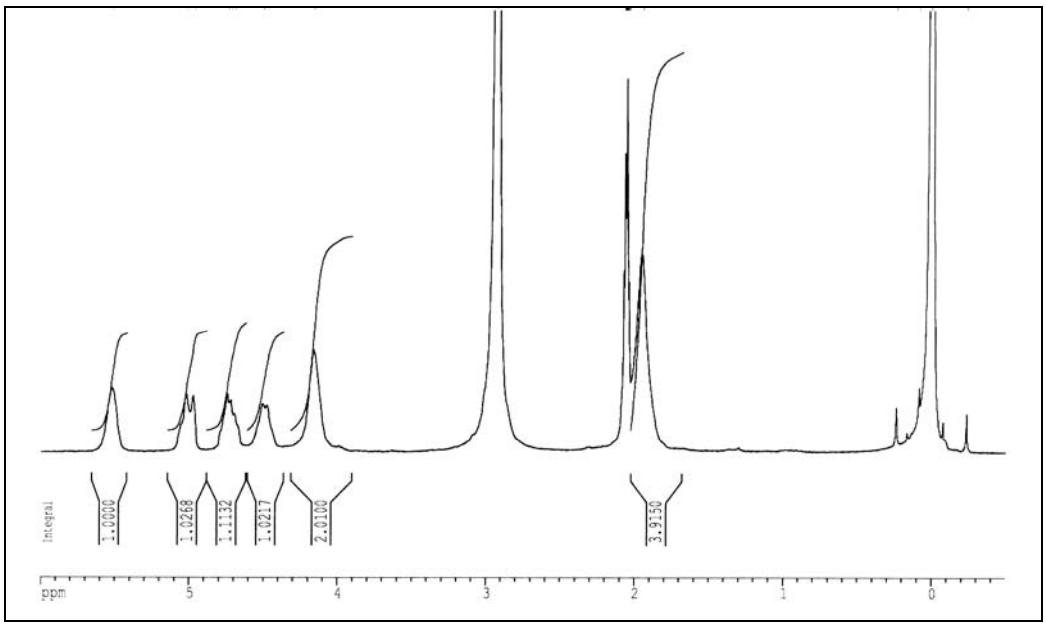

Figure 5.50 ^{1}H NMR spectrum (acetone-d_6 + H_2O) of random linear poly [P-4,5-dinitratopent-1-oxy/P-2,2,2-trifluoroethoxyphosphazene], after re-precipitation from acetone in *n*-hexane.

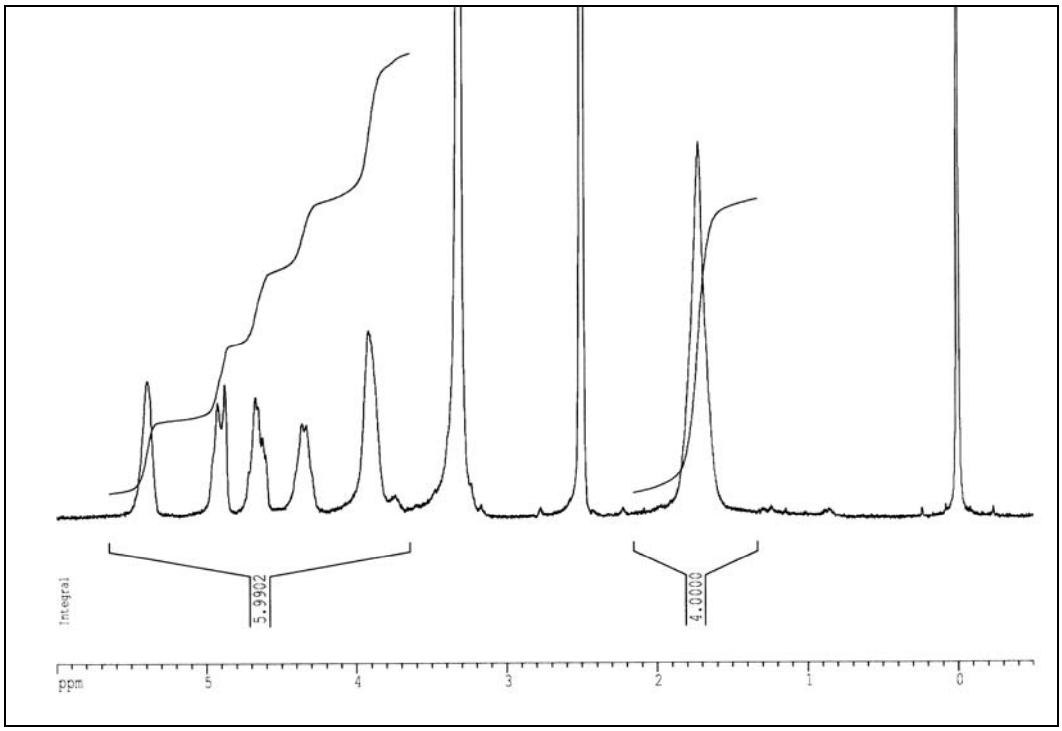

Figure 5.51 ^{1}H NMR spectrum (DMSO-d_6 + H_2O) of random linear poly[P-4,5-dinitratopent-1-oxy/P-2,2,2-trifluoroethoxyphosphazene], after re-precipitation from acetone in *n*-hexane.

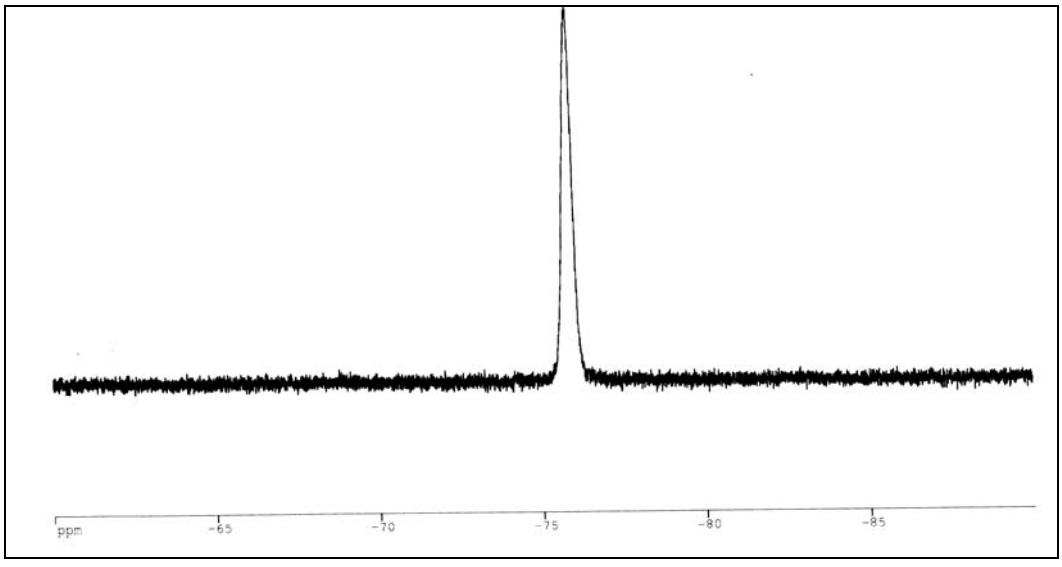

Figure 5.52 ^{19}F NMR spectrum (acetone-d_6) of random linear poly[P-4,5-dinitratopent-1-oxy/P-2,2,2-trifluoroethoxyphosphazene], after re-precipitation from acetone in *n*-hexane.

Relating to Section 4.2.8.1.

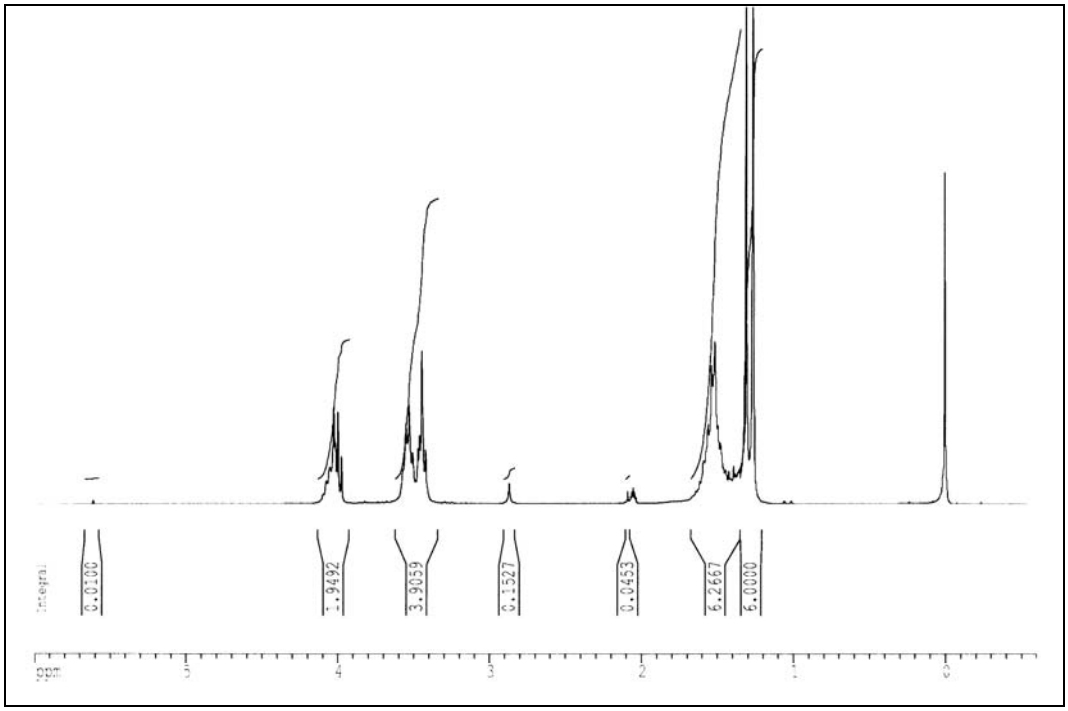

Figure 5.53 ^{1}H NMR spectrum (acetone-d_6) of 4-(4'-hydroxybutyl)-2,2-dimethyl-1,3-dioxolan.

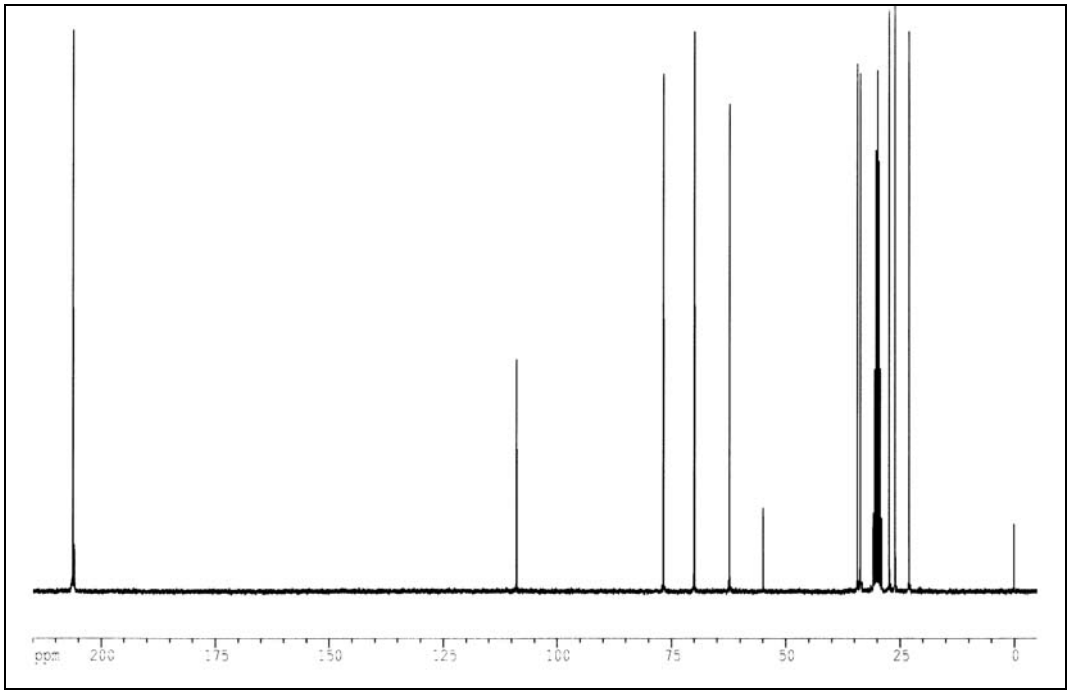

Figure 5.54 ^{13}C NMR spectrum (acetone-d_6) of 4-(4'-hydroxybutyl)-2,2-dimethyl-1,3-dioxolan.

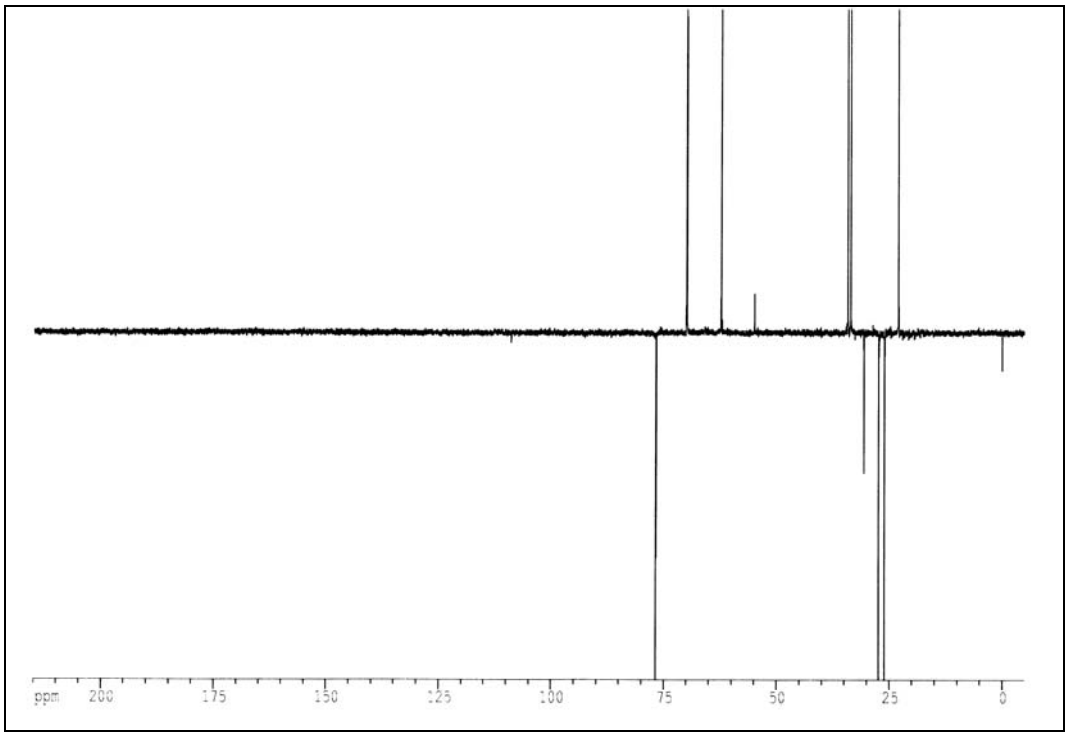

Figure 5.55 ^{13}C DEPT135 NMR spectrum (acetone-d_6) of 4-(4'-hydroxybutyl) -2,2-dimethyl-1,3-dioxolan.

Relating to Section 4.2.8.2.

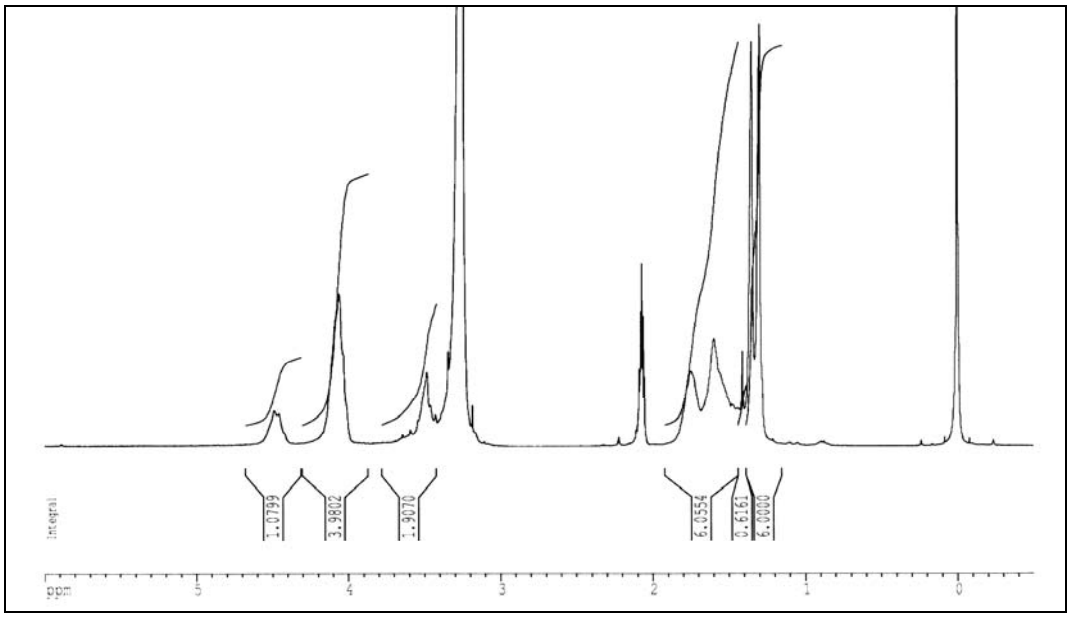

Figure 5.56 ^{1}H NMR spectrum (acetone-d_6 + H_2O) of random linear poly[P-4-(2',2'-dimethyl-1',3'-dioxolan- 4'-yl)butoxy/P-2,2,2-trifluoroethoxy phosphazene].

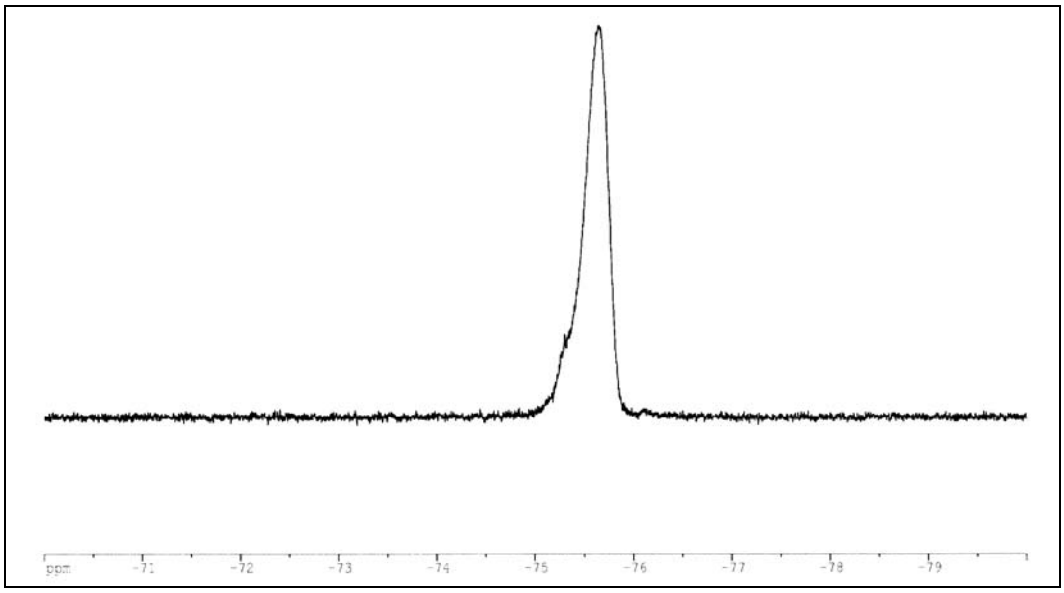

Figure 5.57 ^{19}F NMR spectrum (acetone-d_6) of random linear poly[P-4-(2',2'-dimethyl-1',3'-dioxolan- 4'-yl)butoxy/P-2,2,2-trifluoroethoxyphosphazene].

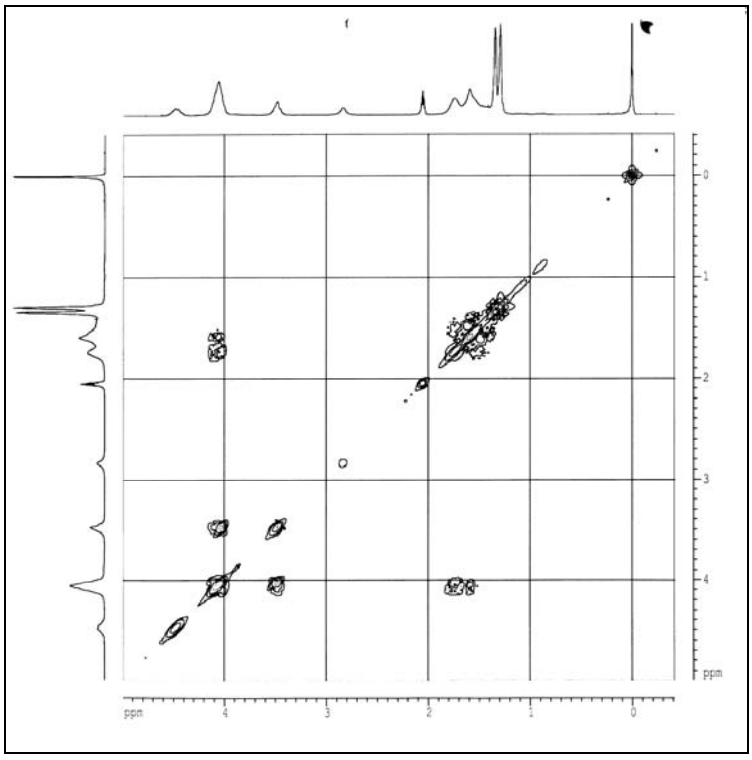

Figure 5.58 ^{1}H-^{1}H correlation (COSY45) NMR spectrum (acetone-d_6) of random linear poly[P-4-(2',2'-dimethyl-1',3'-dioxolan-4'-yl)butoxy/P-2,2,2-trifluoroethoxyphosphazene].

Relating to Section 4.2.8.3.

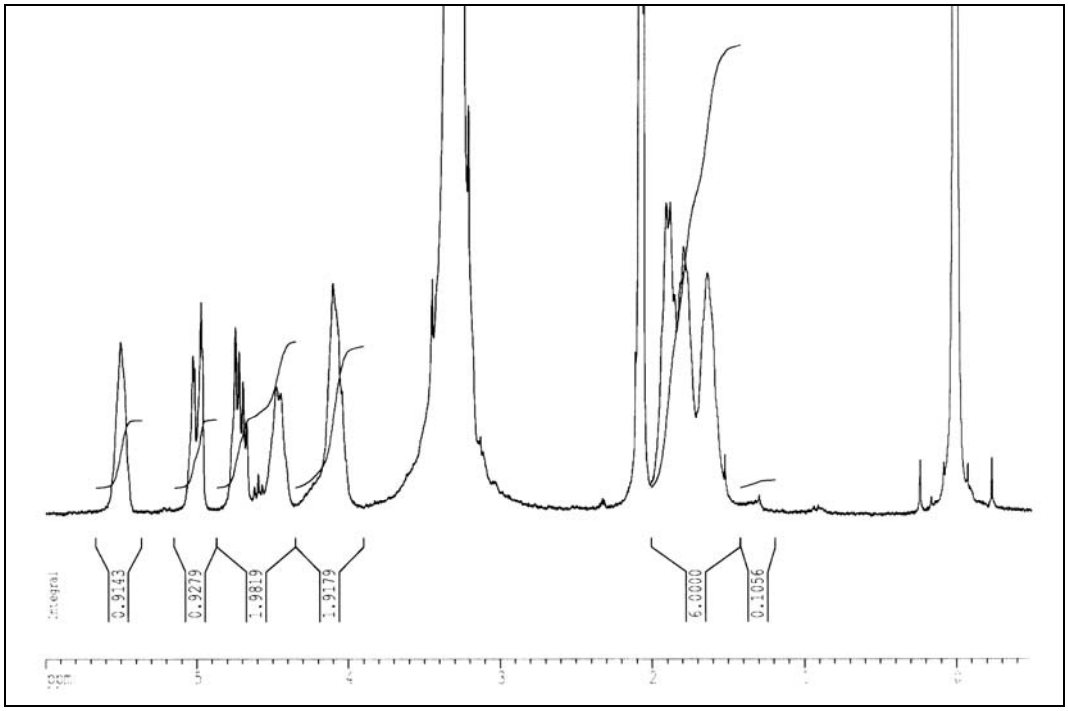

Figure 5.59 ^{1}H NMR spectrum (acetone-d_6 + H_2O) of random linear poly[P-5,6-dinitratohex-1-oxy/P-2,2,2-trifluoroethoxyphosphazene] (unwashed material).

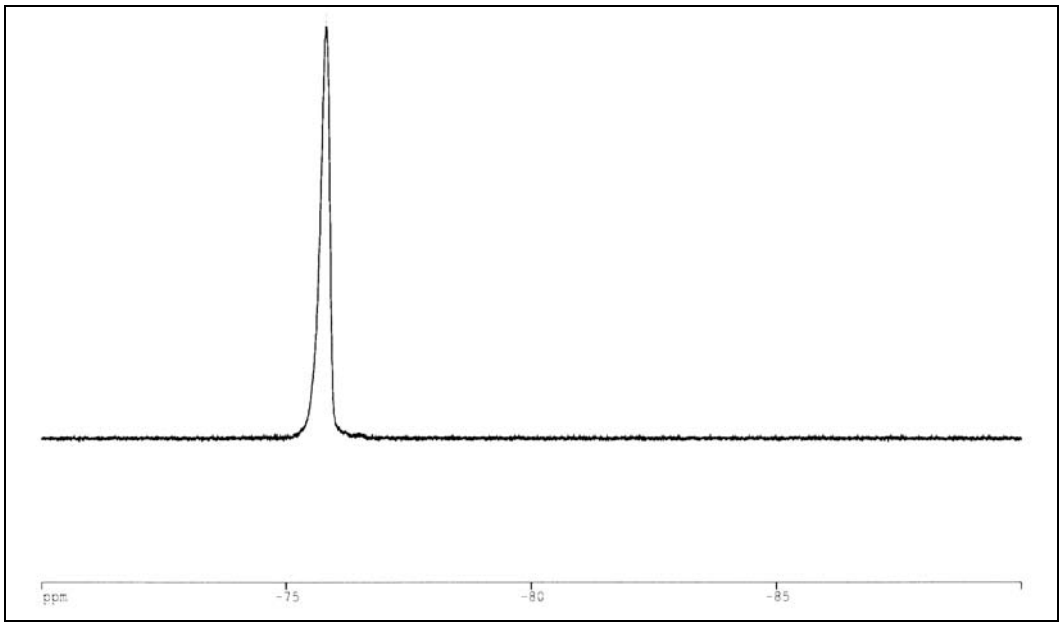

Figure 5.60 ^{19}F NMR spectrum (acetone-d_6) of random linear poly[P-5,6-dinitratohex-1-oxy/P-2,2,2-trifluoroethoxyphosphazene].

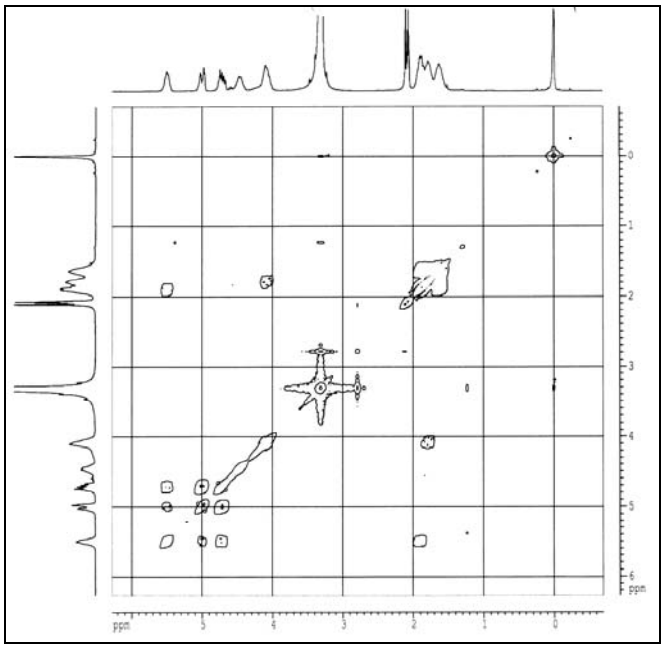

Figure 5.61 ^{1}H-^{1}H correlation (COSY45) NMR spectrum (acetone-d_6 + H_2O) of random linear poly[P-5,6-dinitratohex-1-oxy/P-2,2,2-trifluoroethoxy phosphazene] (unwashed material).

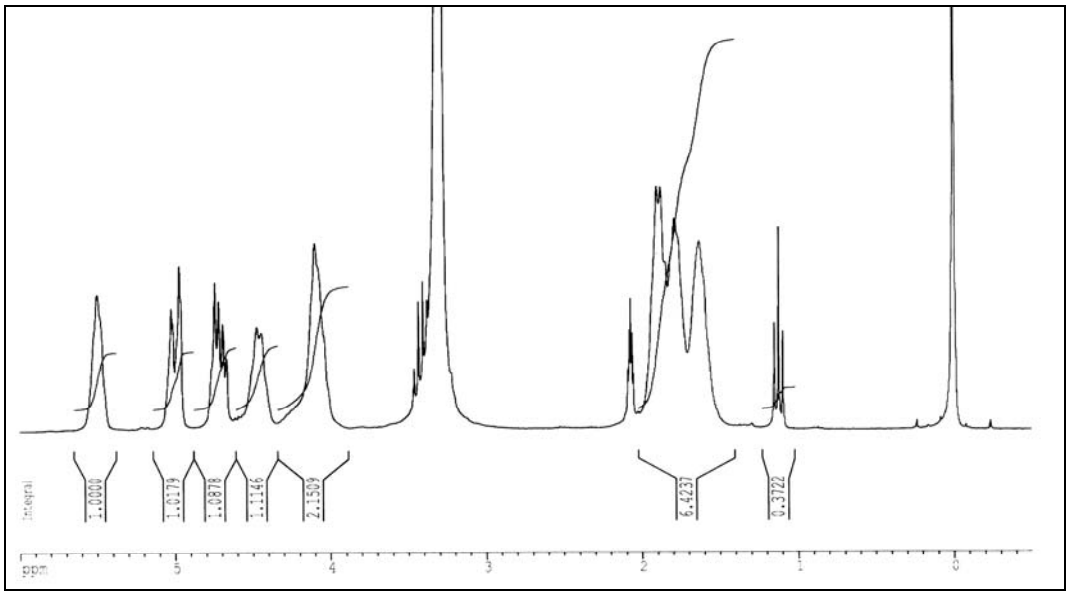

Figure 5.62 ^{1}H NMR spectrum (acetone-d_6 + H_2O) of random linear poly[P-5,6-dinitratohex-1-oxy/P-2,2,2-trifluoroethoxyphosphazene] (Et_2O washed material, Et_2O still present).

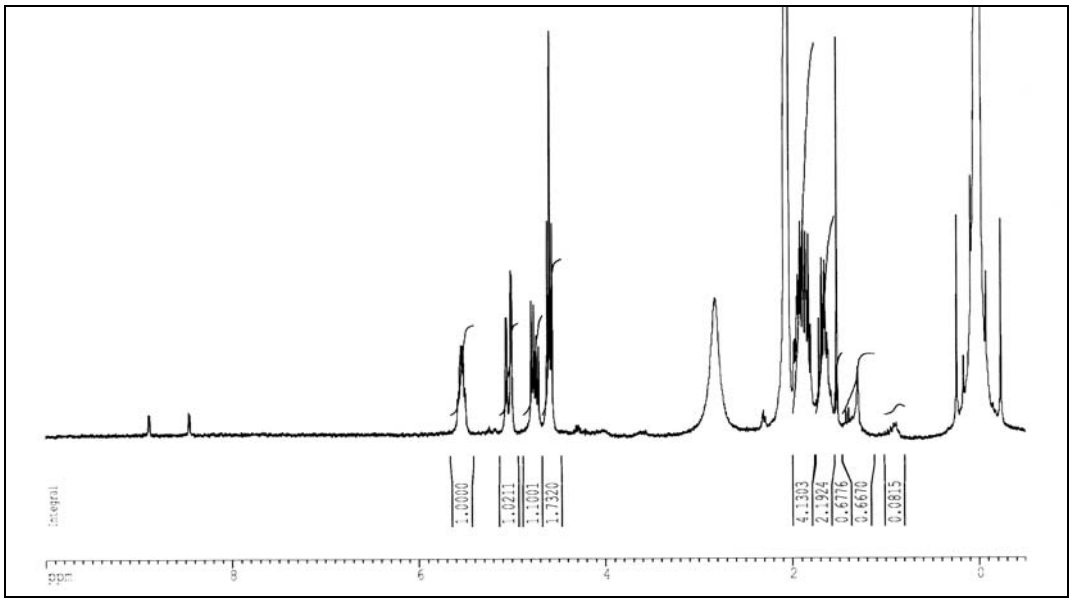

Figure 5.63 ^{1}H NMR spectrum (acetone-d_6) of the evaporated Et_2O extract, showing the presence of hexane-1,2,6-triol trinitrate.

Relating to Section 4.2.8.4.

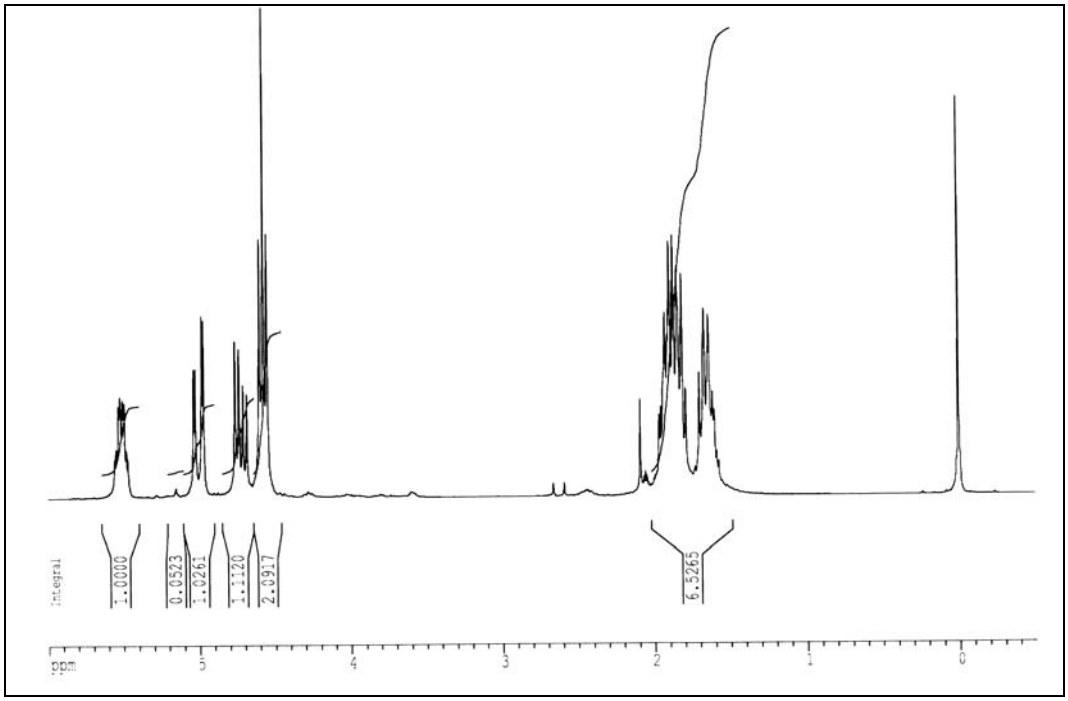

Figure 5.64 ^{1}H NMR spectrum (acetone-d_6) of hexane-1,2,6-triol trinitrate.

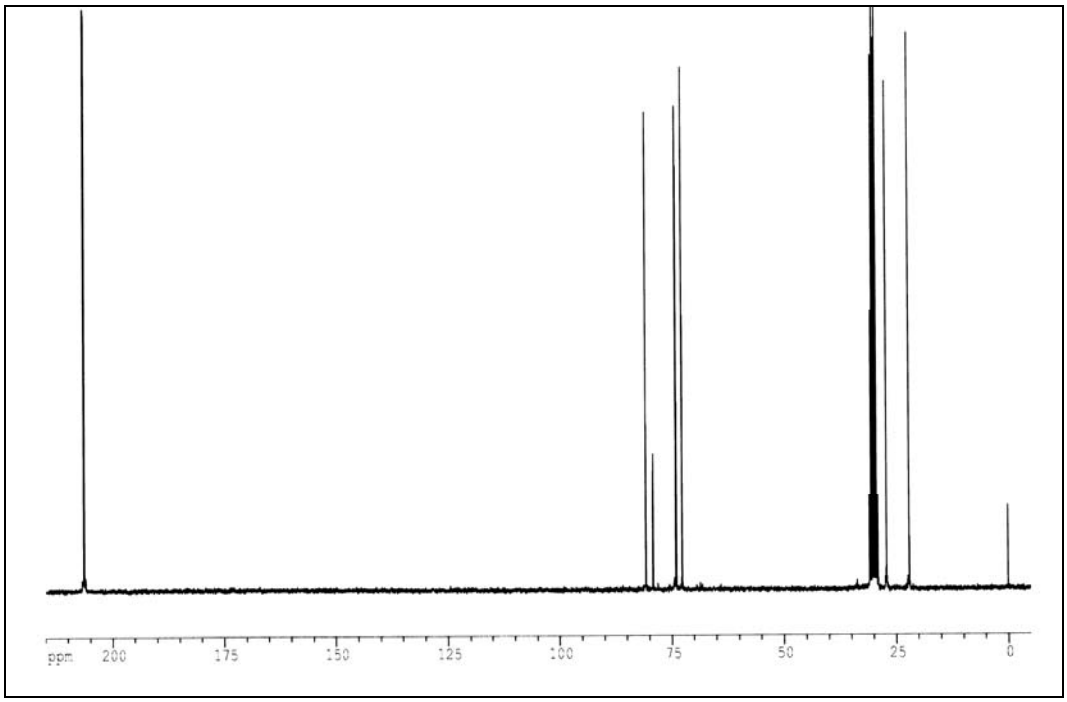

Figure 5.65 ^{13}C NMR spectrum (acetone-d_6) of hexane-1,2,6-triol trinitrate.

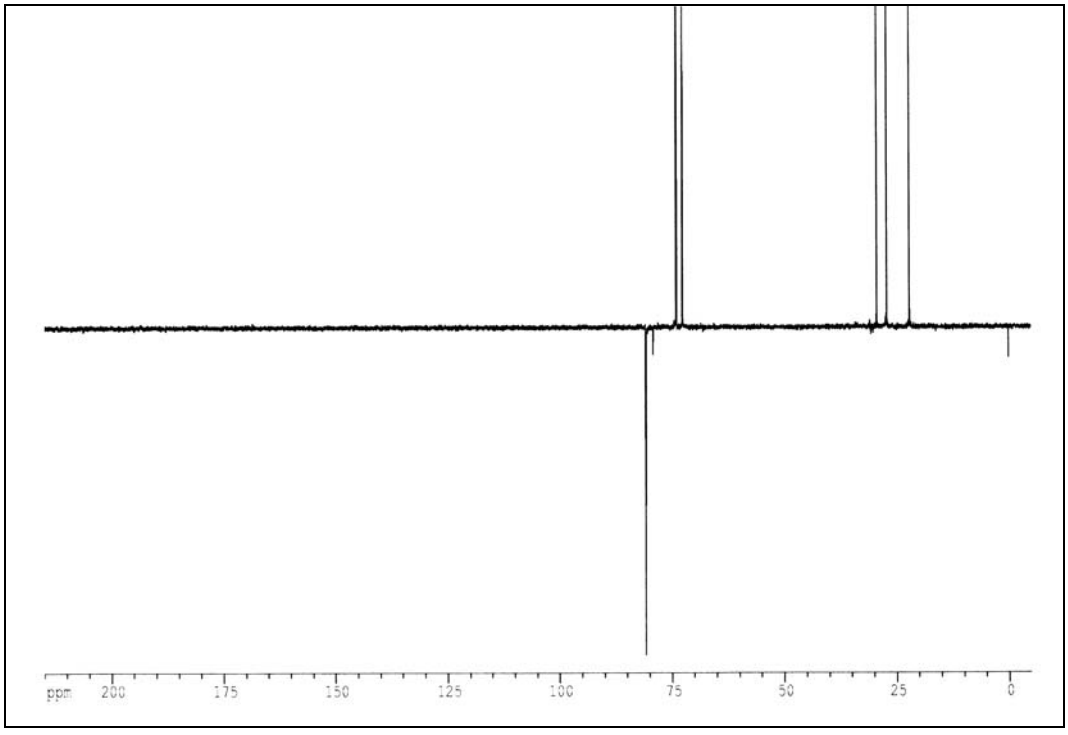

Figure 5.66 ^{13}C DEPT135 NMR spectrum (acetone-d_6) of hexane-1,2,6-triol trinitrate.

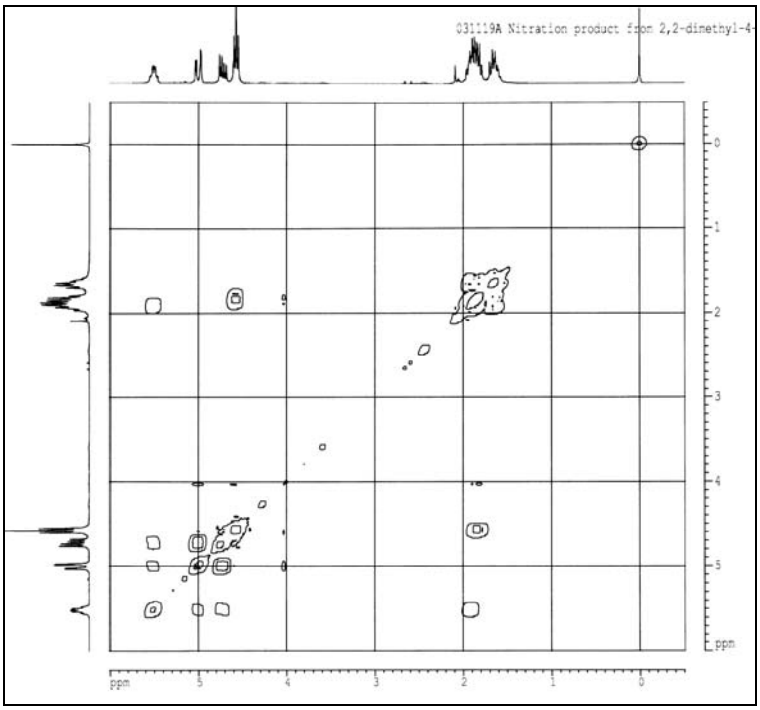

Figure 5.67 ^{1}H-^{1}H NMR (COSY45) spectrum (acetone-d$_6$) of hexane-1,2,6-triol trinitrate.

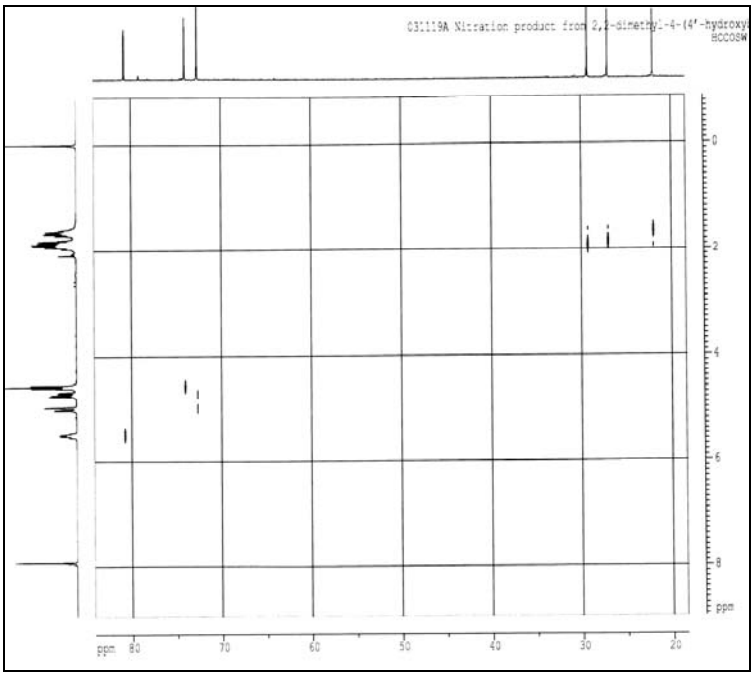

Figure 5.68 ^{1}H-^{13}C correlation NMR spectrum (acetone-d$_6$) of hexane-1,2,6-triol trinitrate.

Relating to section 4.2.9.1.

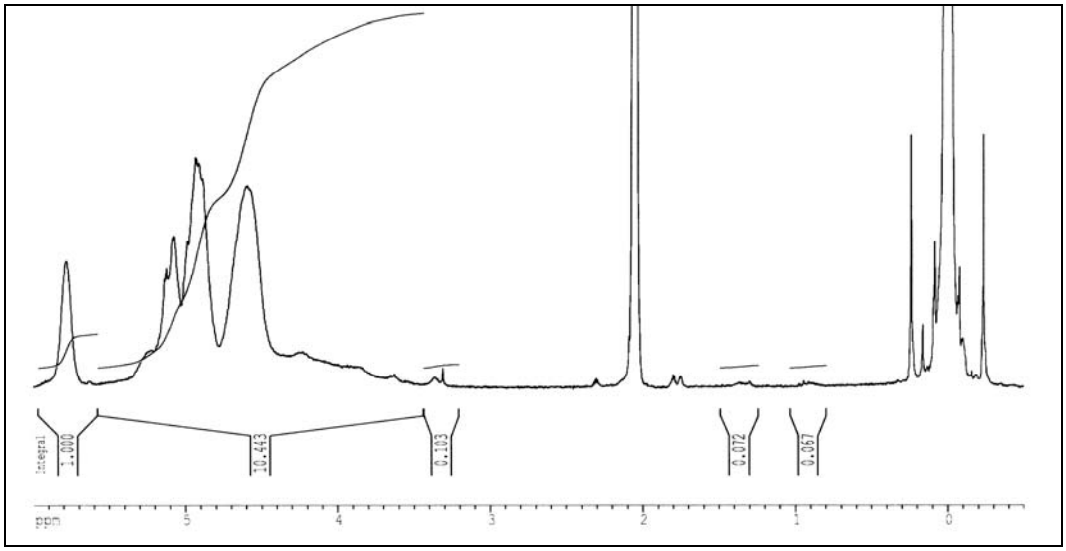

Figure 5.69 ^{1}H NMR spectrum (acetone-d_6) of random linear poly[P-2,3-dinitratoprop-1-oxy/P-2,2,2-trifluoroethoxyphosphazene] obtained by two-phase nitration ($CHCl_3/HNO_3$).

Relating to Section 4.2.9.2.

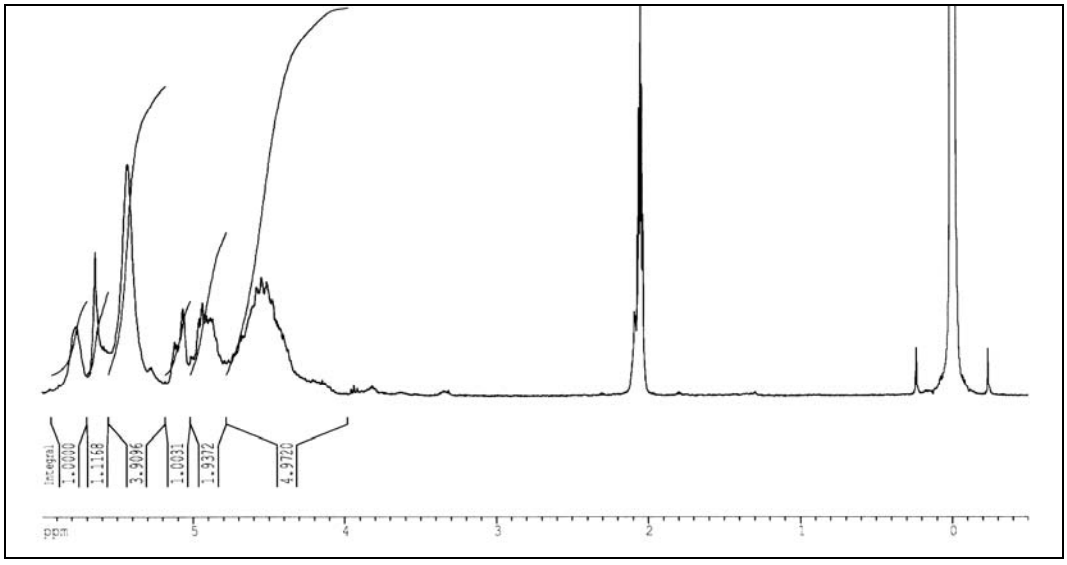

Figure 5.70 ^{1}H NMR spectrum (acetone-d_6) of the product of nitration of random linear poly[P-(2',2'-dimethyl-1',3'-dioxolan-4'-yl)methoxy/P-2,2,2-trifluoroethoxy phosphazene] using N_2O_5 (10 equivalents) in CH_2Cl_2 (Nitration 2).

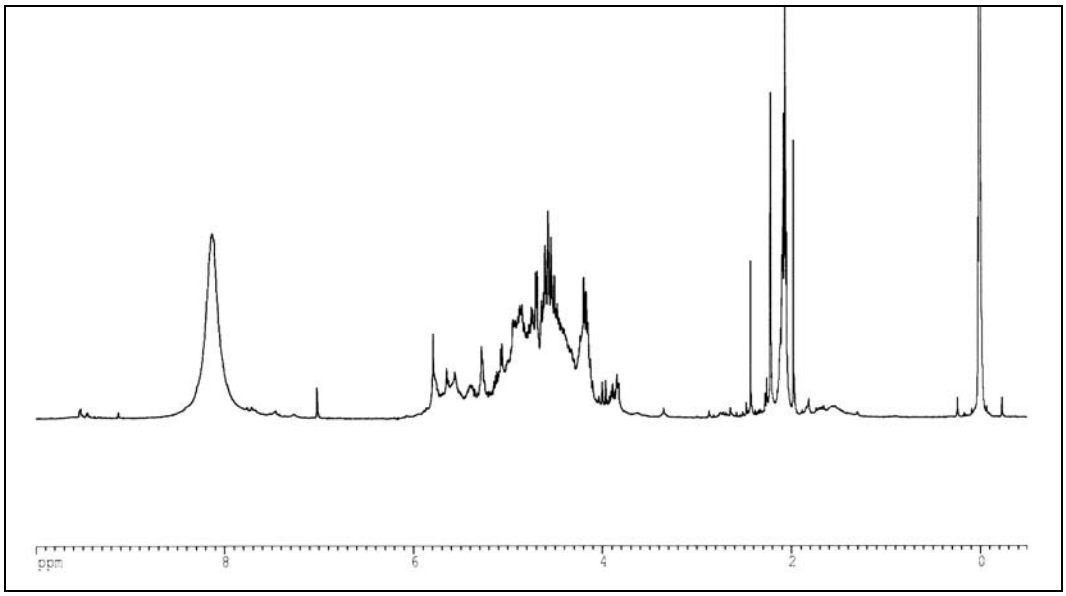

Figure 5.71 ^{1}H NMR spectrum (acetone-d_6) of the product of nitration of random linear poly[P-(2',2'-dimethyl-1',3'-dioxolan-4'-yl)methoxy/P-2,2,2-trifluoroethoxy phosphazene] using N_2O_5 in CH_3CN (Nitration 4).

<u>Relating to Section 4.3.1.1.</u>

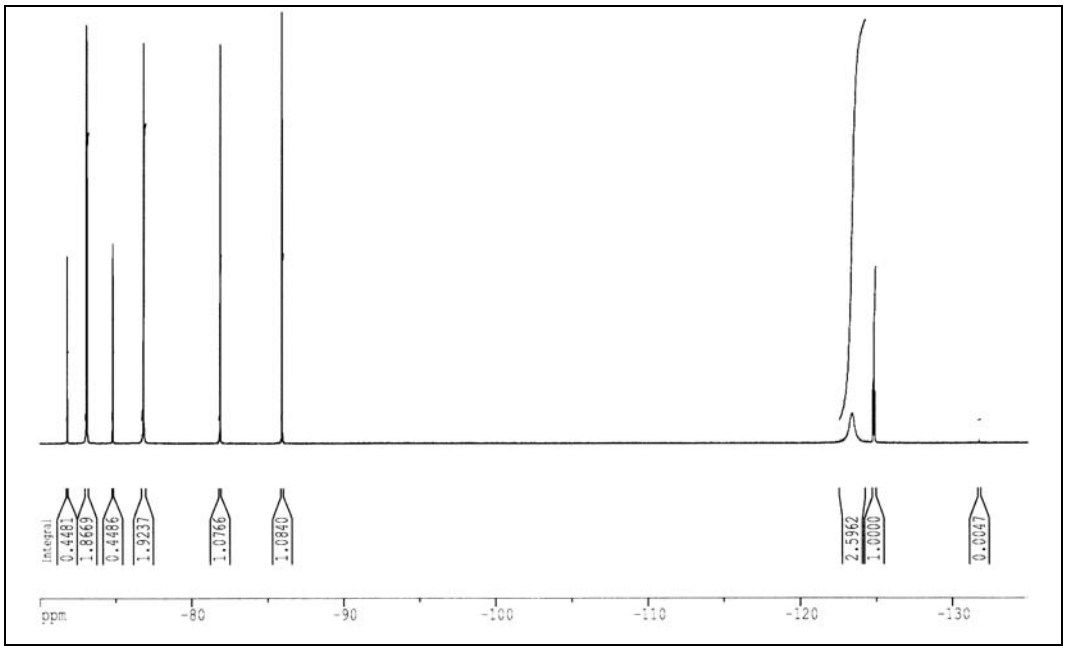

Figure 5.72 ^{19}F NMR spectrum (acetone-d_6 probe) of "salt mixture" A in aqueous imidazole/imidazolium oxalate buffer (pH 7).

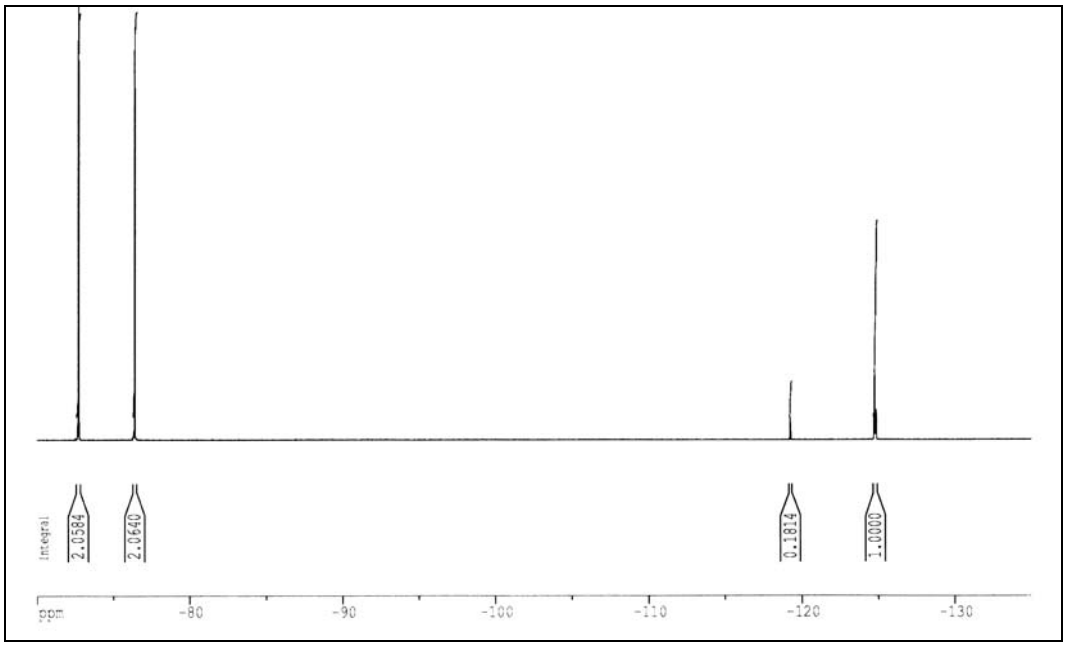

Figure 5.73 ^{19}F NMR spectrum (acetone-d_6 probe) of "salt mixture" B in aqueous imidazole/imidazolium oxalate buffer (pH 7).

APPENDIX B THERMOCHEMICAL DATA FOR SELECTED POLYMERS

Combustion Experiment Number	Cotton Weight (g)	Sample Weight (g)	ΔTcorr (K)	Weight of residue in crucible (mg)	-Q (Total bomb energy change) (J)	Amount of N present in sample (mmol)	Amount of P present in sample (mmol)	HNO_3 formed as detected by IC (mmol)	H_3PO_4 formed as detected by IC (mmol)	Amount of N which converted to HNO_3 (molar%)	Amount of P which converted to H_3PO_4 (molar%)	A: Energy contributed by formation of HNO_3 (J)	B: Energy contributed by dilution of H_3PO_4 (J)	A+ B Energy contributed (as a % of the total energy bomb change)	$-\Delta U_c$ ($J\ g^{-1}$) rounded to 4 signif. figures
1	0	0.2695	0.257	6.9	2802.3	2.645	1.061	0.137	0.624	5.18	58.8	8.1	7.3	0.55	10340
2	0	0.2703	0.269	7.4	2927.2	2.683	1.064	0.143	0.623	5.32	58.5	8.5	7.3	0.54	10770
3	0	0.2816	0.279	7.2	3037.5	2.795	1.108	0.146	0.651	5.22	58.7	8.7	7.7	0.54	10730
4	0	0.2703	0.261	7.0	2844.5	2.683	1.064	0.146	0.626	5.44	58.8	8.7	7.4	0.57	10460
5	0	0.2810	0.270	11.5	2942.4	2.790	1.106	0.148	0.632	5.30	57.1	8.8	7.4	0.55	10410
6	0	0.3023	0.291	8.9	3167.8	3.001	1.189	0.154	0.652	5.13	54.8	9.2	7.7	0.53	10420
Mean and S.D. after propagation of error															**10520 ± 180 (± 1.7%)**

Table 5.1 Experimental measurement of the internal energy of combustion of Polymer 1 (ES%=76, Batch 1).

Combustion Experiment Number	Cotton Weigh t (g)	Sample Weight (g)	ΔT corr (K)	Weight of residue in crucible (mg)	-Q Total bomb energy change (J)	Amount of N present in sample (mmol)	Amount of P present in sample (mmol)	HNO_3 formed as detected by IC (mmol)	H_3PO_4 formed as detected by IC (mmol)	Amount of N which converted to HNO_3 (molar %)	Amount of P which converted to H_3PO_4 (molar %)	A: Energy contributed by formation of HNO_3 (J)	B: Energy contributed by solution of H_3PO_4 (J)	A+B Energy contributed (as a % of the total energy bomb change)	$-\Delta U_c$ ($J\ g^{-1}$) rounded to 4 signif. figures
1	0	0.2431	0.240	5.0	2611.8	2.837	0.946	0.186	0.679	6.55	71.8	11.1	8.0	0.73	10670
2	0	0.2458	0.261	3.5	2847.0	2.868	0.956	0.202	0.710	7.04	74.3	12.1	8.3	0.72	11500
3	0	0.2219	0.232	4.7	2524.4	2.589	0.863	0.163	0.637	6.29	73.8	9.7	7.5	0.68	11300
4	0	0.2279	0.238	3.3	2591.7	2.659	0.886	0.174	0.624	6.54	70.4	10.4	7.3	0.68	11300
5	0	0.1546	0.160	4.9	1743.4	1.804	0.601	0.119	0.380	6.59	63.2	7.1	4.4	0.66	11200
Mean and S.D. (and %SD) after propagation of error															**11190 ± 320 (± 2.9%)**

Table 5.2 Experimental measurement of the standard internal energy of combustion of Polymer 1 (ES%=100, AWE).

Combustion Experiment Number	Cotton Weight (g)	Sample Weight (g)	ΔTcorr (K)	Weight of residue in crucible (mg)	-Q (Total bomb energy change) (J)	Amount of N present in sample (mmol)	Amount of P present in sample (mmol)	HNO_3 formed as detected by IC (mmol)	H_3PO_4 formed as detected by IC (mmol)	Amount of N which converted to HNO_3 (molar %)	Amount of P which converted to H_3PO_4 (molar %)	A: Energy contributed by formation of HNO_3 (J)	B: Energy contributed by solution of H_3PO_4 (J)	A+B Energy contributed (as a % of the total energy bomb change)	$-\Delta U_c$ ($J\ g^{-1}$) rounded to 4 signif. figures
1	0	0.2424	0.196	5.2	2131.8	1.853	0.823	0.084	0.267	4.53	32.4	5.0	3.1	0.38	8760
2	0	0.2857	0.238	4.0	2591.7	2.184	0.970	0.115	0.378	5.27	39.0	6.9	4.4	0.44	9030
3	0	0.2325	0.191	5.0	2083.6	1.777	0.790	0.092	0.292	5.18	36.9	5.5	3.4	0.43	8920
4	0	0.2783	0.230	8.0	2502.9	2.127	0.945	0.109	0.329	5.12	34.8	6.5	3.8	0.41	8960
5	0	0.1652	0.133	3.5	1448.0	1.262	0.561	0.064	0.217	5.07	38.7	3.8	2.5	0.44	8730
Mean and S.D. (and %SD) after propagation of error															**8880 ± 140 (± 1.6%)**

Table 5.3 Experimental measurement of the internal energy of combustion of less-substituted Polymer 2 (ES%=31).

Combustion Experiment Number	Cotton Weight (g)	Sample Weight (g)	ΔT corr (K)	Weight of residue in crucible (mg)	-Q (Total bomb energy change) (J)	Amount of N present in sample (mmol)	Amount of P present in sample (mmol)	HNO_3 formed as detected by IC (mmol)	H_3PO_4 formed as detected by IC (mmol)	Amount of N which converted to HNO_3 (molar %)	Amount of P which converted to H_3PO_4 (molar %)	A: Energy contributed by formation of HNO_3 (J)	B: Energy contributed by dilution of H_3PO_4 (J)	A+B Energy contributed (as a % of the total energy bomb change)	$-\Delta U_c$ ($J\ g^{-1}$) rounded to 3 signif. figures
1	0	0.1038	0.082	1.5	894.7	1.067	0.297	0.039	0.164	3.69	55.4	2.3	1.9	0.47	8580
2	0	0.0934	0.074	0.3	804.6	0.961	0.267	0.037	0.161	3.83	60.2	2.2	1.9	0.51	8570
3	0	0.0974	0.079	1.0	857.1	1.002	0.278	0.038	0.163	3.81	58.6	2.3	1.9	0.49	8760
Mean and S.D. (and 5SD) after propagation of error															**8640 ± 105 (± 1.2%)**

Table 5.4 Experimental measurement of the internal energy of combustion of Polymer 2 (ES%= 65, Batch 1)

Combustion Experiment Number	Cotton Weight (g)	Sample Weight (g)	ΔTcorr (K)	Weight of residue in crucible (mg)	-Q (Total bomb energy change) (J)	Amount of N present in sample (mmol)	Amount of P present in sample (mmol)	HNO_3 formed as detected by IC (mmol)	H_3PO_4 formed as detected by IC (mmol)	Amount of N which converted to HNO_3 (molar %)	Amount of P which converted to H_3PO_4 (molar %)	A: Energy contributed by formation of HNO_3 (J)	B: Energy contributed by solution of H_3PO_4 (J)	A+B Energy contributed (as a % of the total energy bomb change)	$-\Delta U_c$ ($J\ g^{-1}$) rounded to 4 signif. figures
1	0	0.2823	0.243	3.0	2647.4	3.134	0.761	0.185	0.567	5.90	74.5	11.0	6.60	0.66	9320
2	0	0.2869	0.239	2.1	2606.2	3.185	0.773	0.199	0.593	6.25	76.7	11.9	6.90	0.72	9020
3	0	0.2501	0.220	0.5	2397.0	2.776	0.674	0.157	0.505	5.66	74.9	9.40	5.90	0.64	9520
4	0	0.2910	0.242	2.8	2630.0	3.230	0.784	0.186	0.603	5.76	76.9	11.1	7.00	0.69	8980
5	0	0.2581	0.221	2.6	2408.3	2.865	0.695	0.169	0.542	5.90	78.0	10.1	6.30	0.68	9270
Mean and S.D. (and %S.D) after propagation of error															**9220 ± 230 (± 2.5%)**

Table 5.5 Experimental measurement of the internal energy of combustion of Polymer 2 (ES%=78, Batch 3).

Combustion Experiment Number	Cotton Weight (g)	Sample Weight (g)	ΔTcorr (K)	Weight of residue in crucible (mg)	-Q (Total bomb energy change) (J)	Amount of N present in sample (mmol)	Amount of P present in sample (mmol)	HNO_3 formed as detected by IC (mmol)	H_3PO_4 formed as detected by IC (mmol)	Amount of N which converted to HNO_3 (molar %)	Amount of P which converted to H_3PO_4 (molar %)	A: Energy contributed by formation of HNO_3 (J)	B: Energy contributed by dilution of H_3PO_4 (J)	A+B Energy contributed (as a % of the total energy bomb change)	$-\Delta U_c$ ($J\ g^{-1}$) rounded to 4 signif. figures
1	0	0.1304	0.132	1.9	1434.0	1.230	0.366	0.064	0.197	5.23	53.8	3.8	2.3	0.43	10950
2	0	0.1010	0.100	0.2	1086.4	0.952	0.283	0.056	0.166	5.85	58.6	3.3	3.3	0.48	10700
3	0	0.0624	0.064	0.7	689.9	0.588	0.175	0.032	0.088	5.39	50.3	1.9	1.0	0.42	11010
Mean and S.D. (and %S.D.) after propagation of error															**10890 ± 160 (± 1.5%)**

Table 5.6 Experimental measurement of the internal energy of combustion of Polymer 3 (ES% = 59, Batch 1).

Combustion Experiment Number	Cotton Weight (g)	Sample Weight (g)	ΔTcorr (K)	Weight of residue in crucible (mg)	-Q (Total bomb energy change) (J)	Amount of N present in sample (mmol)	Amount of P present in sample (mmol)	HNO_3 formed as detected by IC (mmol)	H_3PO_4 formed as detected by IC (mmol)	Amount of N which converted to HNO_3 (molar%)	Amount of P which converted to H_3PO_4 (molar%)	A: Energy contributed by formation of HNO_3 (J)	B: Energy contributed by dilution of H_3PO_4 (J)	A+B Energy contributed (as a % of the total energy bomb change)	$-\Delta U_c$ ($J\ g^{-1}$) rounded to 4 signif. figures
1	0	0.3043	0.314	7.5	3416.2	2.897	0.844	0.201	0.555	6.96	65.7	12.0	6.5	0.54	11170
2	0	0.2873	0.295	6.0	3217.4	2.735	0.797	0.195	0.540	7.11	67.7	11.6	6.4	0.56	11140
3	0	0.3097	0.324	8.0	3528.4	2.948	0.859	0.215	0.573	7.28	66.7	12.8	6.7	0.55	11330
4	0	0.2506	0.259	8.8	2816.4	2.386	0.695	0.164	0.469	6.86	67.5	9.8	5.5	0.54	11180
5	0	0.3037	0.315	8.2	3432.0	2.892	0.843	0.204	0.561	7.06	66.5	12.2	6.6	0.54	11240
6	0	0.2562	0.270	9.6	2939.6	2.439	0.711	0.168	0.443	6.88	62.3	10.0	5.2	0.52	11410
Mean and S.D. (and %SD) after propagation of error															**11250 ± 100 (± 0.9%)**

Table 5.7 Experimental measurement of the internal energy of combustion of Polymer 3 (ES%=61, Batch 2).

Combustion Experiment Number	Cotton Weight (g)	Sample Weight (g)	ΔTcorr (K)	Weight of residue in crucible (mg)	-Q (Total bomb energy change) (J)	Amount of N present in sample (mmol)	Amount of P present in sample (mmol)	HNO_3 formed as detected by IC (mmol)	H_3PO_4 formed as detected by IC (mmol)	Amount of N which converted to HNO_3 (molar %)	Amount of P which converted to H_3PO_4 (molar %)	A: Energy contributed by formation of HNO_3 (J)	B: Energy contributed by solution of H_3PO_4 (J)	A+B Energy contributed (as a % of the total energy bomb change)	$-\Delta U_c$ ($J\ g^{-1}$) rounded to 4 signif. figures
1	0	0.2337	0.276	2.1	3009.9	2.203	0.599	0.176	0.449	7.98	75.0	10.5	5.2	0.52	12810
2	0	0.2431	0.293	3.6	3194.1	2.292	0.623	0.193	0.428	8.42	68.7	11.5	5.0	0.49	13070
3	0	0.2472	0.302	1.5	3286.2	2.331	0.633	0.180	0.412	7.72	65.1	10.7	4.8	0.47	13230
Mean and S.D. (and %SD) after propagation of error															**13040 ± 210 (± 1.6%)**

Table 5.8 Experimental measurement of the internal energy of combustion of Polymer 4 (ES%= 67).

Combustion Experiment Number	Cotton Weight (g)	Sample Weight (g)	ΔTcorr (K)	Weight of residue in crucible (mg)	-Q (Total bomb energy change) (J)	Amount of N present in sample (mmol)	Amount of P present in sample (mmol)	HNO_3 formed as detected by IC (mmol)	H_3PO_4 formed as detected by IC (mmol)	Amount of N which converted to HNO_3 (molar %)	Amount of P which converted to H_3PO_4 (molar %)	A: Energy contributed by formation of HNO_3 (J)	B: Energy contributed by dilution of H_3PO_4 (J)	A+B Energy contributed (as a % of the total energy bomb change)	$-\Delta U_c$ ($J\ g^{-1}$) rounded to 4 signif. figures
1	0	0.0897	0.111	1.0	1199.7	0.733	0.245	0.048	0.158	6.60	64.7	2.8	1.8	0.38	13320
2	0	0.0853	0.111	0.5	1208.0	0.697	0.233	0.065	0.165	9.38	70.9	3.9	1.9	0.48	14090
3	0	0.0837	0.111	1.5	1202.3	0.684	0.228	0.050	0.143	7.25	62.9	3.0	1.7	0.39	14310
Mean and S.D. after propagation of error															**13910 ± 520 (± 3.7%)**

Table 5.9 Experimental measurement of the internal energy of combustion of Polymer 5 (ES%= 50, Batch 1).

Combustion Experiment Number	Cotton Weight (g)	Sample Weight (g)	ΔTcorr (K)	Weight of residue in crucible (mg)	-Q (Total bomb energy change) (J)	Amount of N present in sample (mmol)	Amount of P present in sample (mmol)	HNO_3 formed as detected by IC (mmol)	H_3PO_4 formed as detected by IC (mmol)	Amount of N which converted to HNO_3 (molar%)	Amount of P which converted to H_3PO_4 (molar%)	A: Energy contributed by form/ation of HNO_3 (J)	B: Energy contributed by dil.ution of H_3PO_4 (J)	A+B Energy contributed (as a % of the total energy bomb change)	$-\Delta U_c$ ($J\ g^{-1}$) rounded to 4 signif. figures
1	0	0.2381	0.316	7.1	3442.5	1.954	0.645	0.152	0.374	7.8	58.0	9.1	4.4	0.39	14400
2	0	0.2410	0.325	5.5	3544.4	1.978	0.653	0.186	0.393	9.4	60.2	11.1	4.6	0.44	14640
3	0	0.2408	0.325	6.4	3540.2	1.976	0.652	0.166	0.369	8.4	56.6	9.9	4.3	0.40	14640
4	0	0.2590	0.339	7.5	3695.8	2.125	0.702	0.176	0.471	8.3	67.1	10.5	5.5	0.43	14210
5	0	0.2109	0.278	6.4	3031.7	1.730	0.571	0.152	0.321	8.8	56.2	9.1	3.8	0.43	14310
6	0	0.2481	0.332	6.8	3615.3	2.036	0.672	0.171	0.375	8.4	55.8	10.2	4.4	0.40	14510
Mean and S.D. (and %SD) after propagation of error															**14450 ± 180 (± 1.2%)**

Table 5.10 Experimental measurement of the internal energy of combustion of Polymer 5 (ES%=51, Batch 2).

Combustion Experiment Number	Cotton Weight (g)	Sample Weight (g)	ΔT corr (K)	Weight of residue in crucible (mg)	-Q (Total bomb energy change) (J)	Amount of N present in sample (mmol)	Amount of P present in sample (mmol)	HNO_3 formed as detected by IC (mmol)	H_3PO_4 formed as detected by IC (mmol)	Amount of N which converted to HNO_3 (molar %)	Amount of P which converted to H_3PO_4 (molar %)	A: Energy contrib. by formation of HNO_3 (J)	B: Energy contrib. by solution of H_3PO_4 (J)	A+B (as a % of the total energy bomb change)	$-\Delta U_c$ ($J\ g^{-1}$) rounded to 4 signif. figures
1	0	0.2900	0.366	13.6 *	3987.8	2.619	0.704	0.223	0.546	8.51	77.6	13.3	6.4	0.49	13680 *
2	0	0.2608	0.344	2.5	3846.5	2.356	0.633	0.210	0.467	8.91	73.8	12.5	5.5	0.47	14680
3	0	0.2230	0.289	1.2	3242.7	2.014	0.541	0.175	0.411	8.69	76.0	10.5	4.8	0.47	14470
4	0	0.2644	0.340	3.0	3768.8	2.388	0.642	0.198	0.481	8.29	74.9	11.8	5.6	0.46	14190
5	0	0.2549	0.335	1.9	3732.1	2.302	0.619	0.200	0.432	8.68	69.8	11.9	5.1	0.46	14570
6	0	0.2673	0.344	2.8	3835.1	2.414	0.649	0.214	0.487	8.86	75.0	12.8	5.7	0.48	14280
Mean , S.D. after propagation of error	* Experiment 1 was rejected.														**14440 ± 210 (± 1.5%)**

Table 5.11 Experimental measurement of the internal energy of combustion of Polymer 5 (ES%=68, AWE).

Combustion Experiment Number	Cotton Weight (g)	Sample Weight (g)	ΔT corr (K)	Weight of residue in crucible (mg)	-Q (Total bomb energy change) -Q cotton(J	Amount of N present In sample (mmol)	Amount of P present In sample (mmol)	HNO_3 formed as detected by IC (mmo)	H_3PO_4 formed as detected by IC (mmol)	Amount of N to HNO_3 (molar %)	Amount of P which converted to H_3PO_4 (molar %)	A: Energy contribut.d by formation of HNO_3 (J)	B: Energy contribut. d by solution of H_3PO_4 (J)	A+B (as a % of the total energy bomb change)	$-\Delta U_c$ ($J\ g^{-1}$) rounded to 4 signif. figures
1	0.0675	0.1778	0.267	3.2	1723.9	0.732	0.732	0.036	0.249	4.91	34.0	2.1	2.9	0.29	9670
2	0.0851	0.1927	0.299	2.0	1765.2	0.793	0.793	0.043	0.269	5.42	33.9	2.6	3.1	0.32	9130
3	0.0857	0.1947	0.302	5.0	1789.3	0.801	0.801	0.040	0.300	4.99	37.4	2.4	3.5	0.33	9160
4	0.0996	0.1813	0.317	6.3	1704.3	0.750	0.750	0.042	0.297	5.60	39.6	2.5	3.5	0.35	9370
5	0.0847	0.1956	0.309	4.1	1833.8	0.805	0.805	0.039	0.270	4.84	33.5	2.3	3.1	0.29	9350
Mean and S.D. after propagation of error															**9340 ± 210 (± 2.3%)**

Table 5.12 Experimental measurement of the internal energy of combustion of linear poly[bis(2,2,2-trifluoroethoxy)phosphazene].

Combustion No.	Sample weight (mg)	Weight of dry residue (mg)	**F^- (mmol)**	**$PO_2F_2^-$ (mmol)**	**PO_3F^{2-} (mmol)**	**PF_6^- (mmol)**	**PO_4^{3-} (mmol)**	Amount of F present in sample (mmol)	Total F recovered (mmol)	Amount of P present in sample (mmol)	Total P recovered (mmol)	**F recovered (%)**	**P recovered (%)**
1	313.6	2.7	0.944	0.082	0.434	0	0.587	1.779	1.542	1.234	1.103	**86.7**	**89.4**
2	299.0	5.0	0.945	0.070	0.424	0	0.639	1.696	1.509	1.178	1.133	**89.0**	**96.2**
3	380.4	2.5	1.137	0.101	0.546	0	0.744	2.158	1.885	1.498	1.391	**87.3**	**92.9**

Table 5.13 Results of the analysis (^{19}F NMR spectroscopy and IC) of the bomb solutions from the combustion experiments of Polymer 1 (ES%=76), cf. Table 5.1.

Combustion No.	Sample weight (mg)	Weight of dry residue (mg)	F^- (mmol)	$PO_2F_2^-$ (mmol)	PO_3F^{2-} (mmol)	PF_6^- (mmol)	PO_4^{3-} (mmol)	Amount of F present in sample (mmol)	Total F recovered (mmol)	Amount of P present in sample (mmol)	Total P recovered (mmol)	**F recovered (Molar %)**	**P recovered (Molar %)**
1	259.0	2.5	0.634	0.046	0.186	0	0.289	0.921	0.912	0.698	0.521	**99.0**	**74.6**
2	207.3	4.3	0.436	0.025	0.089	0	0.160	0.737	0.575	0.558	0.274	**78.0**	**49.1**

Table 5.14 Results of the analysis (^{19}F NMR spectroscopy and IC) of the bomb solutions from the combustion experiments of Polymer 2 (ES%=78, Batch 3), cf. Table 5.5.

Combustion No.	Sample weight (mg)	Weight of dry residue (mg)	**F^- (mmol)**	**$PO_2F_2^-$ (mmol)**	**PO_3F^{2-} (mmol)**	**PF_6^- (mmol)**	**PO_4^{3-} (mmol)**	Amount of F present in sample (mmol)	Total F recovered (mmol)	Amount of P present in sample (mmol)	Total P recovered (mmol)	**F recovered (%)**	**P recovered (%)**
1	266.9	1.0	0.799	0.026	0.193	0	0.472	1.457	1.044	0.742	0.691	**71.7**	**93.0**
2	286.3	1.7	0.819	0.045	0.232	0	0.440	1.563	1.141	0.797	0.717	**73.0**	**90.0**
3	223.2	3.0	0.562	0.029	0.127	0	0.271	1.218	0.747	0.621	0.427	**61.3**	**68.7**

Table 5.15 a (top) and b (bottom). Results of the analysis (^{19}F NMR spectroscopy and IC) of the bomb solutions from the combustion experiments of Polymer 3 (ES%=61, Batch 2), cf. Table 5.7.

Combustion No.	Sample weight (mg)	Weight of dry residue (mg)	F^- (mmol)	$PO_2F_2^-$ (mmol)	PO_3F^{2-} (mmol)	PF_6^- (mmol)	PO_4^{3-} (mmol)	Amount of F present in sample (mmol)	Total F recovered (mmol)	Total F recovered (mmol)	Amount of P present in sample (mmol)	Total P recovered (mmol)	**F recovered (Molar %)**	**P recovered (Molar %)**
1	276.8	3.1	0.977	0.064	0.224	0	0.316	1.411	1.329	1.329	0.709	0.604	**94.2**	**85.2**
2	239.2	2.6	0.715	0.045	0.157	0	0.240	1.219	0.962	0.962	0.613	0.442	**78.9**	**72.1**

Table 5.16 a (top) and b (bottom). Results of the analysis (^{19}F NMR spectroscopy and IC) of the bomb solutions from the combustion experiments of Polymer 4 (ES%=67), cf. Table 5.8.

Combustion No.	Sample weight (mg)	Weight of dry residue (mg)	**F^- (mmol)**	**$PO_2F_2^-$ (mmol)**	**PO_3F^{2-} (mmol)**	**PF_6^- (mmol)**	**PO_4^{3-} (mmol)**	Amount of F present in sample (mmol)	Total F recovered (mmol)	Amount of P present in sample (mmol)	Total P recovered (mmol)	**F recovered (%)**	**P recovered (%)**
1	266.5	3.5	0.971	0.029	0.169	0	0.387	2.129	1.198	0.722	0.585	**56.3**	**81.0**

Table 5.17 a (top) and b (bottom). Results of the analysis (^{19}F NMR spectroscopy and IC) of the bomb solutions from the combustion experiments of Polymer 5 (ES%=51, Batch 2), cf. Table 5.10.

Combustion No.	Sample weight (mg)	Weight of dry residue (mg)	F^- (mmol)	$PO_2F_2^-$ (mmol)	PO_3F^{2-} (mmol)	PF_6^- (mmol)	PO_4^{3-} (mmol)	Amount of F present in sample (mmol)	Total F recovered (mmol)	Amount of P present in sample (mmol)	Total P recovered (mmol)	**F recovered (Molar %)**	**P recovered (Molar %)**
1	253.0	3.1	0.940	0.022	0.142	0	0.378	1.179	1.126	0.614	0.542	**95.5**	**88.3**
2	290.8	2.5	1.030	0.020	0.167	0	0.462	1.356	1.237	0.706	0.649	**91.2**	**93.0**
3	274.1	3.0	0.889	0.034	0.138	0	0.321	1.278	1.095	0.666	0.493	**85.7**	**74.0**

Table 5.18 a (top) and b (bottom). Results of the analysis (^{19}F NMR spectroscopy and IC) of the bomb solutions from the combustion experiments of Polymer 5 (ES%=68, AWE), cf. Table 5.11.

Combustion No.	$PO_2F_2^-$ (mmol) / sample mass (mg) [$x10^{-4}$]	$PO_3F_2^-$ (mmol) / sample mass (mg) [$x10^{-3}$]	Corrected $-\Delta U^\circ_c$ (Jg^{-1})
1	3.029	1.598	10548.7
2	2.642	1.592	10548.1
3	3.050	1.643	10550.1
Mean and S.D %S.D.	2.907 ± 0.229 (± 8.0%)	1.611 ± 0.028 (± 1.7%)	10549.0 ± 1.0 (±0.01%)

Table 5.19 Ratios of the 'scaled up' amounts (mmol) of monofluoro- and difluoro-phosphoric acids formed and the mass of sample burnt (mg) for Polymer 1 (ES%=76) and corrected values of measured ΔU_c, cf. Table 5.1.

Combustion No.	$PO_2F_2^-$ (mmol) / sample mass (mg) [$x10^{-3}$]	PO_3F^{2-} (mmol) / sample mass (mg) [$x10^{-3}$]	Corrected $-\Delta U^\circ_c$ ($J\,g^{-1}$)
1	0.178	0.718	9233
2	0.121	0.429	9228
Mean and S.D %S.D.	0.149 ± 0.04 (± 26.9%)	0.574 ± 0.20 (± 35.6%)	9230 ± 4.0 (±0.04%)

Table 5.20 Ratios of the 'scaled up' amounts (mmol) of monofluoro- and difluoro-phosphoric acids formed and the mass of sample burnt (mg) for Polymer 2 (ES%=78, Batch 3) and corrected values of measured ΔU_c, cf. Table 5.5.

Combustion No.	$PO_2F_2^-$ (mmol) / sample mass (mg) [$x10^{-4}$]	$PO_3F_2^-$ (mmol) / sample mass (mg) [$x10^{-3}$]	Corrected $-\Delta U^\circ_c$ (Jg^{-1})
1	1.349	1.008	11267.3
2	2.166	1.111	11270.1
3	2.106	0.924	11267.1
Mean and S.D. %S.D.	1.872± 0.455 (± 24.3%)	1.014± 0.094 (± 9.2%)	11268.2 ± 1.7 (±0.01%)

Table 5.21 Ratios of the 'scaled up' amounts (mmol) of monofluoro- and difluoro-phosphoric acids formed and the mass of sample burnt (mg) for Polymer 3 (ES%= 61, Batch 2) and corrected values of measured ΔU_c, cf. Table 5.7.

Combustion No.	$PO_2F_2^-$ (mmol) / sample mass (mg) [$x10^{-3}$]	PO_3F^{2-} (mmol) / sample mass (mg) [$x10^{-3}$]	Corrected $-\Delta U°_c$ ($J\ g^{-1}$)
1	0.245	0.856	13057
2	0.238	0.832	13056
Mean and S.D %S.D.	0.241 ± 0.05 (± 2.0%)	0.844 ± 0.02 (± 2.01%)	13056.5 ± 0.70 (±0.005%)

Table 5.22 Ratios of the 'scaled up' amounts (mmol) of monofluoro- and difluoro-phosphoric acids formed and the mass of sample burnt (mg) for Polymer 4 (ES%= 67) and corrected values of measured ΔU_c, cf. Table 5.8.

Combustion No.	$PO_2F_2^-$ (mmol) / sample mass (mg) [$x10^{-4}$]	$PO_3F_2^-$ (mmol) / sample mass (mg) [$x10^{-3}$]	Corrected $-\Delta U°_c$ (Jg^{-1})
1	1.951	1.126	14469.9

Table 5.23 Ratio of the 'scaled up' amounts (mmol) of monofluoro- and difluoro-phosphoric acids formed and the mass of sample burnt (mg) for Polymer 5 (ES%= 51, Batch 2) and corrected value of measured ΔU_c, cf. Table 5.10

Combustion No.	$PO_2F_2^-$ (mmol) / sample mass (mg) [$x10^{-5}$]	PO_3F^{2-} (mmol) / sample mass (mg) [$x10^{-4}$]	Corrected $-\Delta U°_c$ ($J\ g^{-1}$)
1	9.091	5.889	14450.3
2	7.565	6.293	14450.0
3	14.59	5.874	14451.0
Mean and S.D %S.D.	10.40 ± 3.7 (± 35.5%)	6.000 ± 0.24 (± 4.0 %)	14450.4 ± 0.51 (±0.04%)

Table 5.24 Ratio of the 'scaled up' amounts (mmol) of monofluoro- and difluoro-phosphoric acids formed and the mass of sample burnt (mg) for Polymer 5 (ES%= 68, AWE) and corrected value of measured ΔU_c, cf. Table 5.11.

APPENDIX C PUBLISHED PAPER 1

Paper presented at the Insensitive Munitions & Energetic Materials Technology Symposium, November 15-17, 2004, San Francisco, California.

APPENDIX D PUBLISHED PAPER 2

Paper presented at the 8th International Seminar "New Trends in Research of Energetic Materials" April 19-21, 2005,
Pardubice, Czech Republic.

APPENDIX E PUBLISHED PAPER 3

Paper presented at the 36th International Annual Conference of ICT & 32nd International Pyrotechnics Seminar, June 28-July 1, 2005, Karlsruhe, Federal Republic of Germany

[1] Sikder A.K. and Sikder N., *Journal of Hazardous Materials*, 2004, **A112**, 1-15.

[2] Geetha M., Nair U.R., Sarwade D.B., Gore G.M., Ashtana S.N. and Singh H., *J. Thermal Analysis and Calorimetry*, 2003, **73**, 913-22.

[3] Chavez D.E., Hiskey A. and Naud D.L., *Propellants, Explosives, Pyrotechnics*, 2004, **29(4)**, 209-15.

[4] Bailey A. and Murray S.G., *Explosives, Propellants & Pyrotechnics*, Brassey's, London, 1989.

[5] Wild R. and Maasberg W.; *Energetic Materials for Insensitive Munitions*, Paper presented at the 5th Seminar: New Trends in Research of Energetic Materials, 2002, Pardubice, Czech Republic.

[6] Isler J., Propellants, Explosives, Pyrotechnics, 1998, 23(6), 283-91.

[7] Burrows, K.S., *New Explosives for Insensitive Munitions: A Comparative Evaluation*, Paper presented at the Insensitive Munitions and Energetic Materials Symposium, 2001, Bordeaux, France.

[8] Akhavan J., *The Chemistry of Explosives*, RSC Paperbacks, Cambridge, 1998.

[9] Govindan G. and Athithan, S.K., *Propellants, Explosives, Pyrotechnics*, 1994, **19(5)**, 240-4.

[10] Lu Y.C. and Kuo K.K., *Thermochimica Acta*, 1996, **275(2)**, 181-91.

[11] Desai H., Cunliffe A.V., Stewart M.J. and Amass A.J., *Polymer*, 1993, **34(3)**, 642.

[12] Desai H.J., Cunliffe A.V., Hamid J., Honey P.J., Stewart M.J. and Amass A.J., *Polymer*, 1996, **37(15)**, 3461-69.

[13] Bala K. and Golding P., *The Influence of Molecular Weight on Explosive Hazard*, Paper presented at the Insensitive Munitions & Energetic Materials Technology Symposium, San Francisco, 2004.

[14] Frankel M.B. and Flanagan J.E., US Patent No. *4268450*, 1981.

[15] Miller R. S***, Research on new energetic materials,*** Materials Research Society Symposium Proceedings, 1996, **418** (Decomposition, Combustion, and Detonation Chemistry of Energetic Materials), 3-14.

[16] Jin R.C., Young G.C., Jin S.K., Hyun S.K. and Hyung S.K., *A New Energetic Prepolymer, M-PGN and its Undegradable Elastomer*; Paper presented at the

Insensitive Munitions & Energetic Materials Technology Symposium, San Francisco, 2004.

[17] Simmons R.L., *Thermochemistry of NENAs Plasticizers*, Paper presented at the 25th International Annual Conference of ICT, 1994, Karlshrue, Germany.

[18] Christiansen M. and Johansen O.H., *The development of a two-step batch-synthesis to a two-step continuous synthesis*, Paper presented at the 33rd International Annual Conference of ICT, 2002, Karlshrue, Germany.

[19] Golding P. and Trussell S.J., *Energetic Polyphsophazenes – A New category of Binders for Energetic Formulations*; Paper presented at the Insensitive Munitions & Energetic Materials Technology Symposium, San Francisco, 2004.

[20] Provatas A., *Journal of Energetic Materials*, 2003, **21(4)**, 237-45.

[21] Allcock H.R., *Chemistry and Applications of Polyphosphazenes*, Wiley-Interscience, Hoboken, New Jersey, 2003.

[22] Allcock H.R., *Phosphorus-Nitrogen Compounds*, Academic Publishing, New York, 1972.

[23] Billmeyer F.W., *Textbook of Polymer Science*, Wiley Interscience, New York, 1984.

[24] Wang B., Rivard E. and Manners I., *Inorganic Chemistry*, 2002, **41(7)**, 1690-91.

[25] Matyjaszewski K., Lindenberg M.S., Moore M.K. and White M.L., *J. Polymer Science*, 1994, **32**, 465-73.

[26] Allcock H.R., Chester A.C., Morrissey C.T., Nelson J.M. and Reeves S.D., *Macromolecules*, 1996, **29**, 7740-47.

[27] Allcock H.R., Powell E.S., Maher A.E., Prange R.L. and Denus C.R., *Macromolecules*, 2004, **37**, 3635-41.

[28] Allcock H.R.., Reeves S.D., Nelson J.M. and Crane C.A., *Macromolecules*, 1997, **30**, 2213-15.

[29] Greenwood N.N., and Earnshaw A., *Chemistry of the Elements*, Pergamon Press, Oxford, 1984.

[30] Liebig J. *Ann. Chem*., 1834, 11, 139-49.

[31] Rose H., *Ann. Chem.*, 1834, **11**, 131-50.

[32] Gladstone J.H. and Holmes J.D., *J. Chem. Soc.*, 1864, **17**, 225-37.

[33] Stokes H.N., *Amer. Chem. J.*, 1895, **17**, 275-90.

[34] Neilson R.H. and Wisian-Neilson P., *Chem. Rev.*, 1988, **88**, 541-562.

[35] Gleria M., Bertani R. and De Jaeger R., *J. Inorg. And Organomet. Polymers*., 2004, **14(1)**, 1-28.

[36] Allcock, H.R., Pucher, S.R., Fitzpatrick, R.J. and Rashid, K., *Biomaterials*, 1992, **13**, 857.

[37] Allcock, H.R. and Kim, C., *Macromolecules*, 1991, **24**, 2846.

[38] Frech, R.; York, S.; Allcock, H.and Kellam, C. *Macromolecules* (2004), **37(23)**, 8699-8702.

[39] Paulsdorf, J.; Burjanadze, M.; Hagelschur, K.; Wiemhoefer, H.-D. , *Solid State Ionics* (2004), **169(1-4)**, 25-33.

[40] llen, G.; Lewis, C. J. and Todd, S. M., *Polymer* (1970), **11(1)**, 44-60.

[41] Allen, C. W.and Hernandez-Rubio, D, *Phosphazenes*, 2004, 485-503.

[42] Zhang, Teng; Cai, Qing; Wu, De-Zhen; Jin, Ri-Guang., *Journal of Applied Polymer Science*, 2005, **95(4)**, 880-889.

[43] Pintauro, P.N. and Wycisk, R., *Phosphazenes* , 2004, 591-620.

[44] Grolleman, C. W. J.; De Visser, A. C.; Wolke, J. G. C.; Van der Goot, H.; Timmerman, H. *Journal of Controlled Release* , 1986, **4(2)**, 119-31.

[45] Laurencin C T; Koh H J; Neenan T X; Allcock H R and Langer R, *Journal of Biomedical Materials Research* , 1987, **21(10)**, 1231-46.

[46] Gaeta, S. N.; Zhang, H.; Drioli, E. and Basile, A., *Desalination*, 1991, **80(2-3)**, 181-92.

[47] Dave P.R., Forohar F., Axenrod T., Bedford C.D., Chaykovsky M., Gilardi R., Anderson F. and George C., *Preparation of Cyclotriphosphazene Polynitramines*, Paper presented at the Joint International Symposium on Energetic Materials, American Defence Preparedness Association, New Orleans, 1992.

[48] Colclough M.E., *Studies on the Synthesis of Energetic Phosphazenes*, Paper presented at the International Symposium on Energetic Materials Technology, 1995, Phoenix.

[49] Chapman R.D., Welker M.F. and Kreutzberger C.B., *J. Inorganic and Organomet. Polymers*, 1996, **6(3)**, 267-275.

[50] Allcock H.R., Maher A.E. and Ambler C.M., *Macromolecules*, 2003, **36**, 5566-72.

[51] Allcock, H.R. and kim Y.B., *Macromolecules*, 1994, **27**, 3933-42.

[52] Gabler D.G. and Haw, J.F; *Macromolecules,* **24(14)**, 1991, 4218-20.

[53] AWE, Manuscript in preparation…(100%-substituted polymers).

[54] Flindt, E.P. and Rose H.; *Zeitsschrift fuer Anorganische und Allgemeine Chemi*e, **430**, 1977, 155-60.

[55] Staudinger H.; *Helvetica Chimica Acta*, **2**, 1919, 635.

[56] Allcock, H.R., Chem. Reviews, 1972, **72**, 315.

[57] Private conversation with Dr S. Trussell, Polymer Synthetic Team, AWE Aldermaston.

[58] Lora S, Palma G., Bozio R., Caliceti P. and Pezzin G.; *Biomaterials*, 1993, **14(6)**, 430-6.

[59] Tur, D.R., Korshak, V.V., Vinogradova S.V., Dobrova N.B., Novikova S.P., Ll'ina M.B. and Sidorenko E.S.; *Acta Polymerica*, 1985, **36(11)**, 627-31.

[60] Nakamura H., Masuko T., Kojima M. and Magill J.H., *Macromolecular Chemistry and Physics*, 1999, **200(11)**, 2519-24.

[61] McCaffrey R.R., McAtee, R.E., Grey A.E., Allen C.A., Cummings D.G., Apelhans A.D., Wright R.B. and Jolley J.G, *Separation Science and Technology*, 1987, **22(2)**, 873-87.

[62] Flindt E.P. and Rose H.; *Zeitschrift fuer Anorganische und Allgemeine Chemie*, **428**, 1977, 204-8.

[63] Montague R.A., Green J.B. and Matyjaszewski K., *Journal of Macromolecular Science, Pure and Applied Chemistry*, **A32 (8&9)**, 1995, 1497-1519.

[64] Matyjaszewski K., Moore M.M. and White, M.L.; *Macromolecules*, **26**, 1993, 6741.

[65] Matyjaszewski K., Lindberg, M.S., Moore M.M. and White M.L., *Journal of Polymer Science, Series A*, **32**, 1994, 465.

[66] Moore, W.J., *Physical Chemistry*, Longman, London, 1972.

[67] Warn J.R.W. and Peters A.P.H., *Concise Chemical Thermodyna*mics, Stanley Thornes Publishers, Cheltenham, 1999.

[68] IUPAC Compendium of Chemical Terminology, 2nd Edition, 1997.

[69] Freeman, R.D., *J. Chemical Education*, 1985, **62(8)**, 681-6.

[70] Atkins, P.W., *Physical Chemistry*, 5th edn, Oxford University Press, 1999.

[71] Barrow, G.M., *Physical Chemistry*, McGraw-Hill, New York, 1972.

[72] Schmidt R.D. and Manser G.E., *Heats of Formation of Energetic Oxetane Monomers and Polymers*; Paper presented at the 32nd International Conference of ICT, 2001, Karlshrue, Germany.

[73] Bourasseau S.; *Journal of Energetic Materials*, **8(5)**, 1990, 416-441.

[74] Volk F.; *Philosophical Transactions of the Royal Society. Lond. A*, **339**, 335-343.

[75] Ornellas D.L., *Propellants, Explosives, Pyrotechnics*, 1989, **14**, 122-3.

[76] Cox J., *J. Chem. Thermodynamics*, 1978, **10(10)**, 903-6.

[77] Cox J.D. and Pilcher G., *Thermochemistry of Organic and Organometallic Compounds, Academic Press*, London, 1970.

[78] Feng-qi Z., Chen P., Hu R.Z., Luo Y., Zhang Z.Z., Zhou Y.S., Yang X.W., Gao Y., Gao S.L. and Shi Q.Z., *Journal of Hazardous Materials*, 2004, **A113**, 67-71.

[79] Desai H.J., Cunliffe A.V., Lewis T., Millar R.W. Paul N.C., Stewart M.J. and Amass A.J.; *Polymer*, **37(15)**, 1996, 3471-76.

[80] McGuire R.R., Ornellas D.L. and Akst I.B., *Propellants and Explosives*, 1979, **4**, 23-6.

[81] Taylor J., *Detonation in condensed explosives*, Monographs on the Physics and Chemistry of Materials, Oxford University Press, London, 1952.

[82] Ornellas D.L., Carpenter J.H. and Gunn S. R., *Review of Scientific Instruments*, 1966, **37(7)**, 907-912.

[83] Cudzilo S., Trębinsky R., Trzcinky W., Waldemar A. and Wolanski P., *Comparison of Heat Effects on Combustion and Detonation of Explosives in a Calorimetric Bomb*, 29th International Annual Conference of ICT, **1998**, Karlshrue, Germany.

[84] Ornellas D.L., *J. Physical Chemistry*, 1968, **72(7)**, 2390-95.

[85] Volk F. and Schedlbauer F.; *Khimicheskaya Fizika*, **20(8)**, 2001, 43-49.

[86] Keshauarz M.H. and Pouretedal H.R.; *Thermochimica Acta*, **414**, 2004, 203-208.

[87] Chen, P.C., Wu J.C. and Chen S.C.; *Computers and Chemistry*, **25**, 2001, 439-445.

[88] Muthurajan H., Sivabalan R., Talawar M.B. and Ashtana S.N.; *Computer Code for Qualitative Prediction of Heat of Formation of High Energetic Materials-Part I*; Proceedings of the 7th Seminar 'New Trends in Research of Energetic Materials', **2004**, Pardubice, Czech Republic.

[89] Mathieu D. and Simonetti P.; *Thermochimica Acta,* **384**, 2002, 369-375.

[90] Duchowicz P., Castro E.A. and Chen P.C.; *Journal of the Korean Chemical Society*, **47(2)**, 2003, 89-91.

[91] Bensen S.W., *Thermochemical Kinetics, Methods for the estimation of thermochemical data and rate parameters*, John Wiley, New York, 1968.

[92] Walters, N.R., Hackett, S.M. and Lyon R.E., *Fire and Materials*, **24**, 2000, 245-52.

[93] Babrauskas, V., *Heat Release in Fires*, Elsevier, London, 1992.

[94] Pasquetto S. and Patrone L., *Chimica Fisica, Termodinamica Chimica, Elettrochimica*, Volume 3, Masson Editori, Milan, 1992.

[95] Sunner S. and Månsson M., *Combustion Calorimetry, Experimental Chemical Thermodynamics*, IUPAC Series, Pergamon Press, Oxford, 1979.

[96] Bradford H.R., *J. Mining Engineering*, 1957,, **9**, 78-9.

[97] Haines P.J. (Editor), *Principles of Thermal Analysis and Calorimetry*, RSC Paperbacks, 1999.

[98] Rossini F.D. (Editor), *Experimental Thermochemistry*, Interscience Publishers, New York, 1956.

[99] Rojas A. and Valdes A., *J. Chem. Thermodynamics*, 2003, **35**, 1309-19.

[100] Rojas-Aguilar A., *J. Chem. Thermodynamics*, 2002, **34**, 1729-43.

[101] Sakiyama M. and Kiyobayashi T., *J. Chem. Thermodynamics*, 2000, **32**, 269-79.

[102] Private telephone conversation with Dr Hugh Davies, Thermodynamics Modelling Team, National Physical Laboratory, Teddington.

[103] Hubbard W.N., Katz C. and Waddington G., *Journal of Physical Chemistry*,1954, **58**, 142-52.

[104] Matthews G.P., *Experimental Physical Chemistry*, Clarendon Press, Oxford, 1985.

[105] Washburn E.W., *J. Res. Natl. Bur. Stand.*, 1933, **10**, 525.

[106] Siegel B. and Schieler L., Energetics of Propellant Chemistry, John Wiley & Sons, New York, 1964.

[107] Gallazzi M.C., Freddi G., Sanvito G. And Viscardi G., *Journal of Inorganic and Organometallic Polymers*, 1996, **6(4)**, 277-300.

[108] Taber D.F., Xu M. and Hartnett J.C.; *Journal of the American Chemical Society*, **124**, 2002, 13121-6.

[109] Meyers A.I. and Lawson J.P.; *Tetrahedron Letters*, **47**, 1982, 4883-6.

[110] Marton D., Stivanello D. and Tagliavini G.; *Gazzetta Chimica Italiana*, **124**, 1994, 265-70.

[111] Michael A. and Carlson G.H.; *Journal of the American Chemical Society*, **57**, 1935, 1268-76.

[112] Strazzolini P. and Runcio A.; *European Journal of Organic Chemistry*, **3**, 2003, 526-36.

[113] Strazzolini P., Dall'Arche M.G. and Giumanini A.G.; *Tetrahedron Letters*, **39**, 1998, 9255-58.

[114] Grummit O. and stearns J.A.; *Organic Syntheses*, **29**, 1949, 89-91.

[115] Brimble M.A., Park J.H. and taylor C.M.; *Tetrahedron*, **59(31)**, 2003, 5861-68.

[116] Kuehnert S.M. and Maier M.E.*; Organic Letters*, **4(4)**, 2002, 643-46.

[117] Manners I., Wang B. and Rivard E.; *Inorganic Chemistry*, 2002, **41(7)**, 1690-91.

[118] Pinciroli V., Biancardi R., Visentin G. And Rizzo V.; *Organic Process Research & Development*, 2004, **8**, 381-84.

[119] IUPAC Commission on Atomic Weights and Isotopic Abundances, *J. Phys. Chem. Ref. Data*, **24(4)**, 1995, 1561-76.

[120] Sanping C., Gang X., Guang F., Shengli G. and Qizhen S.; *J. Chemical Thermodynamics*, **37**, 2005, 397-404.

[121] Diaz E., Brousseau P., Ampleman G. and Prud'Homme R.E.; *Propellants, explosives, Pyrotechnics*, **28(3)**, 2003, 101-106.

[122] Sanden, R. Determination of the heat of formation of poly(dimethylsiloxane); Internationale Jahrestagung - Fraunhofer-Institut fuer Treib- und Explosivstoffe, 17th , 1986, 65/1-65/13.

[123] Sabbah T., Xu-Wu A., Chickos J.S., Planas Leitão M.S. Roux M.V. and Torres L.A., *Thermochimica Acta*, **331**, 1999, 93-204.

[124] Brimblecombe P., *Air Composition and Chemistry*, Cambridge University Press, 1995.

[125] Parr Inc., *Isothermal Calorimeter's Instruction Manual*.

[126] Unpublished work found on the WWW: http://www.colby.edu/chemistry/PChem/lab/EnthalpyofFormation.pdf

[127] H.W.Salzberg, J.I. Morrow and M.E. Green, *Physical Chemistry Laboratory: Principles and Experiments*, Macmillan, New York, 1978.

[128] Wadso I, *Sci. Tools*, 1966, **13(3)**, 33-39.

[129] Christian G.C., *Analytical Chemistry*, J. Wiley and Son, Oxford, 1994.

[130] Garner W.E. and Abernethy C.L., *Proceedings of the Royal Society*, A, **99**, 1921, 213, cited in Urbanski T., *Chemistry and Technology of Explosives*, Volume 1, Pergamon Press, Oxford, 1986.

[131] Urbanski T., *Chemistry and Technology of Explosives*, Volume 2, Pergamon Press, Oxford, 1986.

[132] Federoff, B.T., *Encyclopedia of Explosives and Related Items*, Volume 2, Dover, NJ.; Picatinny Arsenal, 1960.

[133] Gibbs T.R. and Popolato A., (Editors), *LASL Explosive property Data*, University of California press, Berkeley, 1980.

[134] Bugaut F., Performances des Noveaux Explosifs Insensibles, Cas du NTO, Deuxiemens Journeés Scientifiques, Paul Vielle, 16-18 Oct. 1991, Brest.

[135] Finch A., Gardner, P.J., Head A.J. and Majdi H.S., *Journal of Chemical thermodynamics*, 1991, **23**, 1169-73.

[136] Harrop D. and Head A.J., *Journal of Chemical Thermodynamics*, 1977, **9**, 1067-76.

[137] Bedford A.F. and Mortimer C.T., *Journal of the Chemical Society*, 1960, 1622-25.

[138] Kirklin D.R. and Domalski E.S., *Journal of Chemical thermodynamics*, 1988, **20**, 743-54.

[139] Holmes W.S., *Transactions of the Faraday Society*, 1962, **58**, 1916-25.

[140] Wagenaar W., *Journal of the Chemical Society*, 1912, **100(II)**, 931.

[141] Belcher R., *Quantitative Inorganic Analysis*, Butterworth Scientific Publications, London, 1955.

[142] Parr 1108Cl halogen-resistant bomb instruction and manteinence manual.

[143] Britske E.V. and Dragunov S.S., *Journal of Chemical Industry*, 1927, **4**, 49-51.

[144] Chess W.B. and Bernhart D.N., *Analytical chemistry*, 1959, **31**, 1116-19

[145] Altynikova P.M., Kharakoz A.E., Osipova T.P. and Bleshinskii S.V., *Ser. Fiz. Mat. Estet. Nauk*., 1950, **3**, 63-7.

[146] Smith N.K., Scott D.W. and McCullough J.P., *Journal of Physical Chemistry*, **68(4)**, 1964, 934-39.

[147] Hajiev S.N. and Agarunov M.J., *J. Organometallic Chemistry*, **22**, 1970, 305-311.

[148] Hu, A.T. and Sinke G.C*., J. Chemical Thermodynamics*, 1969, **1**, 507-13.

[149] Hubbard W.N., Knowlton J.W. and Hugh, M.H., *J. Physical Chemistry*, **58**, 1954, 396-402.

[150] Good W.D., Scott D.W. and Waddington G., *Journal of Physical Chemistry*, 1956, **60**, 1080-89.

[151] Cox J.D., Gundry H.A. and head A.J., *Transactions of the Faraday Society*, 1964, **60**, 653-65.

[152] Krech M., Price S.J.W. and Yared W.F., *Canadian Journal of Chemistry*, **50(18)**, 1972, 2935-38.

[153] Krech M.J., Price S.J.W and Yared W.F., *Canadian Journal of Chemistry*, 1973, **51(22)**, 3662-64.

[154] Domalski E.S. and Armstrong, G.T., *J. Research of the National Bureau of Standards, Section A: Physics and Chemistry*, 1967, **71(2)**, 105-18.

[155] Good W.D., Douslin D.R. and McCullough J.P, *J. Physical Chemistry*, 1963, **67**, 1312-14.

[156] Swarts F., *J. Chim. Phys.*, 1949, **3**, 317.

[157] Cox J.D. and Head A.J., *Transactions of the Faraday Society*, 1962, **58**, 1839-45.

[158] Peters H., Tappe E. and Urbanczik M., *Monatsberichte zu Berlin*, 1967, **9**, 703-14.

[159] Williams M.M., McEwan W.S. and Henry R.A. *Journal of Physical Chemistry*, 1957, **61**, 261-7.

[160] Roux M.V., Torres L.A. and Davalos J.Z., *Journal of Chemical Thermodynamics*, 2000, **33**, 949-57.

[161] Jiménez P., Roux M.V. and Turrión C., *J. Chemical Thermodynamics*, 1992, **24**, 1145-49.

[162] Becker, G. and Roth W.A., *Zhurnal Physik. Chem*., 1935, **174**, 104-14.

[163] Aleksandrov Y., Mikina V.D. and Novikov G.A., *Trudy Metrologicheskikh Insitutov SSSR*, 1969, **111**, 95-102.

[164] Uman, M., The lightning discharge, …….

[165] Harris G.W., McKay G.I., Iguchi T., Schiff H.I., Harold I. and Schuetzle D., *Environmental Science and Technology*, 1987, 21(3), 299-304.

[166] Faour M. and Akasheh T.S., *Journal of the Chemical Society, Perkin transactions 2: Physical organic Chemistry*, 1985, **6**, 811-13.

[167] Kongpricha S. and Jache A.W., *Journal of Fluorine Chemistry*, 1971, **72**, 79-84.

[168] Plakhotnik V.N., Shamakhova N.N., Tul'chinskii B.V. and Ll'in E.G.; *Zhurnal Neorgranicheskoi Khimii*, 1985, **30(11)**, 2773-77.

[169] Ames D.P., Ohashi S., Callis C.F., Van Wazer J.R., *Journal of the American Chemical Society*, 1959, **81**, 6350-57.

[170] Larson J.W. and Su B., *Journal of Chemical & Engineering Data*, 1994, **39**, 36-38.

[171] Yoza N., Nakashima S., Ueda N., Miyajima T., Nakamura T. and Vast P., *Journal of Chromatography A*, 1994, **664**, 111-16.

[172] Vast P., Semmoud A., Addou A. and Palavit G., *Journal of Fluorine Chemistry*, **27(3)**, 1985, 319-325.

[173] Nixon J.F. and Schmutzler R.S., *Sopectrochimica Acta*, **20(12)**, 1964, 1835-42

[174] Gebala A.E. and Jones M.M., J. *Inorganic & Nuclear Chemistry*, **31**, 1969, 771-76.

[175] Reddy G.S. and Schmutzler R., *Zeitschrift fur Naturforschung, Teil B (Anorganische Chemie)*, **25(11)**, 1970, 1199-1214.

[176] Lindahl C.B., *Fluorine compounds of Inorganic Phosphorus*, Kirk-Othmer Encyclopedia of Chemical technology (3rd Edition), Wiley, New York.

[177] Pelletier P. and Durant J.L., *Zeitschrift fuer Anorganische und Allgemeine Chemie*, 1990, **581**, 190-98.

[178] Ryss, I.G. and Tul'chinskii, V.B., *Zhurnal Neorganischeskoi Khimii*, 1962, **7**, 1313-15.

[179] Skoog D.A. and West D.M., *Fundamentals of Analytical Chemistry*, Holt, Rinehart and Winston Publishing, 1976, New York.

[180] Vast P., Semmoud A., Addou A. and Plavit G., *Journal of Fluorine Chemistry*, **27**, 1985, 319-25.

[181] Addou A., and Vast P., *Journal of Fluorine Chemistry*, **14**, 1979, 163-69.

[182] Gaudiano A. and Gauduiano G., *Vademecum di Chimica per Chimici, Biochimici e Farmacisti*, Masson Italia Editori, Milan, 1982.

[183] Kazakov A.I., *Bulletin of the Academy of Sciences, USSR, Division Chemical Sciences*, 1990, 1565-70. Cited in ICT thermochemical code…

[184] Benson S.W., Cohen N.; *Chemical Reviews*, 1993, **93**, 2419-38.

[185] Kolesov V.P., *Russian Journal of Physical Chemistry* (English translation), **45**, 1971, 303-5. Cited in the ICT thermochemical code.

[186] Larson J.W. and Su B.; *Journal of Chemical Engineering Data*, 1994, **39**, 36-38.

[187] Cox, J.D., Wagman, D.D. and Medvedev, V.A., *CODATA Key Values for Thermodynamics*, Hemisphere Publishing Corporation, New York, 1989.

[188] Lau, J.K. and Li, W., *Journal of Molecular Structure (Theochem)*, 2002, **578**, 221-28.

[189] Miroshnichenko E.A., Lebedev V.P., Kostikova, L.M., Vorob'eva V.P., Voro'ev A.B. and Inozemtcev J.O.; *Enthalpy characteristics of nitro- and fluorine-nitro derivatives heterocyclic compounds*, Paper presented at the 34th Internation Conference of ICT, 2003, Karshrue, Germany.

[190] Private conversation with Dr P. Gill, …

[191] Deepak D., Sridharan P. and Padmanbhan M.S.; *Journal of Propulsion and Power*, 1998, *14(3)*, 290-94.

[192] Milyokhin Y.M., Klyuchnikov A.N., Fedorychev A.V. Gunin S.V. and Serushkin V.V., *'Identification of experimental dependences of propellant burning rate on pressure'*; Paper presented at the 34th International Conference of ICT, 2003, Karshrue, Germany.

[193] Siegel B. and Schieler L.,*Energetic of Propellant Chemistry*, J. Wiley & Sons, New York, 1964.

[194] Desai H.J., Cunliffe A.V., Lewis T., Millar R.W., Paul N.C. and Stewart M.J.; *Polymer*, **37(15)**, 1996, 3471-76.

[195] Suzuki, H. and Okada, F; ***Japan*** *Kokai Tokkyo Koho* ***No. JP 04134086***, 1992.

[196] Ranu B.C. and Hajra A., *Journal of the Chemical Society, Perkin Transactions 1*, 2001, 2262-65.